Etudes de différentes voies de transduction du signal afin de mettre à jour de nouveaux mécanismes moléculaires et de nouvelles cibles thérapeutiques

Béatrice Vallée

UNIVERSITÉ D'ORLÉANS

CENTRE de BIOPHYSIQUE MOLÉCULAIRE

HDR présentée par :

Béatrice VALLÉE MÉHEUST

soutenue le :

Discipline/ Spécialité : Sciences de la Vie

Etudes de différentes voies de signalisation cellulaire afin de mettre à jour de nouveaux mécanismes moléculaires et de nouvelles cibles thérapeutiques

RAPPORTEURS :

Eric PASMANT	PU-PH, Université de Paris Descartes, CHU de Paris, UFR de Pharmacie
Laurence LAFANECHÈRE	DR, Institut pour l'Avancée des Biosciences CNRS, Grenoble
Jean-Vianney BARNIER	DR, Institut des Neurosciences, CNRS, Paris-Saclay

---

JURY :

Pascal BONNET	Professeur, ICOA, CNRS/Université d'Orléans
Sandrine RUCHAUD	CR, Station Biologique de Roscoff, CNRS/Sorbonne Université
Franck VERRECCHIA	DR, Phy-OS, INSERM Nantes
Hélène BÉNÉDETTI	DR, CBM, CNRS Orléans

Dans la vie, rien n'est à craindre, tout est à comprendre.

Marie Skłodowska Curie

Table des matières

I. CURRICULUM VITÆ - *BÉATRICE VALLÉE MÉHEUST*

Née le 4 mai 1973, 46 ans
Mariée, 2 enfants
Nationalité française
✆ +33 6 30 70 65 67

✉ Centre de Biophysique Moléculaire
UPR 4301 - CNRS
Rue Charles Sadron
F-45071 Orléans Cedex 2
☎ +33 2 38 25 76 11
💻 beatrice.vallee@cnrs-orleans.fr

Expériences de recherche

Depuis mi-2016 Chargée de recherche au **Centre de Biophysique Moléculaire** - **CNRS** d'Orléans (45-France), dans l'équipe « Biologie cellulaire, Cibles moléculaires et Thérapies innovantes », groupe thématique « Signalisation cellulaire ».

- ***Etude des LIM kinases, nouvelles cibles thérapeutiques pour traiter la neurofibromatose de type 1 (NF1), les cancers et certaines maladies neuronales.***
- ***Etude des bases moléculaires de la Neurofibromatose de type 1, maladie hautement prévalente.***

2008-2016 Chargée de recherche au **Centre de Biophysique Moléculaire** - **CNRS** d'Orléans (45-France), dans l'équipe d'Hélène Bénédetti « Signalisation cellulaire et Neurofibromatose ».

- ***Etude des bases moléculaires de la Neurofibromatose de type 1, maladie hautement prévalente.***
- ***Mise à jour d'une nouvelle fonction de Nf1 dans la réorganisation du cytosquelette d'actine via la kinase LIMK2.***
- ***Etude des isoformes de LIMK2.***

2004-2007 Chargée de recherche 2ème classe au **Centre de Biophysique Moléculaire** - **CNRS** d'Orléans (45-France), dans l'équipe d'Hélène Bénédetti.

- ***Etude des PEBPs (Phosphatidyl Ethanolamine Binding Proteins) chez la levure Saccharomyces cerevisiae***.

2000-2003 Stage Post-Doctoral dans le laboratoire du Pr. Howard Riezman dans les départements de Biochimie du **Biozentrum - Université de Bâle**, puis de **Sciences II – Université de Genève** (à partir du 1er octobre 2002) en Suisse.

- ***Etude de la synthèse des céramides chez la levure Saccharomyces cerevisiae***.

1996-1999 Thèse de Biochimie dans l'équipe de Françoise Schoentgen au **Centre de Biophysique Moléculaire** - **CNRS** d'Orléans (45-France).

- ***Etude structurale et fonctionnelle de la protéine PEBP (Phosphatidyl Ethanolamine Binding Protein) extraite du cerveau de bœuf***.

1996 *5 mois* Stage de fin d'études et de DEA sous la direction du Pr. Jean-Paul Lellouche au **Service des Molécules Marquées - CEA** de Saclay (91-France).

- ***Synthèse organique et caractérisation de complexes dièniques du Fer***.

1995 *3 mois* Stage ingénieur à l'**Institut für Pflanzenbau und Pflanzenzüchtung der Justus Liebig Universität** à Gieβen en Allemagne.

- ***Biologie végétale : étude de caryotypes de générations de tournesols***.

Formation

1996-1999	Doctorat en **Biologie et Biophysique Moléculaires et Cellulaires** - Université d'Orléans.
1995-1996	DEA de **Chimie Organique des Biomolécules** - Université de Montpellier II.
1993-1996	**Ingénieur Chimiste à l'Ecole Nationale Supérieure de Chimie de Montpellier**. Option Chimie Organique Fine, Bioorganique.
1991-1993	Classes Préparatoires aux Grandes Ecoles – Lycée Pothier, Orléans.

Mérites et Distinctions

2002-2003	Bourse du groupe européen de recherche sur les Sphingolipides.
2000-2001	Long-term FEBS Fellowship.
Décembre 1999	Doctorat en Biologie et Biophysique Moléculaires et Cellulaires avec les "Félicitations écrites du Jury".
1996-1999	"Bourse de Docteur Ingénieur".
Juin 1996	DEA Mention Bien
Juin 1996	Classement Ecole de Chimie de Montpellier : 13ème sur 98.
Juin 1991	Baccalauréat C : Mention Bien.

Compétences

Biochimie	Purification et caractérisation de protéines et de lipides dans différentes lignées cellulaires et chez la levure *Saccharomyces cerevisiae*. Isolation de complexes protéiques actifs et de protéines membranaires. Purification et isolation de différentes organelles. Tests d'activité enzymatique. Western Blot.
Biologie Moléculaire	Clonage de gènes, amplification et purification d'ADN plasmidique et génomique, mutagenèse dirigée. Biologie Moléculaire et Génétique de la levure *Saccharomyces cerevisiae.*
Biologie Cellulaire	Culture de bactérie, de levure et de différentes lignées de cellules de mammifères. Transfections transitoires. Préparation d'extraits cellulaires à partir de ces diverses cellules. Immunofluorescence.
Biophysique	Etude structurale de protéines et peptides par dichroïsme circulaire et fluorescence. Caractérisation de l'interaction de protéines ou peptides avec des membranes modèles.
Chimie	Synthèse peptidique sur support solide et synthèse organique.
Langues	Anglais courant, "Certificate of Proficiency of Cambridge in English" obtenu en décembre 2003. Allemand d'un niveau correct.
Enseignement	Enseignement aux étudiants de Master 2 Biologie moléculaire et cellulaire de l'université d'Orléans (2h/an). Co-responsable d'un module de Travaux Pratiques à l'Université de Genève (1 semaine en 2003). Encadrement de Travaux Pratiques au Biozentrum (Bâle, Suisse) 3 fois 1 semaine (2000, 2001, et 2002).
Qualités Humaines	Communications orales et écrites, spécialisées et grand public, en français et en anglais. Membre de la Commission Communication du CBM. Encadrement d'étudiants (Master 2, Master 1, BTS). Co-encadrement d'un thésard (depuis octobre 2016). Membre d'un réseau européen de recherche sur les sphingolipides (EC network on Sphingolipids 2000-2004), associant 8 laboratoires de divers pays européens.

Production scientifique

1 demande d'invention, brevet en cours de rédaction
18 publications parues dans des revues à comité de lecture
15 communications orales dont une conférence plénière
41 communications par affiches

Demande d'invention

Demande d'invention déposée en décembre 2018, brevet en cours de rédaction. *Inhibiteurs des kinases LIMK et/ou ROCK comme anticancéreux agissant sur le cytosquelette.*

Publications

1. **Vallée, B,** Doudeau, M., Godin, F., Benedetti, H., (2019) J Vis Exp, 148, doi: 10.3791/59820.
   Characterization at the Molecular Level using Robust Biochemical Approaches of a New Kinase Protein
2. **Vallée, B.,** Tastet, J., Cuberos, H., Toutain, A., Marouillat, S., Thepault, R.-A., Laumonnier, F., Bonnet-Brilhault, F., Vourc'h, P., Andres, C.R., Benedetti, H. (2019) Neuroscience 399:199-210. doi: 10.1016.
   LIMK2-1 is a hominidae-specific isoform of LIMK2 expressed in central nervous system and associated with intellectual disability
3. **Vallée, B.,** Cuberos, H., Doudeau, M., Godin, F., Gosset, D., Vourc'h, P., Andres, C.R., Bénédetti, H. (2018). Biochem J. 475(23):3745-3761. doi: 10.1042/BCJ20170961.
   LIMK2-1, a new isoform of Human-LIMK2, regulates actin cytoskeleton remodeling via a different signaling pathway than its two homologs, LIMK2a/2b.
4. Cuberos, H**.**, **Vallée B**., Vourc'h, P., Tastet, J., Andres, C.R. and Bénédetti, H. (2016) FEBS Letters *589*, 3795-3806.
   Roles of LIM kinases in central nervous system function and dysfunction.
5. **Vallée, B**., Doudeau, M., Godin, F., Gombault, A., Tchalikian, A., de Tauzia, M.L., and Bénédetti, H. (2012) PLoS One 7(10):e47283.
   Nf1 RasGAP Inhibition of LIMK2 Mediates a New Cross-Talk between Ras and Rho Pathways.
6. Beaufour, M., Godin, F., **Vallée, B**., Cadène, M., and Bénédetti, H. (2012) *J. Proteome Res. 11, 3211–3218*
   Interaction Proteomics Suggests a New Role for the Tfs1 Protein in Yeast.
7. Tastet, J., Vourc'h, P., Laumonnier, F., Vallée, B., Michelle, C., Duittoz, A., Bénédetti, H., and Andres, CR. (2012) *BBRC 420, 247-52*.
   LIMK2d, a truncated isoform of Lim kinase 2 regulates neurite growth in absence of the LIM kinase domain.
8. Godin, F., Villette, S., **Vallée, B.**, Doudeau, M., Morisset-Lopez, S., Ardourel, M., Hevor, T., Pichon, C., and Bénédetti, H. (2012) *BBRC 418*, 689-694.
   A fraction of neurofibromin interacts with PML bodies in the nucleus of the CCF astrocytoma cell line.
9. Gombault, A., Warringer, J., Caesar, R., Godin, F., **Vallée, B**., Doudeau, M., Chautard, H., Blomberg, A., and Benedetti, H (2009) *FEMS Yeast Res. 9*, 867-874.
   A phenotypic study of TFS1 mutants differentially altered in the inhibition of Ira2p or CPY.
10. Gombault, A., Godin, F., Sy, D., Legrand, B., Chautard, H., **Vallée, B**., Vovelle, F., and Benedetti, H. en révision dans *J. Mol. Biol.* (2007) *J. Mol. Biol. 374*, 604-617.
    Molecular basis of the Tfs1/Ira2 interaction: a combined protein engineering and molecular modelling study.
11. **Vallée, B**. and Riezman, H. (2005) *EMBO J. 24*, 730-741.
    Lip1p : a novel subunit of acyl-CoA ceramide synthase.
12. Funato, K., Lombardi, R., **Vallée, B**. and Riezman, H. (2003) *J.Biol. Chem. 278*, 7325-7334.

Lcb4p is a Key Regulator of Ceramide Synthesis from Exogenous Long Chain Sphingoid Base in Saccharomyces cerevisiae.

13. **Vallée, B.,** Coadou, G., Labbé, H., Sy, D., Vovelle, F. and Schoentgen, F. (2003) *J. of Peptide Research 61,* 47-57.
    Peptides corresponding to the N-and C-terminal parts of PEBP are well-structured in solution: new insights into their possible interaction with partners in vivo.
14. **Vallée, B.,** Funato, K. and Riezman, H. (2002) *Biochemistry 41,* 15105-15114.
    Biosynthesis and Trafficking of Sphingolipids in the Yeast Saccharomyces cerevisiae.
15. **Vallée, B.,** Schorling, S., Barz, W.P., Riezman, H. and Oesterhelt, D. (2001) *Mol. Biol. Cell 12*, 3417-27.
    Lag1p and Lac1p Are Essential for the Acyl-CoA-dependent Ceramide Synthase Reaction in Saccharomyces cerevisiae.
16. **Vallée, B.,** Tauc, P., Brochon, J.C., Maget-Dana, R., Lelièvre, D., Metz-Boutigue, M.H., Bureaud, N. and Schoentgen, F. (2001) *Eur. J. Biochem. 268*, 5831-5841.
    Behaviour of bovine phosphatidylethanolamine-binding protein with model membranes.
17. **Vallée, B**., Teyssier, C., Maget-Dana, R., Ramstein, J., Bureaud, N. and Schoentgen, F. (1999) *Eur. J. Biochem. 266*, 40-52.
    Stability and physicochemical properties of the bovine brain phosphatidylethanolamine-binding protein.
18. Serre, L., **Vallée, B**., Bureaud, N., Schoentgen, F. and Zelwer, C. (1998) *Structure 6*, 1255-1265.
    Crystal structure of the phosphatidylethanolamine-binding protein from bovine brain: a novel structural class of phospholipid-binding protein.

Présentations orales

Mai 2019, **Mansigné, France**. Cancéropôle Grand Ouest, Colloque du Réseau Molécules marines, métabolisme et cancer. *Détermination et mise en œuvre d'un modèle in vivo pour tester de nouveaux inhibiteurs originaux des LIM kinases, cibles thérapeutiques émergentes dans le cancer*.

Mai 2018, Mansigné, France. Cancéropôle Grand Ouest, 14ème colloque du Réseau Produits de la mer en cancérologie, 5ème colloque du Réseau Canaux ioniques et cancer. *Développement de modulateurs des LIM kinases*.

Janvier 2018, Orléans, France. Journée Fédération de Recherche Physique et Chimie du Vivant – FR2708. *Développement de petites molécules inhibitrices des LIM kinases, nouvelles cibles thérapeutiques pour lutter contre le cancer, les maladies neurologiques et la neurofibromatose*.

Juin 2017, Cracovie, Pologne. LIA miR Tango. *Neurofibromatosis type I : from basic to applied research.*

Mars 2016, Orléans, France. Séminaire Café équipe Bénédetti au CBM. *Nf1 : un couteau suisse dans la cellule. Multiples cibles thérapeutiques potentielles pour la neurofibromatose de type 1*.

Octobre 2010, Orléans, France. Séminaire interne au CBM. *LIMK2 : le lien manquant entre la neurofibromatose de type I et la dynamique du cytosquelette d'actine.*

Juin 2010. Baltimore, Etats-Unis. 2010 NF Conference. *A new partner of NF1 protein directly connects neurofibromatosis type I to actin cytoskeleton dynamics.*

Avril 2003, Genève, Suisse. Levures, Modèles et outils VI. *Caractérisation de l'activité "céramide synthase" chez la levure Saccharomyces cerevisiae*.

Décembre 2002, Rehovot, Israël. EC network on Sphingolipids. *The ceramide synthase complex in Saccharomyces cerevisiae.*

Septembre 2002, Graz, Autriche. **Conférence plénière** au congrès ICBL-43rd International Conference on the Bioscience of Lipids. *Synthesis, transport and functions of ceramides in the yeast Saccharomyces cerevisiae.*

Mai 2002, Utrecht, Pays-Bas. EC network on Sphingolipids. *Characterisation of the ceramide synthase activity in Saccharomyces cerevisiae.*

Novembre 2001, Heidelberg, Allemagne. EC network on Sphingolipids. *LAG1 and LAC1 are essential for the acyl-CoA-dependent and fumonisin B1 sensitive ceramide synthase activity in Saccharomyces cerevisiae*.

Février 2001, Naples, Italie. EC network on Sphingolipids. *LAG1 and LAC1 are essential for the acyl-CoA-dependent ceramide synthase activity Saccharomyces cerevisiae*.

Janvier 1999, Aussois, France. 11ème réunion Peptides et Protéines. *Propriétés physico-chimiques de la Phosphatidylethanolamine-binding protein extraite du cerveau de bœuf.*

Mai 1997, Orléans, France. Sciences en Sologne. *Etudes structurales et fonctionnelles comparées: la phosphatidylethanolamine-binding protein et ses peptides N- et C-terminaux.*

Présentations orales de Mohammed Bergoug

Juin 2019, Varsovie, Pologne. LIA miR Tango*Neurofibromin a new SUMO target involved in neurofibromatosis type 1 disease.*

Novembre 2018, Paris, France. Joint Global Neurofibromatosis conference. *Neurofibromin a new SUMO target involved in neurofibromatosis type 1 disease*.

Communications écrites - Posters

The ubiquitin system: Biology, mechanisms and roles in disease. Septembre 2019. Cavtat, Croatie.

Mohammed Bergoug, Iva Sošić, Michel Doudeau, Fabienne Godin, Béatrice Vallée, Hélène Bénédetti. "Neurofibromin, a new SUMO target involved in neurofibromatosis type1 disease".

Hélène Bénédetti, Mohammed Bergoug, Iva Sošić, Fabienne Godin, Michel Doudeau, Béatrice Vallée. "Study of the different forms of sumoylation of the neurofibromin SecPH domain".

ICYGMB XXIX International Congress on Yeast Genetics and Molecular Biology. Août 2019. Göteborg, Suède.

Christine Mosrin, Bilal Handelaoui, Hélène Bénédetti, Régis Guégan, and Béatrice Vallée. "Yeast Biosensors To Detect Environmental Pollutants Into Effluent Waters."

FEBS Meeting. Juillet 2019. Cracovie, Pologne.

Béatrice Vallée, Aurélie Cosson, Michel Doudeau, Fabienne Godin, Anthony Champiré, Thomas Lelièvre, Karen Plé, Abdennour Braka, Samia Aci-Sèche, Stéphane Bourg, Norbert Garnier, Pascal Bonnet, Sylvain Routier, and Hélène Bénédetti. LIM kinases, new therapeutic targets to treat cancers, neurological disorders and Neurofibromatosis: development of small molecule inhibitors.

Joint Global Neurofibromatosis conference. Novembre 2018. Paris.

Beatrice Vallee, Aurelie Cosson, Michel Doudeau, Fabienne Godin, Anthony Champire, Thomas Lelievre, Karen Ple, Abdennour Braka, Samia Aci Seche, Stephane Bourg, Norbert Garnier, Pascal Bonnet, Sylvain Routier, Helene Benedetti. *Development of small molecule inhibitors of LIM kinases, new therapeutic targets to treat Neurofibromatosis type I*

Helene Benedetti, Michel Doudeau, Fabienne Godin, Beatrice Vallee, Aurelie Cosson, Mohammed Bergoug. *LARP6, a RNA-binding protein involved in translation and stability of collagen mRNA, is a new partner of Neurofibromin (Nf1): Molecular studies and functional implications*

Biotechnocentre. Novembre 2018. Seillac, France. Mohammed Bergoug, Aurélie Cosson, Michel Doudeau, Fabienne Godin, Béatrice Vallée, Hélène Bénédetti. *Neurofibromin, a new SUMO target involved in neurofibromatosis type1 disease*

LIA miR Tango. Mai 2018. Orléans, France. Mohammed Bergoug, Aurélie Cosson, Michel Doudeau, Fabienne Godin, Béatrice Vallée, Hélène Bénédetti. *Neurofibromin, a new SUMO target involved in neurofibromatosis type1 disease*

Biotechnocentre. Novembre 2017. Seillac, France. Mohammed Bergoug, Aurélie Cosson, Michel Doudeau, Fabienne Godin, Béatrice Vallée, Hélène Bénédetti. *Study of the sumoylation of neurofibromin, the protein responsible for neurofibromatosis type1*

EMBO Conference, Ubiquitin and SUMO: From molecular mechanisms to system-wide responses. Septembre 2017. Cavtat-Dubrovnik, Croatie. Mohammed Bergoug, Aurélie Cosson, Michel Doudeau, Fabienne Godin, Béatrice Vallée, Hélène Bénédetti. *Study of the sumoylation of neurofibromin, the protein responsible for neurofibromatosis type1*

VII International Symposium on Advances in Synthetic and Medicinal Chemistry (EFMC). Août 2017. Vienne, Autriche. Anthony Champiré, Abdennour Braka, Béatrice Vallée, Michel Doudeau, Fabienne Godin, Karen Plé, Samia Aci-Sèche, Stéphane Bourg, Norbert Garnier, Hélène Cubéros, Sylviane Marouillat, Rose-Anne Thepault, Patrick Vour'ch, Christian Andrès, Pierre Castelnau, Pascal Bonnet, Sylvain Routier, Hélène Bénédetti. *LIM kinases as new therapeutic targets for the treatment of neurofibromatosis type 1*

Journée Jeunes Chercheurs SCT. Février 2017. Châtenay-Malabry, (France). Anthony Champiré, Abdennour Braka, Béatrice Vallée, Michel Doudeau, Fabienne Godin, Karen Plé, Samia Aci-Sèche, Stéphane Bourg, Norbert Garnier, Hélène Cubéros, Sylviane Marouillat, Rose-Anne Thepault, Patrick Vour'ch, Christian Andrès, Pierre Castelnau, Pascal Bonnet, Sylvain Routier, Hélène Bénédetti. *Design, synthesis and biological evaluation of LIMK inhibitors*

EMBO meeting. Septembre 2016. Mannheim, Allemagne. Béatrice Vallée, Michel Doudeau, Fabienne Godin, Anthony Champiré, Karen Plé, Abdennour Braka, Samia Aci-Sèche, Stéphane Bourg, Hélène Cubéros, Sylviane Marouillat, Rose-Anne Thepault, Patrick Vour'ch, Christian Andrès, Pierre Castelnau, Pascal Bonnet, Sylvain Routier, and Hélène Bénédetti. *LIM kinases: new therapeutic targets to treat Neurofibromatosis type I*

EMBL Symposium: Actin in action: From Molecules to Cellular Functions. Septembre 2016. Heidelberg, Allemagne. Béatrice Vallée, Hélène Cubéros, Michel Doudeau, Fabienne Godin, Patrick Vourc'h, Christian Andres and Hélène Bénédetti. *The three isoforms of human LIMK2 regulate actin cytoskeleton remodeling via different pathways*

10th FENS (Federation of European Neurosciences Societies). Juillet 2016. Copenhague, Danemark.

Béatrice Vallée, Hélène Cubéros, Julie Tastet, Michel Doudeau, Fabienne Godin, Patrick Vourc'h, Christian Andres and Hélène Bénédetti. *LIMK2-1, a new primate-specific isoform of LIMK2, is associated with intellectual disability.*

Hélène Bénédetti, Fabienne Godin, Michel Doudeau, Béatrice Vallée, Marie-Ludivine de Tauzia, Laëtitia Cobret, and Séverine Morisset. *LINGO-1, a protein involved in various neurodevelopmental processes, interacts with neurofibromin (Nf1), the protein responsible for neurofibromatosis type I: molecular studies and functional implications*

Journée Fédération ICOA-CBM. Janvier 2016. Orléans. France. Béatrice Vallée, Michel Doudeau, Fabienne Godin, Hélène Cubéros, Anthony Champiré, Karen Plé, Abdennour Braka, Samia Aci-Sèche, Stéphane Bourg, Hélène Cubéros, Sylviane Marouillat, Rose-Anne Thepault, Patrick Vour'ch, Christian Andres, Pierre Castelnau, Pascal Bonnet, Sylvain Routier, et Hélène Bénédetti. *Projet Région LiCorNe: LIMK protein inhibitors, new therapeutic agents for treatment of cognitive disorders associated with type I Neurofibromatosis*

EMBO Conference "Neural Development. Décembre 2015. Taipei. Taïwan. Hélène Bénédetti, Hélène Cubéros, Béatrice Vallée, Julie Tastet, Michel Doudeau, Fabienne Godin, Patrick Vourc'h, and Christian Andres. *LIMK2-1, a primate-specific isoform of LIMK2 associated with intellectual disability: molecular and functional characterization.*

Nf conference 2015. Juin 2015. Monterey, Etats-Unis. Fabienne Godin, Marie-Ludivine de Tauzia, Séverine Morisset, Béatrice Vallée; Michel Doudeau, Hélène Bénédetti. *Lingo1, a protein involved in various neurodevelopmental processes, is a new partner of Neurofibromin (Nf1): Molecular studies and functional implications.*

Conférence Jacques Monod "Actin and microtubule cytoskeleton in cell motility and morphogenesis: an integrative view". Mai 2015. Roscoff. France. Béatrice Vallée, Michel Doudeau, Fabienne Godin, Kevin Lesage, Mélissa Thomas, Hélène Cubéros, Patrick Vourc'h, Christian Andres, and Hélène Bénédetti. *LIMK2: a new molecular link between Neurofibromatosis type I and actin cytoskeleton dynamics.*

16th European Neurofibromatosis Meeting. Septembre 2014. Barcelone, Espagne. Hélène Bénédetti, Béatrice Vallée, Michel Doudeau, Fabienne Godin, Hélène Henrie, Kevin Lesage, Reine Néhmé. *LIM kinases: new therapeutic targets for NF1 treatment*

FENS-Forum of neurosciences. Juillet 2014. Milan, Italie. Hélène Cuberos, Julie Tastet, Patrick Vourc'h, Marie-Ludivine de Tauzia, Annick Toutain, Martine Raynault, Rose-Anne Thepault, Frédéric Laumonnier, Frédérique Bonnet-Brilhault, Béatrice Vallée, Hélène. Bénédetti, Christian Andres. *A primate specific isoform of Lim Kinase 2, LIMK2-1, is implicated in the regulation of neurite outgrowth and intellectual disability.*

Journée Fédération ICOA-CBM. Juin 2014. Orléans, France. Hélène Henrie, Béatrice Vallée, Elodie Sevestre, Michel Doudeau, Racha El-Debs, Hélène Cuberos, Fabienne Godin, Phillipe Morin, Bérengère Claude, Sylvain Routier, Reine Nehmé, et Hélène Bénédetti. *Développement de protocoles pour étudier les inhibiteurs des LIM kinases par électrophorèse capillaire et évaluation de leurs effets cellulaires*

EMBO Meeting. Septembre 2013. Amsterdam, Pays-Bas. Béatrice Vallée, Michel Doudeau, Fabienne Godin, Aurélie Gombault, Aurélie Tchalikian, Marie-Ludivine De Tauzia, Hélène Bénédetti. *A new cross-talk between Ras and Rho signaling pathways is mediated via the inhibition of LIMK2 by the Ras GAP Nf1*.

JFSM. Septembre 2012. Orléans, France. Martine Beaufour, Fabienne Godin, Béatrice Vallée, Hélène Bénédetti, and Martine Cadène. *Interaction proteomics suggests a new role for the Tfs1 protein in the general stress response in yeast.*

EMBO Meeting. Septembre 2011. Vienne, Autriche. Béatrice Vallée, Michel Doudeau, Fabienne Godin, Aurélie Gombault, Aurélie Tchalikian, Marie-Ludivine de Tauzia, and Hélène Bénédetti. *Neurofibromin, a GTPase activating protein of Ras, connects Ras to the actin cytoskeleton dynamics by inhibiting LIMK2*

2011 NF Conference. Juin 2011. Jackson Hole, Wyoming, Etats-Unis. Béatrice Vallée, Michel Doudeau, Fabienne Godin, Aurélie Gombault, Aurélie Tchalikian, Marie-Ludivine de Tauzia, and Hélène Bénédetti. *LIMK2, a new partner of Nf1 protein, directly connects neurofibromatosis type I to actin cytoskeleton dynamics*

NF European Conference. Septembre 2010. Oslo, Norvège.

Béatrice Vallée, Michel Doudeau, Fabienne Godin, Tobias Hevor, Aurélie Gombault, Aurélie Tchalikian, Marie-Ludivine de Tauzia, Hélène Bénédetti. *LIMK2, a new partner of NF1 protein, directly connects neurofibromatosis type I to actin cytoskeleton dynamics.*

Fabienne Godin, Sandrine Villette, Béatrice Vallée, Michel Doudeau, Tobias Hevor, Séverine Morisset-Lopez, Chantal Pichon, Hélène Bénédetti. *Neurofibromin partially colocalizes with PML bodies and splicing speckles in the nucleus of the CCF astrocytoma cell line.*

2009 NF Conference. Juin 2009. Portland, Etats-Unis. Fabienne Godin, Sandrine Villette, Béatrice Vallée, Michel Doudeau, Chantal Pichon, Jean-Vianney Barnier, Tobias Hévor, Aurélie Gombault, and Hélène Bénédetti. *NF1 and RKIP (Raf kinase inhibitor protein) are partially co-localized in the nucleus of astrocytes.*

Congrès Levures, Modèles et Outils VIII. Octobre 2008. La Colle sur Loup, France.

Béatrice Vallée, Aurélie Gombault, Michel Doudeau, Fabienne Godin, et Hélène Bénédetti. *Tfs1p, un maillon clef dans le rétro-contrôle négatif de la réponse au stress thermique de la voie Ras/AMPc/PKA chez la levure Saccharomyces cerevisiae.*

Aurélie Gombault, Béatrice Vallée, Fabienne Godin, Aurélie Tchalikian, Sandrine Villette, Michel Doudeau et Hélène Bénédetti. *La levure outil modèle pour étudier la neurofibromatose de type 1.*

Congrès Levures, Modèles et outils VII. Septembre 2006. Paris, France. Gombault, A., Vallée, B., Godin, F., Barnier, J.-V. et Bénédetti, H. *Nouveaux modes de régulation des protéines Ras chez la levure. Transposition chez l'homme.*

Gordon conference "Molecular and Cellular biology of Lipids". Juillet 2003. Meriden, NH, United States. Vallée, B. and Riezman, H. *Characterisation of the ceramide synthase activity in S. cerevisiae.*

ICBL-43rd International Conference on the Bioscience of Lipids. Graz, Autriche. **Septembre 2002.** Vallée, B**.** and Riezman, H. *Characterisation of the ceramide synthase activity in S. cerevisiae.*

ELSO Meeting. Juin 2002. Nice, France. Vallée, B. and Riezman, H. *The ceramide synthase complex in Saccharomyces cerevisiae.*

"MAP kinases, a nexus for mediating cellular functions". Novembre 2001. Paris, France. Vallée, B., Bénédetti, H., Serre, L., Zelwer, C. and Schoentgen, F. *Phosphatidylethanolamine-binding protein: a new type of MAP-kinase inhibitor.*

Euroconference on microdomains, lipids rafts and caveolae. Mai 2001. San Feliu de Guixols, Espagne. Vallée, B., Schorling, S., Oesterhelt, D. and Riezman, H. *LAG1 and LAC1 are essential for the acyl-CoA-dependent ceramide synthase activity Saccharomyces cerevisiae.*

Fourth European Symposium of The Protein Society. Avril 2001. Paris, France. Vallée, B., Maget-Dana, R. ,Sy. D., Vovelle, F., Serre, L., Zelwer, C., Bureaud, N. and Schoentgen, F. *Phosphatidylethanolamine-binding protein : a new type of scaffolding protein?*

"Synthesis and Trafficking of Glycolipids and Glycolipid Anchored Proteins". Mars 2001. Les Diablerets, Suisse. Vallée, B., Schorling, S., Oesterhelt, D. and Riezman, H. *LAG1 and LAC1 are essential for the acyl-CoA-dependent ceramide synthase activity Saccharomyces cerevisiae.*

3ème colloque du groupe thématique "phosphorylation des protéines". Octobre 2000. Saint-Malo, France. Vallée, B., Bureaud, N., Maget-Dana, R., Sy, D., Vovelle, F., Serre, L., Zelwer, C. and Schoentgen, F. *La "phosphatidylethanolamine-binding protein" (PEBP) intervient dans la signalisation cellulaire en reconnaissant des protéines phosphorylées.*

8ème GEIMM. Octobre 1998. Anglet-Biarritz, France. Vallée, B., Maget-Dana, R., Lelièvre, D.and Schoentgen, F. *Interaction de la Phosphatidylethanolamine-binding protein avec des membranes modèles.*

AFC 98. Février 1998. Orléans, France. Vallée, B., Serre, L., Schoentgen, F. and Zelwer, C. *Cristallisation de la Phosphatidylethanolamine-binding protein extraite du cerveau de bœuf.*

2nd EBSA (European Biophysics Congress). Juillet 1997. Orléans, France. Maget-Dana, R., Vallée, B., Lelièvre, D.and Schoentgen, F. *Bovine Brain cytosolic 21 kDa protein: adsorption kinetics at the air/water interface and penetration into phospholipid monolayers.*

Encadrement d'étudiants

Depuis octobre 2016	Co-encadrement de la thèse de Mohammed Bergoug. ***Etude de la SUMOylation de la Neurofibromine.***
2015-2018	Supervision de la thèse d'Anthony Champiré
2013-2016	Supervision de la thèse d'Hélène Cuberos
2008-2012	Supervision de la thèse de Julie Tastet
2004-2008	Supervision de la thèse d'Aurélie Gombault
2020	Encadrement du stage de Master 2 de Célina Chalal
2019	Encadrement de Janusz Koszucki (3 semaines) lors de son Master 2 dans le cadre de la collaboration du LIA miR TANGO (Pologne)
2018	Encadrement du stage de Master 2 de Déborah Cassas (6 mois)
2016	Encadrement du stage de Master 2 de Lauren Blot (5 mois)
2015	Encadrement du stage de Master 2 de Mélissa Thomas (5 mois)
2014	Encadrement du stage de Master 2 de Kevin Lesage (5 mois)
2014	Supervision du stage de Master 2 de Hélène Henrie (5 mois)
2010	Encadrement du stage de Master 2 de Morgane Placet (5 mois)

Enseignement

2018 et 2019	2h/an aux étudiants de Master 2 Biologie Moléculaire et Cellulaire de l'Université d'Orléans
2003	Co-responsable d'un module de Travaux Pratiques à l'Université de Genève, Suisse, niveau Master 1, (1 semaine)
2000-2002	Encadrement de Travaux Pratiques au Biozentrum, Université de Bâle, Suisse, niveau Master 1, (3 x 1 semaine)

Diffusion de la culture scientifique

Participation récurrente à la Fête de la Science, accueil de stagiaires, membre de la cellule communication du CBM.

Financements

2020-2024	Financement ANR. *First pre-clinical validation of LIMK/ROCK inhibitors for the treatment of Neurofibromatosis Type 1*. Porteure: Karen Plé (ICOA, Orléans). 42 mois.
2019-2021	Financement Prématuration CNRS. *Validation préclinique d'inhibiteurs de LIMK dans le cancer*. Porteurs : Hélène Bénédetti et Sylvain Routier. 18 mois
2019-2020	Financement ARD2020 Cosmétosciences LYMFLU. *Développement de sondes fluorescentes pour l'identification d'actifs restaurant le tonus du système lymphatique.* Porteur : Sylvain Routier (ICAO, Orléans). 1 an.

Depuis 2015	Financement de trois projets par la Région Centre-Val de Loire. *MONITOPOL : Suivi de polluants des cours d'eau par des bio-capteurs à base de matériaux lamellaires et levures.* Porteur : Régis Guégan (ISTO, Orléans). 2018-2020. *FLUPO : Optimisation structurale et validation de sondes pour la sécurité d'actifs cosmétiques.* Porteur : Sylvain Routier (ICOA, Orléans). 2016-2018. *LiCoRNe : Développement de nouveaux médicaments potentiels contre la neurofibromatose de type I.* Porteure : Hélène Bénédetti. 2015-2017.
2018-2019	Financement ARSLA. *ILIADE : Evaluation de nouveaux inhibiteurs de LIMK1 et LIMK2, kinases de la voie des Rho-GTPases, dans un modèle murin de la Sclérose Latérale Amyotrophique*. Porteure : Hélène Bénédetti.
2013-2018	Financement ANR en tant que partenaire. *ChaDock : Cinétique des inhibiteurs de protéines kinases et Affinité par Docking flexible.* Porteure : Samia Aci−Sèche (Equipe Modélisation, ICOA - Orléans).
Depuis 2012	Financements récurrents de l'Association Neurofibromatoses et Recklinghausen
2018, 2017, 2008-2015	Financements de la Ligue contre le Cancer

Collaborations

Sylvain Routier, Karen Plé	Chimie Médicinale, ICOA, Orléans
Pascal Bonnet, Samia Aci-Sèche	Modélisation, ICOA, Orléans
Christian Andres, Patrick Vourc'h	iBrain – Neurogénétique et Physiopatologie neuronale, U1253, Tours
Sandrine Ruchaud	Phosphorylation des protéines et pathologies humaines, UMR8227, Roscoff
Franck Verrecchia	Sarcomes osseux et remodelage des tissus calcifiés, UMR1238, Nantes
Michal Sarna	Département de Biophysique, Jagiellonian University, Cracovie, Pologne
Régis Guégan	ISTO, Orléans et Université de Waseda, Tokyo, Japon

II. ACTIVITÉS DE RECHERCHE ANTÉRIEURES

1. Travaux de thèse

J'ai réalisé ma thèse au Centre de Biophysique Moléculaire de 1996 à 1999 sous la direction du Dr Françoise Schœntgen. Mon sujet portait sur l'étude structurale et fonctionnelle d'une protéine, la Phosphatidyléthanolamine Binding Protein, PEBP, extraite du cerveau de bœuf.

La Phosphatidylethanolamine-binding protein (PEBP) est une protéine cytosolique de 21 kDa extraite du cerveau de bœuf. Elle avait été initialement caractérisée par son affinité vis-à-vis des phospholipides, et plus particulièrement de la phosphatidyléthanolamine (Bernier and Jolles, 1984). La PEBP bovine appartient à une famille de protéines largement répandues à travers de nombreuses espèces. Plusieurs rôles avaient été suggérés pour ces protéines. Chez les mammifères, la PEBP semblait impliquée dans la morphogenèse et le développement des cellules, mais à cette époque sa fonction restait énigmatique.

Mon travail de thèse a consisté à mieux caractériser cette protéine dans le but de découvrir son ou ses rôles biologiques.

Tout d'abord, en collaboration avec l'équipe de Charles Zelwer au CBM, j'ai contribué à la résolution de la structure tridimensionnelle de la PEBP par cristallographie aux Rayons X. Un repliement atypique et nouveau de cette protéine a été mis à jour, qui ne permettait de l'apparenter à aucune famille de protéines alors connue : la PEBP définissait donc une nouvelle famille structurale de protéines (Figure 1). Un site de fixation de petits ligands, en particulier de la tête polaire de la phosphatidyléthanolamine, a aussi été mis à jour proche de la surface et accessible (Serre et al., 1998).

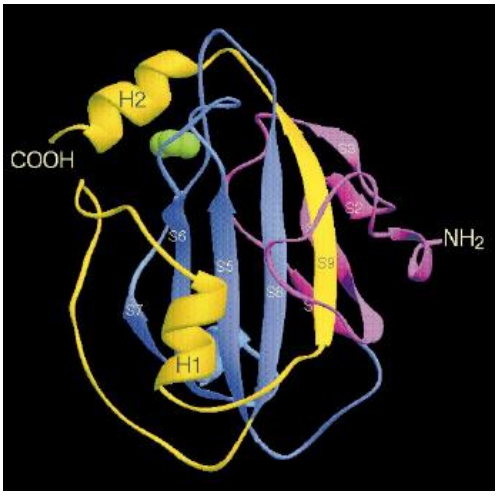

Figure 1 : Structure tridimensionnelle de la PEBP bovine (Serre et al., 1998)

J'ai ensuite déterminé les propriétés physicochimiques et la stabilité de la PEBP par différentes techniques biophysiques de dichroïsme circulaire, fluorescence, infra-rouge, et microcalorimétrie. J'ai montré que la conformation de cette protéine est peu stable et sensible aux conditions hydrophobes, suggérant une certaine flexibilité et adaptabilité de cette dernière (Vallee et al., 1999).

J'ai aussi étudié son interaction avec des membranes modèles en collaboration avec Jean-Claude Brochon et Patrick Tauc, à l'ENS de Cachan. J'ai alors mis à jour le rôle des extrémités N- et C-terminales de la PEBP dans son interaction avec des membranes anioniques (Vallee et al., 2001b).

Enfin, j'ai caractérisé plus avant le rôle de ses extrémités N et C-terminales dans d'éventuelles nouvelles interactions *in vivo* (Vallee et al., 2003).

Mes travaux de thèse m'ont permis d'aborder de nombreuses techniques de biophysique (Dichroïsme circulaire, Fluorescence, microcalorimétrie), de biochimie (purification de protéines, Western Blot, cristallogenèse) et de biologie moléculaire (clonage, mutagenèse dirigée) et de collaborer avec plusieurs équipes.

2. Stage Post-doctoral

J'ai ensuite effectué un stage post-doctoral de 2000 à 2003 dans l'équipe du Professeur Howard Riezman, au Biozentrum à l'Université de Bâle puis à Sciences II à l'Université de Genève en Suisse.

J'ai alors étudié la synthèse des sphingolipides chez la levure *Saccharomyces cerevisiae* (Funato et al., 2003; Funato et al., 2002). Les sphingolipides jouent un rôle clé dans de nombreux processus, tel que la transduction du signal, la réponse au choc thermique, l'homéostasie du calcium, et le trafic membranaire. Ils sont aussi impliqués dans des pathologies, telles les maladies de Gaucher et de Niemann-Pick.

Les sphingolipides sont des lipides complexes et très particuliers, formés par une liaison amide entre un amino-alcool (sphingosine) et un acide gras. Leur voie de synthèse n'était pas totalement élucidée au début des années 2000.

Au cours de mon stage post-doctoral, j'ai isolé le complexe enzymatique de synthèse des céramides, un intermédiaire clé dans la vie métabolique des sphingolipides. Ce complexe est

membranaire et localisé au niveau du réticulum endoplasmique. J'ai tout d'abord caractérisé les protéines Lac1p et Lag1p (Vallee et al., 2001a). J'ai ensuite mis à jour et caractérisé une nouvelle protéine, Lip1p, impliquée dans la synthèse des céramides (Figure 2) (Vallee and Riezman, 2005).

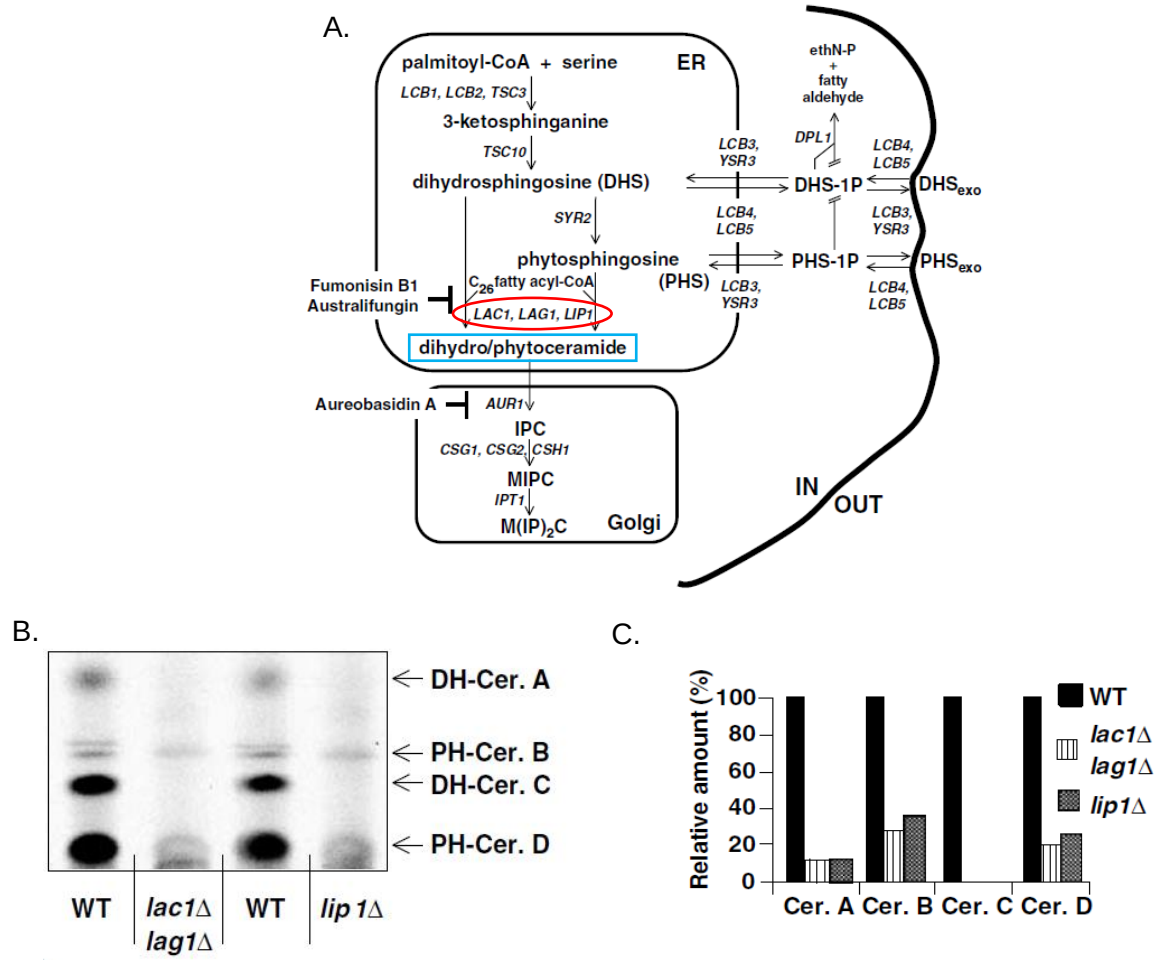

Figure 2 : Les protéines Lac1p, Lag1p et Lip1p sont impliquées dans la synthèse des céramides (Vallee and Riezman, 2005; Vallee et al., 2001a). A. Voie métabolique des sphingolipides. B. Séparation par chromatographie sur couche mince des céramides extraits de levure sauvage ou mutée après marquage au [^{3}H]-DHS. Quantification des céramides de la figure B.

J'ai acquis de solides compétences dans les domaines de la génétique de la levure, de la biologie moléculaire et de la biochimie tant des lipides que des protéines et complexes protéiques membranaires. Cette expérience m'a aussi permis d'évoluer dans un cadre de recherche international au quotidien et de faire partie d'un réseau européen de recherche.

3. Travaux de chargée de recherche au CBM

Fin 2003, j'ai été recrutée au Centre de Biophysique Moléculaire dans l'équipe d'Hélène Bénédetti, qui travaillait alors sur les PEBPs (Phosphatidyléthanolamine Binding Proteins) de la levure *Saccharomyces cerevisiae*, Tfs1p et Ylr179c.

A cette époque, le rôle des PEBPs de levure, Tfs1p et Ylr179cp, était assez obscur. Tfs1p avait été décrite comme inhibant la carboxypeptidase Y (Bruun et al., 1998), rien n'était connu sur Ylr179cp. L'objectif était donc d'en savoir plus sur ces protéines en combinant des approches de génétique de la levure, de modélisation moléculaire, de biologie moléculaire et de biochimie. Par un crible double hybride, l'équipe d'Hélène avait mis à jour une interaction entre la PEBP de levure Tfs1p et la RasGAP (GTPase Activating Protein) Ira2p (Chautard et al., 2004). Cependant, Ylr179cp, homologue de Tfs1p, n'interagit pas avec Ira2p. Notre premier objectif a été de mettre à jour les déterminants moléculaires nécessaires à l'interaction entre Tfs1p et Ira2p. La structure tridimensionnelle de Tfs1p en complexe avec la carboxypeptidase CPY était connue (Mima et al., 2005). La structure tridimensionnelle de Ylr179cp a alors été modélisée à partir de celle de Tfs1p, des protéines chimères entre Tfs1p et Ylr179cp ont aussi été modélisées. Ces protéines ont été surproduites dans la levure et leur activité a été testée. Trois éléments de la structure de Tfs1p jouant un rôle clé dans son interaction avec Ira2p ont été mis en évidence : (i) l'accessibilité d'une poche en surface, (ii) sa région N-terminale et (iii) des propriétés électrostatiques particulières sur une large zone de surface comprenant ces deux zones (Gombault et al., 2007).

Ensuite, nous avons réalisé une étude phénotypique de Tfs1p basée sur des mutants interagissant et inhibant spécifiquement soit CPY, soit Ira2p. Ce travail a été réalisé en collaboration avec Anders Blomberg, de l'université de Göteborg en Suède. Nous avons montré que : (i) l'acétylation N-terminale de Tfs1p est requise pour inhiber CPY, mais pas pour inhiber Ira2p, (ii) la poche d'interaction en surface de Tfs1p est requise pour inhiber Ira2p mais pas CPY, (iii) l'inhibition de Ira2p par Tfs1p semble prépondérante dans les conditions testées dans notre étude (Gombault et al., 2009).

Nous avons aussi réalisé des études de protéomique pour en savoir plus sur Tfs1p, en collaboration avec l'équipe de Martine Cadène au CBM. 14 nouveaux partenaires de Tfs1p ont été identifiés suggérant un rôle de Tfs1p dans le métabolisme intermédiaire et mettant à jour la régulation par Tfs1p d'une nouvelle protéine GAP, Glo3p, une GAP des petites protéines G

Arf. Tfs1p serait donc un nœud de coordination entre la transduction du signal et le métabolisme des levures (Figure 3) (Beaufour et al., 2012).

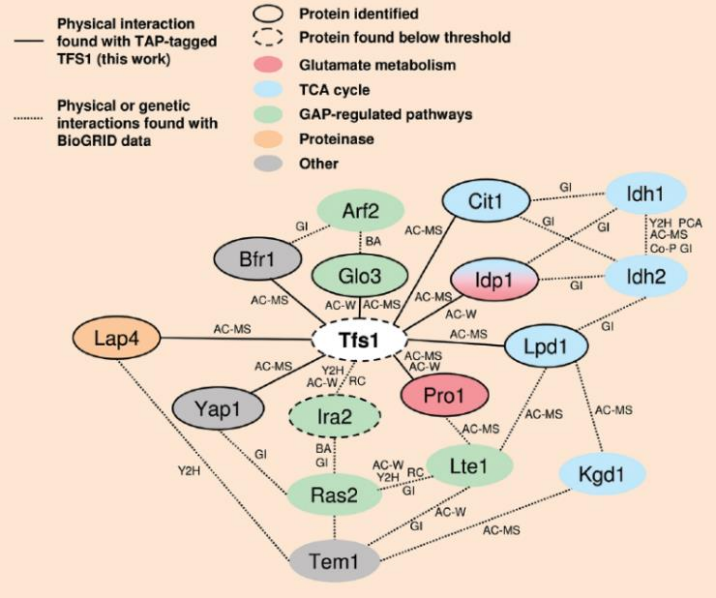

Figure 3 : Réseau d'interaction de Tfs1p (Beaufour et al., 2012)

Progressivement et parallèlement à ces études sur les PEBPs de levure, nous avons commencé à nous intéresser aux eucaryotes supérieurs. En effet, l'homologue humain de Ira2p est Nf1, la neurofibromine, protéine codée par le gène *NF1*, qui est responsable de la Neurofibromatose de type I. La Neurofibromatose de type I est une maladie génétique hautement prévalente, peu étudiée d'un point de vue moléculaire, et dont il n'existe aucun traitement.

Dans un premier temps, nous avons essayé de mettre en évidence une interaction entre Nf1 et l'une des PEBPs humaines, en vain !

En 2007, nous avons réalisé un crible double-hybride afin de rechercher de façon systématique de nouveaux partenaires de Nf1. Ce crible double-hybride a été très efficace, et nous avons pu identifier 20 nouveaux partenaires de Nf1. J'ai choisi de me concentrer sur l'un d'entre eux, qui me paraissait particulièrement intéressant : LIMK2.

Depuis 2008, mes travaux se concentrent sur Nf1 et LIMK2.

III. ACTIVITÉS DE RECHERCHE ACTUELLES ET FUTURES

1. Introduction

1. *La neurofibromatose de Type I*

La neurofibromatose de type I ou maladie de von Recklinghausen est une maladie monogénétique autosomale dominante très fréquente. Elle touche 1 individu sur 3500, ce qui en fait la deuxième maladie génétique en France après la mucoviscidose (Wolkenstein, 2001). Cette maladie est évolutive et son expression clinique est très variable. Elle se manifeste par des taches café au lait et par des tumeurs qui se développent au niveau du système nerveux central (gliomes, astrocytomes) ou périphérique (neurofibromes cutanés et plexiformes). 20% des neurofibromes cutanés peuvent devenir très invasifs et dégénérer en cancers (MPNST : Malignant Peripheral Nerve Sheath Tumors) dont l'issue est rapidement fatale. Des problèmes osseux, de l'hypertension artérielle et pulmonaire ainsi que des nodules de Lisch au niveau des yeux sont aussi répertoriés. Des troubles cognitifs sont souvent associés à cette maladie (50 à 70% des cas).

Le gène responsable de cette maladie a été identifié en 1987. Il s'agit de *NF1*, qui code pour la neurofibromine, Nf1. *NF1* est un gène suppresseur de tumeurs. *NF1*, très grand gène de plus de 300kb, est un des gènes dont le taux de mutation spontanée est un des plus importants chez l'homme : des néomutations sont observées pour la moitié des malades. Il n'y a pas de « point chaud » de mutation, et une même mutation peut conduire à des phénotypes très différents, bénins comme très graves.

Si la neurofibromatose est bien caractérisée d'un point de vue phénotype et génotype, peu d'études concernant les bases moléculaires de cette maladie sont menées. De par le monde, on compte seulement une dizaine de groupes travaillant sur ces aspects moléculaires. De plus, actuellement, il n'existe aucun traitement pour traiter cette maladie (autres que des traitements symptomatiques).

Mettre à jour les différentes fonctions de Nf1 ainsi que sa régulation constitue donc un enjeu majeur pour lutter contre la neurofibromatose en vue de développer de nouvelles thérapies ciblées.

2. *Recherche systématique de nouveaux partenaires de Nf1 : crible double-hybride*

Afin de mettre à jour de nouvelles fonctions et régulation de Nf1, nous avons décidé de rechercher de façon systématique de nouveaux partenaires de Nf1. Pour cela, en 2007, nous avons réalisé un crible double-hybride chez la levure *Saccharomyces cerevisiae*.

Nf1 étant une grosse protéine de 320 kDa, il nous a fallu choisir un domaine de taille raisonnable pour réaliser ce crible double-hybride. Nf1 est constituée de plusieurs domaines dont le domaine GAP (GTPase Activating Domain), seule activité catalytique connue de Nf1 (voir Figure 4). Un autre domaine a retenu notre attention, le domaine SecPH.

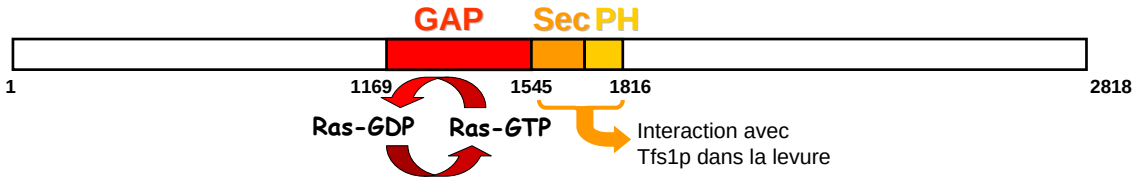

Figure 4 : Les domaines GAP et SecPH de Nf1.

Le domaine SecPH est adjacent au domaine GAP, il pourrait donc le réguler. Il est constitué de deux motifs d'interaction protéine-protéine : Sec (homologue de Sec14p chez la levure) et PH (Pleckstrin Homolog). Ce domaine SecPH a été cristallisé : il possède une structure intrinsèque (D'Angelo et al., 2006) (Figure 5).

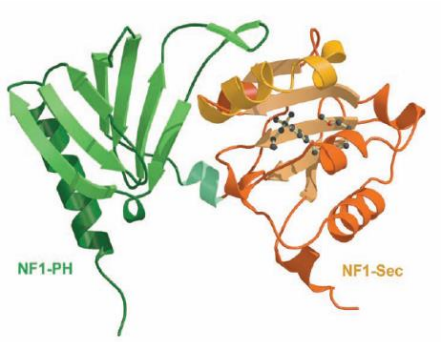

Figure 5 : Structure du domaine SecPH de Nf1 obtenue par cristallographie aux rayons X (D'Angelo et al., 2006).

Ces différentes données nous ont donc suggéré que le domaine SecPH pourrait médier des interactions protéine-protéine. C'est pourquoi notre équipe a réalisé un criblage double hybride en utilisant SecPH comme appât et une banque d'ADNc de cerveau humain comme proie. Ce criblage a été particulièrement réussi puisque 1464 clones positifs ont été isolés. A ce jour, 173 clones ont été séquencés permettant d'identifier 20 cibles différentes.

Je m'intéresse tout particulièrement à l'une de ces cibles : LIMK2.

3. *Présentation de LIMK2, et de son homologue LIMK1*

LIMK2 est une sérine/thréonine et tyrosine kinase appartenant à la famille des LIM-protéines. Les motifs LIM sont des structures très conservées, riches en cystéines et contenant 2 doigts de zinc. Bien que les doigts de zinc lient habituellement l'ADN ou l'ARN, les motifs LIM seraient plutôt impliqués dans des interactions protéine-protéine (Scott and Olson, 2007).

LIMK2 a un unique homologue, LIMK1. LIMK1 et LIMK2 constituent la famille des LIM-kinases. Ces deux protéines sont identiques à 50%.

Chez l'homme, trois isoformes de LIMK2 sont répertoriées dans les banques de données, elles sont issues d'épissages alternatifs. Ces trois isoformes sont schématisées Figure 6. Elles sont strictement identiques en leur partie centrale avec un domaine PDZ, un domaine S/P (Serine Proline Rich) et un domaine kinase. Par contre, elles diffèrent en leurs extrémités. Les isoformes 1 et 2b ont des extrémités N-terminales identiques avec un premier domaine LIM tronqué. L'isoforme 2-1 possède en son extrémité C-terminale un domaine supplémentaire PP1i (Protein Phosphatase 1 inhibitor), identifié par homologie de séquence.

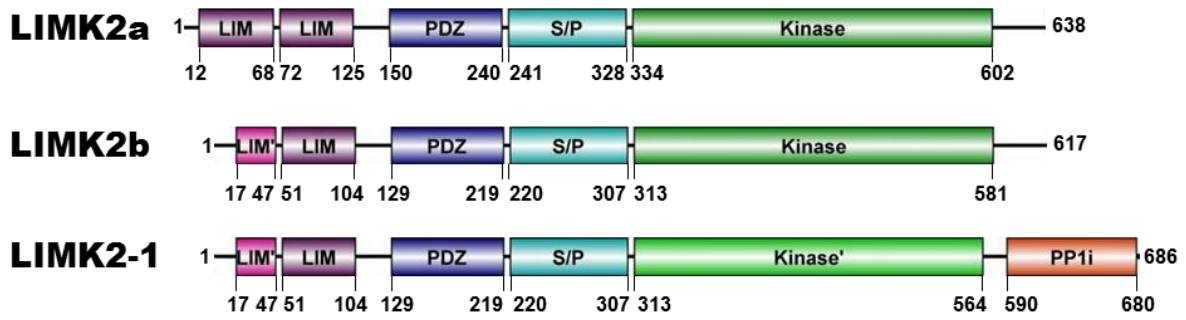

Figure 6 : Alignement des trois isoformes de LIMK2.
Références Entrez Gene des ces isoformes :
LIMK2-1 (NP_001026971.1), LIMK2-2a (NP_005560.1), LIMK2-2b (NP_057952.1).

LIMK2 et LIMK1 jouent des rôles clés dans la dynamique du cytosquelette en régulant indépendamment le remodelage des filaments d'actine et des microtubules (Figure 7). Le mécanisme moléculaire de leur implication dans le remaniement des filaments d'actine est connu : les LIMKs inhibent la cofiline en la phosphorylant. Or, la cofiline est un facteur de dépolymérisation de l'actine. Lorsqu'elle est inhibée, elle ne peut plus dépolymériser les filaments d'actine, des fibres de stress s'accumulent, un phénotype invasif est alors observé (Figure 7) (Maekawa et al., 1999; Sumi et al., 2001). Pour le remaniement des microtubules, les acteurs moléculaires ne sont pas connus, mais les LIMKs favorisent la forme libre dépolymérisée de la tubuline (Gorovoy et al., 2005; Po'uha et al., 2010).

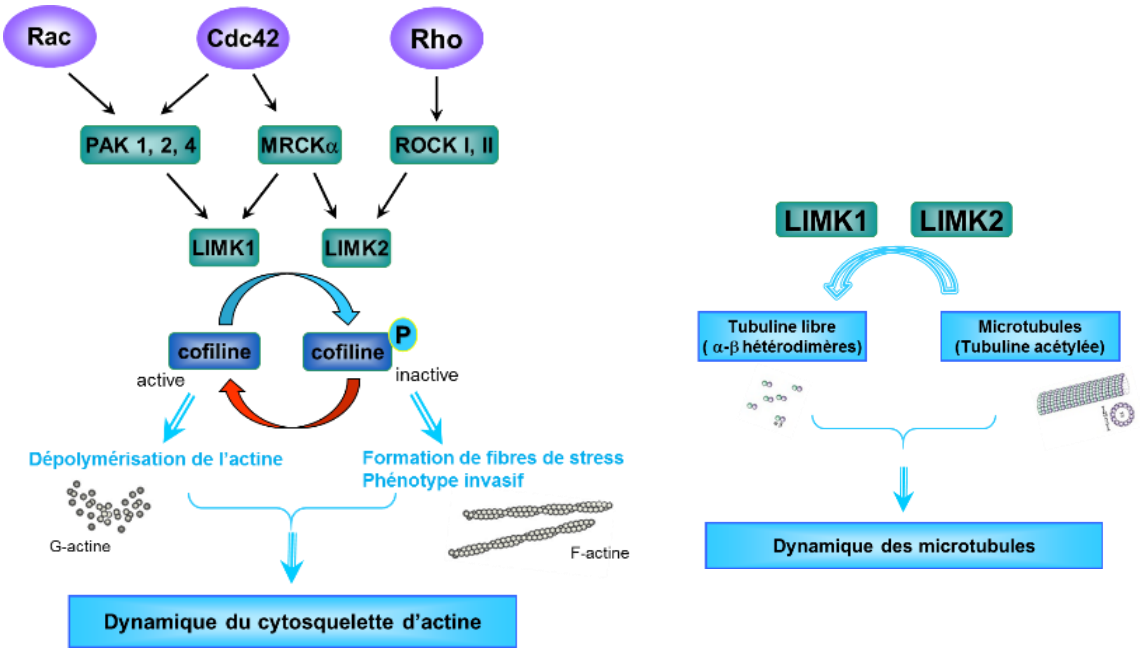

<u>Figure 7 :</u> Voie de transduction du signal des LIMKs dans la dynamique du cytosquelette.

Or la dynamique de remodelage du cytosquelette est impliquée dans de nombreux processus cellulaires, telles la division, la différenciation, la morphogénèse, la mobilité, l'apoptose, la neuritogenèse et la plasticité neuronale, mais aussi dans des processus pathologiques, telles l'oncogenèse, l'invasion tumorale et l'apparition de métastases. De ce fait, ces dernières années de nombreux articles ont montré l'implication des LIMKs dans le cancer (développement et invasion tumorale, formation de métastases, résistance à des drogues), dans certaines maladies neurologiques (déficience intellectuelle, Parkinson, syndrome de Williams-Beuren, …), dans les infections virales, dans l'hyperpression oculaire (glaucome), dans la reproduction et dans la douleur chronique (Figure 8).

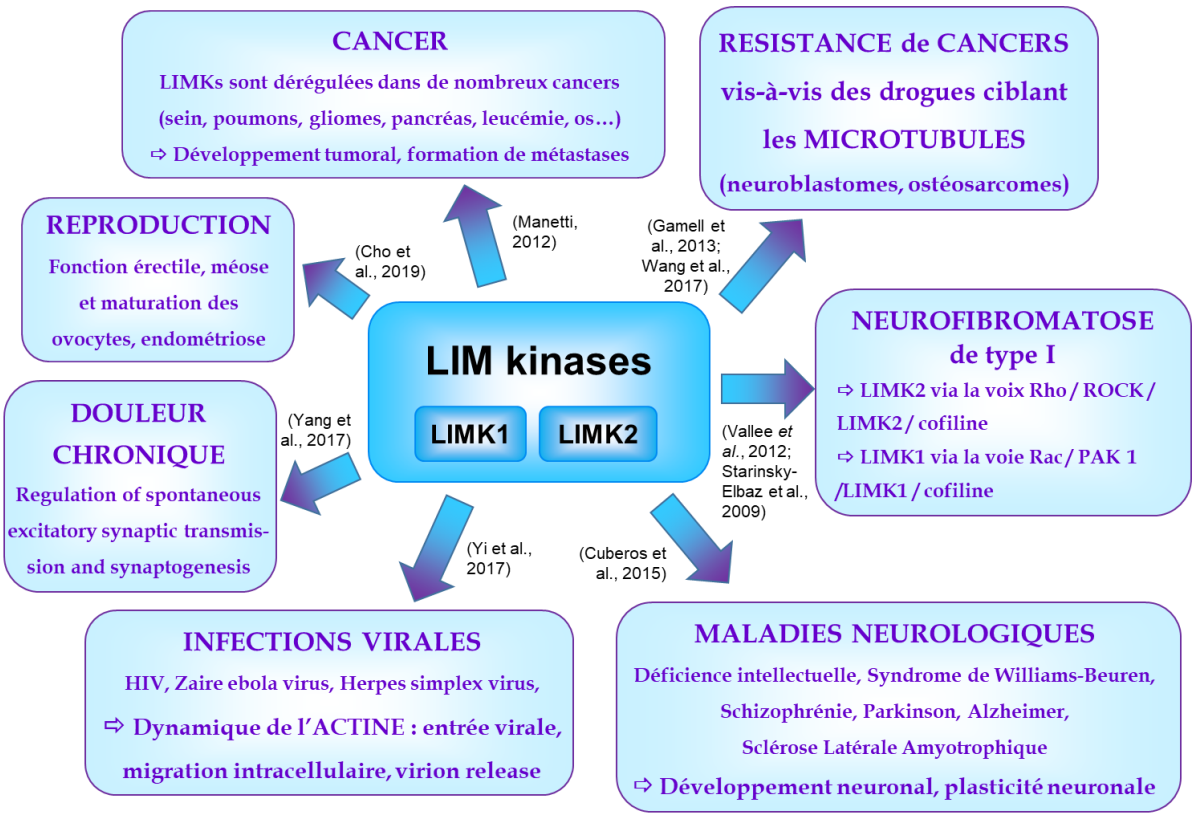

Figure 8 : Les LIMKs : de nouvelles cibles thérapeutiques dans plusieurs pathologies.
(Cho et al., 2019; Cuberos et al., 2015; Gamell et al., 2013; Manetti, 2012; Starinsky-Elbaz et al., 2009; Vallee et al., 2012; Wang et al., 2017; Yang et al., 2017; Yi et al., 2017)

Ayant identifié LIMK2 comme nouveau partenaire de Nf1, cible particulièrement intéressante aussi en elle-même, mes travaux se sont alors répartis en quatre axes majeurs de recherche, qui constituent mes axes de recherche actuels et futurs :

1. **Etude du lien entre LIMK2 et Nf1**
2. **Etude des bases moléculaires de la Neurofibromatose de type I**
3. **Etude des isoformes de LIMK2**
4. **Développement de petites molécules chimiques pour inhiber les LIMKs, nouvelles cibles thérapeutiques dans le traitement de la neurofibromatose de type I, des cancers et de certaines maladies neurologiques**

2. LIMK2 et Nf1

1. *LIMK2 et Nf1 : un nouveau lien entre les voies de signalisation cellulaire Rho et Ras (Vallee et al., 2012)*

Le crible double hybride a permis d'identifier LIMK2, isoforme LIMK2a, comme nouveau partenaire de Nf1. Nous avons confirmé cette interaction par des expériences de co-immunoprécipitation sur les protéines LIMK2a et SecPH-Nf1 surexprimées dans des cellules HEK-293, sur les protéines endogènes LIMK2 et Nf1, et décortiqué les domaines de LIMK2a interagissant avec SecPH-Nf1.

Nous avons mis à jour le rôle physiologique de cette interaction. Par immunofluorescence dans des cellules HeLa, nous avons montré que SecPH inhibe la formation des fibres de stress induites par LIMK2. Moléculairement, nous avons montré que SecPH inhibe la phosphorylation de la cofiline par LIMK2 en empêchant la phosphorylation de la Threonine 505 de LIMK2, et donc son activation par ROCK, la kinase en amont de LIMK2.

Ces résultats ont été publiés dans PLOS One en 2012 (Vallee et al., 2012) et sont résumés Figure 9.

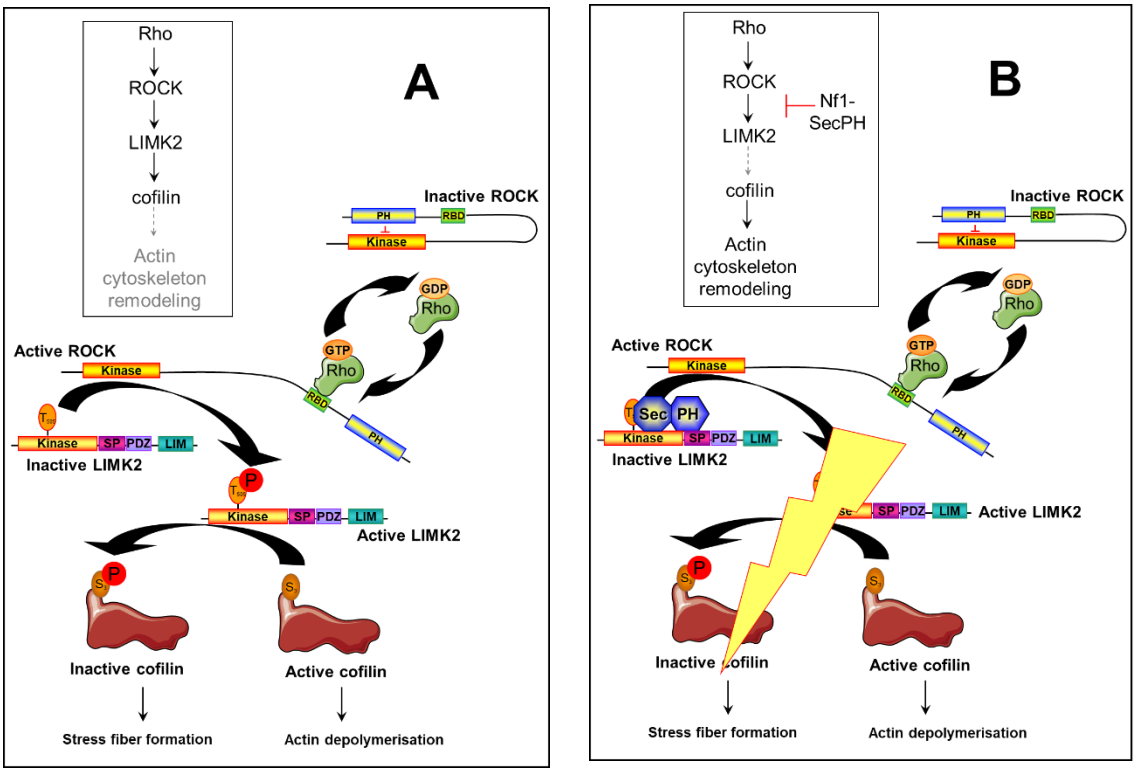

Figure 9 : Résumé des résultats obtenus dans cette étude : *Mise à jour du lien moléculaire entre la neurofibromatose de type I et la dynamique du cytosquelette d'actine (Vallee et al., 2012).*
A. Rho se fixe au RBD (Rho Binding Site) de ROCK et l'active grâce à un changement conformationnel de ROCK. Le domaine PH de ROCK s'éloigne alors de son domaine kinase et ne peut plus l'inhiber. ROCK active alors LIMK2 en la phosphorylant sur sa Thr505. LIMK2 phosphoryle alors la cofiline sur sa Ser3, l'inhibant. Un phénotype invasif est alors observé avec la formation de fibres de stress. B. Par cette étude, nous avons mis en évidence un nouvel acteur de cette voie : Nf1. Ces résultats permettent ainsi de connecter moléculairement la neurofibromatose de type I au remodelage du cytosquelette d'actine. En interagissant avec LIMK2, Nf1-SecPH empêche l'activation de LIMK2 par ROCK. LIMK2 ne peut alors plus phosphoryler la cofiline et donc l'inhiber.

2. *LIMK2 et Nf1 : mécanisme moléculaire de l'inhibition par SecPH-Nf1 de l'activation de LIMK2 par ROCK*

Nous avons alors voulu comprendre plus finement le mécanisme d'inhibition par SecPH-Nf1 de l'activation de LIMK2 par ROCK en allant à l'échelle moléculaire. L'idée était d'identifier des régions protéiques clés de ce processus afin éventuellement d'identifier un peptide qui pourrait mimer l'action de SecPH sur LIMK2. On pourrait alors envisager de développer un peptide thérapeutique contre la neurofibromatose de type I.

Ce sujet a été traité par les stagiaires successifs de Master 2 que j'ai encadrés : Kevin Lesage (2014), Mélissa Thomas (2015) et Lauren Blot (2016).

Dans un premier temps, les domaines minimaux d'interaction entre LIMK2 et ROCK ont été déterminés. Différentes versions tronquées de ROCK ont été construites et testées contre LIMK2a entière (Figure 10).

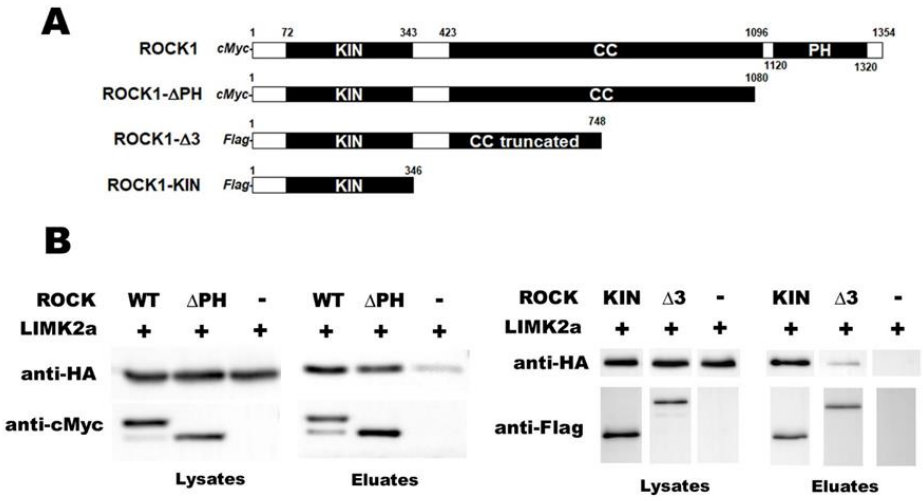

<u>Figure 10 :</u> Interaction entre LIMK2a entière et différents domaines de ROCK.
A. Représentation schématique des domaines de ROCK.
B. *A gauche*. Des cellules HEK sont transfectées par LIMK2a(HA) et ROCK(cMyc) entière ou ROCK-ΔPH(cMyc), puis lysées. Une immunoprécipitation avec des billes greffées avec des anticorps anti-cMyc est réalisée. Les lysats et éluats sont analysés par Western Blot. *A droite.* Des cellules HEK sont transfectées par LIMK2a(HA) et ROCK-Δ3(Flag) ou ROCK-KIN(Flag), puis lysées. Une immunoprécipitation avec des billes greffées avec des anticorps anti-Flag est réalisée. Les lysats et éluats sont analysés par Western Blot.

LIMK2 interagit avec toutes les constructions de ROCK, en particulier la version la plus courte correspondant à son domaine kinase. Nous avons donc ensuite testé l'interaction de ce domaine de ROCK avec les différents domaines de LIMK2 (Figure 11).

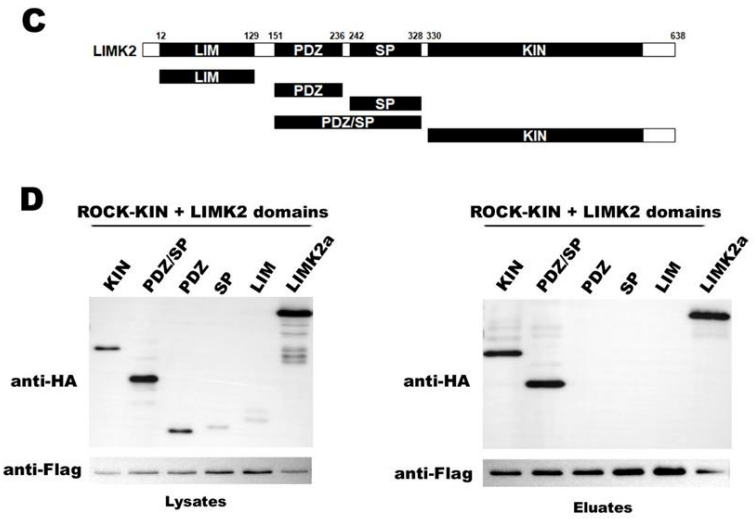

Figure 11 : Interaction entre KIN-ROCK et les différents domaines de LIMK2.
C. Représentation schématique des domaines de LIMK2.
D. Des cellules HEK sont transfectées par ROCK-KIN(Flag) et différents domaines de LIMK2, puis lysées. Une immunoprécipitation avec des billes greffées avec des anticorps anti-Flag est réalisée. Les lysats et éluats sont analysés par Western Blot.

Le domaine KIN de ROCK interagit avec 2 domaines de LIMK2 : LIMK2-KIN et LIMK2-PDZ/SP.

Précédemment, nous avons montré que SecPH ne perturbe pas l'interaction entre les protéines entières LIMK2a et ROCK (Vallee *et al.*, 2012). Qu'en est-il des domaines d'interaction entre LIMK2 et ROCK que nous venons d'identifier ?
Les interactions entre ROCK-KIN et LIMK2-KIN d'une part, et ROCK-KIN et LIMK2-PDZ/SP ont été testées en présence ou non de SecPH-Nf1 (Figure 12).

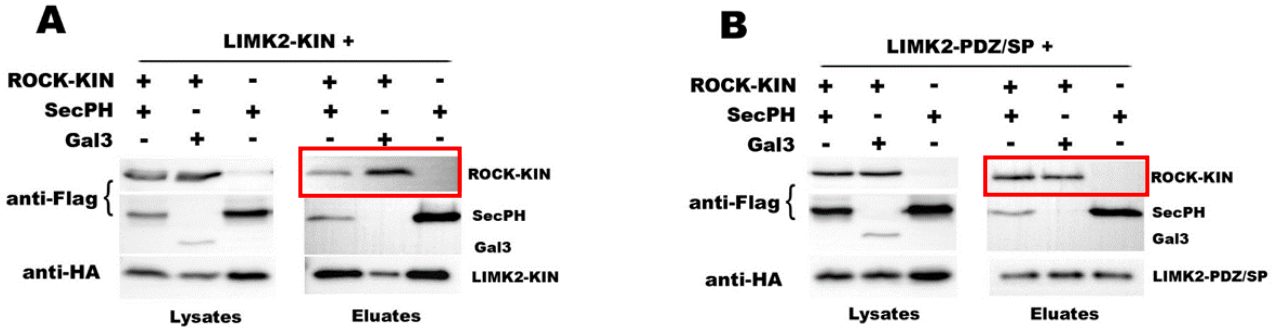

Figure 12 : SecPH-Nf1perturbe l'interaction entre ROCK-KIN et LIMK2-KIN mais pas entre ROCK-KIN et LIMK2-PDZ/SP.
A. Des cellules HEK sont transfectées par LIMK2-KIN(HA) et ROCK-KIN(Flag) ou le plasmide parental vide (p3x-Flag) et SecPH-Nf1(Flag) ou Gal3(Flag) en contrôle négatif. Une immunoprécipitation avec des billes greffées avec des anticorps anti-HA est réalisée. Les lysats et éluats sont analysés par Western Blot.
B. Des cellules HEK sont transfectées par LIMK2-PDZ/SP(HA) et ROCK-KIN(Flag) ou le plasmide parental vide (p3x-Flag) et SecPH-Nf1(Flag) ou Gal3(Flag) en contrôle négatif. Une immunoprécipitation avec des billes greffées avec des anticorps anti-HA est réalisée. Les lysats et éluats sont analysés par Western Blot.

Une diminution de l'interaction entre LIMK2-KIN et ROCK-KIN est observée en présence de SecPH-Nf1 (Figure 12). Par contre, SecPH-Nf1 ne perturbe pas l'interaction entre LIMK2-PDZ/SP et ROCK-KIN (Figure 12). Par ailleurs, on constate que SecPH-Nf1 interagit moins avec les domaines de LIMK2 lorsque ROCK est présent. Ces résultats sont particulièrement intéressants car ils montrent que SecPH perturbe l'interaction entre ROCK-KIN et LIMK2-KIN.

Précédemment, nous avions montré que SePH-Nf1 empêche la phosphorylation et donc l'activation de LIMK2 par ROCK (Vallée et al., 2012). Qu'en est-il pour les domaines réduits ROCK-KIN et LIMK2-KIN ?
Tout d'abord, nous avons vérifié que ROCK-KIN était suffisant pour phosphoryler LIMK2-KIN. Pour cela, nous avons réalisé deux tests : (i) un marquage *in vitro* au γ-[^{32}P]-ATP (ii) un immunoblot avec des anticorps spécifiques anti-Phospho-Thr505 de LIMK2 (Figure 13).

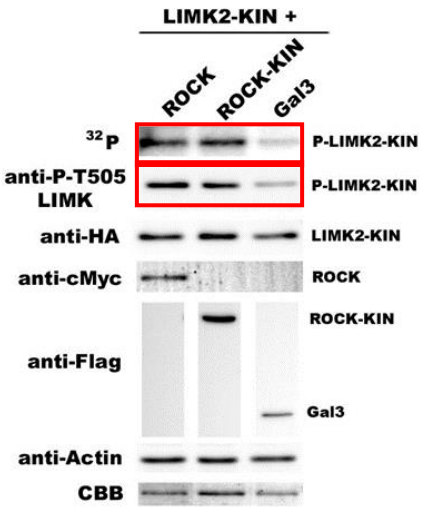

Figure 13 : ROCK-KIN phosphoryle LIMK2-KIN.
Des cellules HEK sont transfectées avec LIMK2-KIN(HA) et soit ROCK entière, soit ROCK-KIN soit le contrôle négatif Gal3. Une immunoprécipitation avec des billes greffées avec des anticorps anti-HA est réalisée, ces billes sont ensuite incubées avec du γ-[^{32}P]-ATP, et éluées. L'éluat est analysé par autoradiographie. Les lysats sont analysés par Western Blot.

Ces deux expériences montrent que ROCK-KIN est suffisant pour phosphoryler LIMK2-KIN sur sa Thréonine 505.
Nous avons alors testé si SecPH-Nf1 perturbait cette phosphorylation (Figure14).

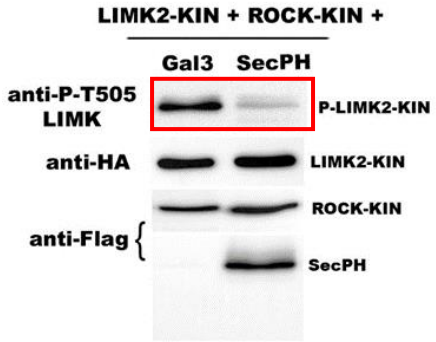

Figure 14 : SecPH diminue la phosphorylation de LIMK2-KIN par ROCK-KIN.
Des cellules HEK sont transfectées par LIMK2-KIN, ROCK-KIN et SecPH ou le contrôle Galectine 3, puis lysées. Les lysats sont analysés par Western Blot.

Une nette diminution de la phosphorylation de la Thréonine 505 de LIMK2-KIN par ROCK-KIN est observée en présence de SecPH-Nf1.

En conclusion, ces travaux montrent que SecPH-Nf1 ne perturbe pas l'interaction entre ROCK-KIN et LIMK2-PDZ/SP. Par contre, il perturbe l'interaction entre ROCK-KIN et LIMK2-KIN, ce qui conduit à une diminution de la phosphorylation de LIMK2-KIN par ROCK-KIN.

Ces résultats suggèrent que la diminution de phosphorylation de la Thr505 de LIMK2 par ROCK observée en présence de SecPH (Vallee *et al.*, 2012) est la conséquence de la perte d'interaction entre ROCK-KIN et LIMK2-KIN en présence de SecPH. Cette compétition d'interaction est en accord avec le fait que SecPH et KIN-ROCK se fixent tous les deux aux mêmes domaines de LIMK2 (les domaines KIN et PDZ/SP, (Vallee et al., 2012)). Ces résultats sont résumés Figure 15.

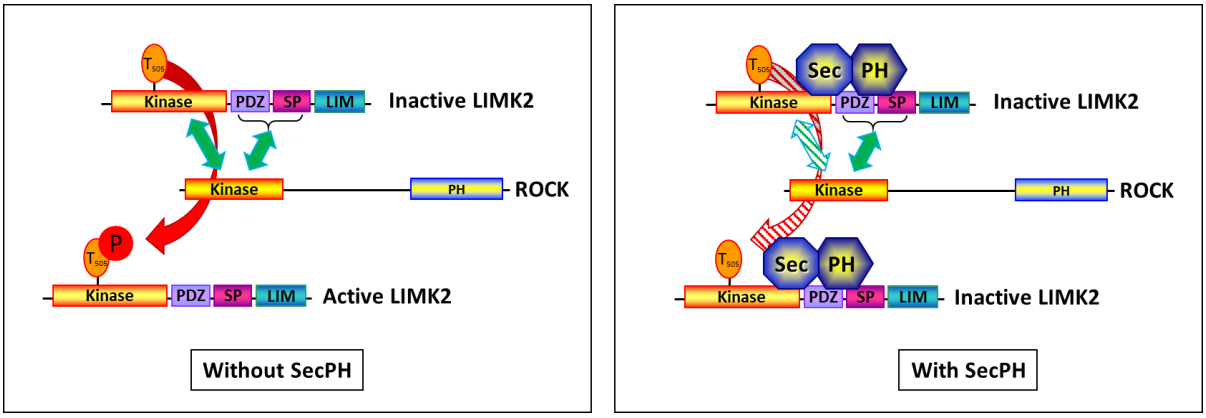

Figure 15 : Résumé des résultats obtenus dans cette étude.
A gauche, en l'absence de SecPH, ROCK et LIMK2 interagissent via leurs domaines KIN et KIN et PDZ/SP respectivement. ROCK phosphoryle LIMK2 sur sa Thr505 et l'active.
A droite, en présence de SecPH, ce dernier se fixe sur LIMK2 via ses domaines KIN et PDZ/SP (Vallee *et al.*, 2012). ROCK-KIN ne peut plus interagir avec LIMK2-KIN, il ne phosphoryle donc pas sa Thr505. LIMK2 reste inactive.

J'aurais voulu aller plus loin dans cette étude, mais elle n'est pas une priorité par rapport aux autres sujets que je veux développer. J'ai donc décidé de l'arrêter à ce stade. Une publication regroupant l'ensemble de ces résultats est en cours de rédaction.

3. *Etude du rôle fonctionnel des trois isoformes de LIMK2 vis-à-vis de Nf1*

Chez l'homme, trois isoformes de LIMK2 sont décrites dans les bases de données, les isoformes 2-1, 2a et 2b (voir Figure 6). LIMK2a interagit avec SecPH-Nf1, qu'en est-il des autres isoformes de LIMK2 ?

Nous avons mis en évidence l'interaction entre SecPH-Nf1 et chacune des trois isoformes de LIMK2 (Figure 16).

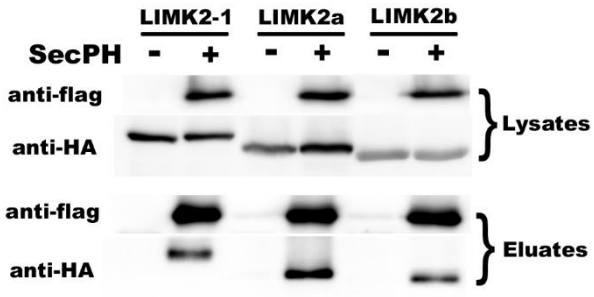

Figure 16 : Interaction des isoformes de LIMK2s avec le domaine SecPH de Nf1.
Des cellules HEK sont transfectées par l'une des isoformes de LIMK2(HA) et SecPH-Nf1(Flag) ou le plasmide parental vide (p3x-Flag). Une immunoprécipitation avec des billes greffées avec des anticorps anti-Flag est réalisée. Les lysats et éluats sont analysés par Western Blot.

Nous avons aussi testé l'interaction entre chacune des isoformes de LIMK2 et Nf1 endogène (Figure 17). Il s'avère que l'isoforme LIMK2-1 n'interagit pas ou extrêmement faiblement avec Nf1. En poussant la révélation une très faible bande de LIMK2-1 apparaît dans la co-immunoprécipitation avec Nf1. Nous avons pensé que ce résultat pouvait être dû au fait que LIMK2-1(HA) est plus faiblement exprimée que ses deux homologues. Nous avons alors réalisé la même expérience avec les versions étiquetées YFP des isoformes de LIMK2, leur expression étant plus homogène. A nouveau, l'isoforme LIMK2-1 n'interagit pas ou extrêmement faiblement avec Nf1 (Figure 17).

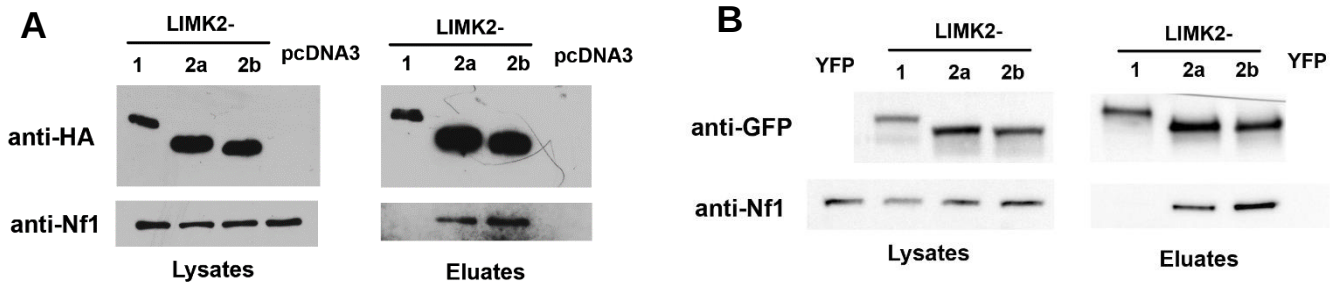

Figure 17 : Interaction des isoformes de LIMK2s avec Nf1.
A. Des cellules HEK sont transfectées par l'une des isoformes de LIMK2(HA) ou le plasmide parental vide (pcDNA3). Une immunoprécipitation avec des billes greffées avec des anticorps anti-HA est réalisée. Les lysats et éluats sont analysés par Western Blot.
B. Des cellules HEK sont transfectées par l'une des isoformes de LIMK2(YFP) ou le plasmide parental vide (peN1-YFP). Une immunoprécipitation avec des billes greffées avec des anticorps anti-GFP est réalisée. Les lysats et éluats sont analysés par Western Blot.

Ce résultat peut paraître déroutant. Cependant, plusieurs explications sont possibles :
- (i) selon les conditions physiologiques, Nf1, qui est une très grosse protéine de 320 kDa, peut subir des changements conformationnels qui peuvent masquer ou dévoiler le domaine SecPH modulant l'interaction avec LIMK2-1,
- (ii) Nf1 possède plusieurs sites putatifs de coupure aux caspases, ainsi qu'une putative séquence PEST. Selon les conditions physiologiques, Nf1 pourrait être clivée conduisant à la formation de fragments où SecPH serait accessible à LIMK2-1,
- (iii) Nf1 et LIMK2-1 ne sont pas localisés dans les mêmes compartiments cellulaires, LIMK2-1 est quasi-exclusivement dans le cytoplasme (Vallee et al., 2018), tandis que Nf1 est majoritairement dans le noyau (Godin et al., 2012). Cette différence de localisation pourrait expliquer l'absence d'interaction. Peut-être existe-t-il des conditions dans lesquelles ces deux protéines se rencontrent (activation, …) ?

Au niveau fonctionnel, nous avons montré que Nf1-SecPH empêche la phosphorylation et donc l'activation de l'isoforme LIMK2a par ROCK. Qu'en est-il des deux autres isoformes LIMK2-1 et LIMK2b ? Les trois isoformes de LIMK2 sont-elles inhibées de la même façon par Nf1-SecPH ? Y a-t-il des différences entre ces trois isoformes comme pour la p53 (Croft et al., 2011; Hsu et al., 2010) ?

Par ailleurs, il serait intéressant de compléter ces observations par des études structurales. Des articles récents et le développement de nouveaux outils permettent de l'envisager.
Jusque récemment, il était extrêmement difficile de cloner NF1 entier dans un plasmide pour pouvoir exprimer la neurofibromine. La construction s'avérait instable du fait de la taille énorme de ce gène et de sa séquence (360 kb). L'optimisation des codons avait permis d'améliorer la stabilité de cette construction (Bonneau et al., 2009). Une nouvelle étape vient d'être franchie en sous-clonant successivement différents fragments de NF1 et en introduisant un mini-intron dans sa séquence (Cui and Morrison, 2019). Nf1 entière a pu être clonée de façon stable et surproduite. Cette avancée ouvre de nombreuses perspectives. En particulier, des études structurales en microscopie électronique ont permis de montrer que Nf1 forme un dimère et de déterminer les régions de Nf1 impliquées dans cette dimérisation (Sherekar et al., 2019).
La structure du domaine kinase de LIMK2 a été résolue par cristallographie aux rayons X (pdb 3S95) par le groupe de Stefan Knapp et Alex Bullock en 2011. Nous les avions alors contactés pour réaliser des études structurales sur LIMK2-1, et sur le complexe LIMK2a-SecPH. Ces études n'ont pas abouti à cause de problèmes pour produire le domaine kinase de LIMK2. Dans

un article récent où le groupe de Knapp a résolu la structure tridimensionnelle du complexe du domaine kinase de LIMK1 avec la cofiline, le rendement de production de KIN-LIMK2 est de 0.2 mg/L de culture de cellules d'insecte, comparé à celui de KIN-LIMK1 de 2.0 mg/L de culture de cellules d'insecte (Salah et al., 2019). Cependant, un article a récemment montré qu'il était possible de produire et purifier LIMK1 entière (Somogyi et al., 2019).
Il serait intéressant de résoudre la structure de LIMK2a et LIMK2-1 entières, ainsi que celle du complexe LIMK2a-Nf1. Ces structures pourraient nous donner des informations précieuses quant au mode d'action et d'interaction de ces différentes protéines.
Dans la structure résolue par microscopie électronique de Nf1, le domaine SecPH se situe au niveau de la zone de dimérisation de Nf1, et une cavité apparaît dans cette zone (Sherekar et al., 2019). On peut postuler que l'interaction de SecPH avec ces ligands pourrait être modulée par la dimérisation de Nf1 et par la flexibilité de ce complexe.

3. Nf1 : étude des bases moléculaires de la Neurofibromatose de type I

L'étude intrinsèque de Nf1 se poursuit aussi afin de mieux caractériser cette protéine et son implication dans la Neurofibromatose de type I. Des études ont montré que Nf1 est partiellement localisée dans le noyau de différentes cellules (neurones télencéphaliques, neuroblastomes, cellules de cancer du sein, cellules de Schwann saines ou cancéreuses). Mais aucun rôle fonctionnel n'a été associé à cette localisation de Nf1.
Nous avons montré que Nf1 est partiellement localisée dans le noyau des astrocytes, et plus particulièrement dans le sous-compartiment nucléaire des PML bodies (Godin et al., 2012). Ces PML nuclear bodies (Promyelocytic Leukemia), structures très dynamiques, sont impliqués dans de nombreux processus liés au noyau, telles la réparation de l'ADN, l'apoptose, la prolifération cellulaire, la protéolyse, la suppression de tumeurs ou encore la réponse antivirale. D'autre part, les PML nuclear bodies contiennent de nombreuses protéines SUMOylées (dont PML), de nombreuses protéines contenant des motifs SIM (SUMO Interacting Motif), et des enzymes du cycle de SUMOylation, dont l'unique SUMO-conjugating enzyme E2, Ubc9 (Lallemand-Breitenbach and de The, 2018).

Or, Nf1 est prédite comme étant potentiellement SUMOylée par les logiciels SUMOPlot et JASSA (Beauclair et al., 2015), et des études systématiques ont montré que Nf1 est SUMOylée (Hendriks et al., 2014; Hendriks and Vertegaal, 2016; Schimmel et al., 2014).

SUMO (Small Ubiquitin-like Modifier) est une modification post-traductionnelle, qui correspond à l'établissement d'une liaison covalente entre la Glycine de la protéine SUMO et le NH_2-ε d'une Lysine de la protéine cible. Il existe trois isoformes de SUMO, SUMO1, SUMO2 et SUMO3. SUMO2 et SUMO3 sont très proches en séquence. Les protéines SUMO ont une taille d'environ 15 kDa. Le processus de SUMOylation d'une protéine cible se déroule en trois étapes bien décrites dans la littérature, de façon comparable à celle de l'ubiquitination. Un motif consensus de SUMOylation a été décrit, ψKxD/E (ψ acide aminé hydrophobe, K Lysine cible) faisant intervenir Ubc9, mais des Lysines n'appartenant pas à ces sites consensus peuvent aussi être SUMOylées, en particulier celles appartenant à des sites SIM (Hay, 2013).
Au niveau moléculaire, la SUMOylation d'une protéine cible peut réguler (i) son réseau d'interaction en favorisant ou empêchant son interaction avec ses partenaires, (ii) sa stabilité en la ciblant ou non vers le protéasome, (iii) sa localisation subcellulaire. D'un point de vue fonctionnel, il a été démontré que la SUMOylation est impliquée dans certaines pathologies telles que le cancer, les maladies d'Alzheimer, de Parkinson, et de Huntington (Droescher et al., 2013; Eifler and Vertegaal, 2015; Flotho and Melchior, 2013; Seeler and Dejean, 2017; Zhao, 2018).

Le sujet de thèse de Mohammed Bergoug, étudiant que je co-encadre actuellement avec Hélène Bénédetti, porte sur cette modification post-traductionnelle SUMO de Nf1.

Mohammed a montré que SecPH-Nf1 est SUMOylé. Plusieurs bandes de SUMOylation sont observées correspondant à de la mono-SUMOylation (+15kDa) et à de la di-SUMOylation (+30kDa) (Figure 18).

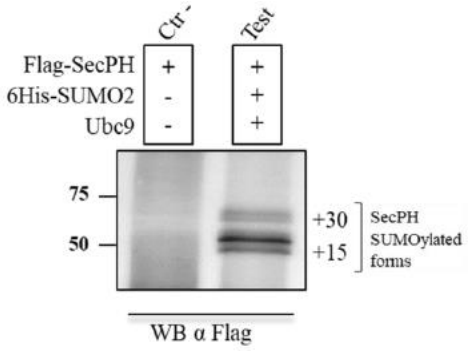

Figure 18 : Le domaine SecPH de Nf1 est SUMOylé.
Des cellules HEK sont transfectées par SecPH-Flag, SUMO-His en présence ou non de Ubc9. Un pull-down avec des billes de Cobalt est réalisé, les éluats sont analysés par Western Blot.

Mohammed a aussi montré que le domaine GRD de Nf1 et Nf1 entière endogène sont SUMOylés. Il a déterminé un site majeur de SUMOylation de SecPH, la Lysine K1731 (Figure 19), une autre Lysine semble aussi être SUMOylée, Lys1634, mais ces résultats doivent être confirmés.

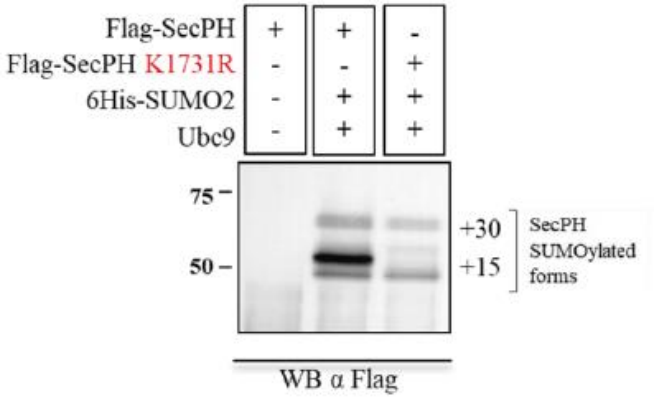

Figure 19 : La Lys1731 du domaine SecPH de Nf1 est SUMOylée.
Des cellules HEK sont transfectées par SecPH-Flag ou SecPH-K1731R-Flag, SUMO-His en présence de Ubc9. Un pull-down avec des billes de Cobalt est réalisé, les éluats sont analysés par Western Blot.

Mohammed a étudié le rôle fonctionnel de la SUMOylation de cette Lys1731. Il a montré que le mutant SecPH-K1731R restaurait moins efficacement la phosphorylation de ERK dans des cellules délétées de *NF1* (Figure 20).

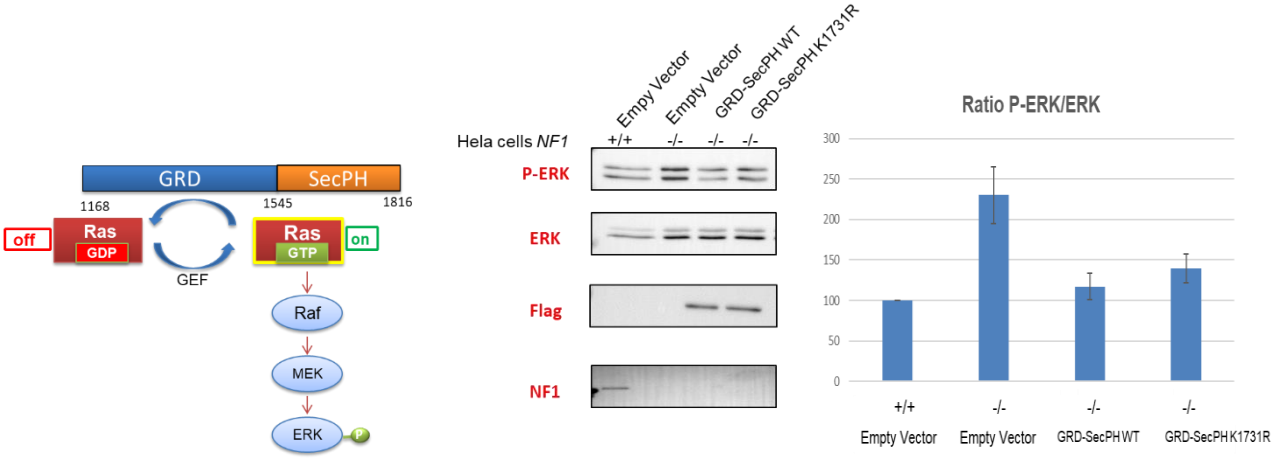

Figure 20 : La SUMOylation de la Lys1731 du domaine SecPH de Nf1 régule le taux de phosphorylation de ERK.
Des cellules HeLa *Nf1*$^{-/-}$ sont transfectées par GRD-SecPH-Flag ou GRDSecPH-K1731-Flag, SUMO-His en présence de Ubc9. Les extraits totaux sont analysés par Western Blot avec différents anticorps. Le ratio Phospho-ERK versus ERK est quantifié et normalisé par rapport aux cellules HeLa *NF1*$^{+/+}$ (100%).

Mohammed a aussi étudié si des mutations présentes au niveau du domaine SecPH de Nf1 de malades atteints de la neurofibromatose pouvaient influencer le profil de SUMOylation de ce domaine. 6 mutations ont été étudiées : D1623G, Δ1719-1736, S1578F, L1602R, L1584V,

ΔIY1658-59. Hormis le mutant 1584, tous ces mutants ont un profil de SUMOylation différent de celui de SecPH sauvage : la bande identifiée comme correspondant à la SUMOylation de la Lys1731 disparaît ou diminue fortement, et une bande juste au-dessus de cette dernière apparaît et est plus ou moins intense. De plus, tous ces mutants sont moins bien exprimés que SecPH sauvage (Figure 21).

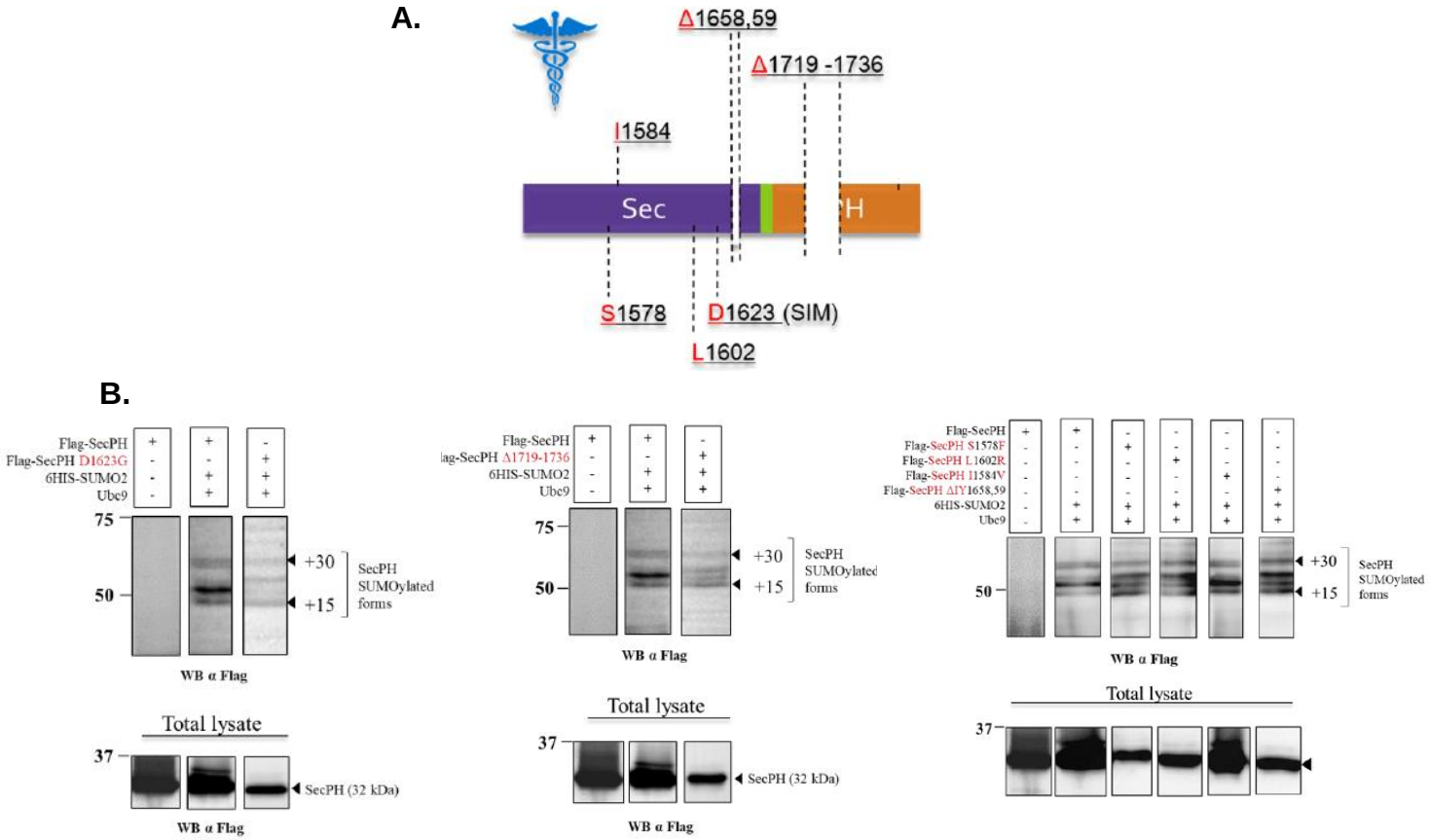

<u>Figure 21 :</u> Etude de la SUMOylation du domaine SecPH de Nf1 portant des mutations correspondant à celles trouvées chez des malades NF1.
A. Mutations décrites dans les bases de données (HGMD)
B. Des cellules HEK sont transfectées par SecPH-Flag ou un des mutants de SecPH-Flag, SUMO-His en présence de Ubc9. Un pull-down avec des billes de Cobalt est réalisé, les éluats sont analysés par Western Blot.

On peut penser que ces mutations engendrent des changements conformationnels de la structure de SecPH, résultant à une accessibilité modifiée des Lysine SUMOylées ou bien qu'elles modifient les interactions avec les différents composants de la machinerie de SUMOylation. Le mutant D1623G est certainement dans ce cas, vu qu'il appartient à un site SIM (SUMO Interacting Motif). Par ailleurs, les mutants dont les profils de SUMOylation sont affectés s'avèrent moins stables que le SecPH sauvage. Ce défaut de stabilité pourrait aussi être une explication sur le dysfonctionnement de ces mutants.

Nous voulons poursuivre ses études, en particulier en caractérisant plus avant la mutation 1634 et son profil de mutation. Nous voulons aussi aller plus loin dans la caractérisation du rôle fonctionnel de la SUMOylation de Nf1, en particulier en étudiant l'impact des mutations 1731 et 1634 sur la stabilité de Nf1, sur sa localisation, sur son réseau d'interaction avec les différents partenaires que nous avons mis en évidence lors de notre crible double hybride.

4. Etude des isoformes de LIMK2

1. *Caractérisation des trois isoformes de LIMK2*

L'étude intrinsèque des isoformes de LIMK2 est aussi menée en parallèle. Etant donné que LIMK2 est une nouvelle cible thérapeutique pour traiter le cancer, la neurofibromatose de type I et certaines maladies neurologiques (Figure 8), il nous est apparu important de caractériser plus précisément ses isoformes d'un point de vue biochimique (Vallee et al., 2018).

Trois isoformes de LIMK2 sont décrites dans les bases de données : LIMK2-1, LIMK2a et LIMK2b. Elles sont strictement identiques sur leur partie centrale et ne diffèrent qu'en leurs extrémités N- et C-terminales (voir Figure 6). LIMK2-1 et LIMK2b sont identiques en leur extrémité N-terminale avec un premier domaine LIM tronqué comparé à LIMK2a. LIMK2a et LIMK2b sont identiques en leur extrémité C-terminale, alors que LIMK2-1 possède un domaine supplémentaire PP1i (Protein Phosphatase 1 inhibitory Domain) identifié par homologie de séquence. La plupart des études concernent LIMK2a. Cependant, des données de la littérature suggèrent que LIMK2a et LIMK2b n'ont pas des rôles identiques. Leur expression au cours du développement, leur distribution dans les tissus, leur localisation dans la cellule et leur stabilité sont différentes. Elles sont différemment dérégulées selon les types de cancers. LIMK2b et LIMK2-1, mais pas LIMK2a, sont régulées par la p53 (Hsu et al., 2010 ; Croft et al., 2011).

Au début de cette étude, LIMK2-1 n'était mentionnée que dans un seul article, en tant que mRNA (Croft et al., 2011). Tout d'abord, nous avons montré que LIMK2-1 existait en tant que protéine (Vallee et al., 2018). Nous avons montré que les trois isoformes ont des localisations cellulaires différentes : LIMK2-1 est strictement dans le noyau, LIMK2b est majoritairement dans le cytosol et peu dans le noyau, LIMK2a apparaît dans ces deux compartiments subcellulaires.

D'un point de vue fonctionnel, les trois isoformes remodèlent le cytosquelette d'actine : elles induisent des fibres de stress. Par contre, LIMK2a et LIMK2b phosphorylent la cofiline, alors

que, de façon surprenante, LIMK2-1 ne la phosphoryle pas (tests *in vivo* et *in vitro*), bien qu'elle possède une activité kinase sur un substrat plus universel la MBP, Myelin Basic Protein (voir Figure 22).

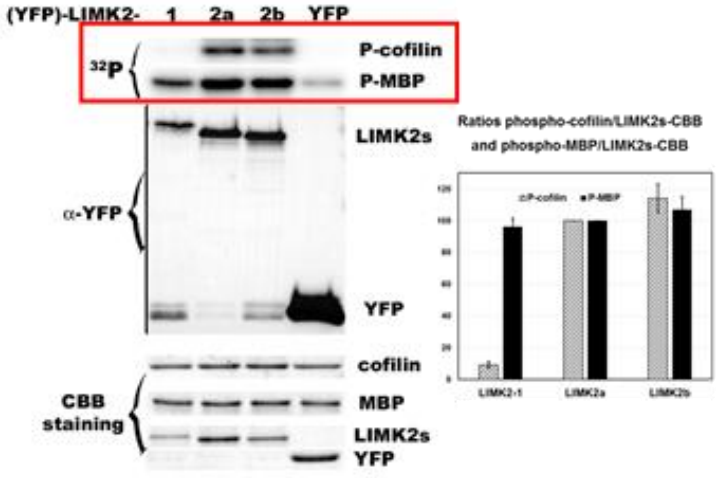

Figure 22 : LIMK2a et 2b, mais pas LIMK2-1, phosphorylent la cofiline.
Essai *in vitro*. Des cellules HEK sont transfectées par l'une des isoformes de LIMK2 étiquetées YFP ou YFP seule, puis lysées. Une immunoprécipitation avec des billes greffées avec l'anticorps anti-GFP est réalisée. Les éluats sont utilisés pour le test d'activité, marquage γ^{32}P-[ATP], avec la GST-cofiline ou la MBP pour substrat. L'éluat est aussi analysé par Western blot et par bleu de Coomassie.

Nous avons alors voulu comprendre comment LIMK2-1 pouvait remodeler le cytosquelette d'actine sans phosphoryler la cofiline. Nous avons émis l'hypothèse que le domaine spécifique PP1i de LIMK2-1 pouvait jouer un rôle dans ce processus en inhibant l'activité phosphatase de PP1 sur la phospho-cofiline.
Hélène Cubéros, étudiante en thèse en co-tutelle entre notre équipe et le laboratoire de Christian Andres à Tours (2013-2016), a montré que LIMK2-1 interagit avec PP1 via son domaine PP1i. J'ai alors montré que LIMK2-1 pouvait inhiber partiellement, mais de façon reproductible, la déphosphorylation de la cofiline par LIMK2-1 *in cellulo*.

En conclusion, nos travaux montrent que les trois isoformes de LIMK2 régulent la dynamique du cytosquelette d'actine en augmentant le taux intracellulaire de cofiline phosphorylée. Cependant, elles n'ont pas le même mode d'action. LIMK2a et LIMK2b phosphorylent directement la cofiline alors que LIMK2-1 inhibe partiellement la déphosphorylation de la cofiline par la phosphatase PP1. Ces résultats ont été publiés en 2018 dans Biochemical Journal (Vallee et al., 2018) et sont résumés Figure 23.

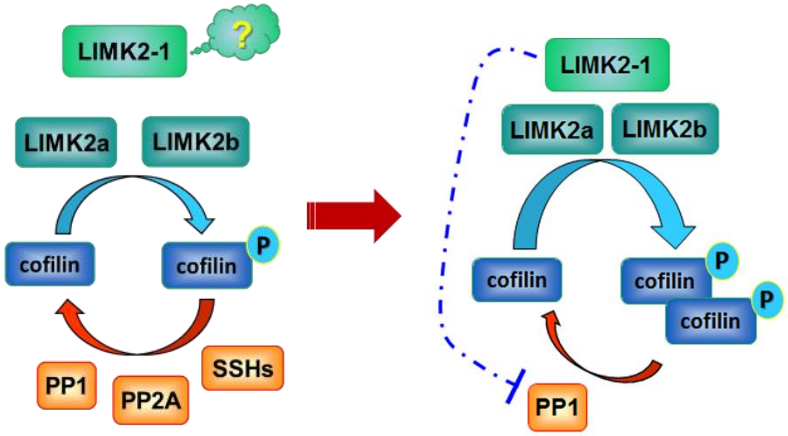

Figure 23 : Les trois isoformes de LIMK2 régulent le taux intracellulaire de cofiline phosphorylée par des mécanismes différents (Vallee et al., 2018).
LIMK2a et LIMK2b phosphorylent directement la cofiline. LIMK2-1 inhibe partiellement la déphosphorylation de la cofiline par la phosphatase PP1.

2. *Etude moléculaire des trois isoformes de LIMK2*

Nous voulons maintenant comprendre pourquoi LIMK2a et LIMK2b phosphorylent la cofiline et pas LIMK2-1, alors que ces protéines ont de fortes homologies de séquences.
Cette étude est d'autant plus intéressante que nous développons aussi de petites molécules inhibitrices des LIMKs en vue de nouvelles thérapies ciblées (§ 5.). LIMK2-1, ne possédant pas d'activité kinase sur la cofiline, elle pourrait être un point de résistance dans cette stratégie.

La spécificité de LIMK2-1 vient de son extrémité C-terminale qui possède un domaine PP1i en plus par rapport à LIMK2a/2b, et son domaine kinase est tronqué d'une dizaine d'acides aminés (Figure 24).

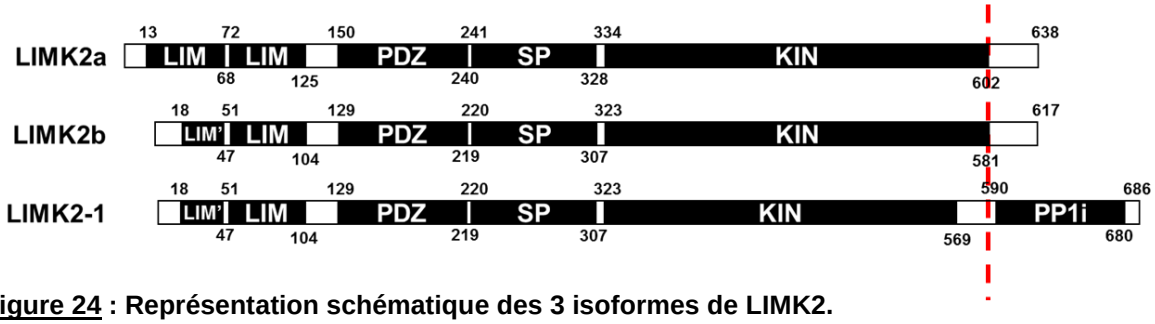

Figure 24 : Représentation schématique des 3 isoformes de LIMK2.

Tout d'abord, nous avons vérifié si LIMK2-1 pouvait interagir avec la cofiline. En effet, son extrémité C-terminale supplémentaire PP1i, pourrait gêner cette interaction.

Ces expériences ont été réalisées par Déborah Cassas, étudiante en M2 que j'ai encadrée en 2018.

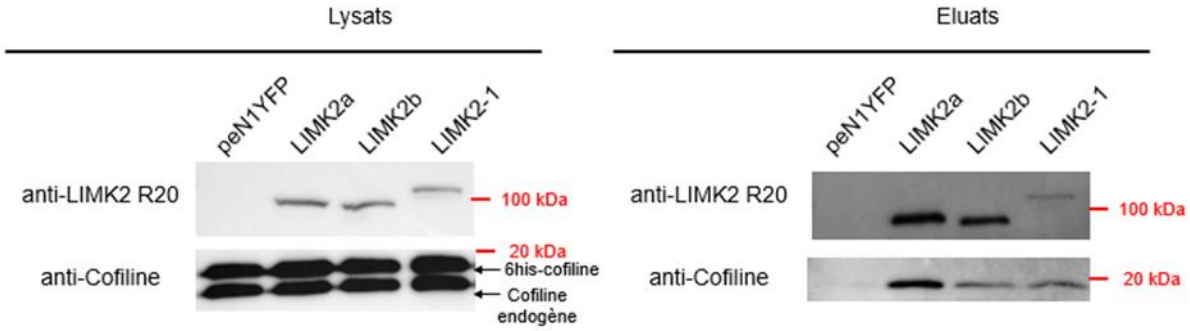

Figure 25 : **Interaction des isoformes de LIMK2 avec la cofiline.**
Des cellules HEK sont co-transfectées par des vecteurs exprimant une des isoformes de LIMK2 étiquetées YFP et la cofiline étiquetée 6His. Les cellules sont lysées. Le lysat est incubé avec des billes greffées avec l'anticorps anti-GFP. Les lysats et éluats sont analysés par Western Blot.

LIMK2-1, comme LIMK2a et LIMK2b, interagit avec la cofiline (Figure 25).

Nous avons alors émis l'hypothèse que le manque d'activité kinase de LIMK2-1 vis-à-vis de la cofiline pouvait être dû à son domaine kinase tronqué en comparaison avec LIMK2a et LIMK2b. Hélène Cubéros et Déborah Cassas ont construit différentes protéines chimères de LIMK2a plus ou moins tronquées en leur extrémité C-terminale. Ces protéines chimères interagissent avec la cofiline mais sont incapables de phosphoryler la cofiline *in cellulo* et *in vitro* (Figure 26). Le domaine kinase de LIMK2a est donc nécessaire pour phosphoryler la cofiline mais pas suffisant.

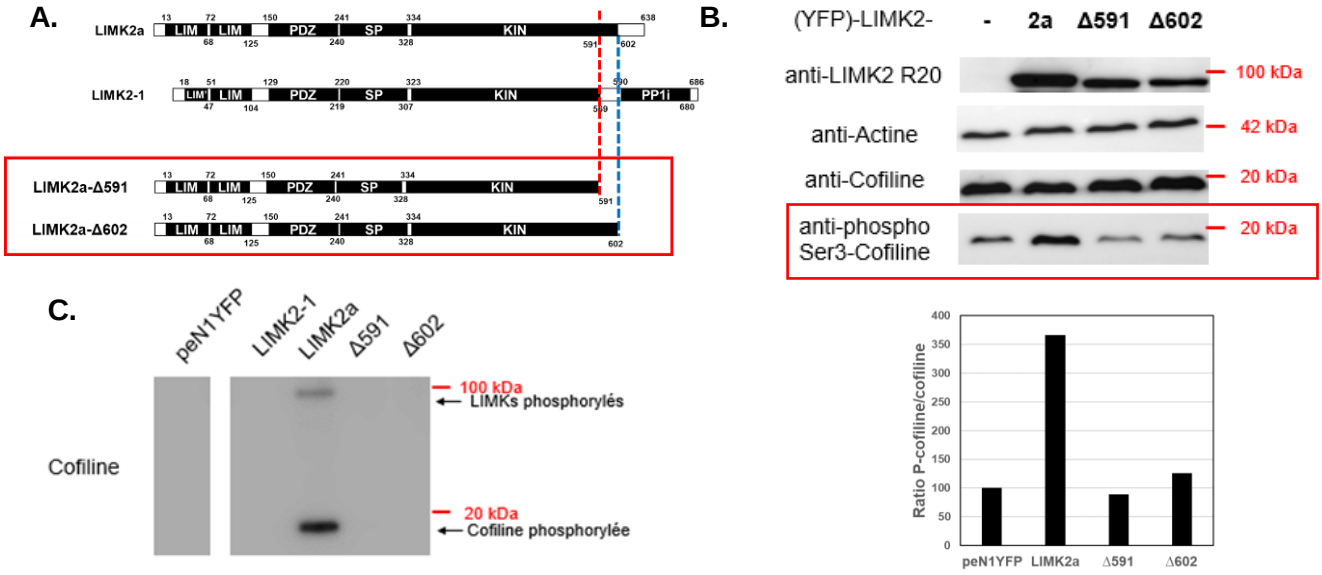

Figure 26 : **Etude de deux formes tronquées de LIMK2a : LIMK2-Δ591 et LIMK2-Δ602**
A. Représentation schématique
B. Phosphorylation *in cellulo* de la cofiline. Des cellules HEK-293 sont transfectées par une des constructions. Les cellules sont lysées. Le lysat est analysé par Western Blot. Histogramme : quantification du ratio phospho-cofiline *versus* cofiline normalisé à 100% pour la condition contrôle peN1-YFP.
C. Phosphorylation *in vitro* de la cofiline. Des cellules HEK sont transfectées par l'une des constructions étiquetées YFP ou YFP seule, puis lysées. Une immunoprécipitation avec des billes greffées avec l'anticorps anti-GFP est réalisée. Les éluats sont utilisés pour le test d'activité, marquage γ^{32}P-[ATP], avec la GST-cofiline pour substrat. Autoradiogramme.

La structure tridimensionnelle du domaine kinase de LIMK2a a été résolue par cristallographie aux rayons X. En analysant cette structure au niveau des acides aminés qui ont été tronqués dans nos constructions, nous nous sommes rendu compte que nous avions éliminé deux hélices qui pourraient avoir un rôle structurant d'après les modélisateurs (Figure 27). Nous avons donc décidé de construire deux autres protéines tronquées de LIMK2a conservant l'avant-dernière hélice de l'extrémité C-terminale : LIMK2-Δ609 possède l'avant-dernière hélice α et LIMK2-Δ611 possède en plus deux acides aminés dont une Proline qui pourrait avoir un rôle de structuration.

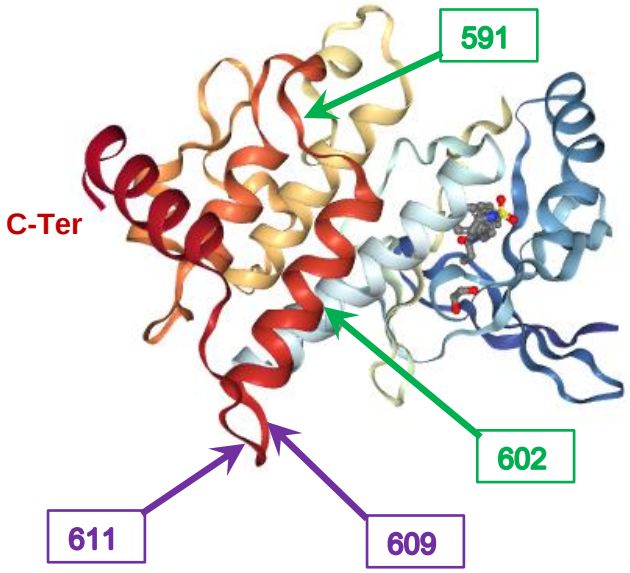

Figure 27 : Structure cristallographique du domaine kinase de LIMK2 (PDB : 5NXD). Les deux hélices C-terminales sont en rouge. Les extrémités C-terminales des deux premières protéines tronquées LIMK2-Δ591 et LIMK2-Δ602 sont en vert, tandis que les extrémités C-terminales des deux autres protéines tronquées LIMK2-Δ609 et LIMK2-Δ611 sont en violet.

Ces deux nouvelles protéines tronquées LIMK2-Δ609 et LIMK2-Δ611 interagissent avec la cofiline, mais sont incapables de la phosphoryler *in cellulo* et *in vitro* (Figure 28).

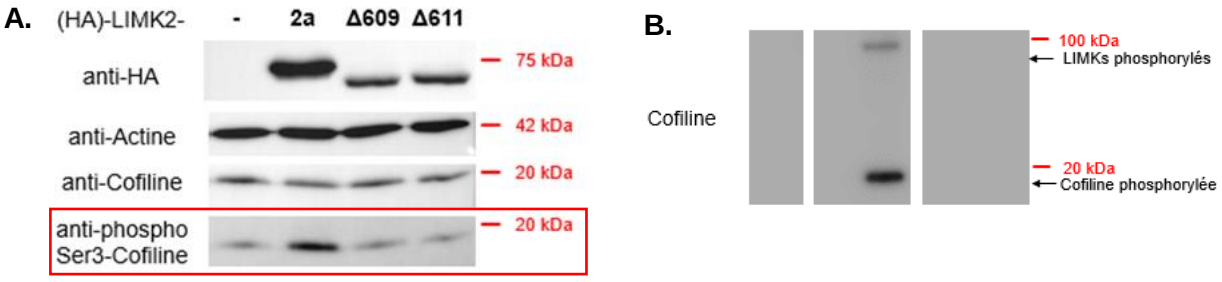

Figure 28 : Etude des deux nouvelles formes tronquées de LIMK2a : LIMK2-Δ609 et LIMK2-Δ611
A. Phosphorylation *in cellulo* de la cofiline. Des cellules HEK-293 sont transfectées par une des constructions. Les cellules sont lysées. Le lysat est analysé par Western Blot.
B. Phosphorylation *in vitro* de la cofiline. Des cellules HEK sont transfectées par l'une des constructions étiquetées YFP ou YFP seule, puis lysées. Une immunoprécipitation avec des billes greffées avec l'anticorps anti-GFP est réalisée. Les éluats sont utilisés pour le test d'activité, marquage γ^{32}P-[ATP], avec la GST-cofiline pour substrat. Autoradiogramme.

La partie C-terminale de LIMK2a (dernière hélice α) apparaît donc comme étant cruciale pour l'activité kinase de cette dernière vis-à-vis de la cofiline. Par ailleurs, lors des tests de phosphorylation *in vitro*, nous avons remarqué que LIMK2-1 ainsi que les 4 protéines tronquées de LIMK2a n'étaient pas phosphorylées contrairement à LIMK2a (Figures 26C et 28B, bande haute de l'autoradiogramme). Or, dans des expériences antérieures nous avons montré que, *in cellulo*, LIMK2-1 est phosphorylée par ROCK sur sa Thr505 (Vallee et al., 2018). Il nous faudra vérifier que les 4 protéines tronquées de LIMK2a (Δ591, Δ602, Δ609 et Δ611) interagissent avec ROCK et sont phosphorylées par cette dernière *in cellulo*. Ces expériences sont en cours de réalisation par Célina Chalal, étudiante en M2, que j'encadre depuis fin de janvier 2020. Nous avons aussi émis l'hypothèse que l'extrémité C-terminale de LIMK2a pourrait contenir un acide aminé qui doit être phosphorylé *in vitro* pour permettre l'activité kinase de LIMK2a sur la cofiline. Plusieurs Thréonine, Sérine et Tyrosine sont présentes dans cette zone (Figure 29).

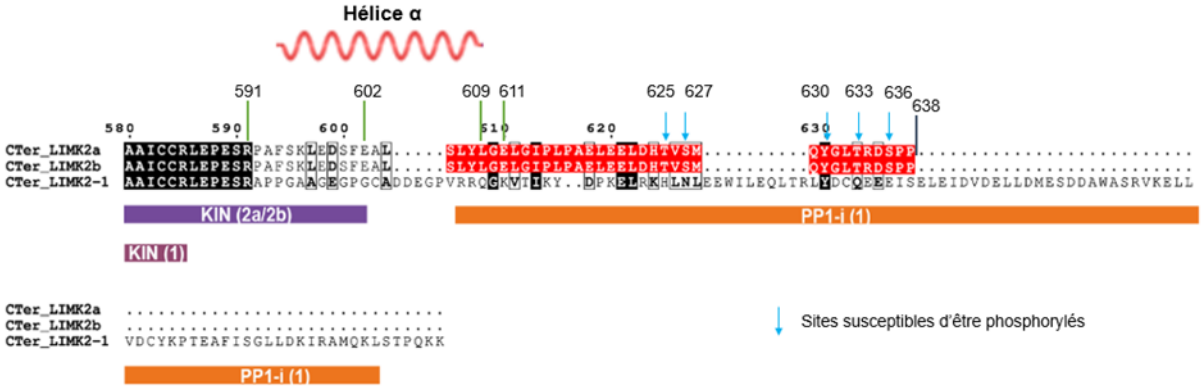

Figure 29 : **Extrémités C-terminales des 3 isoformes de LIMK2.**
A. Les domaines kinases de LIMK2a et LIMK2b sont indiqués en violet, celui de LIMK2-1 en grenat, le domaine PP1i de LIMK2-1 en orange. Les 4 constructions tronquées sont indiquées avec les traits verts. Les acides aminés potentiellement phosphorylés sur l'extrémité C-terminale sont marqués par des flèches bleues.

Célina va muter ces résidus un à un et testera leur activité kinase sur la cofiline et leur phosphorylation *in vitro*. Nous identifierons peut-être un nouveau site de phosphorylation et donc d'activation de LIMK2a. Il sera alors intéressant d'identifier la kinase responsable de cette phosphorylation.

D'autre part, la structure tridimensionnelle du complexe entre le domaine kinase de LIMK1 et la cofiline a été résolue par cristallographie aux Rayons X par deux groupes différents et publiée en même temps dans la PDB (PDB 5HVK et 5L6W) (Hamill et al., 2016; Salah et al., 2019).

L'interaction entre LIMK1 et la cofiline est non canonique. L'hélice α5 de la cofiline se loge spécifiquement et fortement dans une cavité hydrophobe du C-lobe de LIMK1 créée par une conformation inhabituelle de la boucle αFG. La Sérine 3 de la cofiline est alors orientée dans le site actif pour être phosphorylée (Figure 41).

Or, dans la structure de ce complexe, l'extrémité C-terminale de LIMK1 est loin du site d'interaction avec la cofiline, et nous avons montré que toutes nos protéines tronquées interagissent avec le cofiline. L'extrémité C-terminale de LIMK2 ne semble donc pas avoir de rôle dans son interaction avec la cofiline. Cependant, elle est cruciale pour l'activité kinase sur la cofiline. Nous avons aussi testé l'activité kinase de nos constructions tronquées sur un substrat universel, la Myelin Basic Protein, MBP. De façon surprenante, toutes nos constructions phosphorylent la MBP (résultats de Déborah). Identifier le rôle de cette extrémité C-terminale de LIMK2 vis-à-vis de la cofiline pourrait mettre un jour un nouveau mécanisme de régulation de l'activité kinase des LIMKs vis-à-vis de la cofiline.

3. *Etude de LIMK2-1 en tant que potentielle nouvelle PPP1R14*

Le domaine PP1i de LIMK2-1 a été identifié par homologie de séquence avec CPI-17, une protéine inhibant la protéine phosphatase 1 (Eto et al., 1997). Toute une famille de protéines inhibitrices de PP1 et homologues à CPI-17 a par la suite été décrite, elles sont dénommées PPP1R14 (Korrodi-Gregorio et al., 2014). Par homologie de séquence, LIMK2-1 pourrait appartenir à cette famille. La séquence du domaine PP1i de LIMK2-1 est particulièrement proche de celle de PHI-1, elles partagent 93 % d'identité (Figure 30).

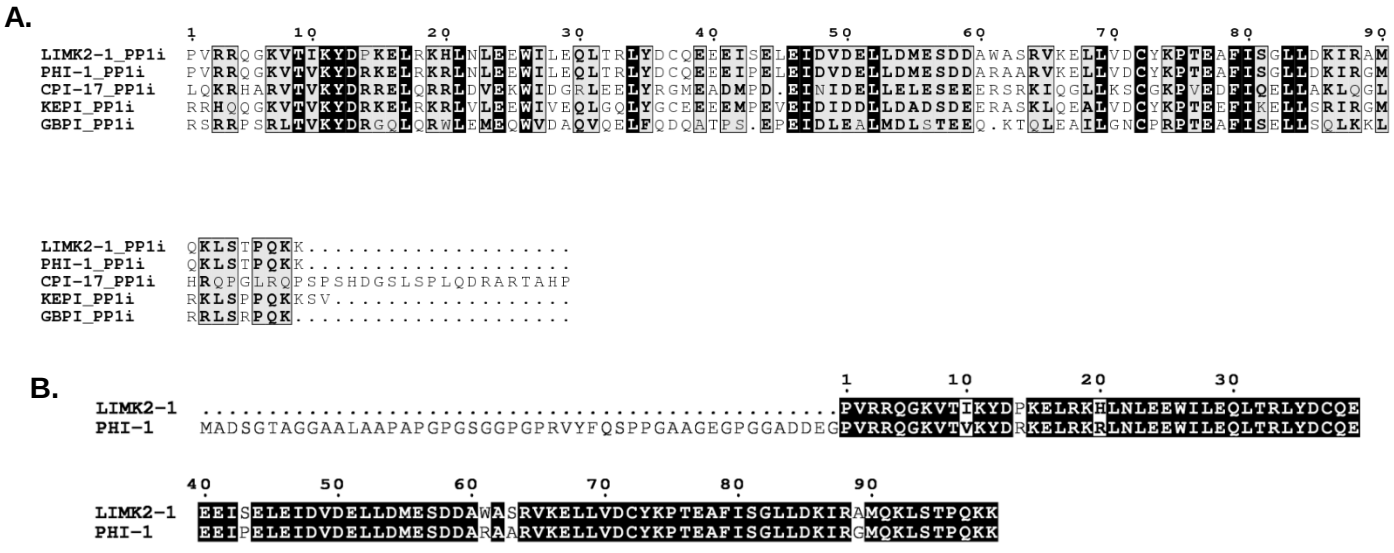

Figure 30 : **Alignement des domaines PP1i de la famille des PPP1R14 et de LIMK2-1**
A. Alignement du domaine PP1i de LIMK2-1 avec celui de tous les membres de la famille PPP1R14
B. Alignement du domaine PP1i de LIMK2-1 avec PHI-1

La régulation des protéines phosphatases est encore mal connue de nos jours. Contrairement aux kinases, qui sont plus de 500 dans le protéome humain, les protéases sont peu nombreuses, une centaine de Tyrosine phosphatases et une quarantaine de Ser/Thr phosphatases (Bollen et al., 2010). Leur spécificité vient du fait qu'elles forment des complexes ou phosphatase holoenzymes contenant l'unité catalytique et des unités régulatrices qui vont déterminer la spécificité de leur substrat et leur régulation. Les Ser/Thr phosphatases PP1 et PP2A assurent plus de 90% de l'activité phosphatase chez les eucaryotes, PP1 catalysant la majorité de ces déphosphorylations puisqu'elle forme environ 700 holoenzymes contre 70 pour PP2A.

Nous avons montré, *in cellulo*, que LIMK2-1 inhibe partiellement la déphosphorylation de la cofiline par PP1 (Vallee et al., 2018). Nous avons voulu mettre au point un test *in vitro* pour évaluer l'inhibition de LIMK2-1 sur PP1 sans succès. Dans ce test, nous avons purifié l'unité catalytique PP1α à partir de cellules HEK-293 transfectées par un vecteur codant pour le gène de PP1α étiqueté Flag. Notre PP1α purifiée s'est avérée incapable de déphosphoryler la phospho-cofiline *in vitro*. Les articles anciens décrivant l'activité phosphatase de PP1 utilisaient des extraits de tissus (muscles de lapin, aorte de porc) pour isoler cette protéine et caractériser son activité. Au moment de notre étude, PP1 recombinante active n'était plus vendue par aucun fournisseur. Cependant, un article récent sur PP2A donne de nouvelles pistes pour travailler avec les phosphatases, nous allons les explorer (Gao et al., 2019). Par ailleurs, nous avons travaillé sur PP1α, or il existe trois gènes codant pour PP1 : PP1α, PP1β/δ, PP1γ. Il faudrait tester ces autres unités catalytiques PP1.
Si nous parvenons à mettre au point un test *in vitro* où nous observons la déphosphorylation de la phospho-cofiline par PP1, nous pourrons alors tester si LIMK2-1 inhibe cette activité *in vitro*. Par ailleurs, les membres de PPP1R14 possèdent une Thr conservée qui, lorsqu'elle est phosphorylée, décuple le pouvoir d'inhibition de ces dernières. LIMK2-1 possède cette Thr (Thr596) qui appartient à son domaine PP1i. Il serait intéressant de tester si la phosphorylation de cette Thréonine exacerbe l'activité de LIMK2-1 sur PP1, et d'identifier la kinase responsable de cette phosphorylation.

4. *Etude de l'isoforme LIMK2-1 : implication dans la déficience intellectuelle*

Au cours de leurs thèses respectives, Julie Tastet et Hélène Cubéros (thèse en cotutelle avec Patrick Vourc'h et Christian Andres, 2008-2012 et 2013-2016) ont mis en évidence

l'implication de LIMK2-1 dans la déficience mentale. Chez des patients déficients mentaux, Julie a mis à jour une mutation Ser668Pro spécifique du domaine PP1i de LIMK2-1, et elle a montré que ce mutant influence la neuritogenèse. Ces résultats ont été publiés en 2019 dans Neuroscience (Tastet et al., 2019). Nous voulons poursuivre l'étude de ce mutant, en particulier des résultats préliminaires montrent qu'il interagit plus faiblement avec SecPH-Nf1. Nous voulons aussi déterminer si le domaine PP1i de ce mutant est fonctionnel, et si c'est la présence de la Pro en position 668 ou l'absence de la Ser 668 qui est délétère.

5. *Etude des propriétés nanomécanistiques de cellules surexprimant une des isoformes de LIMK2*

Je viens d'initier une nouvelle collaboration avec Michal Sarna (Université de Jagellonne, Cracovie, Pologne), dans le cadre du Laboratoire International Associé (LIA) miR Tango. Nous voulons étudier les propriétés nanomécanistiques de cellules surexprimant une des isoformes de LIMK2 par différentes techniques biophysiques, en particulier l'AFM (Microspcopie à Force Atomique). En effet, nous avons montré que les isoformes de LIMK2 induisent la formation de fibres de stress. Cependant, celles induites par l'isoforme LIMK2-1 semblent différentes de celles induites par LIMK2a/2b en immunofluorescence (Vallee et al., 2018). Or ces fibres de stress influencent certainement les propriétés nanomécanistiques des cellules. Ces propriétés nanomécanistiques des cellules, en particulier leur élasticité, jouent un rôle clé dans le potentiel métastatique des cellules (Kilpatrick et al., 2015; Luo et al., 2016; Sokolov et al., 2013). Cette nouvelle collaboration a concrètement débuté en janvier 2019 avec un étudiant en Master 2, Janusz Koszucki, qui est venu s'initier à la culture cellulaire trois semaines dans notre équipe et que j'ai encadré. Il a ensuite réalisé des expériences de biophysique à Cracovie en combinant l'AFM et la microscopie confocale afin de déterminer des paramètres reflétant l'élasticité des cellules. Il a travaillé sur des cellules HeLa transfectées par l'une des isoformes de LIMK2 étiquetées YFP. Il a montré que chacune des isoformes induit une augmentation de l'épaisseur moyenne du cortex d'actine et du nombre de points d'adhésion focale. Il a aussi déterminé le module de Young dans chacune de ces conditions. Ce module de Young permet de quantifier les propriétés élastiques d'une cellule. Plus la valeur de ce module est faible, plus la cellule est « élastique ». Ainsi, les adipocytes sont les cellules les plus souples avec un module de Young de 0,1 kPa, tandis que les ostéoblastes sont très rigides avec un module de Young de 10 kPa, les myofibroblates sont intermédiaires avec un module de Young d'environ 3,5 kPa. Janusz a montré que chacune des isoformes de LIMK2 induit une rigidité des cellules

avec une augmentation du module de Young par rapport à des cellules transfectées par le plasmide parental. Or il a été montré que l'élasticité des cellules est corrélée à la structure du cytosquelette d'actine. Lorsque le cytosquelette d'actine d'une cellule est désorganisé par ajout d'agents pharmacologiques, on observe une diminution du module de Young (Rotsch and Radmacher, 2000). Les résultats de Janusz sont cohérents avec ces données. Les isoformes de LIMK2 induisent la formation de fibres de stress, qui conduit à une rigidification de la cellule et donc à une augmentation du module de Young. Cette étude doit être complétée pour reproduire et consolider ces données.

5. Développement d'inhibiteurs des LIMKs, nouvelles cibles thérapeutiques dans le traitement de la neurofibromatose de type I, des cancers et de certaines maladies neurologiques

1. *Inhibiteurs « Petites molécules chimiques » à partir de la molécule LX7101*

Nous avons démontré l'implication de LIMK2 dans la neurofibromatose de type I. Starinsky-Elbaz *et al*. ont montré l'implication de LIMK1 dans la neurofibromatose de type I (Starinsky-Elbaz et al., 2009). Par ailleurs, de nombreuses données de la littérature montrent que les LIMKs jouent un rôle majeur dans le développement de nombreux cancers et dans le caractère invasif et donc métastasique des tumeurs cancéreuses. Les LIMKs sont aussi impliquées dans un certain nombre de maladies du système nerveux (Figure 8).

Ces protéines apparaissent donc comme de nouvelles cibles thérapeutiques. Elles sont d'autant plus intéressantes qu'elles agissent et sur le cytosquelette d'actine et sur les microtubules, en comparaison des taxanes qui ciblent uniquement les microtubules. Les LIMKs sont donc des cibles alternatives très intéressantes, tout particulièrement dans les cancers résistants.

Depuis une dizaine d'années, des inhibiteurs petites molécules sont développés contre les LIMKs. Cependant, seulement deux de ces inhibiteurs sont allés en phase préclinique et ont montré des effets sur des tumeurs xénogreffées chez la souris : tumeurs du sein, du pancréas et leucémie (Prudent et al., 2012; Prunier et al., 2016; Rak et al., 2014), et un (LX7101) est entré en phases cliniques I et II pour le traitement du glaucome, sans résultats publiés.

Le champ d'investigation est donc très ouvert, et nous nous y sommes lancés en 2015.

Nous avons développé un projet collaboratif en nous associant à des modélisateurs (équipe de Pascal Bonnet), et à des chimistes (équipe de Sylvain Routier) de l'ICOA à Orléans.

Les travaux de modélisation ont été réalisés par Abdennour Braka, étudiant en thèse encadré par Samia Aci-Sèche, les travaux de synthèse chimique par Anthony Champiré étudiant en thèse, Margaux Sainjon, étudiante en Master 2 et les CDD Gwenaël Bourdeau et Thomas Lelièvre encadrés par Karen Plé, et les travaux de biologie par Aurélie Cosson, CDD IE, que j'ai encadrée.

En s'inspirant du squelette chimique de la molécule développée par Lexicon et qui est allée en phases cliniques I et II, LX7101, (Figure 31), (Harrison et al., 2015) et de son précurseur n°23 (Harrison et al., 2009), les chimistes ont synthétisé une librairie de 138 composés.

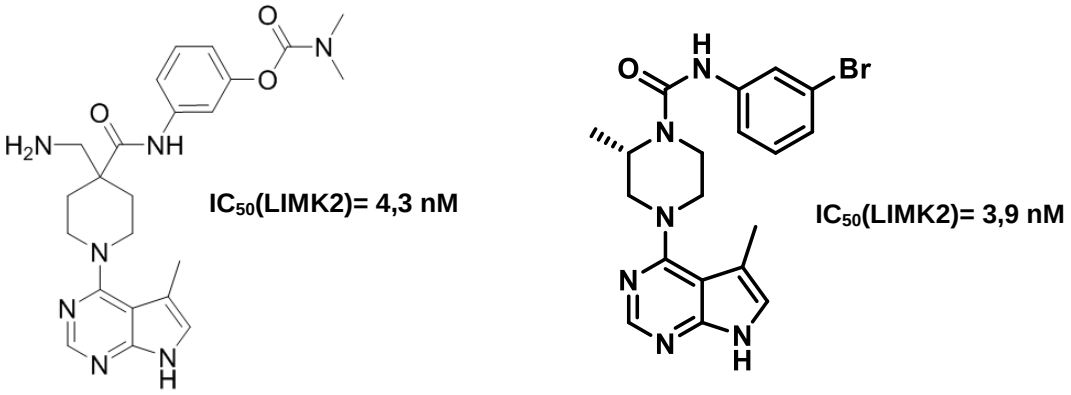

Figure 31 : Structures chimiques du LX7101 et de son précurseur n°23

Les chimistes ont modifié le squelette du précurseur n°23 selon trois grandes zones (Figure 32) : (i) au Nord, en vert, la substitution de l'aromatique, (ii) au centre, en rouge, la modulation du cycle central, (iii) au Sud, en bleu, la modification de la base hétérocyclique.

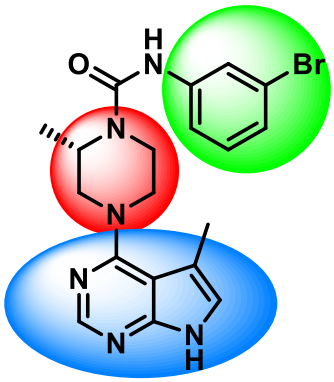

Figure 32 : Modifications chimiques sur lesquelles les chimistes ont travaillé

L'activité *in vitro* de ces 138 molécules a été déterminée par le prestataire Invitrogen-Life Technologies sur LIMK1 et LIMK2 en utilisant le test « Lanthascreen Eu Kinase Binding Assay » qui est basé sur une compétition d'interaction entre un traceur et notre inhibiteur à caractériser (détermination de Ki).

A.

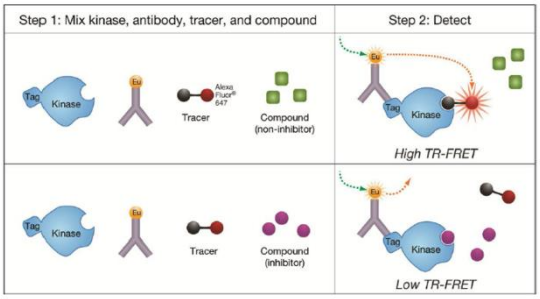

B.

	Nombre de composés dont Ki <10 nM	Nombre de composés dont 10<Ki<50 nM
LIMK1	**16**	**44**
LIMK2	**12**	**41**

C.

Compounds	IC50(LIMK1) nM	IC50(LIMK2) nM
LIMKi3 (BMS5)	7	8
LX7101		4,3
Pyr1	50	75
T56-LIMKi		
Damnacanthal	800	1530
aminothiazole pyrimidines	58	38
sulfonamide derivative	3200	39
CRT0105446	8	32

Figure 33 : Activités *in vitro* de nos composés sur LIMK1 et LIMK2.
A. Principe du test réalisé par Invitrogen-Life Technologies.
B. Résultats de nos composés
C. Données de la littérature

Plus de 50 de nos inhibiteurs ont des Ki sur LIMK1 et LIMK2 inférieurs à 50 nM et plus d'une dizaine ont un Ki inférieur à 10 nM. Ces résultats sont tout à fait satisfaisants comparés aux données de la littérature (Figure 33).

L'activité de nos composés a aussi été testée sur ROCK1 et ROCK2, à une seule concentration de 1µM en utilisant le test « Z'-LYTE » réalisé par le prestataire Invitrogen-Life Technologies. Ce test est basé sur le clivage protéolytique sélectif d'un peptide non-phosphorylé par rapport à sa forme phosphorylée, ce peptide possédant à chacune de ses extrémités un couple de fluorophores FRET. Nous avons alors pu classer nos composés en deux groupes : ceux inhibant spécifiquement les LIMKs, et ceux possédant une activité duale LIMKs/ROCKs. Pour caractériser précisément ces deux groupes, il faudrait déterminer les IC_{50} de nos composés sur

ROCK1 et ROCK2 (prioritairement ceux ayant un pourcentage d'inhibition entre 30 et 60%), pour des raisons de coût, nous ne l'avons pas fait systématiquement, mais nous pensons le faire sur quelques composés prometteurs de par les résultats qu'ils ont donnés sur d'autres tests.
La sélectivité de 18 de nos composés a été testée par la société Eurofins sur un panel de 100 kinases à la concentration de 1 µM. 8 de nos composés sont particulièrement sélectifs des LIMKs (Figure 34).

	Nombre de kinases inhibées à >60 %	Nombre de kinases inhibées à 40-60%	Nombre de kinases inhibées à 20-40%
AC419	2	6	11
TL09	1+2	2	14
AC572	2+2	2	22
GB126	2+2	5	13
TL23	2+2	6	29
AC549	3+2	1	17
TL154	3+2	3	8
TL144	5+2	6	21

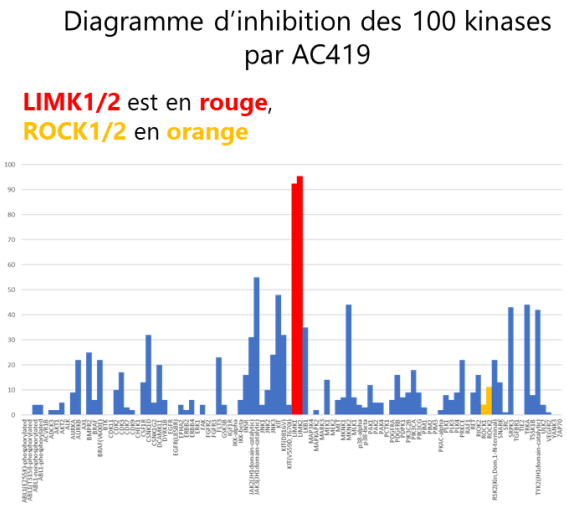

Figure 34 : Sélectivité de nos composés sur un panel de 100 kinases, réalisés par Eurofins.

Nous avons testé la cytotoxicité de nos composés sur différentes lignées cellulaires en utilisant le test CellTiter-Glo® Luminescent Cell Viability de chez Promega, qui permet de mesurer la quantité d'ATP, reflétant le métabolisme des cellules vivantes. Les inhibiteurs sont incubés pendant 48h à différentes concentrations (Figure 35).

Lignées cellulaires	Nombre de composés dont la cytotoxicité < 10 µM	Nombre de composés dont la cytotoxicité 10-25 µM	Nombre de composés dont la cytotoxicité > 25 µM	Nombre de composés testés
HeLa	2	19	29	50
MPNST88-14	0	0	17	17
NSC34	0	8	9	17
hTERT-RPE	2	18		20
HCT116	8	12		20
MDA-MB-231	1	19		20
SH-SY5Y	1	19		20
U2OS	5	15		20
fibroblastes	0	0	4	4

Figure 35 : Cytotoxicité de nos composés sur différentes lignées cellulaires.
Les essais sur 4 colonnes ont été réalisés par Aurélie au CBM, les essais sur 3 colonnes ont été réalisés à Roscoff sur la plateforme KISSf dirigée par Sandrine Ruchaud.

Nos composés montrent des gammes de cytotoxicité assez larges, ce qui permet d'envisager de les utiliser pour différentes indications : cancer pour les plus toxiques, troubles neurologiques pour les moins toxiques.

L'activité cellulaire de nos composés a été évaluée sur l'inhibition de la phosphorylation de la cofiline par Western Blot, grâce à un anticorps spécifique anti-phospho-Ser3-cofiline, sur trois lignées cellualires : HeLa, MPNST88-14 et MPNST90-8. Les MPNST (Malignant Peripheral Nerve Sheath Tumors) sont des tumeurs malignes très agressives des gaines nerveuses périphériques de patients atteints de NF1. 73 composés ont été testés sur les HeLa. Deux composés de référence ont été inclus dans ces tests : LIMKi3, un des tout premiers inhibiteurs des LIMKs décrit dans la littérature (Ross-Macdonald et al., 2008) et LX7101. 26 de nos composés sont plus efficaces que la référence LX7101, résultant à plus de 85% d'inhibition de la phosphorylation de la cofiline. Trois de ces composés sont particulièrement actifs, inhibant à plus de 95% la phosphorylation de la cofiline (Figure 36).

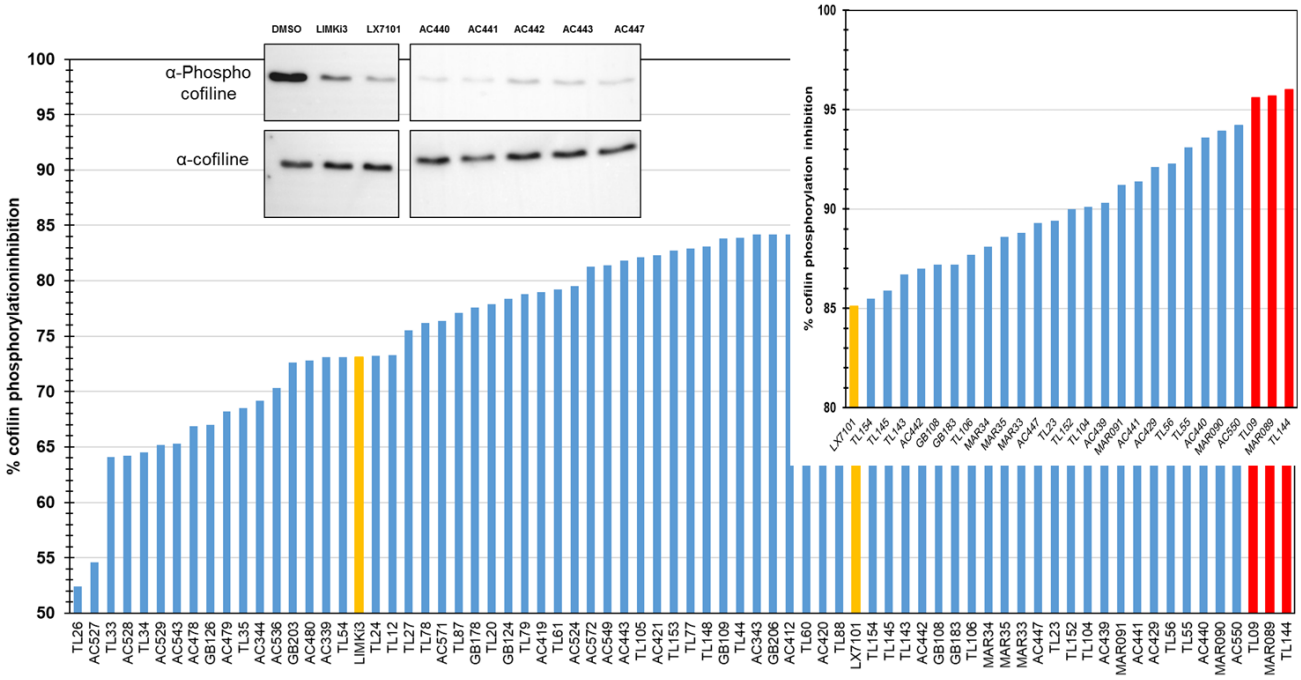

Figure 36 : Inhibition de la phosphorylation de la cofiline par nos composés sur les cellules HeLa. Les cellules HeLa sont incubées avec 25 µM de chacun des composés pendant 2 heures. Les cellules sont lysées. L'extrait est analysé par Western Blot avec des anticorps anti-phospho-cofiline et anti-cofiline.

20 composés ont été testés sur cellules MPNST88-14 (Figure 37), et 12 sur cellules MPNST90-8. Respectivement, 5 et 4 de nos composés sont plus efficaces que la référence LX7101. L'étude n'est pas assez exhaustive pour observer une différence entre ces deux lignées.

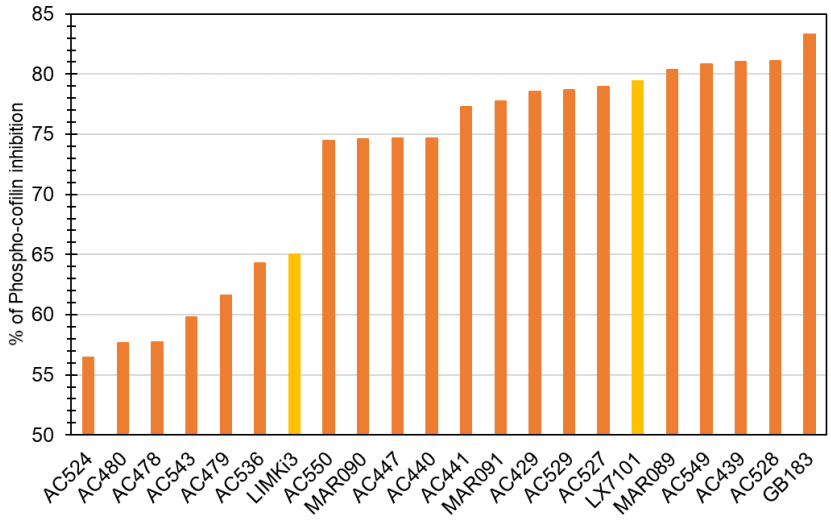

Figure 37 : Inhibition de la phosphorylation de la cofiline par nos composés sur les cellules MPNST88-14.
Les cellules MPNST88-14 sont incubées avec 25 µM de chacun des composés pendant 2 heures. Les cellules sont lysées. L'extrait est analysé par Western Blot avec des anticorps anti-phospho-cofiline et anti-cofiline.

Trois composés ont tout particulièrement retenu notre attention, AC527, AC528 et AC529. Ils inhibent modérément la phosphorylation de la cofiline des cellules HeLa, par contre ils sont très actifs sur les cellules MPNST88-14 (Figure 38)

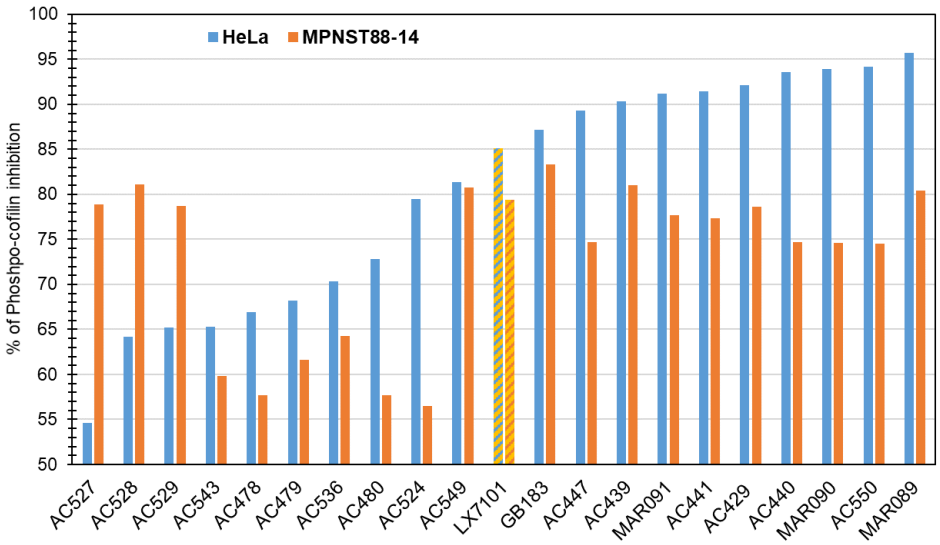

Figure 38 : Comparaison de l'inhibition de la phosphorylation de la cofiline par nos composés sur les cellules HeLa et MPNST88-14.

Nous avons aussi observé la formation des fibres de stress induites par la surexpression de LIMK2 en présence ou non de deux de nos inhibiteurs (Figure 39). Sans aucun traitement ou en présence de DMSO (condition contrôle), on observe des fibres de stress, qui disparaissent en présence de nos composés.

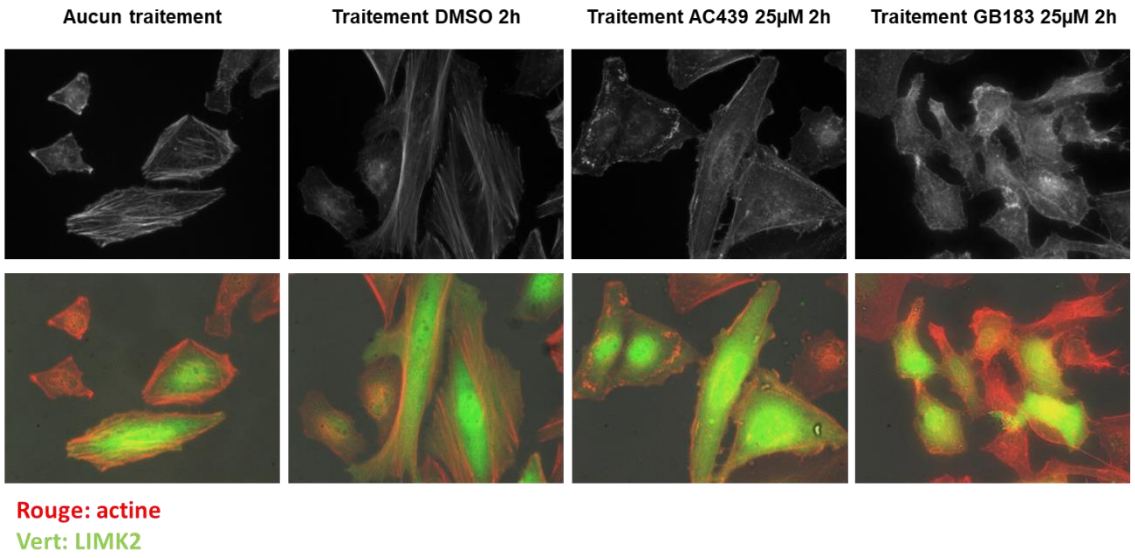

<u>Figure 39</u> : Observation des fibres de stress induites par LIMK2 en présence ou non de deux de nos composés.
Des cellules HeLa sont transfectées avec un plasmide contenant LIMK2 pendant 48h, puis incubées pendant 2 heures avec 25µM de nos composés (DMSO contrôle négatif). Les fibres de stress sont visualisées par un marquage à la phalloïdine.

La migration cellulaire de cellules U2OS (ostéosarcomes) a été testée par Béatrice Josselin de l'équipe de Sandrine Ruchaud à Roscoff, par un test de « wound healing » (Figure 40).

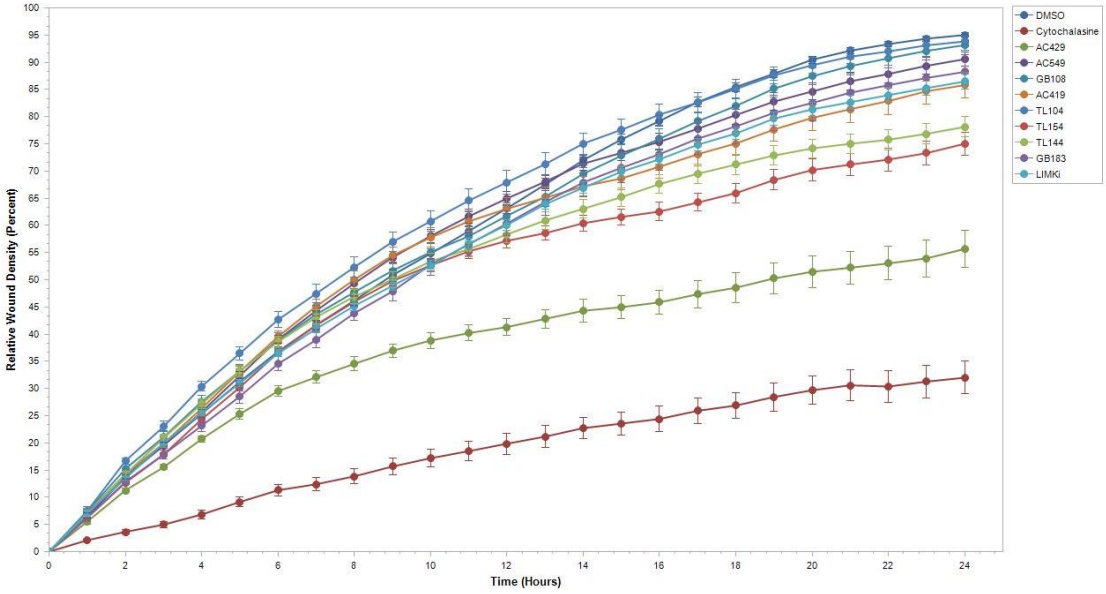

<u>Figure 40</u> : Test de migration cellulaire (Wound Healing).
Des cellules U2OS sont incubées avec 2.5 µM de nos composés 5 heures après starvation (0,5% SVF). La migration cellulaire est observée pendant 24 heures par l'IncuCyte® S3.

Le contrôle positif de cette expérience est la cytochalasine, un inhibiteur de la polymérisation de l'actine, qui inhibe la migration cellulaire. Un de nos composés se détache nettement, AC429, et deux autres de façon moins prononcée, TL154 et TL144. Ces trois composés bloquent donc partiellement la migration des cellules U2OS, ce qui démontre leur efficacité *in cellulo*.

L'effet de ces trois composés a aussi été étudié sur les microtubules sur la plateforme KISSf à Roscoff. AC429 a un effet drastique, entraînant une disparition quasi-totale des microtubules astraux.

Aurélie a aussi caractérisé l'effet de 10 de nos inhibiteurs sur la croissance des neurites de cellules NSC34 (motoneurones de souris). 4 de nos composés induisent une augmentation significative de la longueur des neurites de ces cellules.

Nous voulons aussi caractériser l'effet de ces composés sur le cycle cellulaire et sur la dynamique des microtubules, et déterminer leurs propriétés pharmacologiques. La stabilité de 5 composés en présence de microsomes de souris a été testée sur la plate-forme TechMed^{ILL} à Strasbourg. Deux composés ont des durées de vie proches de celle de LX7101 (entre 15 et 20 minutes), les autres sont très peu stables.

Quand nous aurons bien caractérisé nos inhibiteurs par ces différents tests, nous pourrons alors commencer des expériences précliniques en testant nos « meilleurs » inhibiteurs sur 3 pathologies différentes dans le cadre de trois projets :

1. Projet ILIADE, (financement ARSLA) : sur un modèle de souris *SOD1*^{G93A}, modèle de Sclérose Latérale Amyotrophique (SLA) (Gurney, 1994), en collaboration avec Patrick Vourc'h et Christian Andres à Tours ;
2. Projet Prématuration CNRS : sur des tumeurs d'ostéosarcome en collaboration avec Franck Verrecchia à Nantes. De récentes publications ont montré l'implication des LIMKs dans le développement des ostéosarcomes, cancer pédiatrique fatal (Wang et al., 2017; Yang et al., 2018);
3. Projet ANR, CliNeF1 : sur un tout nouveau modèle de souris *Nf1* développé par Piotr Topilko à Mondor (Radomska et al., 2019), modèle qui récapitule tous les phénotypes de la neurofibromatose de type 1, nous nous intéresserons tout particulièrement aux neurofibromes cutanés et plexiformes.

2. *Développement d'un test physiologique original pour identifier de nouveaux inhibiteurs des LIMKs*

Les inhibiteurs « petites molécules » que nous avons développés sont inspirés du squelette du LX7101. Il serait intéressant d'élargir la diversité chimique des molécules inhibitrices des LIMKs (autres squelettes chimiques, peptides, …).

Les LIMKs étant des cibles thérapeutiques particulièrement intéressantes, depuis une dizaine d'années de nombreux inhibiteurs « petites molécules » de ces kinases ont vu le jour. Différents squelettes chimiques sont répertoriés (Prunier et al., 2017). La résolution de la structure tridimensionnelle du domaine kinase de LIMK1 et LIMK2 a permis d'optimiser ces inhibiteurs « petites molécules » par modélisation moléculaire et docking dans le site actif de ces kinases.

Plusieurs criblages ont été réalisés afin de diversifier ces squelettes chimiques et de pouvoir tester des banques actuellement disponibles commercialement ou des chimiothèques de certains laboratoires. Ces criblages sont basés sur des tests *in vitro* d'inhibition de l'activité kinase des LIMKs sur la cofiline ou d'inhibition de l'interaction entre la cofiline et l'actine en présence des LIMKs (Harrison et al., 2009; Mardilovich et al., 2015; Ohashi et al., 2014; Salah et al., 2019; Sleebs et al., 2011), ou sur leur activité *in cellulo* sur le remodelage des microtubules (Prudent et al., 2012).

Or de nouvelles données structurales montrent que les LIMKs sont des kinases particulièrement atypiques dans leur interaction et phosphorylation de la cofiline (Hamill et al., 2016; Salah et al., 2019). Le site de phosphorylation de la cofiline étant la Serine 3, le mécanisme classique de reconnaissance de l'acide aminé à phosphoryler via la reconnaissance des acides aminés adjacents (motif linéaire, (Ubersax and Ferrell, 2007)) n'est pas possible. Une interaction non canonique entre la cofiline et le domaine kinase de LIMK1 a été décrite par deux équipes différentes (Hamill et al., 2016; Salah et al., 2019). Les résultats sont concordants et démontrent une certaine flexibilité de cette interaction (l'angle d'interaction étant légèrement différent entre ces deux études). Une boucle de la cofiline, non adjacente de la Serine 3 dans la séquence, mais proche dans le repliement 3D s'avère cruciale pour l'interaction de cette dernière avec LIMK1. La boucle va se plaquer dans une cavité hydrophobe de LIMK1, et forcer l'orientation de la Serine 3 vers le site actif de phosphorylation (Figure 41).

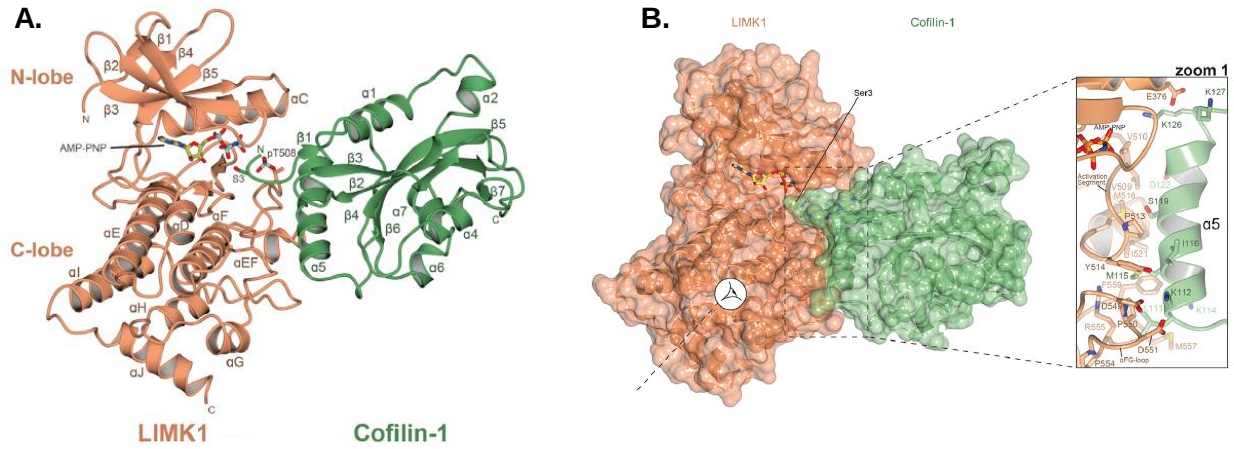

<u>Figure 41</u> : Structure tridimensionnelle de l'interaction entre le domaine kinase de LIMK1 et la cofiline, d'après (Hamill *et al.*, 2016) pdb 5HVK.

LE domaine kinase de LIMK1 est représentée en orange et la cofiline en vert. L'hélice α5 de la cofiline vient se plaquer dans une cavité hydrophobe de LIMK1, ce qui oriente la Serine 3 de la cofiline dans le site actif de LIMK1.

A. Représentation en rubans. La Serine 3 de la cofiline et la phospho-Thr508 de LIMK1 sont représentés sous forme de bâtons.

B. Représentation des surfaces d'interaction. En encadré, détail de l'interaction entre la boucle de la cofiline et la cavité hydrophobe de LIMK1.

Il serait particulièrement intéressant de prendre en compte ce mécanisme d'interaction atypique pour identifier de nouveaux inhibiteurs des LIMKs.

Pour cela, nous proposons de développer un nouveau test physiologique original basé sur l'utilisation de levure *Saccharomyces cerevisiae* thermosensible *cof1-ts*.

Chez la levure *Saccharomyces cerevisiae*, le gène de la cofiline est présent et régule aussi la polymérisation des filaments d'actine (Lappalainen and Drubin, 1997; Moseley and Goode, 2006). Or ce gène est essentiel, la levure n'est pas viable en son absence. L'équipe de David Drubin a développé des souches thermosensibles mutées dans le gène *COF1*. A 25°C, ces souches poussent normalement, tandis qu'à 37 °C elles ne sont pas viables (Lappalainen et al., 1997). Or le gène COF1 humain est capable de complémenter ce gène muté, c'est-à-dire que lorsque la levure *cof1-ts* est transformée par un plasmide permettant l'expression de la cofiline humaine, cette souche est capable de pousser à 37°C. Les LIMKs ne sont pas présentes chez la levure *Saccharomyces cerevisiae*, elles sont apparues plus tard dans l'évolution (Te Velthuis et al., 2007). Chez la levure *Saccharomyces cerevisiae*, l'activité de la cofiline n'est pas régulée par phosphorylation par les LIMKs. On ne sait pas trop comment l'activité de la cofiline est régulée chez la levure *Saccharomyces cerevisiae*. Par contre, il a été mis en évidence que la phosphorylation de la Serine de la cofiline est létale pour la levure : lorsqu'une souche est

transformée par un plasmide permettant l'expression de LIMK1, cette souche n'est pas viable (Lappalainen et al., 1997; Moseley and Goode, 2006).

Nous voulons développer un nouveau test permettant de cribler de potentiels nouveaux inhibiteurs des LIMKs basé sur ces observations (Figure 42).

La souche *cof1-ts* sera utilisée. Elle sera transformée par les plasmides permettant la surexpression constitutive de la cofiline humaine et la surexpression de LIMK2 ou LIMK1 sous contrôle d'un promoteur inductible par le galactose. Lorsque cette souche est cultivée sur milieu Galactose à 37°C, LIMK1 ou LIMK2 sont induites et conduisent à la létalité de la souche. Si dans ces conditions, on ajoute un inhibiteur des LIMKs, la souche devrait alors pouvoir pousser à 37°C. Il faudra tout d'abord valider cette hypothèse. Si ce test est validé, nous pourrons alors cribler différentes banques d'inhibiteurs, telle la banque Prestwick.

L'originalité de ce test réside dans le fait qu'il est réalisé dans des conditions physiologiques, sur un organisme entier, en prenant la phosphorylation de la cofiline comme critère. Il n'est pas basé uniquement sur une compétition d'interaction au niveau du site actif des kinases LIMKs.

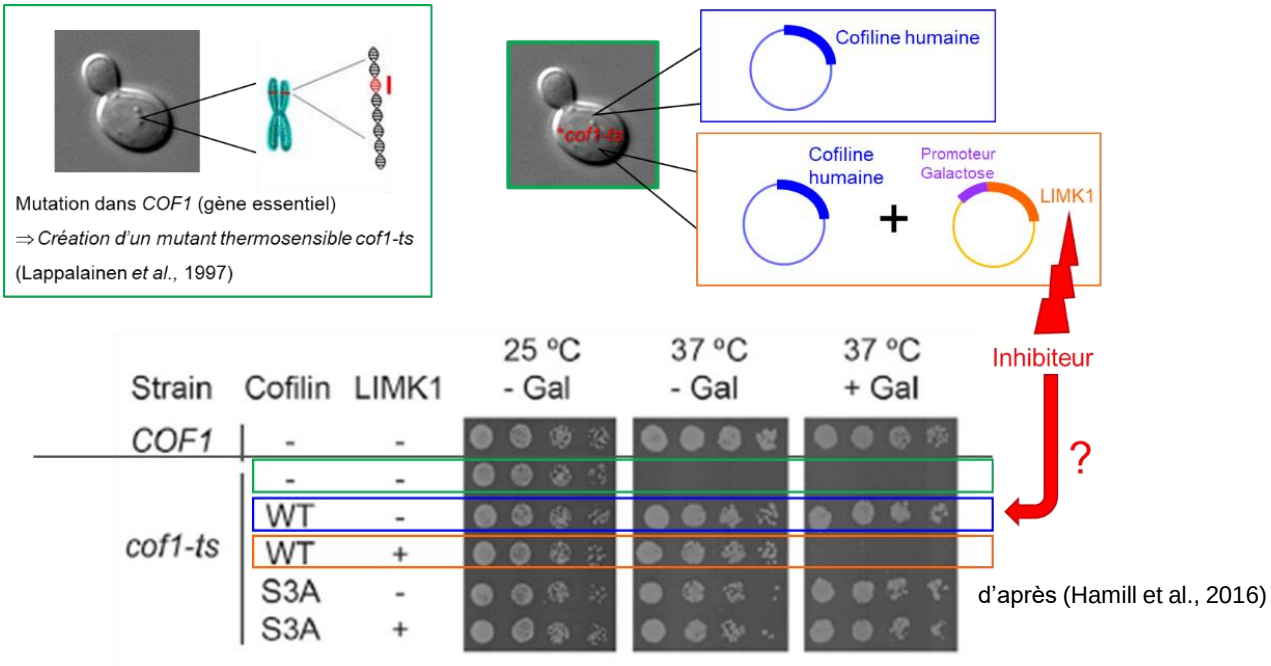

<u>Figure 42</u> : Principe du test sur *Saccharomyces cerevisiae* pour tester de nouveaux inhibiteurs des LIMKs.

Carré vert : Une mutation est introduite dans le gène *COF1*, rendant cette souche thermosensible. Dans un test de croissance en goutte (partie inférieure de la Figure), cette souche pousse à 25°C, température permissive, mais pas à 37°C.

Carré bleu : Lorsque cette souche *cof1-ts* est transformée par un plasmide permettant la surexpression de la cofiline humaine, on restaure le phénotype, *i.e.* la croissance à 37°C. La cofiline humaine complémente la cofiline de levure.

Carré orange : Lorsque la souche *cof1-ts* est cotransformée par un plasmide permettant la surexpression constitutive de la cofiline humaine et par un plasmide permettant la surexpression de LIMK1 sous contrôle d'un promoteur inductible au galactose, on perd cette complémentation. Cette souche n'est pas capable de pousser à 37°C du fait de la phosphorylation de la cofiline par LIMK1, processus létal pour la levure *Saccharomyces cerevisiae.*

6. Mettre à jour un lien moléculaire entre les LIMKs et la dynamique des microtubules

Les LIMKs sont impliquées dans la dynamique des microtubules, elles favorisent la forme libre de la tubuline (Gorovoy et al., 2005; Po'uha et al., 2010). La régulation de la dynamique des microtubules par les LIMKs se révèle être indépendante de celle des filaments d'actine (Heng et al., 2012; Prudent et al., 2012). Les acteurs moléculaires reliant les LIMKs à la dynamique des microtubules ne sont pas connus. Il serait particulièrement intéressant d'identifier cette « potentielle » nouvelle voie de signalisation cellulaire.

Il y a quelque temps, nous avons réalisé une étude protéomique par spectrométrie de masse de l'interactome des trois isoformes de LIMK2 (Figure 43). L'idée était de trouver des partenaires différents entre ces trois isoformes, et peut-être de trouver une explication au fait que LIMK2-1 ne phosphoryle pas la cofiline. Rien de tel n'est apparu concrètement.

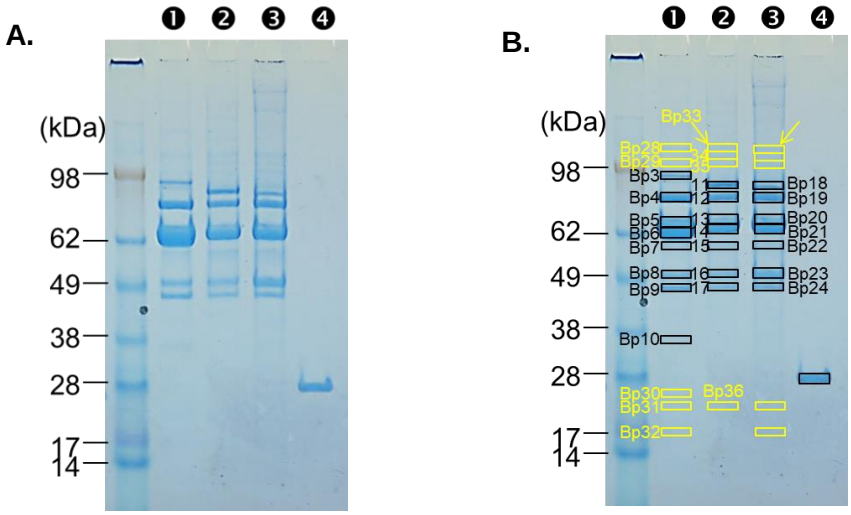

Figure 43 : Approche protéomique de l'interactome des isoformes de LIMK2.
Des cellules HEK293 ont été transfectées par une des isoformes de LIMK2 étiquetée YFP en C-terminal. Une immunoprécipitation est réalisée avec des billes GFP-trap. Les billes sont éluées en tampon Laemmli. L'éluat est chargé sur gel. Après migration, les bandes sont découpées, digérées sur gel à la trypsine. Les échantillons sont analysés par spectrométrie de masse.
A. Gel obtenu. Coloration au Bleu de Coomassie. ❶ LIMK2-1-YFP, ❷ LIMK2a-YFP, ❸ LIMK2b-YFP, ❹ YFP
B. Bandes découpées pour identification.

Par contre, des partenaires identifiés dans cette étude pourraient être de bons candidats pour relier les LIMKs à la dynamique des microtubules. Dans les microtubules, l'acétylation de la tubuline assure la stabilité de ces derniers. Plusieurs protéines en lien avec le processus

d'acétylation ont été identifiées dans cette étude : (i) HDAC1, HDAC2, HDAC6, des histones déacétylases, or HDAC6 est connue pour déacétyler la tubuline (Hubbert et al., 2002; Skultetyova et al., 2017) et (ii) HAT1, une histone acetyl transferase.

Par ailleurs, plusieurs chaînes de la tubuline ont été trouvées en interaction avec les isoformes de LIMK2. Les LIMKs pourraient peut-être agir directement sur la tubuline sans intermédiaire.

7. Développement de biocapteurs à base de levure et de matériaux lamellaires pour détecter des polluants dans les cours d'eau

Fin 2016, Régis Guégan, de l'Institut des Sciences de la Terre d'Orléans (ISTO), m'a contactée pour mes compétences de levuriste. Il voulait développer un nouveau projet original de biocapteurs en combinant des matériaux lamellaires originaux et des levures sensibles à différents analytes afin de détecter en temps réel et à faible coût des polluants en milieu aquatique (dans l'eau des rivières).

Il recherchait donc un biologiste ayant des compétences en levure. Bien que ce projet ne soit pas du tout en rapport avec mes activités de recherche sur NF1 et LIMK2, il m'a semblé très intéressant et particulièrement novateur. Et la littérature montre que ce champ d'investigation des biocapteurs (biosensors) est en pleine expansion (Jarque et al., 2016; Wan et al., 2019).

L'originalité du projet repose sur la combinaison (Figure 44) :

- de levure, organisme vivant connu pour être extrêmement sensible pour détecter différents analytes tels que des éléments traces métaux, des pesticides ou encore des composés pharmaceutiques, et permettant de rapporter leur présence par l'expression de différentes protéines dont l'activité est détectable *in situ,* et
- de matériaux lamellaires de type minéraux argileux, ou de matériaux nanofeuillets (résultants de l'exfoliation ou la délamination des matériaux lamellaires) associés à des matrices de biopolymères (alginates par exemple) ou des hydrogels.

Les matériaux lamellaires permettent l'immobilisation des levures pour créer un système portatif. Mais ils devraient aussi protéger les levures et augmenter leur viabilité et améliorer la sensibilité de détection de ce système.

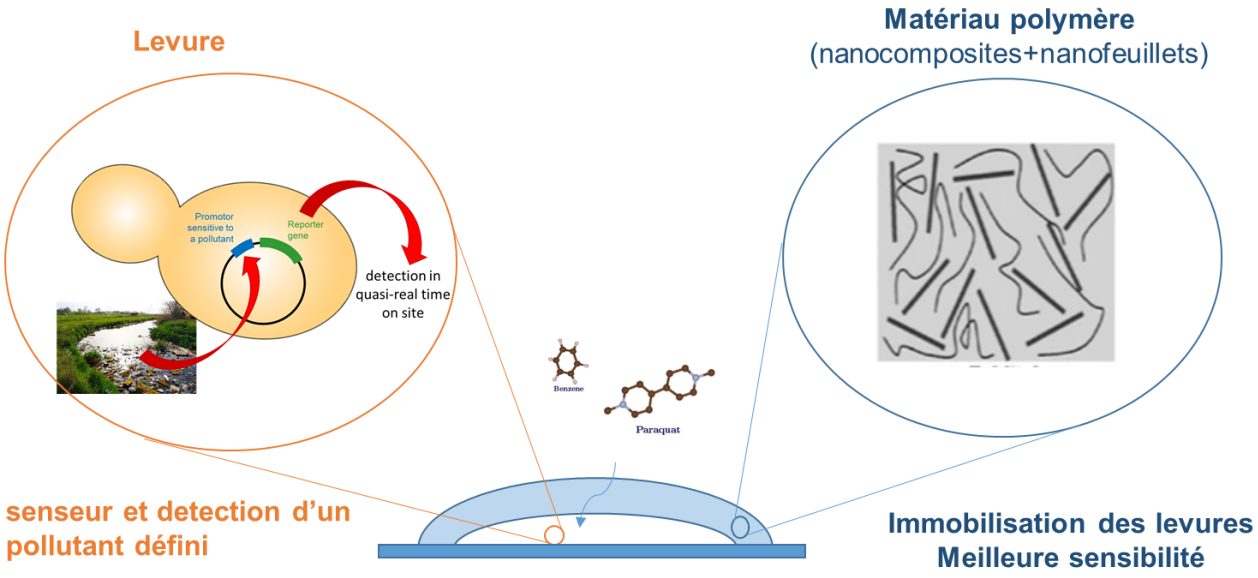

Figure 44 : Représentation schématique de nos biocapteurs combinant des levures (senseurs et rapporteur d'un polluant défini) et des matériaux polymères (pour immobiliser les levures et augmenter la sensibilité du système).

Nous avons donc déposé un projet Région AP-IR, Régis étant le porteur, qui a été financé en 2017. La mise en œuvre du projet a été décalée suite au départ de Régis au Japon.

Ce projet a commencé expérimentalement en avril 2019 avec un étudiant de M1 que j'ai encadré, et surtout avec l'arrivée de Christine Mosrin-Huaman dans notre groupe en juin 2019 pour une durée déterminée, en attente de sa mobilité géographique.

Concernant le génie génétique des levures, j'ai choisi de travailler avec la souche classique *Saccharomyces cerevisiae*, et d'utiliser un tandem de gènes rapporteurs nano-Luciférase et GFP. Il m'est apparu judicieux de combiner deux gènes rapporteurs pour pouvoir tester leur sensibilité et stabilité respectives dans différentes conditions mimant le milieu naturel (variations de température, de pH,… rencontrées dans les cours d'eau). Une séquence PEST a aussi été introduite dans les différentes constructions. La séquence PEST déstabilise la protéine qui la porte, diminuant drastiquement son temps de vie. L'idée est que ce système devrait permettre de détecter des pollutions passagères ou des pics de pollutions.

Tout d'abord, ces deux gènes ont été clonés sous le contrôle d'un promoteur fort constitutif, afin de tester leurs propriétés (expression, stabilité, activité, …) en culture liquide classique

puis dans des conditions mimant les conditions naturelles des cours d'eau, et enfin dans le but de les tester ultérieurement lorsque les levures seront intégrées dans les matériaux lamellaires.
Christine a ensuite réalisé la construction où les gènes rapporteurs tandem (nano-Luciférase et GFP) sont sous contrôle d'un promoteur sensible à la tétracycline, système qu'elle maîtrise tout particulièrement. Cette construction devra nous permettre de faire la preuve de concept de notre système en détectant cet antibiotique dans des cours d'eau.

Ces différentes souches et constructions sont prêtes pour être associées aux matériaux développés par Régis au Japon. Cette étape va bientôt commencer.
Un Post-Doc va être recruté mi-2020 pour poursuivre ce projet. En particulier, il mettra au point de nouvelles constructions de levure (autres promoteurs sensibles à différents polluants, levures mutées dans les processus de détoxification (*PDR*, …), et il associera ces levures modifiées aux différents matériaux lamellaires développés par Régis.

IV. CONCLUSION

Il y a une douzaine d'années quand nous avons décidé de nous orienter vers l'étude de la Neurofibromatose de type I, de passer de la levure aux cellules de mammifères, de découvrir de nouvelles communautés scientifiques, le défi nous paraissait audacieux et incertain.
Aujourd'hui, nous avons réalisé de belles avancées, des recherches passionnantes sont en cours, et tant de découvertes nous attendent !
Le chemin n'a pas été simple, mais la ténacité paie.

J'espère communiquer cet enthousiasme et cette foi en la science à de nouvelles générations, qui traceront ensuite leurs voies…

V. RÉFÉRENCES

Beauclair, G., Bridier-Nahmias, A., Zagury, J.F., Saib, A., and Zamborlini, A. (2015). JASSA: a comprehensive tool for prediction of SUMOylation sites and SIMs. Bioinformatics (Oxford, England) *31*, 3483-3491.

Beaufour, M., Godin, F., Vallee, B., Cadene, M., and Benedetti, H. (2012). Interaction proteomics suggests a new role for the Tfs1 protein in yeast. Journal of proteome research *11*, 3211-3218.

Bernier, I., and Jolles, P. (1984). Purification and characterization of a basic 23 kDa cytosolic protein from bovine brain. Biochimica et biophysica acta *790*, 174-181.

Bollen, M., Peti, W., Ragusa, M.J., and Beullens, M. (2010). The extended PP1 toolkit: designed to create specificity. Trends in biochemical sciences *35*, 450-458.

Bonneau, F., Lenherr, E.D., Pena, V., Hart, D.J., and Scheffzek, K. (2009). Solubility survey of fragments of the neurofibromatosis type 1 protein neurofibromin. Protein expression and purification *65*, 30-37.

Bruun, A.W., Svendsen, I., Sorensen, S.O., Kielland-Brandt, M.C., and Winther, J.R. (1998). A high-affinity inhibitor of yeast carboxypeptidase Y is encoded by TFS1 and shows homology to a family of lipid binding proteins. Biochemistry *37*, 3351-3357.

Chautard, H., Jacquet, M., Schoentgen, F., Bureaud, N., and Benedetti, H. (2004). Tfs1p, a member of the PEBP family, inhibits the Ira2p but not the Ira1p Ras GTPase-activating protein in Saccharomyces cerevisiae. Eukaryotic cell *3*, 459-470.

Cho, M.C., Lee, J., Park, J., Oh, S., Chai, J.S., Son, H., Paick, J.S., and Kim, S.W. (2019). The effects of single versus combined therapy using LIM-kinase 2 inhibitor and type 5 phosphodiesterase inhibitor on erectile function in a rat model of cavernous nerve injury-induced erectile dysfunction. Asian journal of andrology.

Croft, D.R., Crighton, D., Samuel, M.S., Lourenco, F.C., Munro, J., Wood, J., Bensaad, K., Vousden, K.H., Sansom, O.J., Ryan, K.M.*, et al.* (2011). p53-mediated transcriptional regulation and activation of the actin cytoskeleton regulatory RhoC to LIMK2 signaling pathway promotes cell survival. Cell research *21*, 666-682.

Cuberos, H., Vallee, B., Vourc'h, P., Tastet, J., Andres, C.R., and Benedetti, H. (2015). Roles of LIM kinases in central nervous system function and dysfunction. FEBS letters *589*, 3795-3806.

Cui, Y., and Morrison, H. (2019). Construction of cloning-friendly minigenes for mammalian expression of full-length human NF1 isoforms. Human mutation *40*, 187-192.

D'Angelo, I., Welti, S., Bonneau, F., and Scheffzek, K. (2006). A novel bipartite phospholipid-binding module in the neurofibromatosis type 1 protein. EMBO Rep *7*, 174-179.

Droescher, M., Chaugule, V.K., and Pichler, A. (2013). SUMO rules: regulatory concepts and their implication in neurologic functions. Neuromolecular medicine *15*, 639-660.

Eifler, K., and Vertegaal, A.C.O. (2015). SUMOylation-Mediated Regulation of Cell Cycle Progression and Cancer. Trends in biochemical sciences *40*, 779-793.

Eto, M., Senba, S., Morita, F., and Yazawa, M. (1997). Molecular cloning of a novel phosphorylation-dependent inhibitory protein of protein phosphatase-1 (CPI17) in smooth muscle: its specific localization in smooth muscle. FEBS letters *410*, 356-360.

Flotho, A., and Melchior, F. (2013). Sumoylation: a regulatory protein modification in health and disease. Annual review of biochemistry *82*, 357-385.

Funato, K., Lombardi, R., Vallee, B., and Riezman, H. (2003). Lcb4p is a key regulator of ceramide synthesis from exogenous long chain sphingoid base in Saccharomyces cerevisiae. J Biol Chem *278*, 7325-7334. Epub 2002 Dec 7318.

Funato, K., Vallee, B., and Riezman, H. (2002). Biosynthesis and trafficking of sphingolipids in the yeast Saccharomyces cerevisiae. Biochemistry *41*, 15105-15114.

Gamell, C., Schofield, A.V., Suryadinata, R., Sarcevic, B., and Bernard, O. (2013). LIMK2 mediates resistance to chemotherapeutic drugs in neuroblastoma cells through regulation of drug-induced cell cycle arrest. PloS one *8*, e72850.
Gao, X., Zhao, L., Liu, S., Li, Y., Xia, S., Chen, D., Wang, M., Wu, S., Dai, Q., Vu, H.*, et al.* (2019). gamma-6-Phosphogluconolactone, a Byproduct of the Oxidative Pentose Phosphate Pathway, Contributes to AMPK Activation through Inhibition of PP2A. Molecular cell.
Godin, F., Villette, S., Vallee, B., Doudeau, M., Morisset-Lopez, S., Ardourel, M., Hevor, T., Pichon, C., and Benedetti, H. (2012). A fraction of neurofibromin interacts with PML bodies in the nucleus of the CCF astrocytoma cell line. Biochemical and biophysical research communications *418*, 689-694.
Gombault, A., Godin, F., Sy, D., Legrand, B., Chautard, H., Vallee, B., Vovelle, F., and Benedetti, H. (2007). Molecular basis of the Tfs1/Ira2 interaction: a combined protein engineering and molecular modelling study. J Mol Biol *374*, 604-617. Epub 2007 Sep 2026.
Gombault, A., Warringer, J., Caesar, R., Godin, F., Vallee, B., Doudeau, M., Chautard, H., Blomberg, A., and Benedetti, H. (2009). A phenotypic study of TFS1 mutants differentially altered in the inhibition of Ira2p or CPY. FEMS yeast research *9*, 867-874.
Gorovoy, M., Niu, J., Bernard, O., Profirovic, J., Minshall, R., Neamu, R., and Voyno-Yasenetskaya, T. (2005). LIM kinase 1 coordinates microtubule stability and actin polymerization in human endothelial cells. The Journal of biological chemistry *280*, 26533-26542.
Gurney, M.E. (1994). Transgenic-mouse model of amyotrophic lateral sclerosis. The New England journal of medicine *331*, 1721-1722.
Hamill, S., Lou, H.J., Turk, B.E., and Boggon, T.J. (2016). Structural Basis for Noncanonical Substrate Recognition of Cofilin/ADF Proteins by LIM Kinases. Molecular cell *62*, 397-408.
Harrison, B.A., Almstead, Z.Y., Burgoon, H., Gardyan, M., Goodwin, N.C., Healy, J., Liu, Y., Mabon, R., Marinelli, B., Samala, L.*, et al.* (2015). Discovery and Development of LX7101, a Dual LIM-Kinase and ROCK Inhibitor for the Treatment of Glaucoma. ACS medicinal chemistry letters *6*, 84-88.
Harrison, B.A., Whitlock, N.A., Voronkov, M.V., Almstead, Z.Y., Gu, K.J., Mabon, R., Gardyan, M., Hamman, B.D., Allen, J., Gopinathan, S.*, et al.* (2009). Novel class of LIM-kinase 2 inhibitors for the treatment of ocular hypertension and associated glaucoma. Journal of medicinal chemistry *52*, 6515-6518.
Hay, R.T. (2013). Decoding the SUMO signal. Biochemical Society transactions *41*, 463-473.
Hendriks, I.A., D'Souza, R.C., Yang, B., Verlaan-de Vries, M., Mann, M., and Vertegaal, A.C. (2014). Uncovering global SUMOylation signaling networks in a site-specific manner. Nature structural & molecular biology *21*, 927-936.
Hendriks, I.A., and Vertegaal, A.C. (2016). A comprehensive compilation of SUMO proteomics. Nature reviews Molecular cell biology *17*, 581-595.
Heng, Y.W., Lim, H.H., Mina, T., Utomo, P., Zhong, S., Lim, C.T., and Koh, C.G. (2012). TPPP acts downstream of RhoA-ROCK-LIMK2 to regulate astral microtubule organization and spindle orientation. Journal of cell science *125*, 1579-1590.
Hsu, F.F., Lin, T.Y., Chen, J.Y., and Shieh, S.Y. (2010). p53-Mediated transactivation of LIMK2b links actin dynamics to cell cycle checkpoint control. Oncogene *29*, 2864-2876.
Hubbert, C., Guardiola, A., Shao, R., Kawaguchi, Y., Ito, A., Nixon, A., Yoshida, M., Wang, X.F., and Yao, T.P. (2002). HDAC6 is a microtubule-associated deacetylase. Nature *417*, 455-458.
Jarque, S., Bittner, M., Blaha, L., and Hilscherova, K. (2016). Yeast Biosensors for Detection of Environmental Pollutants: Current State and Limitations. Trends in biotechnology *34*, 408-419.
Kilpatrick, J.I., Revenko, I., and Rodriguez, B.J. (2015). Nanomechanics of Cells and Biomaterials Studied by Atomic Force Microscopy. Advanced healthcare materials *4*, 2456-2474.
Korrodi-Gregorio, L., Esteves, S.L., and Fardilha, M. (2014). Protein phosphatase 1 catalytic isoforms: specificity toward interacting proteins. Translational research : the journal of laboratory and clinical medicine *164*, 366-391.
Lallemand-Breitenbach, V., and de The, H. (2018). PML nuclear bodies: from architecture to function. Current opinion in cell biology *52*, 154-161.

Lappalainen, P., and Drubin, D.G. (1997). Cofilin promotes rapid actin filament turnover in vivo. Nature *388*, 78-82.
Lappalainen, P., Fedorov, E.V., Fedorov, A.A., Almo, S.C., and Drubin, D.G. (1997). Essential functions and actin-binding surfaces of yeast cofilin revealed by systematic mutagenesis. The EMBO journal *16*, 5520-5530.
Luo, Q., Kuang, D., Zhang, B., and Song, G. (2016). Cell stiffness determined by atomic force microscopy and its correlation with cell motility. Biochimica et biophysica acta *1860*, 1953-1960.
Maekawa, M., Ishizaki, T., Boku, S., Watanabe, N., Fujita, A., Iwamatsu, A., Obinata, T., Ohashi, K., Mizuno, K., and Narumiya, S. (1999). Signaling from Rho to the actin cytoskeleton through protein kinases ROCK and LIM-kinase. Science (New York, NY) *285*, 895-898.
Manetti, F. (2012). Recent findings confirm LIM domain kinases as emerging target candidates for cancer therapy. Current cancer drug targets *12*, 543-560.
Mardilovich, K., Baugh, M., Crighton, D., Kowalczyk, D., Gabrielsen, M., Munro, J., Croft, D.R., Lourenco, F., James, D., Kalna, G*., et al.* (2015). LIM kinase inhibitors disrupt mitotic microtubule organization and impair tumor cell proliferation. Oncotarget *6*, 38469-38486.
Mima, J., Hayashida, M., Fujii, T., Narita, Y., Hayashi, R., Ueda, M., and Hata, Y. (2005). Structure of the carboxypeptidase Y inhibitor IC in complex with the cognate proteinase reveals a novel mode of the proteinase-protein inhibitor interaction. Journal of molecular biology *346*, 1323-1334.
Moseley, J.B., and Goode, B.L. (2006). The yeast actin cytoskeleton: from cellular function to biochemical mechanism. Microbiology and molecular biology reviews : MMBR *70*, 605-645.
Ohashi, K., Sampei, K., Nakagawa, M., Uchiumi, N., Amanuma, T., Aiba, S., Oikawa, M., and Mizuno, K. (2014). Damnacanthal, an effective inhibitor of LIM-kinase, inhibits cell migration and invasion. Molecular biology of the cell *25*, 828-840.
Po'uha, S.T., Shum, M.S., Goebel, A., Bernard, O., and Kavallaris, M. (2010). LIM-kinase 2, a regulator of actin dynamics, is involved in mitotic spindle integrity and sensitivity to microtubule-destabilizing drugs. Oncogene *29*, 597-607.
Prudent, R., Vassal-Stermann, E., Nguyen, C.H., Pillet, C., Martinez, A., Prunier, C., Barette, C., Soleilhac, E., Filhol, O., Beghin, A*., et al.* (2012). Pharmacological inhibition of LIM kinase stabilizes microtubules and inhibits neoplastic growth. Cancer research *72*, 4429-4439.
Prunier, C., Josserand, V., Vollaire, J., Beerling, E., Petropoulos, C., Destaing, O., Montemagno, C., Hurbin, A., Prudent, R., de Koning, L*., et al.* (2016). LIM Kinase Inhibitor Pyr1 Reduces the Growth and Metastatic Load of Breast Cancers. Cancer research *76*, 3541-3552.
Prunier, C., Prudent, R., Kapur, R., Sadoul, K., and Lafanechere, L. (2017). LIM kinases: cofilin and beyond. Oncotarget *8*, 41749-41763.
Radomska, K.J., Coulpier, F., Gresset, A., Schmitt, A., Debbiche, A., Lemoine, S., Wolkenstein, P., Vallat, J.M., Charnay, P., and Topilko, P. (2019). Cellular Origin, Tumor Progression, and Pathogenic Mechanisms of Cutaneous Neurofibromas Revealed by Mice with Nf1 Knockout in Boundary Cap Cells. Cancer discovery *9*, 130-147.
Rak, R., Haklai, R., Elad-Tzfadia, G., Wolfson, H.J., Carmeli, S., and Kloog, Y. (2014). Novel LIMK2 Inhibitor Blocks Panc-1 Tumor Growth in a mouse xenograft model. Oncoscience *1*, 39-48.
Ross-Macdonald, P., de Silva, H., Guo, Q., Xiao, H., Hung, C.Y., Penhallow, B., Markwalder, J., He, L., Attar, R.M., Lin, T.A*., et al.* (2008). Identification of a nonkinase target mediating cytotoxicity of novel kinase inhibitors. Molecular cancer therapeutics *7*, 3490-3498.
Rotsch, C., and Radmacher, M. (2000). Drug-induced changes of cytoskeletal structure and mechanics in fibroblasts: an atomic force microscopy study. Biophysical journal *78*, 520-535.
Salah, E., Chatterjee, D., Beltrami, A., Tumber, A., Preuss, F., Canning, P., Chaikuad, A., Knaus, P., Knapp, S., Bullock, A.N*., et al.* (2019). Lessons from LIMK1 enzymology and their impact on inhibitor design. The Biochemical journal *476*, 3197-3209.
Schimmel, J., Eifler, K., Sigurethsson, J.O., Cuijpers, S.A., Hendriks, I.A., Verlaan-de Vries, M., Kelstrup, C.D., Francavilla, C., Medema, R.H., Olsen, J.V*., et al.* (2014). Uncovering SUMOylation dynamics during cell-cycle progression reveals FoxM1 as a key mitotic SUMO target protein. Molecular cell *53*, 1053-1066.

Scott, R.W., and Olson, M.F. (2007). LIM kinases: function, regulation and association with human disease. Journal of molecular medicine (Berlin, Germany) *85*, 555-568.
Seeler, J.S., and Dejean, A. (2017). SUMO and the robustness of cancer. Nature reviews Cancer *17*, 184-197.
Serre, L., Vallee, B., Bureaud, N., Schoentgen, F., and Zelwer, C. (1998). Crystal structure of the phosphatidylethanolamine-binding protein from bovine brain: a novel structural class of phospholipid-binding proteins. Structure *6*, 1255-1265.
Sherekar, M., Han, S.W., Ghirlando, R., Messing, S., Drew, M., Rabara, D., Waybright, T., Juneja, P., O'Neill, H., Stanley, C.B.*, et al.* (2019). Biochemical and structural analyses reveal that the tumor suppressor neurofibromin (NF1) forms a high-affinity dimer. The Journal of biological chemistry.
Skultetyova, L., Ustinova, K., Kutil, Z., Novakova, Z., Pavlicek, J., Mikesova, J., Trapl, D., Baranova, P., Havlinova, B., Hubalek, M.*, et al.* (2017). Human histone deacetylase 6 shows strong preference for tubulin dimers over assembled microtubules. Scientific reports *7*, 11547.
Sleebs, B.E., Levit, A., Street, I.P., Falk, H., Hammonds, T., C., W.A., Charles, M.D., Olson, M.F., and B., B.J. (2011). Identification of 3-aminothieno[2,3-b]pyridine-2-carboxamides and 4-aminobenzothieno[3,2-d]pyrimidines as LIMK1 inhibitors. Med Chem Comm *2*, 977-981.
Sokolov, I., Dokukin, M.E., and Guz, N.V. (2013). Method for quantitative measurements of the elastic modulus of biological cells in AFM indentation experiments. Methods (San Diego, Calif) *60*, 202-213.
Somogyi, M., Szimler, T., Baksa, A., Vegh, B.M., Bakos, T., Parej, K., Adam, C., Zsigmond, A., Megyeri, M., Flachner, B.*, et al.* (2019). A versatile modular vector set for optimizing protein expression among bacterial, yeast, insect and mammalian hosts. PloS one *14*, e0227110.
Starinsky-Elbaz, S., Faigenbloom, L., Friedman, E., Stein, R., and Kloog, Y. (2009). The pre-GAP-related domain of neurofibromin regulates cell migration through the LIM kinase/cofilin pathway. Molecular and cellular neurosciences *42*, 278-287.
Sumi, T., Matsumoto, K., and Nakamura, T. (2001). Specific activation of LIM kinase 2 via phosphorylation of threonine 505 by ROCK, a Rho-dependent protein kinase. The Journal of biological chemistry *276*, 670-676.
Tastet, J., Cuberos, H., Vallee, B., Toutain, A., Raynaud, M., Marouillat, S., Thepault, R.A., Laumonnier, F., Bonnet-Brilhault, F., Vourc'h, P.*, et al.* (2019). LIMK2-1 is a Hominidae-Specific Isoform of LIMK2 Expressed in Central Nervous System and Associated with Intellectual Disability. Neuroscience *399*, 199-210.
Te Velthuis, A.J., Isogai, T., Gerrits, L., and Bagowski, C.P. (2007). Insights into the molecular evolution of the PDZ/LIM family and identification of a novel conserved protein motif. PloS one *2*, e189.
Ubersax, J.A., and Ferrell, J.E., Jr. (2007). Mechanisms of specificity in protein phosphorylation. Nature reviews Molecular cell biology *8*, 530-541.
Vallee, B., Cuberos, H., Doudeau, M., Godin, F., Gosset, D., Vourc'h, P., Andres, C.R., and Benedetti, H. (2018). LIMK2-1, a new isoform of human LIMK2, regulates actin cytoskeleton remodeling via a different signaling pathway than that of its two homologs, LIMK2a and LIMK2b. The Biochemical journal *475*, 3745-3761.
Vallee, B., Doudeau, M., Godin, F., Gombault, A., Tchalikian, A., de Tauzia, M.L., and Benedetti, H. (2012). Nf1 RasGAP inhibition of LIMK2 mediates a new cross-talk between Ras and Rho pathways. PloS one *7*, e47283.
Vallee, B., and Riezman, H. (2005). Lip1p: a novel subunit of acyl-CoA ceramide synthase. Embo J *24*, 730-741. Epub 2005 Feb 2003.
Vallee, B., Schorling, S., Barz, W.P., Riezman, H., and Oesterhelt, D. (2001a). Lag1p and Lac1p are essential for the Acyl-CoA-dependent ceramide synthase reaction in Saccharomyces cerevisae. Mol Biol Cell *12*, 3417-3427.
Vallee, B., Teyssier, C., Maget-Dana, R., Ramstein, J., Bureaud, N., and Schoentgen, F. (1999). Stability and physicochemical properties of the bovine brain phosphatidylethanolamine-binding protein. Eur J Biochem *266*, 40-52.

Vallee, B.S., Coadou, G., Labbe, H., Sy, D., Vovelle, F., and Schoentgen, F. (2003). Peptides corresponding to the N- and C-terminal parts of PEBP are well-structured in solution: new insights into their possible interaction with partners in vivo. J Pept Res *61*, 47-57.
Vallee, B.S., Tauc, P., Brochon, J.C., Maget-Dana, R., Lelievre, D., Metz-Boutigue, M.H., Bureaud, N., and Schoentgen, F. (2001b). Behaviour of bovine phosphatidylethanolamine-binding protein with model membranes. Evidence of affinity for negatively charged membranes. Eur J Biochem *268*, 5831-5841.
Wan, X., Marsafari, M., and Xu, P. (2019). Engineering metabolite-responsive transcriptional factors to sense small molecules in eukaryotes: current state and perspectives. Microbial cell factories *18*, 61.
Wang, S., Ren, T., Jiao, G., Huang, Y., Bao, X., Zhang, F., Liu, K., Zheng, B., Sun, K., and Guo, W. (2017). BMPR2 promotes invasion and metastasis via the RhoA-ROCK-LIMK2 pathway in human osteosarcoma cells. Oncotarget *8*, 58625-58641.
Wolkenstein, P. (2001). La neurofibromatose 1. Médecine/Sciences *17*, 1158-1167.
Yang, J.Z., Huang, L.H., Chen, R., Meng, L.J., Gao, Y.Y., Ji, Q.Y., and Wang, Y. (2018). LIM kinase 1 serves an important role in the multidrug resistance of osteosarcoma cells. Oncology letters *15*, 250-256.
Yang, X., He, G., Zhang, X., Chen, L., Kong, Y., Xie, W., Jia, Z., Liu, W.T., and Zhou, Z. (2017). Transient inhibition of LIMKs significantly attenuated central sensitization and delayed the development of chronic pain. Neuropharmacology *125*, 284-294.
Yi, F., Guo, J., Dabbagh, D., Spear, M., He, S., Kehn-Hall, K., Fontenot, J., Yin, Y., Bibian, M., Park, C.M., *et al.* (2017). Discovery of Novel Small-Molecule Inhibitors of LIM Domain Kinase for Inhibiting HIV-1. Journal of virology *91*.
Zhao, X. (2018). SUMO-Mediated Regulation of Nuclear Functions and Signaling Processes. Molecular cell *71*, 409-418.

VI. ANNEXES

UNIVERSITE D'ORLEANS
CHÂTEAU DE LA SOURCE
BP 6749 - 45067 ORLEANS CEDEX 2

UNIVERSITE D'ORLEANS

ATTESTATION PROVISOIRE DE DIPLÔME

DE DOCTORAT

N° 854

Le Président de l'Université certifie que .....

Mademoiselle Béatrice **VALLEE**.....

Née le 4 Mai 1973... .....

à Neuville aux Bois..... .....

Titulaire du DEA : Chimie des Biomolécules - Montpellier (1996) .....

a été déclarée le : **6 Décembre 1999** .....

DOCTEUR de L'UNIVERSITE D'ORLEANS

Discipline : Biologie et Biophysique Moléculaires et Cellulaires.....

avec la MENTION : ... **TRES HONORABLE avec félicitations**.....

Le titre de la thèse et les noms et titres des membres du jury figurent au verso de la présente attestation.

Orléans, le 13 Décembre 1999

Le Président de l'Université

Michel MUDRY

Titre de la thèse soutenue par Mademoiselle Béatrice **VALLEE** .....

le 6 Décembre 1999.....

Etudes structurales et fonctionnelles de la « Phosphatidylethanolamine-binding protein » extraite du cerveau de boeuf

Noms et titres des membres du jury :

- Monsieur Jean RAMSTEIN - Professeur - Université d'Orléans - Président
- Monsieur Didier MARION - Directeur de Recherche INRA - Nantes - Rapporteur
- Monsieur Jean - Marie RUYSSCHAERT - Professeur - Université de Bruxelles (Belgique)
- Monsieur Robert VERGER - Directeur de Recherche CNRS - Marseille
- Madame Françoise SCHOENTGEN - Directeur de Recherche CNRS - Orléans

UNIVERSITE D'ORLEANS

RAPPORT DE SOUTENANCE [1]

SOUTENANCE d'une THESE en vue d'obtenir le grade de DOCTEUR de l'UNIVERSITE d'ORLEANS
(arrêté du 30 Mars 1992, relatif aux études doctorales)

Thèse soutenue par Mademoiselle Béatrice **VALLEE**
portant sur le sujet : ***Etudes structurales et fonctionnelles de la « Phosphatidylethanolamine-binding protein » extraite du cerveau de boeuf***

devant le jury suivant* :

- Monsieur Jean RAMSTEIN - Professeur - Université d'Orléans
- Monsieur Didier MARION - Directeur de Recherche INRA - Nantes
- Monsieur Jean - Marie RUYSSCHAERT - Professeur - Université de Bruxelles (Belgique)
- Monsieur Robert VERGER - Directeur de Recherche CNRS - Marseille
- Madame Françoise SCHOENTGEN - Directeur de Recherche CNRS - Orléans

*indiquer quels sont les membres qui ont été désignés en tant que Président et Rapporteur de soutenance (*Article 26,3 de l'arrêté du 30 mars 1992 : " Les membres du jury désignent parmi eux un président et un rapporteur. Le président doit être un professeur ou assimilé ou un enseignant de rang équivalent. Le directeur de thèse ou de travaux du candidat ne peut être choisi comme rapporteur. ")*

Orléans, le **6 Décembre 1999**

Signature des membres du jury :

[1] **Rapport établi au verso de cette feuille**

Château de La Source - BP 6749 - 45067 Orléans cedex 2 - Tél. : (33) 02 38 41 71 71 - Télécopie : (33) 02 38 41 70 69
E-mail : president@univ-orleans.fr - Internet : http://web.univ-orleans.fr/index.html

RAPPORT SUR LA SOUTENANCE ORALE
DE LA THESE DE
MADEMOISELLE BEATRICE VALLEE

Mademoiselle Béatrice Vallée a défendu sa thèse le 6 décembre 1999. L'exposé a été clair et bien structuré ce qui a permis à la candidate de bien faire ressortir et d'expliquer les résultats principaux obtenus au cours de la partie expérimentale de sa thèse. En guise d'introduction la candidate a dressé un panorama complet des connaissances actuelles se rapportant à son domaine de recherche. Par ailleurs elle a su répondre avec beaucoup de brio et de maturité aux questions des membres du jury. Ceci montre à l'évidence que Mademoiselle Béatrice Vallée possède une bonne maitrise de son sujet de recherche. Par ailleurs la qualité d'ensemble de l'exposé oral suggère que la candidate a des aptitudes certaines pour enseigner.

Le Jury décerne à Beatrice Vallée le grade de Docteur de l'Université d'Orléans avec la mention très honorable avec félicitations.

VII. PRINCIPALES PUBLICATIONS

Biochemical Journal (2018) **475** 3745–3761
https://doi.org/10.1042/BCJ20170961

Research Article

LIMK2-1, a new isoform of human LIMK2, regulates actin cytoskeleton remodeling via a different signaling pathway than that of its two homologs, LIMK2a and LIMK2b

Béatrice Vallée[1], Hélène Cuberos[1,2], Michel Doudeau[1], Fabienne Godin[1], David Gosset[1], Patrick Vourc'h[2], Christian R. Andres[2] and Hélène Bénédetti[1]

[1]Centre de Biophysique Moléculaire, CNRS, UPR 4301, University of Orléans and INSERM, 45071 Orléans Cedex 2, France; [2]UMR INSERM U930, University François Rabelais, 37020 Tours Cedex 1, France

Correspondence: Béatrice Vallée (beatrice.vallee@cnrs-orleans.fr)

LIMK1 and LIMK2 (LIMKs, LIM kinases) are kinases that play a crucial role in cytoskeleton dynamics by independently regulating both actin filament and microtubule remodeling. LIMK1 and, more recently, LIMK2 have been shown to be involved in cancer development and metastasis, resistance of cancer cells to microtubule-targeted treatments, neurological diseases, and viral infection. LIMKs have thus recently emerged as new therapeutic targets. Databanks describe three isoforms of human LIMK2: LIMK2a, LIMK2b, and LIMK2-1. Evidence suggests that they may not have completely overlapping functions. We biochemically characterized the three isoforms to better delineate their potential roles, focusing on LIMK2-1, which has only been described at the mRNA level in a single study. LIMK2-1 has a protein phosphatase 1 (PP1) inhibitory domain at its C-terminus which its two counterparts do not. We showed that the LIMK2-1 protein is indeed synthesized. LIMK2-1 does not phosphorylate cofilin, the canonical substrate of LIMKs, although it has kinase activity and promotes actin stress fiber formation. Instead, it interacts with PP1 and partially inhibits its activity towards cofilin. Our data suggest that LIMK2-1 regulates actin cytoskeleton dynamics by preventing PP1-mediated cofilin dephosphorylation, rather than by directly phosphorylating cofilin as its two counterparts, LIMK2a and LIMK2b. This specificity may allow for tight regulation of the phospho-cofilin pool, determining the fate of the cell.

Introduction

LIM kinases (LIMKs) are serine/threonine and tyrosine kinases involved in regulating cytoskeleton dynamics. They phosphorylate cofilin, resulting in its inhibition [1]. Cofilin is a member of the actin-depolymerizing factor (ADF) family and regulates actin polymerization dynamics by promoting rapid turnover of actin filaments [2–4]. LIMKs also control microtubule dynamics, independently from their regulation of actin remodeling. The molecular mechanism by which LIMKs regulate microtubule dynamics is still unknown [5]. LIMKs thus play a crucial role in cytoskeleton remodeling, contributing to many cellular functions, such as cell motility, morphogenesis, division, differentiation, apoptosis, neuronal morphology, neuritogenesis, and oncogenesis.

The LIMK family consists of only two members: LIMK1 and LIMK2. They share 50% overall identity and 70% identity in their kinase domain. They have a unique sequence organization consisting of two LIM (Lin11, Isl-1, and Mec-3) domains at their N-terminus, a central PDZ domain, and a C-terminal kinase domain.

Received: 19 December 2017
Revised: 22 October 2018
Accepted: 29 October 2018

Accepted Manuscript online: 29 October 2018
Version of Record published: 6 December 2018

Biochemical Journal (2018) 475 3745–3761
https://doi.org/10.1042/BCJ20170961

Three isoforms of human LIMK2 are described in databanks: LIMK2a, LIMK2b, and LIMK2-1. These three isoforms differ only at their extremities. The first LIM motif is truncated at the N-terminus of LIMK2b and LIMK2-1, whereas LIMK2-1 has an extra C-terminal domain identified as a protein phosphatase 1 inhibitory (PP1i) domain by sequence homology (Figure 1). Only one paper has shown the existence of LIMK2-1 mRNA [6]. Very little is known about the functional differences between these three isoforms and most studies did not indicate which isoform was under investigation. However, some data suggest that they probably do not have completely overlapping functions. The tissue distribution of LIMK2a and LIMK2b is different and they are differentially expressed according to the developmental stage [7,8]. They also show different subcellular localization: LIMK2a is found in the cytoplasm and the nucleus, whereas LIMK2b is mainly localized to the cytoplasm [8]. LIMK2a is an extremely stable protein with a half-life of ∼24 h, whereas LIMK2b has a much shorter half-life of ∼6 h [9]. LIMK2b and LIMK2-1, but not LIMK2a, are targets of p53. Upon DNA damage, p53 induces up-regulation of *LIMK2b* and *LIMK2-1* mRNA expression, thus modulating G2/M arrest [6,10]. LIMK2 has been described as a cancer cell-survival factor as p53 plays a major role in cancer development [11]. These data further connect LIMK2 to cancer. Indeed, increasing evidence shows a role for LIMK2 in cancer development and metastasis formation. LIMK2 is deregulated in many cancers (such as pancreatic and breast cancers) [12–14], and LIMK2a and 2b deregulation differ depending on cancer type [7,8]. Furthermore, LIMK2 also interacts with Aurora A, a kinase overexpressed in many cancers, and believed to promote tumorigenesis. LIMK2 and Aurora A regulate each other in a positive feedback loop in which LIMK2 appears to be a key oncogenic effector of Aurora A [15]. Recently, LIMK2a and LIMK2b were also shown to play a role in microtubule organization, but the molecular mechanisms involved are not yet known [5,9,16,17]. Gamell et al. [9] showed that LIMK2a and LIMK2b differentially regulate G2/M cell cycle arrest induced by microtubule-targeted drugs. Moreover, LIMK2 expression is elevated in neuroblastoma cells resistant to microtubule-targeted drugs. Thus, LIMK2 may be a possible target to overcome resistance to microtubule-targeted drugs [9,16,17]. We and others have shown that LIMK2 may also be involved in neurofibromatosis type I, a common genetic disease, of which the main manifestations are cancer development and cognitive defects [18,19]. LIMK2 is also involved in neurodevelopmental disorders [20]. Indeed, LIMK2 plays a critical role in growth cone establishment, neurite guidance and outgrowth, synapse plasticity, and neuronal death [21]. More recently, a possible role for LIMK2 in schizophrenia was suggested by gene expression studies in an animal model [22].

These findings all suggest LIMK2 as an emerging therapeutic target to treat cancer, neurofibromatosis type I, and neuronal disorders, and to overcome resistance to chemotherapy treatment with microtubule-targeting drugs. Nonetheless, no exhaustive studies of the three LIMK2 isoforms have yet been performed.

We biochemically characterized the three LIMK2 isoforms, particularly LIMK2-1, to delineate their specific properties. We showed that LIMK2-1 can be found in various cell lines and tissues. All three LIMK2 isoforms interact with each other. They show different subcellular localization with LIMK2-1 being mostly cytoplasmic. They are all phosphorylated by the upstream kinase ROCK on the catalytic regulatory threonine, Thr505/484. However, LIMK2-1 does not phosphorylate cofilin, the canonical substrate of LIM kinases, even though it exhibits kinase activity towards myelin basic protein (MBP) and promotes stress fiber formation. LIMK2-1 interacts with PP1 and partially inhibits it, resulting in an increase in the level of phospho-cofilin. Our data suggest that the three LIMK2 isoforms regulate actin polymerization dynamics by increasing the global pool of phospho-cofilin, either by direct phosphorylation by LIMK2a and LIMK2b or by preventing its dephosphorylation through the action of LIMK2-1. LIMK2 isoforms may provide fine tuning of the balance between cofilin and phospho-cofilin, which may be crucial, depending on the biological context.

Materials and methods

Materials

Antibodies anti-LIMK2 (sc-8390) and anti-GFP (sc-9996) were from Santa Cruz Biotechnology, Inc., anti-cMyc (MA1-21316) from Invitrogen, anti-HA (11687423001) from Roche Applied Science, and anti-phospho-LIMK2 (3841), cofilin (3312, 5175), and phospho-cofilin (3313) from Cell Signaling Technology. Antibody against a 12 amino acid peptide (DKIRAMQKLSTP) belonging to the PP1i domain of LIMK2-1 was developed by Eurogentec. EZview™ Red anti-HA affinity gel (E6779) and anti-Flag®-M2 affinity gel (A2220) were from Sigma–Aldrich Co., as well as antibodies anti-actin (A1978) and anti-Flag (M2 antibody F3165). GFP-trap beads were from Chromotek. Lipofectamine 2000 and Lipofectamine RNAiMAX were from Invitrogen, Opti-MEM from Gibco. Recombinant GST-fused cofilin and MBP were purchased from Upstate Cell Signaling, Inc. The different tissue extracts were from Biochain. Y27632 was from Tocris Bioscience. Plasmids used in this study are listed Table 1.

Biochemical Journal (2018) **475** 3745–3761
https://doi.org/10.1042/BCJ20170961

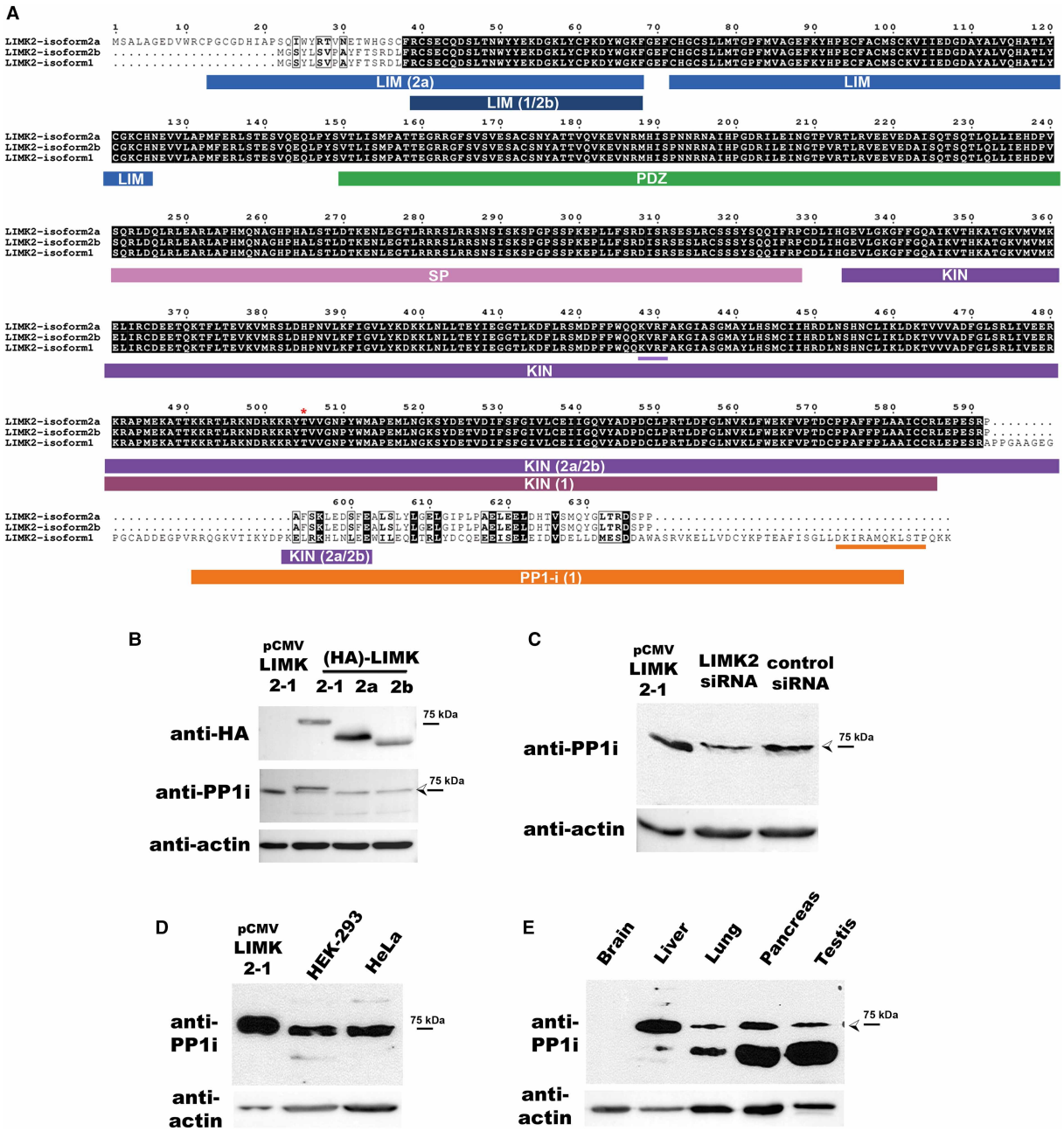

Figure 1. Evidence for the existence of the LIMK2-1 protein.

(**A**) *Sequence alignment and motif representation of the three isoforms of human LIMK2*. LIMK2 isoforms are described in Entrez Gene: LIMK2-1 (NP_001026971.1), LIMK2a (NP_005560.1), and LIMK2b (NP_057952.1). The various domains of LIMK2 are shown: LIM, PDZ, SP (serine proline-rich), KIN (kinase), and PP1i (protein phosphatase 1 inhibitory) domains. * indicates the activatable threonine that modulates LIMK2 activity towards cofilin. The PP1-binding consensus sequence is underlined in purple. The sequence chosen for anti-PP1i antibody design is underlined in orange. (**B**,**C**) *Validation of the anti-LIMK2-1 antibody*. (**B**) HEK-293 cells were transfected with untagged LIMK2-1 (pCMV-LIMK2-1) and HA-tagged isoforms of LIMK2. Lysates were analyzed by western blotting using the indicated antibodies. (**C**) HEK-293 were transfected with LIMK2 siRNA or control siRNA. Lysates were analyzed by western blot. *LIMK2-1 is expressed in various human cell lines* (**D**) *and tissues* (**E**). HEK-293 and HeLa cells were disrupted in 1% Triton X-100 lysis buffer. Tissue extracts were directly purchased. Samples were analyzed by western blotting.

Biochemical Journal (2018) **475** 3745–3761
https://doi.org/10.1042/BCJ20170961

Table 1 Plasmids used in the present study

Plasmid	Description	Source/reference
pcDNA3-$(HA)_2$-LIMK2-1	P_{CMV}-$(HA)_2$-*LIMK2-1*	The present study
pcDNA3-$(HA)_2$-LIMK2-1_ΔPP1i	P_{CMV}-$(HA)_2$-*LIMK2-1_ΔPP1i*	The present study
pcDNA3-$(HA)_2$-LIMK2-1_D430N	P_{CMV}-$(HA)_2$-*LIMK2-1_D430N*	The present study
pcDNA3-$(HA)_2$-LIMK2a	P_{CMV}-$(HA)_2$-*LIMK2a*	[19]
pcDNA3-$(HA)_2$-LIMK2b	P_{CMV}-$(HA)_2$-*LIMK2b*	The present study
pcDNA3-$(HA)_2$-KIN2	P_{CMV}-$(HA)_2$-*KIN2*	[19]
pcDNA3-$(HA)_2$-KIN1-PP1i	P_{CMV}-$(HA)_2$-*KIN1-PP1i*	The present study
pcDNA3-$(HA)_2$-PP1i	P_{CMV}-$(HA)_2$-*PP1i(AA581-686)*	The present study
pCMV-LIMK2-1	P_{CMV}-sport6-*LIMK2-1*	Open Biosystem
pcDNA3-$(HA)_2$-Larp6	P_{CMV}-$(HA)_2$-*LARP6*	The present study
pXJN-*myc*-LIMK2b	pXJN-*myc-LIMK2b*	[10]
pE-YFP-LIMK2-1	pE-YFP-N1-*LIMK2-1*	The present study
pE-YFP-LIMK2a	pE-YFP-N1-*LIMK2a*	The present study
pE-YFP-LIMK2b	pE-YFP-N1-*LIMK2b*	The present study
pcDNA3-$(HA)_2$-LIMK2-T505A	P_{CMV}-$(HA)_2$-*LIMK2-2a-T505A*	The present study
pCAG ROCK1	*ROCK1-myc*	[47]
p3x-Flag-PP1	P_{CMV}-(Flag)-*PP1cα*	The present study

Cell culture and transfection

HEK-293 and HeLa cells were cultured under 5% CO_2 at 37°C in Dulbecco's modified Eagle's medium supplemented with 10% fetal calf serum. HEK-293 cells were transiently transfected with 10 μg of plasmid/100-mm dish with calcium phosphate method, and HeLa cells with Lipofectamine 2000 according to manufacturer's recommendations. Further experiments were conducted 48 h after transfection. For Y27632 experiments, cells were treated for 30 min with 10 μl of a 10 mM stock solution of Y27632 in ethanol (10 μM final concentration) and then lysed.

Cell lysates for endogenous LIMK2-1 detection

HEK-293 and HeLa cells were lysed in 1% Triton X-100 lysis buffer (50 mM Tris–HCl, pH 7.5, 100 mM NaCl, 5 mM EDTA, 50 mM NaF, 10 mM sodium pyrophosphate, 1 mM Na_3VO_4, 20 mM *p*-nitrophenyl phosphate, 20 mM β-glycerophosphate, 10 μg/ml aprotinin, 0.05 μg/ml okaidic acid, 1 μg/ml leupeptin, and 1 mM PMSF).

LIMK2-1 RNAi transfection

LIMK2 siRNA (#s8191) and control siRNA (#AM4611) were from Ambion®. HEK-293 cells were transfected with 2 nM siRNA with Lipofectamine RNAiMAX for 48 h, using manufacturer's instructions.

Cell fractionation

Nuclear and cytoplasmic fractions were prepared as described by Smolich et al. [23]. Briefly, HEK-293 cells were transfected or not with expression plasmids as described above and cultured for 48 h. They were scraped off the dish in PBS and resuspended in 10 mM Tris–HCl (pH 7.6), 10 mM NaCl, 3 mM $MgCl_2$, 0.5% Triton X-100 and a cocktail of protease inhibitors. Cells were homogenized with 20 strokes in a Dounce homogenizer and the nuclei pelleted by centrifugation in a microfuge at 2000×***g*** for 10 min. Supernatant was collected as the cytoplasmic fraction. The nuclear pellet was washed twice in the previous buffer, and the final pellet was solubilized in 10 mM Tris–HCl (pH 7.0), 150 mM NaCl, 1% NP40, 1% Na-deoxycholate, 0.1% SDS, and a cocktail of protease inhibitors.

Biochemical Journal (2018) **475** 3745–3761
https://doi.org/10.1042/BCJ20170961

Immunoprecipitation

HEK-293 cells were transfected with expression plasmids as described above and cultured for 48 h. Cells were lysed in 0.5 ml of 0.1% Triton X-100 lysis buffer (50 mM Tris–HCl, pH 7.5, 100 mM NaCl, 5 mM EDTA, 50 mM NaF, 10 mM sodium pyrophosphate, 1 mM Na_3VO_4, 20 mM *p*-nitrophenyl phosphate, 20 mM β-glycerophosphate, 10 μg/ml aprotinin, 0.05 μg/ml okaidic acid, 1 μg/ml leupeptin, and 1 mM PMSF) and incubated on ice for 10 min. After centrifugation, the supernatants were incubated for 2–3 h at 4°C either with anti-HA affinity gel for HA-LIMK2s or with GFP-trap beads for YFP-LIMK2s. Beads were washed five times with lysis buffer and then eluted with Laemmli sample buffer.

Kinase assay

Immunoprecipitates bound to HA-beads or GFP-beads, as described above, were washed twice with lysis buffer and then three times with kinase buffer (50 mM HEPES-NaOH, pH 7.5, 150 mM NaCl, 5 mM $MgCl_2$, 5 mM $MnCl_2$, 50 mM NaF, 1 mM Na_3VO_4, 20 mM β-glycerophosphate, 1 μg/ml leupeptin, and 1 mM PMSF). Immunoprecipitates were incubated for 20 min at 30°C in 22 μl of kinase buffer containing 50 μM ATP, 5 μCi of $\gamma[^{32}P]$ATP (3000 Ci/mmol), and 2.5 μg of GST-fused cofilin or 10 μg of MBP. The reaction was terminated by heating 5 min at 90°C in Laemmli sample buffer. Samples were then subjected to SDS–PAGE and analyzed by autoradiography.

Cell staining

HeLa cells were fixed with 4% paraformaldelyde in PBS for 20 min and permeabilized with 0.5% Triton-X100 in PBS for 15 min at room temperature. After blocking with 1% fetal calf serum in PBS for 30 min, these cells were incubated with anti-HA antibodies for 1 h and subsequently with FITC-conjugated anti-rat IgG, and simultaneously with AlexaFluor568-conjugated phalloidin for 1 h. The cells were then washed three times with PBS, mounted on glass slides, and then analyzed by confocal microscopy using a Zeiss Axiovert 200 M microscope coupled with a Zeiss LSM 510 scanning device (Carl Zeiss Co. Ltd., Iena, Germany).

Statistics

Statistical significance was determined using one-way ANOVA (***$P < 0.001$, **$P < 0.01$, *$P < 0.05$).

Results

The LIMK2-1 protein is synthesized

LIMK2-1 is mentioned in databanks, but only at the mRNA level by one publication [6]. LIMK2-1 has a PP1i domain at its C-terminus, which LIMK2a and LIMK2b do not (Figure 1A). We first designed an antibody that targets this domain, amino acids 671–684 (Figure 1A, underlined in orange). A blast search of this 12 amino acid sequence against human protein databases showed only one strong similarity within the sequence of the protein phosphatase PHI-1. PHI-1 migrates at 23 kDa on SDS–PAGE gels [24], and thus, it should not interfere with the detection of endogenous LIMK2-1, expected to migrate at ∼75 kDa. We validated this antibody firstly on HEK-293 cells transfected with LIMK2-1, LIMK2a, or LIMK2b. The anti-PP1i antibody recognized transfected LIMK2-1 (pCMV-LIMK2-1) and HA-tagged LIMK2-1, but did not cross-react with transfected HA-tagged LIMK2a or LIMK2b (Figure 1B). We observed a band of endogenous LIMK2-1 in HEK cells transfected with HA-tagged versions of the LIMK2 isoforms (indicated by an arrow in the anti-PP1i blot; Figure 1B). Secondly, we checked if the signal induced by our anti-PP1i antibody was specific to LIMK2-1 using siRNA targeting the three spliced variants of LIMK2 (Figure 1C). In the presence of LIMK2 siRNA, we could observe a reproducible and significant decrease in our band of interest (indicated by an arrow) compared with control conditions, suggesting that our antibody is specific to LIMK2-1. We then used the anti-PP1i antibody to detect LIMK2-1 in two cell line extracts from HEK-293 and HeLa cells and various human tissues (Figure 1D,E). LIMK2-1 appeared to be expressed in HEK-293 and HeLa cell lines (Figure 1D). LIMK2-1 protein levels varied depending on the tissue: we found the highest levels in liver, somewhat less in pancreas, and the lowest in testis and lung. LIMK2-1 was barely detectable in brain (Figure 1E). However, we observed lower molecular mass bands in all tissue samples except liver, suggesting degradation of the full protein probably due to the lysis conditions of these commercial samples (this lysis buffer contains a cocktail of inhibitors not specified on the data sheet, which may be less efficient than our many protease and phosphatase inhibitors, we used in our home-made buffer). These data show that human LIMK2-1 protein is synthesized and differently expressed in the tested tissues.

Biochemical Journal (2018) **475** 3745–3761
https://doi.org/10.1042/BCJ20170961

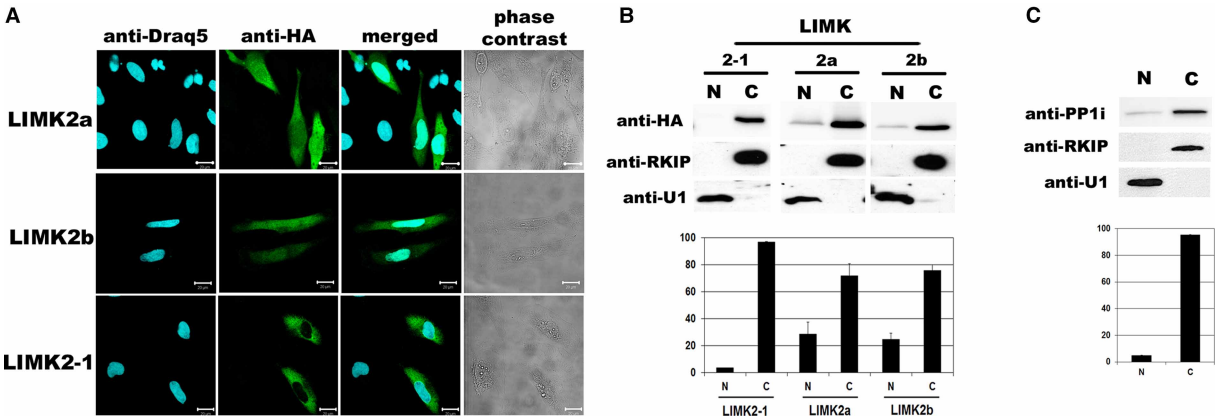

Figure 2. Subcellular localization of LIMK2s.

(**A**) *Immunofluorescence.* HeLa cells were transfected with one of the three HA-tagged LIMK2 isoforms (2-1, 2a, and 2b). Cells were fixed and stained with anti-Draq5 (to label the nucleus) and anti-HA antibodies (to detect the LIMK2 isoforms). Scale bar represents 20 μm. (**B**) *Cell fractionation on transfected cells. Upper panel:* HEK-293 cells were transfected with one of the three HA-tagged LIMK2 isoforms (2-1, 2a, and 2b). Cells were then fractionated as described in Materials and Methods. *Lower panel: Quantification of three independent experiments*. The values obtained for nuclear and cytosolic fractions were first normalized with U1 and RKIP, respectively, and then summed and normalized to 100%. (**C**) *HEK cell fractionation. Upper panel:* HEK-293 cells were fractionated as above. *Lower panel: Quantification of three independent experiments*. The values obtained for nuclear and cytosolic fractions were first normalized with U1 and RKIP, respectively, and then summed and normalized to 100%.

Subcellular localization

Previous studies have shown that the subcellular localization of LIMK2a and LIMK2b is different. Both are found in the cytoplasm and the nucleus, but LIMK2b to a lesser extent in the nucleus [8,23].

We first assessed the subcellular localization of each LIMK2 isoform in HeLa cells transfected with a HA-tagged version of each by immunofluorescence. We found both LIMK2a and LIMK2b in the cytoplasm and the nucleus, whereas LIMK2-1 was exclusively localized to the cytoplasm (Figure 2A).

We further characterized the subcellular localization of LIMK by cell fractionation of HEK cells transfected with each of the HA-tagged LIMK2 isoforms. The results were consistent with those obtained by immunofluorescence. We found LIMK2a and LIMK2b in both the nuclear and cytoplasmic fractions, with less LIMK2b found in the nuclear fraction, whereas LIMK2-1 was mostly found in the cytoplasmic fraction. Quantification of three independent experiments showed that a mean of 3.4% of LIMK2-1 was localized to the nuclear fraction versus 28.4% for LIMK2a and 24.6% for LIMK2b (Figure 2B).

We then checked endogenous LIMK2-1 subcellular localization by repeating this subcellular fractionation on non-transfected HEK cells. LIMK2-1 distribution was analyzed using anti-PP1i antibody (Figure 2C). Endogenous LIMK2-1 appeared mainly localized in the cytoplasmic fraction (95.2% versus 4.8% in the nuclear fraction).

LIMK oligomers

LIMK1 and LIMK2 can form heterodimers [25,26]. We determined whether the various isoforms of LIMK2 could form homo and/or heterodimers. We performed co-transfection experiments on HEK-293 cells using vectors encoding the three HA-tagged isoforms of LIMK2 and a non-tagged LIMK2-1, cMyc-tagged LIMK2b, or YFP-tagged LIMK2a isoform. Cell extracts were then immunoprecipitated using anti-HA antibodies and the co-immunoprecipitated LIMK2 isoforms analyzed by western blotting using anti-LIMK2, anti-cMyc, and anti-GFP antibodies. Each isoform interacted with itself and with its two other counterparts (Figure 3).

Regulation by ROCK

LIMK2 belongs to the Rho/ROCK/LIMK2/cofilin signaling pathway. ROCK activates LIMK2a by direct phosphorylation of Thr505 [27,28]. We first assessed whether the three LIMK2 isoforms can interact with ROCK by co-immunoprecipitation. HEK cells were co-transfected with cMyc-tagged ROCK1 and one of the HA-tagged

Biochemical Journal (2018) **475** 3745–3761
https://doi.org/10.1042/BCJ20170961

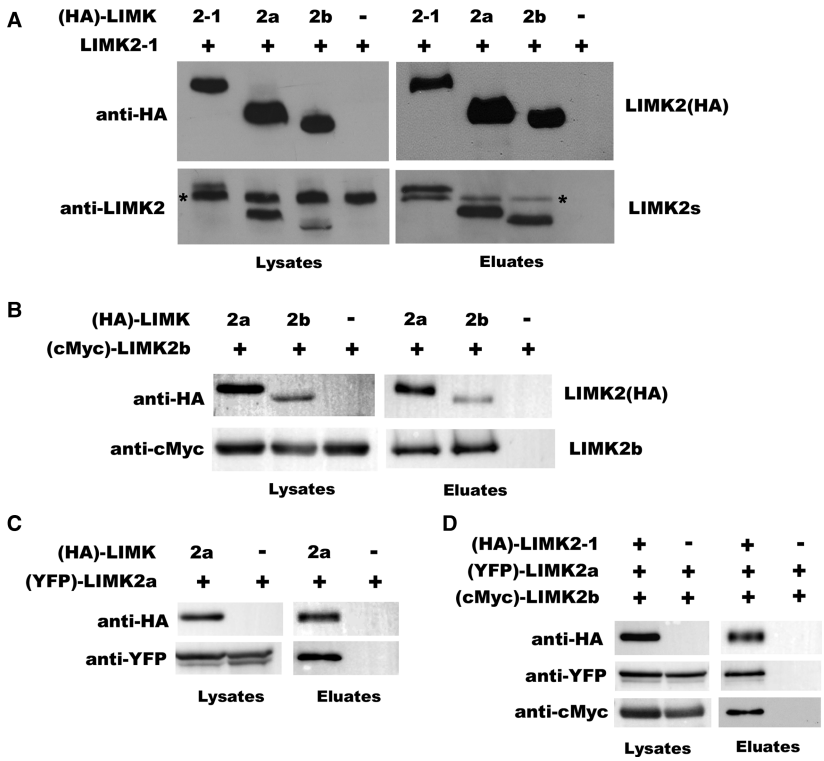

Figure 3. LIMK2 oligomers.

(**A**) *LIMK2-1 interacts with itself and with LIMK2 isoforms 2a and 2b*. HEK-293 cells were co-transfected with LIMK2-1 and one of the three HA-tagged LIMK2 isoforms (2-1, 2a, and 2b) or the empty parental vector pcDNA3. Lysates and anti-HA immunoprecipitates were subjected to western blotting. * indicates non-tagged LIMK2-1. (**B**) *LIMK2b interacts with itself and with LIMK2a.* HEK-293 cells were co-transfected with cMyc-tagged LIMK2b and HA-tagged LIMK2a or 2b or the empty parental vector, pcDNA3. Lysates and anti-HA immunoprecipitates were subjected to western blotting. (**C**) *LIMK2a interacts with itself.* HEK-293 cells were co-transfected with YFP-tagged LIMK2a and HA-tagged LIMK2a or the empty parental vector, pcDNA3. Lysates and anti-HA immunoprecipitates were subjected to western blotting. (**D**) *The three isoforms interact together.* HEK-293 cells were co-transfected with HA-tagged LIMK2-1 or the empty parental vector, pcDNA3, YFP-tagged LIMK2a, and cMyc-tagged LIMK2b. Lysates and anti-HA immunoprecipitates were subjected to western blotting.

LIMK2 isoforms, followed by anti-HA immunoprecipitation. ROCK1 specifically interacted with each isoform of LIMK2 (Figure 4A). We then determined whether ROCK1 can activate each of the three isoforms using an antibody that specifically targets phospho-Thr505 of LIMK2a. HEK cells were transfected by one of the LIMK2 isoforms or the non-phosphorylatable mutant LIMK2a-T505A. Lysates were analyzed with the anti-phospho-Thr505 LIMK2 antibody. This antibody exhibits background signal, as we observed a band for the T505A mutant (Figure 4B). This background signal is probably due to the fact that this antibody was produced by immunization with a synthetic phospho-peptide corresponding to residues surrounding Thr505; these residues may be also slightly recognized. The three isoforms of LIMK2 exhibited basal phosphorylation, which was reduced by treating cells with the ROCK inhibitor Y27632 (Figure 4B, left panels). This signal of phosphorylation increased drastically when cells were co-transfected with ROCK1. These data suggest that ROCK1 phosphorylated the three LIMK2 isoforms on Thr505 for LIMK2a and on the corresponding Thr484 for LIMK2b and LIMK2-1 (Figure 4B).

Kinase activity

Stress fiber formation

We next focused on LIMK2 activity. LIMK2 phosphorylates cofilin on serine 3, resulting in the inhibition of this actin depolymerization factor. Cellular overexpression of LIMK2 inhibits cofilin-mediated actin

Biochemical Journal (2018) **475** 3745–3761
https://doi.org/10.1042/BCJ20170961

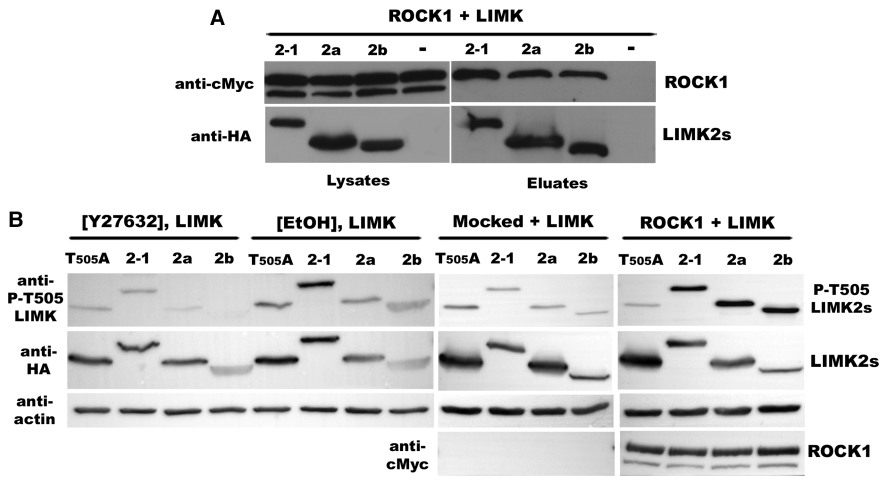

Figure 4. The three isoforms of LIMK2 interact with ROCK1, which specifically phosphorylates them on Thr505/484.
(**A**) *ROCK1 interacts with the three isoforms of LIMK2*. HEK-293 cells were co-transfected with cMyc-tagged ROCK1 and one of the three HA-tagged LIMK2 isoforms (2-1, 2a, and 2b) or the empty parental vector, pcDNA3. Lysates and anti-HA immunoprecipitates were subjected to western blotting. (**B**) *ROCK1 activates the three isoforms of LIMK2. Left panels*: HEK-293 were transfected with one of the three HA-tagged LIMK2 isoforms 2-1, 2a, 2b, or the inactivatable mutant, LIMK2a-T505A. Cells were treated for 30 min with 10 μl of a 10 mM stock solution of Y27632 in ethanol (10 μM final concentration), or with 10 μl of ethanol (negative control). Cells were then lysed, and lysates were analyzed by western blotting. *Right panels*: HEK-293 cells were co-transfected with cMyc-tagged ROCK1 or empty parental plasmid, pCAG, and one of the three HA-tagged LIMK2 isoforms 2-1, 2a, 2b, or the inactivatable mutant, LIMK2a-T505A. Lysates were subjected to western blotting.

depolymerization, leading to the accumulation of stress fibers [19,28,29]. We tested whether this is true for each of the three LIMK2 isoforms by immunofluorescence experiments on fixed intact cells. We transfected HeLa cells with one of the HA-tagged LIMK2 isoforms and visualized the actin filaments by phalloidin staining. Expression of each LIMK2 isoform resulted in the formation of more actin stress fibers than in cells transfected with an unrelated control construct (Larp6) (Figure 5A). LIMK2-1-induced stress fibers appeared to be slightly different from the one induced by LIMK2a or 2b: they are thinner and not present all over the z-plans of the cell (Supplementary Figure S1). Stress fibers were quantified by categorizing them into two batches: (i) thick and numerous stress fibers and (ii) thin or no stress fibers (Figure 5A, right panel). LIMK2-1-transfected cells exhibited less thick and numerous stress fibers (batch (i)) compared with LIMK2a- or 2b-transfected cells; nevertheless, they exhibited significant stress fibers compared with the negative control (Larp6) (Figure 5A, right panel). These data suggest that LIMK2-1, as well as LIMK2a and LIMK2b, plays a role in actin cytoskeleton organization by promoting stress fiber formation.

Phospho-cofilin in intact cells

We then studied LIMK2 kinase activity more directly by measuring the level of endogenous phospho-cofilin in HEK cells overexpressing one of the LIMK2 isoforms. HEK cells were transfected with one of the HA-tagged LIMK2 isoforms or the corresponding empty vector, and lysates were analyzed by western blotting using an antibody specifically targeting phospho-Ser3 cofilin. The presence of LIMK2a or LIMK2b induced a significant and reproducible increase in phospho-cofilin levels over that of control conditions, whereas the presence of LIMK2-1 had no detectable effect (Figure 5B, left panel).

We repeated the same experiment with a C-terminal YFP-tagged version of the three LIMK2 isoforms and an untagged version of LIMK2-1 to rule out possible interference by the N-terminal HA tag. The results were identical with those obtained using the HA-tagged versions of the three isoforms (Figure 5B, right panel for YFP-tagged isoforms).

Biochemical Journal (2018) **475** 3745–3761
https://doi.org/10.1042/BCJ20170961

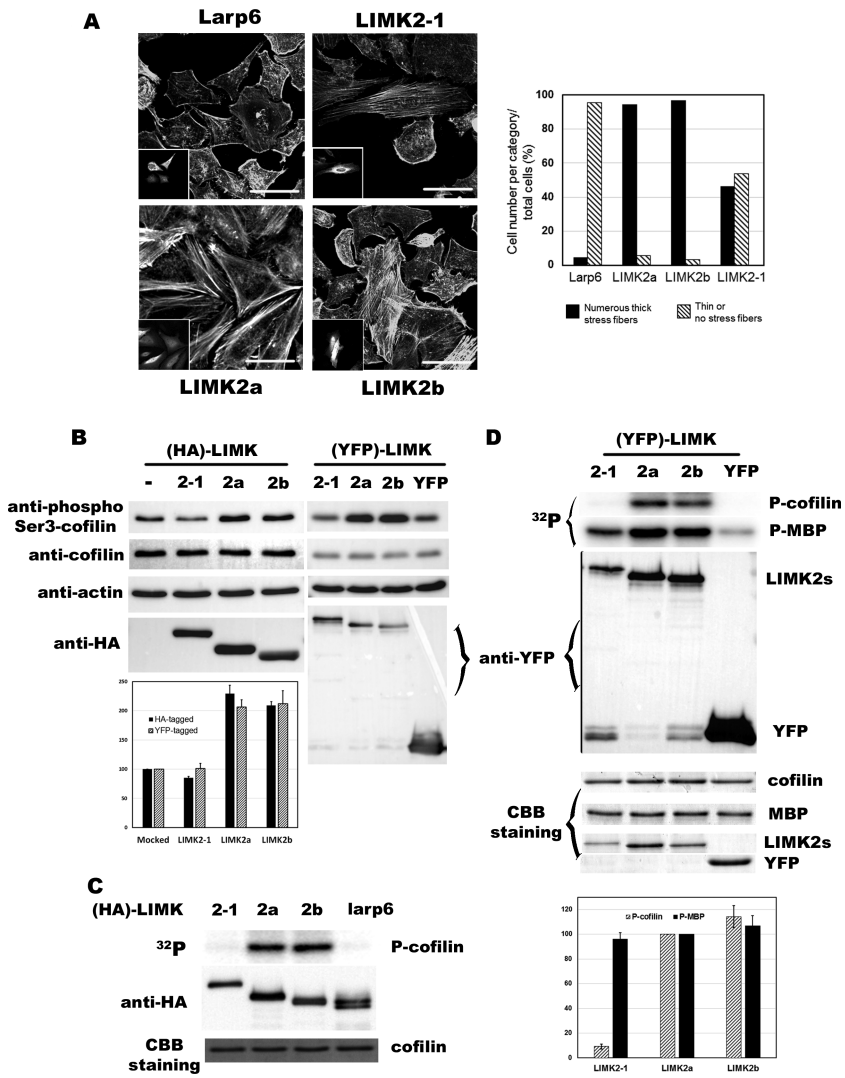

Figure 5. LIMK2-1 remodels the actin cytoskeleton, but has no kinase activity towards cofilin, although it phosphorylates MBP.

(**A**) *Stress fibers induced by LIMK2s.* HeLa cells were transfected with one of the HA-tagged LIMK2 isoform. Cells were fixed and stained with phalloidin (main picture), and anti-HA antibodies (bottom left corner picture). The scale bar represents 50 μm. Right panel: quantification of observed stress fibers by categorizing them into two batches. Four independent experiments were performed, each time 70–90 transfected cells were counted, (**B**) *HEK cells transfected with LIMK2a or LIMK2b exhibit a higher level of endogenous phospho-cofilin than HEK cells transfected with LIMK2-1.* HEK-293 cells were transfected with one of the three HA-tagged LIMK2 isoforms (1, 2a, and 2b) or the empty parental vector, pcDNA3 (left panel), or with one of the three YFP-tagged LIMK2 isoforms or YFP alone (right panel). Lysates were subjected to western blotting. Quantification of the ratio of phospho-cofilin *versus* cofilin is shown in the bottom graph. Phospho-cofilin versus cofilin ratio of mock-transfected cells was normalized to 100. Each value represents the mean ± SE of three independent experiments. (**C**) *LIMK2-1 does not phosphorylate cofilin in vitro.* HEK-293 cells were transfected with one of the three HA-tagged LIMK2 isoforms (2-1, 2a, and 2b) or an unrelated HA-tagged protein, Larp6, as a negative control. Anti-HA immunoprecipitated proteins and GST-cofilin were used in the kinase assay. The anti-HA immunoprecipitates were also subjected to anti-HA immunoblotting and Coomassie blue staining. (**D**) *The three LIMK2 isoforms have kinase activity towards MBP.* HEK-293 cells were transfected with one of the three YFP-tagged LIMK2 isoforms (2-1, 2a, and 2b) or YFP alone. Anti-GFP-immunoprecipitated LIMK2 isoforms and cofilin or MBP were used in the kinase assay. The anti-GFP immunoprecipitates were also subjected to anti-GFP immunoblotting and Coomassie blue staining. Quantification of phospho-cofilin and phospho-MBP is shown in the bottom graph. Phospho-cofilin levels obtained with anti-GFP-immunoprecipitated LIMK2a were normalized to 100. Each value represents the mean ± SE of three independent experiments.

Biochemical Journal (2018) 475 3745–3761
https://doi.org/10.1042/BCJ20170961

In vitro kinase tests

We then studied the kinase activity of the LIMK2 isoforms by *in vitro* labeling with γ[^{32}P]ATP. HEK cells were transfected with each of the HA-tagged versions of the LIMK2 isoforms and the kinase activity of the anti-HA-LIMK2 immunoprecipitates measured using recombinant GST-cofilin as a substrate in the presence of γ[^{32}P]ATP. Immunoprecipitated LIMK2a and LIMK2b phosphorylated cofilin, whereas LIMK2-1 did not (Figure 5C). We obtained similar results using YFP-tagged versions of the three isoforms immunoprecipitated with GFP-trap beads in the presence of recombinant cofilin and γ[^{32}P]ATP (Figure 5D).

We then tested whether LIMK2-1 had no kinase activity or if its activity on cofilin was impaired. We repeated the *in vitro* labeling experiment using MBP as a substrate instead of cofilin. MBP is an efficient substrate for numerous protein kinases. There was a high background signal under the control conditions when the assay was performed in the presence of the HA-tagged versions of the LIMK2 isoforms (data not shown). We overcame this problem by using the YFP-tagged version of these proteins. Under these conditions, the background in the control was low, allowing further studies. GFP-trapped YFP-LIMK2a, LIMK2b, and LIMK2-1 showed kinase activity towards MBP, although the activity of LIMK2-1 was lower (Figure 5D). However, LIMK2-1 was also less efficiently immunoprecipitated under these conditions (see CBB staining and western blotting). Thus, the three isoforms showed comparable activity on MBP when phospho-MBP was normalized to immunoprecipitated LIMK2 levels (by CBB staining) (Figure 5D, lower panel).

Overall, these data show that LIMK2a and LIMK2b have similar activities on cofilin and MBP. Although LIMK2-1 has kinase activity towards MBP comparable to that of the other two isoforms, cofilin is not a good substrate for it.

LIMK2-1 and PP1

LIMK2-1 interacts with PP1

LIMK2-1 has a PP1i domain at its C-terminus, identified by sequence homology, whereas its two counterparts do not. We hypothesized that LIMK2-1 may regulate actin cytoskeleton dynamics via its interaction with PP1. Indeed, PP1 dephosphorylates cofilin [30–33]. LIMK2-1 may indirectly increase the pool of phospho-cofilin by inhibiting its dephosphorylation by PP1.

PP1 is known to interact with many proteins via a consensus motif R/K-V/I-X-F, which serves as an anchor for the initial binding between PP1 and its partner. Furthermore, a secondary interaction site is often present and affects the activity and substrate specificity of PP1 [34–36]. The K-V-R-F motif is present in the sequences of the three LIMK2 isoforms (Figure 1A, underlined in purple and Figure 6A). We tested the interaction between PP1 and each of the three LIMK2 isoforms by co-immunoprecipitation. Flag-tagged PP1 was co-transfected with one of the HA-tagged LIMK2 isoforms or unrelated Larp6 protein and immunoprecipitated with anti-Flag beads. Each isoform of LIMK2 specifically interacted with PP1 (Figure 6B).We then look for the potential secondary interaction site. First, we focused on the potential role of the C-terminal portion of the LIMK2 isoforms by using N-terminal truncated versions of the LIMK2 isoforms, consisting of the kinase domain of LIMK2a/2b, referred to as KIN2, and the kinase-PP1i domain of LIMK2-1, referred to as KIN1-PP1i (Figure 6C, right panel). Flag-tagged PP1 was co-transfected with HA-tagged KIN2 or HA-tagged KIN1-PP1i and immunoprecipitated with anti-Flag beads. PP1 interacted with KIN1-PP1i and a weak band of KIN2 was observed (Figure 6C). It is possible that the interaction between PP1 and KIN1-PP1i is mediated by the extra PP1i domain of LIMK2-1, which may be the secondary interaction site of LIMK2-1 with PP1. Flag-PP1 was then co-transfected with the restricted PP1i domain of LIMK2-1 and immunoprecipitated with anti-Flag beads. PP1i alone interacted with PP1 (Figure 6D).

In conclusion, the three isoforms of LIMK2 interact with PP1. LIMK2-1 seems to have a secondary interaction site present in its PP1i domain.

LIMK2-1 partially inhibits the dephosphorylation of cofilin by PP1

The LIMK2-1 PP1i domain has very strong sequence similarity with the C-terminal portion of PHI-1, a protein which inhibits PP1 (Figure 7A) [24]. We tested whether LIMK2-1 inhibits cofilin dephosphorylation by PP1. We co-transfected HEK-293 cells with various combinations of plasmids and analyzed lysates by western blotting using an antibody that specifically targets phospho-Ser3 cofilin. All the phosphatase inhibitors were omitted in the lysis buffer. The level of phospho-cofilin was much lower in the presence of PP1 than under the control conditions (Gal3 + Larp6, non-related proteins) (Figure 7B): there was detectable PP1 activity towards cofilin in these *in cellulo* conditions. The level of phospho-cofilin was slightly, but significantly, higher when

Biochemical Journal (2018) **475** 3745–3761
https://doi.org/10.1042/BCJ20170961

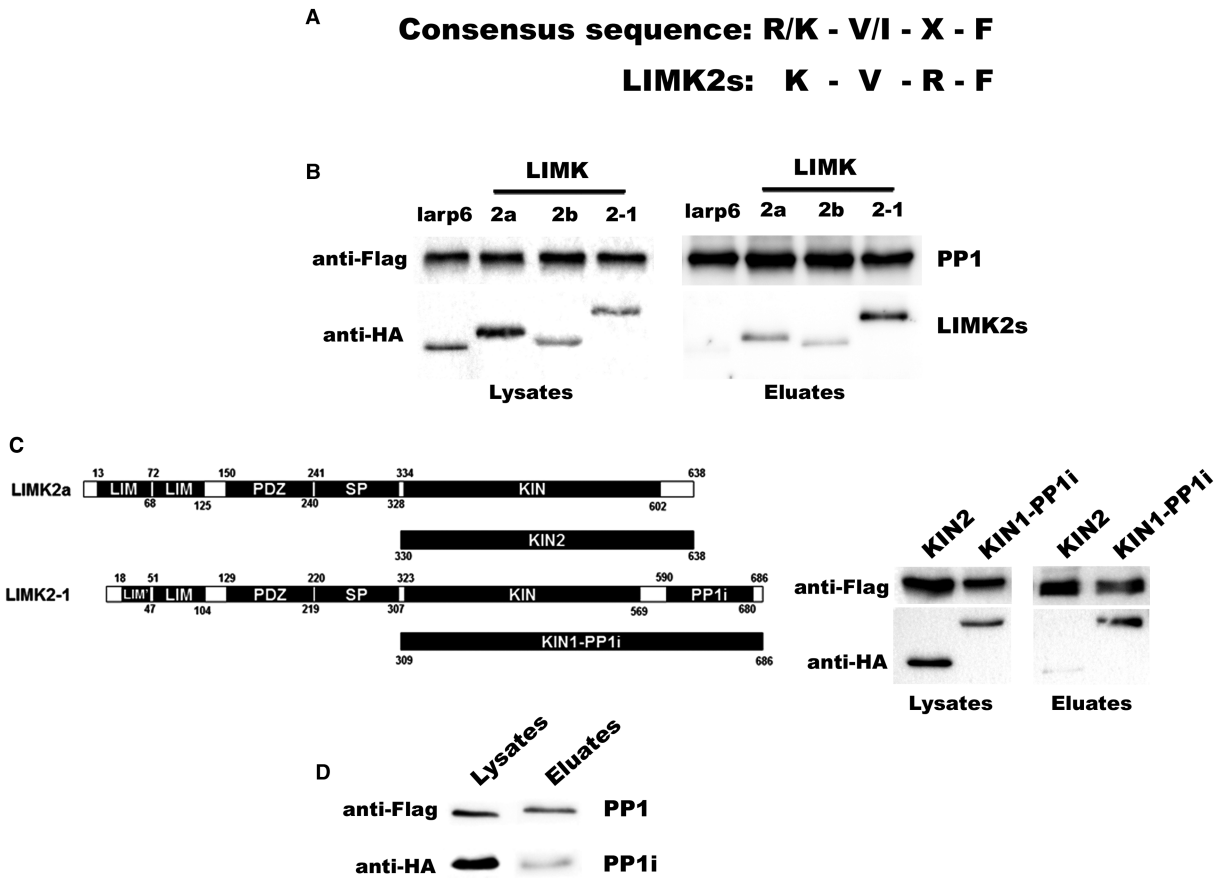

Figure 6. The three LIMK2 isoforms interact with PP1.

(**A**) The consensus PP1 interaction motif is present in the sequence of the three LIMK2 isoforms. (**B**) Interaction between LIMK2 isoforms and PP1. HEK-293 cells were co-transfected with Flag-tagged PP1 and one of the three HA-tagged LIMK2 isoforms (2-1, 2a, and 2b) or the unrelated Larp6 protein. Lysates and anti-Flag immunoprecipitates were subjected to western blotting. (**C**) Interaction between LIMK2 C-terminal fragments and PP1. Left panel: Scheme of KIN1-PP1i and KIN2. Right panel: HEK-293 cells were co-transfected with Flag-tagged PP1 and either the C-terminal domain of LIMK2a/2b (KIN2) or the C-terminal domain of LIMK2-1 (KIN1-PP1i). Lysates and anti-Flag immunoprecipitates were subjected to western blotting. (**D**) Interaction between the PP1i domain of LIMK2-1 and PP1. HEK-293 cells were co-transfected with Flag-tagged PP1 and the HA-tagged PP1i domain of LIMK2-1. Lysates and anti-Flag immunoprecipitates were subjected to western blotting.

LIMK2-1 was co-transfected with PP1 than when PP1 was transfected with the unrelated Larp6 protein. Moreover, when PP1 was co-transfected with LIMK2-1 missing its PP1i part (LIMK2-1_ΔPP1i), the level of phospho-cofilin was comparable to the one of PP1 co-transfected with Larp6, suggesting a role of the PP1i domain in this modulation of phospho-cofilin level. Altogether, these data suggest that LIMK2-1 partially inhibits cofilin dephosphorylation by PP1 under these *in cellulo* conditions.

LIMK2-1 and LIMK2a synergistically phosphorylate cofilin

Our data suggest that LIMK2-1 regulates phospho-cofilin levels and thus cytoskeleton dynamics, not by directly phosphorylating cofilin like LIMK2a and LIMK2b, but by preventing cofilin dephosphorylation by PP1. The three LIMK2 isoforms may have a complementary action, resulting in an increase in the phospho-cofilin pool.

We tested this possibility by cotransfecting HEK-293 cells with LIMK2-1 or LIMK2a alone, or both, and analyzing lysates by western blot using an antibody specific for phospho-Ser3 cofilin. All the phosphatase inhibitors were omitted in the lysis buffer. Phospho-cofilin levels were significantly and reproducibly higher when cells were co-transfected with both LIMK2-1 and LIMK2a than with LIMK2a alone (Figure 7C). When LIMK2a was co-transfected with a kinase dead version of LIMK2-1, LIMK2-1_D430N, this increase was even

Biochemical Journal (2018) **475** 3745–3761
https://doi.org/10.1042/BCJ20170961

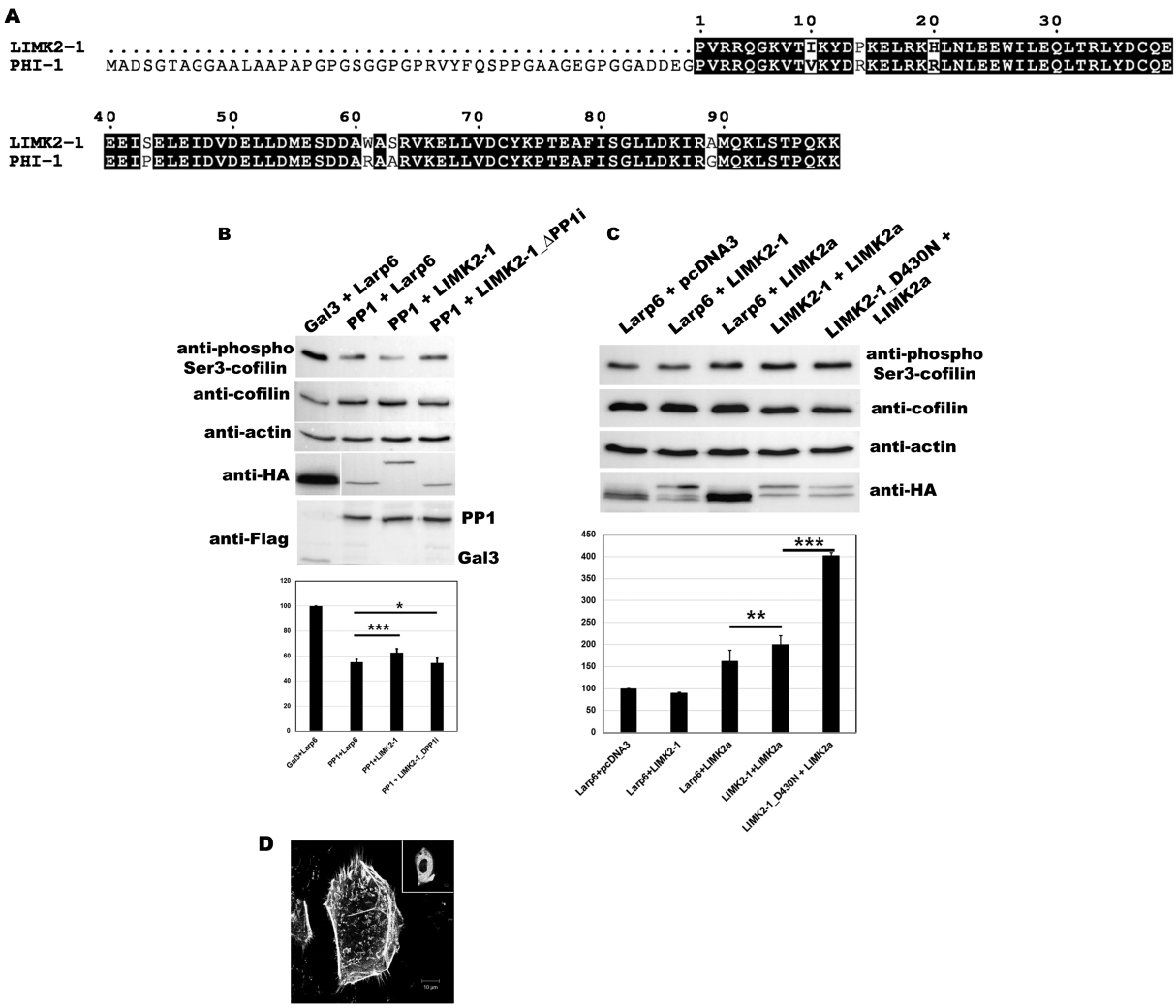

Figure 7. LIMK2-1 regulates cofilin phosphorylation via its PP1i domain.

(**A**) *Alignment between the C-terminal portions of LIMK2-1 and PHI-1*. (**B**) *LIMK2-1 partially inhibits cofilin dephosphorylation by PP1*. HEK-293 cells were co-transfected with the indicated plasmid pairs, resulting in overexpression of the indicated proteins. Lysates were subjected to western blotting. Quantification of the ratio of phospho-cofilin *versus* cofilin is shown in the bottom graph. Phospho-cofilin versus cofilin ratio of mock-transfected cells (Gal3 + Larp6) was normalized to 100. Each value represents the mean ± SE of three independent experiments. (**C**) *LIMK2a and LIMK2-1 act synergistically to increase the pool of phospho-cofilin.* HEK-293 cells were co-transfected with the indicated plasmid pairs, resulting in overexpression of the indicated proteins. Lysates were subjected to western blotting. Quantification of the ratio of phospho-cofilin *versus* cofilin is shown in the bottom graph. Phospho-cofilin versus cofilin ratio of mock-transfected cells (Larp6 + pcDNA3) was normalized to 100. Each value represents the mean ± SE of three independent experiments. (**D**) *LIMK2-1_D430N, the kinase dead mutant of LIMK2-1, induces stress fibers*. HeLa cells were transfected with HA-tagged LIMK2-1_D430N. Cells were fixed and stained with phalloidin (main picture), and anti-HA antibodies (top right corner picture). The scale bar represents 10 μm.

higher. This mutant was also able to induce thin stress fiber formation (Figure 7D). These data suggest that these effects of LIMK2-1 are not due to its kinase activity. LIMK2a and LIMK2-1 act synergistically to increase the pool of phospho-cofilin in the cell.

Discussion

Recent research has shown LIMK2 to have a role in cancer development, metastasis formation, tumor resistance to microtubule-targeting drugs, and neurological disorders [1,21]. Three isoforms of human LIMK2 are

described in databanks: LIMK2a, LIMK2b, and LIMK2-1. Most studies have focused on LIMK2a and, to a lesser extent, LIMK2b. LIMK2-1, which differs from its two counterparts by the presence of a C-terminal PP1i domain, is very poorly studied. Here, we focused on this isoform and further characterized the three LIMK isoforms to better delineate their role in the cell.

We first showed the existence of the LIMK2-1 protein. We developed an antibody against a 12 amino acid peptide of the PP1i domain of LIMK2-1. We could detect endogenous LIMK2-1 expression in HEK293 and HeLa cell lines, as well as in various human tissues (liver, pancreas, testis, and lung). LIMK2-1 expression varied depending on the tissue.

We biochemically characterized the three LIMK2 isoforms. LIMK2 subcellular localization has already been investigated in former studies. Osada et al. [8] showed that both LIMK2a and LIMK2b were located in the cytoplasm and the nucleus, but LIMK2b to a lesser extent in the nucleus, by immunofluorescence of COS cells overexpressing cMyc-tagged LIMK2a or LIMK2b. Smolich et al. [23] showed that LIMK2b was present in both the cytoplasmic and nuclear fractions by fractionation experiments on HEK-293 cells overexpressing LIMK2b. Our data using HeLa and HEK cells are in accordance with these published results. We also showed that transfected as well as endogenous LIMK2-1 is mostly located in the cytoplasm (Figure 2). This result is surprising, given the LIMK2 isoform sequences. Goyal et al. [37,38] identified several nuclear localization signals (NLS) in regions 480–503 and 280–286 of LIMK2a. These domains are identical in all three isoforms (Figure 1) and thus cannot explain the different localization of the LIMK2 isoforms. It is possible that the longer C-terminal domain of LIMK2-1 hides the NLS, thereby preventing its import into the nucleus. LIMK2-1 may also use this extra domain to interact with another partner, segregating it to the cytoplasm. These differences in subcellular localization may also arise from the N-terminal domain of the LIMK2 isoforms. Indeed, LIMK2-1 and LIMK2b are shorter at their N-terminus and the first 18 first amino acids of LIMK2a are different from those of the other two isoforms (their first LIM domain is truncated, Figure 1). Osada et al. [8] suggested that this N-terminal domain could be involved in an interaction with a partner, blocking LIMK2b in the cytoplasm. Alternatively, the extra N-terminal portion of LIMK2a may also interact with a partner, facilitating its import into the nucleus, or retaining it there. Furthermore, LIMK2b and LIMK2-1 have been shown to regulate cell cycle progression via G2/M transition in tumoral cells [6,9,10]. At this cell cycle stage, LIMK2b and LIMK2-1 are most likely present in the nucleus. Thus, shuttling of LIMK2 between the cytoplasm and the nucleus is probably tightly regulated according to environmental conditions. This was suggested by Goyal et al. [37,38] who showed that LIMK2a phosphorylation by PKC on both Ser283 and Thr494 completely inhibited LIMK2a nuclear import in human umbilical vein endothelial cells.

LIMK2a belongs to the Rho/ROCK/LIMK2/cofilin pathway [28,29]. We showed that the three LIMK2 isoforms bind to ROCK1, which specifically phosphorylates them on Thr505 for LIMK2a and Thr484 for LIMK2b and LIMK2-1. Surprisingly, however, LIMK2-1 did not phosphorylate cofilin, either *in cellulo* or *in vitro*, whereas LIMK2a and LIMK2b did. Nevertheless, LIMK2-1 has kinase activity towards MBP, a substrate broadly used to test kinase activity. The role of LIMK2-1 phosphorylation by ROCK is not immediately clear, as LIMK2a phosphorylation by ROCK activates LIMK2 kinase activity towards cofilin [27,28]. Phosphorylation of LIMK2-1 by ROCK may trigger its activation towards another substrate. It is unclear why LIMK2-1 did not phosphorylate cofilin, the canonical substrate of LIM kinases, as the three isoforms of LIMK2 have kinase domains with almost identical sequences. There are several possible explanations for these results: (i) the extra PP1i domain at the LIMK2-1 C-terminus may hide the cofilin-binding site, (ii) LIMK2-1 is missing a few amino acids at the end of the kinase domain with respect to that of LIMK2a/2b, which may perturb kinase activity or cofilin binding, or (iii) a second protein that interacts with or processes LIMK2-1 (maybe by cleavage of the extra PP1i domain) may be necessary for LIMK2-1 to phosphorylate cofilin. The crystal structure of a complex between the kinase domain of LIMK1 and cofilin has been recently resolved [39]. The LIMK1 residues involved in the interaction with cofilin are conserved in the three LIMK2 isoforms, and thus, the LIMK2–cofilin interaction should be preserved. However, we cannot exclude that the PP1i domain of LIMK2-1 may destabilize this interaction, although the C-terminal portion of LIMK1 is distant from the cofilin interaction site in the crystal structure of the complex.

Although LIMK2-1 is unable to phosphorylate cofilin, it still remodels the actin cytoskeleton and promotes stress fiber formation. The mechanism by which LIMK2-1 regulates cytoskeleton dynamics may reside in the C-terminal PP1i domain. This domain receives its name in the databanks because it shows strong homology with PP1 inhibitor proteins, especially PHI-1, which shares 93% identity with this domain (Figure 7A). The mammalian genome encodes far fewer Ser/Thr phosphatases than Ser/Thr kinases (~40 versus ~400) [35]. Phosphatases get their diversity by forming holoenzymes. This is particularly true for the Ser/Thr phosphatase,

Biochemical Journal (2018) **475** 3745–3761
https://doi.org/10.1042/BCJ20170961

PP1. PP1 holoenzymes consist of a catalytic subunit and one or two variable regulatory (PPP1R-) subunits that determine the substrate specificity, allosteric regulation, and subcellular compartmentalization of PP1. One family of such PPP1Rs, the PPP1R14s, encode members of the PHI/CPI-17 family, also called phosphatase holoenzyme inhibitors, comprising CPI-17, PHI1/2, KEPI, and GBPI [40,41]. These specific regulators of PP1 complexes act in addition to, not instead of, regulatory subunits and result in PP1 holoenzyme inhibition. LIMK2-1 may belong to this family, as the PP1i domain of LIMK2-1 exhibits 93% sequence identity with PHI-1. Here, the three LIMK2 isoforms interacted with PP1, consistent with the fact that they all possess the consensus sequence R/K-V/I-X-F, which constitutes the anchoring motif between PP1 and its partners. Moreover, PP1i domain of LIMK2-1 alone interacts with PP1, suggesting that this domain may constitute a second PP1 interaction site. The second binding site has been shown to be crucial, as it brings PP1 into close proximity with its PPP1R, resulting in additional interactions that determine the activity and substrate specificity of the holoenzyme [42]. PP1 has been shown to dephosphorylate cofilin in various cell lines [30–33]. Our data are in good accordance with these results as we observed a strong decrease in phospho-cofilin levels in HEK-293 cells transfected with PP1 catalytic subunit α (Figure 7B). Moreover, co-transfection of PP1 with LIMK2-1 resulted in a weak but relevant increase in phospho-cofilin levels, suggesting slight inhibition of PP1-mediated cofilin dephosphorylation by LIMK2-1 in our *in cellulo* conditions. This effect seems to be correlated with PP1i domain as it was abolished when LIMK2-1 missed its PP1i domain. The faintness of the effect of LIMK2-1 on PP1 activity may come from the fact that we may have missed activation of this inhibition, as reported for PHI/CPI-17 family member PPP1R14s. Indeed, PHI/CPI-17 family members become potent inhibitors of PP1 holoenzymes after phosphorylation on a conserved threonine by diverse kinases including PKC, ROCK, MYPT-associated kinase, or integrin-linked kinase [24,43–45]. LIMK2-1 has this conserved threonine (Thr 596). We attempted to mimic this threonine phosphorylation by substituting it with aspartic acid residue. However, this mutant no longer inhibited cofilin dephosphorylation by PP1 (data not shown). These results are not surprising as substituting Thr38 of CPI-17 by Asp or Glu did not result in an increase in inhibition, but rather destabilized the interaction between CPI-17 and PP1 [46]. We are currently studying whether LIMK2-1 can be phosphorylated by a kinase on Thr596, and whether such phosphorylation enhances LIMK2-1-mediated inhibition of cofilin dephosphorylation by PP1. We also attempted to develop an *in vitro* assay to further characterize this inhibition, but were unsuccessful. We probably missed regulatory unit(s) necessary to trigger catalytic activity of the PP1 holoenzyme towards cofilin. It may be necessary to identify this or these regulatory

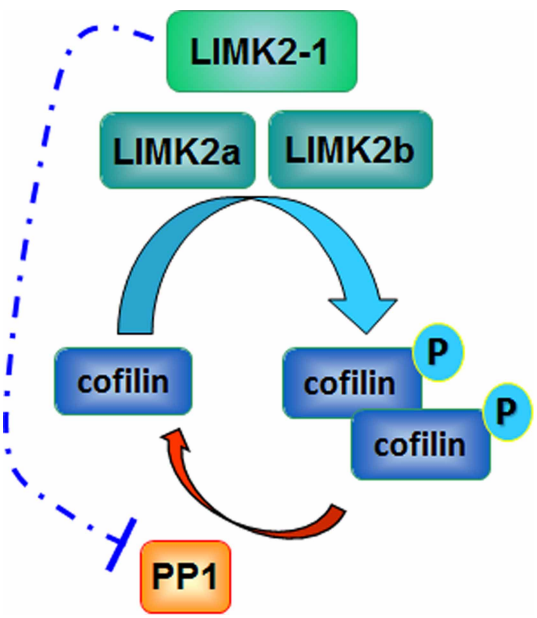

Figure 8. Schematic representation of our findings.

LIMK2a, LIMK2b, and LIMK2-1 form a complex that regulates the balance between cofilin and phospho-cofilin. LIMK2a and LIMK2b directly phosphorylate cofilin, whereas LIMK2-1 prevents cofilin dephosphorylation by the phosphatase PP1.

subunits to further understand the action of PP1 on cofilin. PP1 appears to act as a hub as it interacts with specific partners to form holoenzymes, according to specific signaling mechanisms (normal or tumorigenic conditions, cell types). Multiple holoenzyme-specific strategies have evolved for fine and acute regulation of phosphatase activity. The underlying molecular mechanisms are mostly still poorly understood. This field will provide many challenges in coming years as phosphatases are emerging as new therapeutic targets. Indeed, the role of phosphatases in many diseases is well established and new therapies that target phosphatases may be an attractive alternative to those that target kinases.

Here, we have characterized a new isoform of human LIMK2, LIMK2-1. LIMK2-1 regulates actin cytoskeleton dynamics, as its two counterparts, LIMK2a and LIMK2b, but through a distinct signaling pathway. LIMK2a and LIMK2b directly phosphorylate cofilin, whereas LIMK2-1 appears to partially prevent its dephosphorylation by PP1 (Figure 8). The cofilin/phospho-cofilin balance mediates actin dynamics, which, in turn, control many physiological mechanisms and are involved in many pathological processes. Currently, small molecules inhibiting the kinase activity of LIMK2 are developed as LIM kinases appear to be new therapeutic targets. As LIMK2-1 has no kinase activity towards cofilin, it may constitute a by-pass for these inhibitors. Our work provides a better understanding of the regulation of actin dynamics by the cofilin/phospho-cofilin balance via the action of LIMK2s, providing new elements for the development of future therapies.

Abbreviations

LIMKs, LIM kinases; MBP, myelin basic protein; NLS, nuclear localization signals; PP1, protein phosphatase 1; PP1i, protein phosphatase 1 inhibitory.

Author Contribution

B.V., H.C., M.D., and F.G. performed experiments. D.G. did immunofluorescence image treatment. B.V. and H.B. were involved in the concept, design, and interpretation of data. P.V. and C.A. discussed the manuscript. B.V. and H.B. wrote the manuscript.

Funding

This work was supported by La ligue contre le Cancer, l'Association Neurofibromatoses et Recklinghausen, and la Région Centre Val de Loire.

Acknowledgements

We thank S. Shieh who kindly provided cMyc-LIMK2b plasmid. Many thanks to Aurélie Cosson and Déborah Casas for their support.

Competing Interests

The Authors declare that there are no competing interests associated with the manuscript.

References

1 Scott, R.W. and Olson, M.F. (2007) LIM kinases: function, regulation and association with human disease. *J. Mol. Med.* **85**, 555–568 https://doi.org/10.1007/s00109-007-0165-6

2 Bamburg, J.R. and Bernstein, B.W. (2010) Roles of ADF/cofilin in actin polymerization and beyond. *F1000 Biol. Rep.* **2**, 62 https://doi.org/10.3410/B2-62

3 Mizuno, K. (2013) Signaling mechanisms and functional roles of cofilin phosphorylation and dephosphorylation. *Cell. Signal.* **25**, 457–469 https://doi.org/10.1016/j.cellsig.2012.11.001

4 Pollard, T.D. and Borisy, G.G. (2003) Cellular motility driven by assembly and disassembly of actin filaments. *Cell* **112**, 453–465 https://doi.org/10.1016/S0092-8674(03)00120-X

5 Prunier, C., Prudent, R., Kapur, R., Sadoul, K. and Lafanechère, L. (2017) LIM kinases: cofilin and beyond. *Oncotarget* **8**, 41749–41763 https://doi.org/10.18632/oncotarget.16978

6 Croft, D.R., Crighton, D., Samuel, M.S., Lourenco, F.C., Munro, J., Wood, J. et al. (2011) p53-mediated transcriptional regulation and activation of the actin cytoskeleton regulatory RhoC to LIMK2 signaling pathway promotes cell survival. *Cell Res.* **21**, 666–682 https://doi.org/10.1038/cr.2010.154

7 Nomoto, S., Tatematsu, Y., Takahashi, T. and Osada, H. (1999) Cloning and characterization of the alternative promoter regions of the human LIMK2 gene responsible for alternative transcripts with tissue-specific expression. *Gene* **236**, 259–271 https://doi.org/10.1016/S0378-1119(99)00280-2

8 Osada, H., Hasada, K., Inazawa, J., Uchida, K., Ueda, R., Takahashi, T. et al. (1996) Subcellular localization and protein interaction of the human LIMK2 gene expressing alternative transcripts with tissue-specific regulation. *Biochem. Biophys. Res. Commun.* **229**, 582–589 https://doi.org/10.1006/bbrc.1996.1847

9 Gamell, C., Schofield, A.V., Suryadinata, R., Sarcevic, B. and Bernard, O. (2013) LIMK2 mediates resistance to chemotherapeutic drugs in neuroblastoma cells through regulation of drug-induced cell cycle arrest. *PLoS ONE* **8**, e72850 https://doi.org/10.1371/journal.pone.0072850

Biochemical Journal (2018) **475** 3745–3761
https://doi.org/10.1042/BCJ20170961

10 Hsu, F.F., Lin, T.Y., Chen, J.Y. and Shieh, S.Y. (2010) p53-Mediated transactivation of LIMK2b links actin dynamics to cell cycle checkpoint control. *Oncogene* **29**, 2864–2876 https://doi.org/10.1038/onc.2010.40
11 Rak, R. and Kloog, Y. (2014) Targeting LIM kinase in cancer and neurofibromatosis. *Cell Cycle* **13**, 1360–1361 https://doi.org/10.4161/cc.28748
12 Manetti, F. (2012) Recent findings confirm LIM domain kinases as emerging target candidates for cancer therapy. *Curr. Cancer Drug Targets* **12**, 543–560 https://doi.org/10.2174/156800912800673266
13 Suyama, E., Wadhwa, R., Kawasaki, H., Yaguchi, T., Kaul, S.C., Nakajima, M. et al. (2004) LIM kinase-2 targeting as a possible anti-metastasis therapy. *J. Gene Med.* **6**, 357–363 https://doi.org/10.1002/jgm.491
14 Vlecken, D.H. and Bagowski, C.P. (2009) LIMK1 and LIMK2 are important for metastatic behavior and tumor cell-induced angiogenesis of pancreatic cancer cells. *Zebrafish* **6**, 433–439 https://doi.org/10.1089/zeb.2009.0602
15 Johnson, E.O., Chang, K.H., Ghosh, S., Venkatesh, C., Giger, K., Low, P.S. et al. (2012) LIMK2 is a crucial regulator and effector of Aurora-A-kinase-mediated malignancy. *J. Cell Sci.* **125**, 1204–1216 https://doi.org/10.1242/jcs.092304
16 Po'uha, S.T., Shum, M.S., Goebel, A., Bernard, O. and Kavallaris, M. (2010) LIM-kinase 2, a regulator of actin dynamics, is involved in mitotic spindle integrity and sensitivity to microtubule-destabilizing drugs. *Oncogene* **29**, 597–607 https://doi.org/10.1038/onc.2009.367
17 Prudent, R., Vassal-Stermann, E., Nguyen, C.H., Pillet, C., Martinez, A., Prunier, C. et al. (2012) Pharmacological inhibition of LIM kinase stabilizes microtubules and inhibits neoplastic growth. *Cancer Res.* **72**, 4429–4439 https://doi.org/10.1158/0008-5472.CAN-11-3342
18 Starinsky-Elbaz, S., Faigenbloom, L., Friedman, E., Stein, R. and Kloog, Y. (2009) The pre-GAP-related domain of neurofibromin regulates cell migration through the LIM kinase/cofilin pathway. *Mol. Cell. Neurosci.* **42**, 278–287 https://doi.org/10.1016/j.mcn.2009.07.014
19 Vallée, B., Doudeau, M., Godin, F., Gombault, A., Tchalikian, A., de Tauzia, M.L. et al. (2012) Nf1 RasGAP inhibition of LIMK2 mediates a new cross-talk between Ras and Rho pathways. *PLoS ONE* **7**, e47283 https://doi.org/10.1371/journal.pone.0047283
20 Cuberos, H., Vallée, B., Vourc'h, P., Tastet, J., Andres, C.R. and Bénédetti, H. (2015) Roles of LIM kinases in central nervous system function and dysfunction. *FEBS Lett.* **589**, 3795–3806 https://doi.org/10.1016/j.febslet.2015.10.032
21 Manetti, F. (2012) LIM kinases are attractive targets with many macromolecular partners and only a few small molecule regulators. *Med. Res. Rev.* **32**, 968–998 https://doi.org/10.1002/med.20230
22 Genis-Mendoza, A.D., Gallegos-Silva, R.I., Lopez-Casamichana, M., Lopez-Rubalcava, C. and Nicolini, H. (2013) Gene expression profiles of nucleus accumbens, prefrontal cortex and hippocampus in an animal model of schizophrenia: proposed candidate genes. *Actas Esp. Psiquiatr.* **41**, 154–163 PMID:23803799
23 Smolich, B., Vo, M., Buckley, S., Plowman, G. and Papkoff, J. (1997) Cloning and biochemical characterization of LIMK-2, a protein kinase containing two LIM domains. *J. Biochem.* **121**, 382–388 https://doi.org/10.1093/oxfordjournals.jbchem.a021599
24 Eto, M., Karginov, A. and Brautigan, D.L. (1999) A novel phosphoprotein inhibitor of protein type-1 phosphatase holoenzymes. *Biochemistry* **38**, 16952–16957 https://doi.org/10.1021/bi992030o
25 Acevedo, K., Moussi, N., Li, R., Soo, P. and Bernard, O. (2006) LIM kinase 2 is widely expressed in all tissues. *J. Histochem. Cytochem.* **54**, 487–501 https://doi.org/10.1369/jhc.5C6813.2006
26 Hiraoka, J., Okano, I., Higuchi, O., Yang, N. and Mizuno, K. (1996) Self-association of LIM-kinase 1 mediated by the interaction between an N-terminal LIM domain and a C-terminal kinase domain. *FEBS Lett.* **399**, 117–121 https://doi.org/10.1016/S0014-5793(96)01303-8
27 Amano, T., Tanabe, K., Eto, T., Narumiya, S. and Mizuno, K. (2001) LIM-kinase 2 induces formation of stress fibres, focal adhesions and membrane blebs, dependent on its activation by Rho-associated kinase-catalysed phosphorylation at threonine-505. *Biochem. J.* **354**, 149–159 https://doi.org/10.1042/bj3540149
28 Sumi, T., Matsumoto, K. and Nakamura, T. (2001) Specific activation of LIM kinase 2 via phosphorylation of threonine 505 by ROCK, a Rho-dependent protein kinase. *J. Biol. Chem.* **276**, 670–676 https://doi.org/10.1074/jbc.M007074200
29 Maekawa, M., Ishizaki, T., Boku, S., Watanabe, N., Fujita, A., Iwamatsu, A. et al. (1999) Signaling from Rho to the actin cytoskeleton through protein kinases ROCK and LIM-kinase. *Science* **285**, 895–898 https://doi.org/10.1126/science.285.5429.895
30 Ambach, A., Saunus, J., Konstandin, M., Wesselborg, S., Meuer, S.C. and Samstag, Y. (2000) The serine phosphatases PP1 and PP2A associate with and activate the actin-binding protein cofilin in human T lymphocytes. *Eur. J. Immunol.* **30**, 3422–3431 https://doi.org/10.1002/1521-4141(2000012)30:12<3422::AID-IMMU3422>3.0.CO;2-J
31 Li, G.B., Cheng, Q., Liu, L., Zhou, T., Shan, C.Y., Hu, X.Y. et al. (2013) Mitochondrial translocation of cofilin is required for allyl isothiocyanate-mediated cell death via ROCK1/PTEN/PI3K signaling pathway. *Cell Commun. Signal.* **11**, 50 https://doi.org/10.1186/1478-811X-11-50
32 Oleinik, N.V., Krupenko, N.I. and Krupenko, S.A. (2010) ALDH1L1 inhibits cell motility via dephosphorylation of cofilin by PP1 and PP2A. *Oncogene* **29**, 6233–6244 https://doi.org/10.1038/onc.2010.356
33 Samstag, Y. and Nebl, G. (2003) Interaction of cofilin with the serine phosphatases PP1 and PP2A in normal and neoplastic human T lymphocytes. *Adv. Enzyme Regul.* **43**, 197–211 https://doi.org/10.1016/S0065-2571(02)00031-6
34 Bollen, M., Peti, W., Ragusa, M.J. and Beullens, M. (2010) The extended PP1 toolkit: designed to create specificity. *Trends Biochem. Sci.* **35**, 450–458 https://doi.org/10.1016/j.tibs.2010.03.002
35 Ceulemans, H., Stalmans, W. and Bollen, M. (2002) Regulator-driven functional diversification of protein phosphatase-1 in eukaryotic evolution. *BioEssays* **24**, 371–381 https://doi.org/10.1002/bies.10069
36 Wakula, P., Beullens, M., Ceulemans, H., Stalmans, W. and Bollen, M. (2003) Degeneracy and function of the ubiquitous RVXF motif that mediates binding to protein phosphatase-1. *J. Biol. Chem.* **278**, 18817–18823 https://doi.org/10.1074/jbc.M300175200
37 Goyal, P., Pandey, D., Behring, A. and Siess, W. (2005) Inhibition of nuclear import of LIMK2 in endothelial cells by protein kinase C-dependent phosphorylation at Ser-283. *J. Biol. Chem.* **280**, 27569–27577 https://doi.org/10.1074/jbc.M504448200
38 Goyal, P., Pandey, D. and Siess, W. (2006) Phosphorylation-dependent regulation of unique nuclear and nucleolar localization signals of LIM kinase 2 in endothelial cells. *J. Biol. Chem.* **281**, 25223–25230 https://doi.org/10.1074/jbc.M603399200
39 Hamill, S., Lou, H.J., Turk, B.E. and Boggon, T.J. (2016) Structural basis for noncanonical substrate recognition of cofilin/ADF proteins by LIM kinases. *Mol. Cell* **62**, 397–408 https://doi.org/10.1016/j.molcel.2016.04.001
40 Eto, M. (2009) Regulation of cellular protein phosphatase-1 (PP1) by phosphorylation of the CPI-17 family, C-kinase-activated PP1 inhibitors. *J. Biol. Chem.* **284**, 35273–35277 https://doi.org/10.1074/jbc.R109.059972

41 Eto, M. and Brautigan, D.L. (2012) Endogenous inhibitor proteins that connect Ser/Thr kinases and phosphatases in cell signaling. *IUBMB Life* **64**, 732–739 https://doi.org/10.1002/iub.1067
42 Verbinnen, I., Ferreira, M. and Bollen, M. (2017) Biogenesis and activity regulation of protein phosphatase 1. *Biochem. Soc. Trans.* **45**, 89–99 https://doi.org/10.1042/BST20160154
43 Deng, J.T., Sutherland, C., Brautigan, D.L., Eto, M. and Walsh, M.P. (2002) Phosphorylation of the myosin phosphatase inhibitors, CPI-17 and PHI-1, by integrin-linked kinase. *Biochem. J.* **367**, 517–524 https://doi.org/10.1042/bj20020522
44 Liu, Q.R., Zhang, P.W., Lin, Z., Li, Q.F., Woods, A.S., Troncoso, J. et al. (2004) GBPI, a novel gastrointestinal- and brain-specific PP1-inhibitory protein, is activated by PKC and inactivated by PKA. *Biochem. J.* **377**, 171–181 https://doi.org/10.1042/bj20030128
45 Liu, Q.R., Zhang, P.W., Zhen, Q., Walther, D., Wang, X.B. and Uhl, G.R. (2002) KEPI, a PKC-dependent protein phosphatase 1 inhibitor regulated by morphine. *J. Biol. Chem.* **277**, 13312–13320 https://doi.org/10.1074/jbc.M107558200
46 Ohki, S., Eto, M., Shimizu, M., Takada, R., Brautigan, D.L. and Kainosho, M. (2003) Distinctive solution conformation of phosphatase inhibitor CPI-17 substituted with aspartate at the phosphorylation-site threonine residue. *J. Mol. Biol.* **326**, 1539–1547 https://doi.org/10.1016/S0022-2836(03)00048-2
47 Ishizaki, T., Naito, M., Fujisawa, K., Maekawa, M., Watanabe, N., Saito, Y. et al. (1997) p160ROCK, a Rho-associated coiled-coil forming protein kinase, works downstream of Rho and induces focal adhesions. *FEBS Lett.* **404**, 118–124 https://doi.org/10.1016/S0014-5793(97)00107-5

NEUROSCIENCE

RESEARCH ARTICLE

J. Tastet et al. / Neuroscience xxx (2018) xxx–xxx

LIMK2-1 is a Hominidae-Specific Isoform of LIMK2 Expressed in Central Nervous System and Associated with Intellectual Disability

Julie Tastet, [a,b,f†] **Hélène Cuberos,** [a,b†] **Béatrice Vallée,** [b†] **Annick Toutain,** [a,c] **Martine Raynaud,** [a,c] **Sylviane Marouillat,** [a] **Rose-Anne Thépault,** [a] **Frédéric Laumonnier,** [a] **Frédérique Bonnet-Brilhault,** [a,d] **Patrick Vourc'h,** [a,e] **Christian R. Andres** [a,e] **and Hélène Bénédetti** [b*]

[a] *UMR INSERM U1253, Université François Rabelais, Tours, France*

[b] *CNRS UPR 4301, CBM, Orléans, France*

[c] *CHRU de Tours, Service de Génétique, Tours, France*

[d] *CHRU de Tours, Service de Pédopsychiatrie, Tours, France*

[e] *CHRU de Tours, Service de Biochimie et de Biologie Moléculaire, Tours, France*

[f] *Department of Translational Neuroscience, Brain Center Rudolf Magnus, University Medical Center Utrecht, Utrecht, Netherlands*

Abstract—LIMK2 is involved in neuronal functions by regulating actin dynamics. Different isoforms of LIMK2 are described in databanks. LIMK2a and LIMK2b are the most characterized. A few pieces of evidence suggest that LIMK2 isoforms might not have overlapping functions. In this study, we focused our attention on a less studied human LIMK2 isoform, LIMK2-1. Compared to the other LIMK2 isoforms, LIMK2-1 contains a supplementary C-terminal phosphatase 1 inhibitory domain (PP1i). We found out that this isoform was hominidae-specific and showed that it was expressed in human fetal brain and faintly in adult brain. Its coding sequence was sequenced in 173 patients with sporadic non-syndromic intellectual disability (ID), and we observed an association of a rare missense variant in the PP1i domain (rs151191437, p.S668P) with ID. Our results also suggest an implication of LIMK2-1 in neurite outgrowth and neurons arborization which appears to be affected by the p.S668P variation. Therefore our results suggest that LIMK2-1 plays a role in the developing brain, and that a rare variation of this isoform is a susceptibility factor in ID.

Key words: LIM kinase, hominidae-specific, neuron morphology, cytoskeleton remodeling, intellectual deficiency, patient mutation.

INTRODUCTION

LIM kinase (LIMK) family comprises two members: LIMK1 and LIMK2. These two proteins share 50% identity. They possess a Ser/Thr/Tyr kinase activity involved in cytoskeleton remodeling. LIMKs phosphorylate and subsequently inactivate cofilin, an actin depolymerizing factor (Arber et al., 1998). Their role on actin dynamics through their regulation of the balance between phospho-cofilin and cofilin has been widely described (Aizawa et al., 2001; Hsieh et al., 2006; Endo et al., 2007). They also regulate microtubule stability (Gorovoy et al., 2005), and play a role in mitotic spindle integrity (Po'uha et al., 2010; Heng et al., 2012). They are involved in cancer development and metastasis propagation (Scott and Olson, 2007; Manetti, 2012) and in viral infection (Yi et al., 2017). They also play a role in neuronal functions, particularly in neurite outgrowth and synaptic plasticity, and in several neurologic diseases (Cuberos et al., 2015). Recent studies suggest a role for LIMKs independently of cofilin phosphorylation, especially in neuronal functions. Other substrates of LIMK1 have been identified in the central nervous system (CNS) (Yang et al., 2004; Sacchetti et al., 2006). One of them, CREB, is involved in long-term late-phase potentiation (L-LTP) and long-term memory (Todorovski et al., 2015). Furthermore, LIMKs seem to exert functions independently of their kinase activity since overexpression of the N-terminal non-catalytic region of LIMK1 in PC12 cells has been shown to inhibit neurite outgrowth (Birkenfeld et al., 2001) whereas overexpression of LIMK2d, a rat LIMK2 isoform lacking the kinase domain, in NSC-34 cells led to a significant increase in neurite length (Tastet et al., 2012).

Several pieces of evidence suggest that LIMK1 and LIMK2 most probably play distinct roles particularly in the CNS. Indeed, deletions of *Limk1* or *Limk2* genes

*Corresponding author.
E-mail address: helene.benedetti@cnrs-orleans.fr (H. Bénédetti).
† These authors contributed equally to this work.
Abbreviations: PP1i, phosphatase 1 inhibitory domain; ID, intellectual disability; LIMK, LIM kinase.

https://doi.org/10.1016/j.neuroscience.2018.12.017
0306-4522/

Table 1. Primer sequences used for sequencing and PCR

Gene	Location	Forward primer (5′–3′)	Reverse primer (5′–3′)	Amplified fragment (bp)
LIMK2-1	Exon 16-1	CCAAGGACCACGCATCTACT	CGGTATTGCTGTTGCTACGA	453
	Exons 15 to 16-1	ATGACAGGGCCTTTTATG	GGGAGTTACTTGTCAGTCCC	149
GAPDH	Exons 7 to 8	CTGCACCACCAACTGCTTAG	GTCTTCTGGGTGGCAGTGAT	108

result in relatively mild but different phenotypes in mice (Meng et al., 2002; Meng et al., 2004), they are differently regulated by Rho family GTPases (Edwards et al., 1999; Sumi et al., 2001a; b) and they have different subcellular localizations and activities during the different stages of the cell cycle (Foletta et al., 2004; Acevedo et al., 2006; Sumi et al., 2006).

Different isoforms of LIMK2 are described in the databanks, LIMK2a and LIMK2b are the most studied. However, we have shown that rat isoform LIMK2d regulates neurite growth in NSC-34 cells (Tastet et al., 2012), and that human isoform LIMK2-1 is expressed in different cell lines and tissues (Vallée et al., 2018). Different arguments indicate that LIMK2 isoforms might display functional differences. For example, LIMK2a and LIMK2b exhibit different tissue distribution and are differently expressed during development stages (Osada et al., 1996; Nomoto et al., 1999). Furthermore, their cellular localization and stability differs (Osada et al., 1996; Gamell et al., 2013). In addition, LIMK2b as well as LIMK2-1, but not LIMK2a, are regulated by p53 (Croft et al., 2011). Moreover, LIMK2-1 does not phosphorylate cofilin, the canonical substrate of LIM kinases, whereas it remodels actin cytoskeleton (Vallée et al.; 2018).

In the present study, we decided to further characterize human isoform LIMK2-1 and more specifically its role in neurodevelopment. Compared to the two other human isoforms, LIMK2-1 lacks a few amino acids in its kinase C-terminal domain and contains a supplementary phosphatase 1 inhibitory domain (PP1i) at its C-terminal extremity. By *in silico* analysis, we showed that this isoform is specific to Hominidae primates. We demonstrated that LIMK2-1 is expressed in human fetal brain and in specific areas of adult brain, both at mRNA and protein level. These observations, together with the known involvement of LIM kinases in neurodevelopment, prompted us to further study this particular isoform in cognitive disorders. We found out an association between a rare coding variant in the PP1i domain of LIMK2-1 and non-syndromic intellectual disability (ID). On a functional level, our results suggest that LIMK2-1 might have a distinct effect on neurite outgrowth and neuron arborization compared to LIMK2b, and that the variation associated with ID disturbs this effect.

EXPERIMENTAL PROCEDURES

Subjects

Patients with non-syndromic ID were examined in the Child Psychiatry Unit and the Clinical genetics Unit of the University Hospital of Tours (France) (n = 173). Recognizable genetic diseases have been excluded by clinicians and cytogeneticists. All patients tested were negative for fragile X mutation. A practitioner from the Center of Clinical Investigations in Tours examined control individuals. These control individuals and their family did not present any psychiatric or developmental diseases. Written consents were obtained from patients (or parents) and from control individuals.

Genetic analysis

Genomic DNA was extracted from peripheral blood samples using standard procedures. The sequence coding the PP1i domain was analyzed by sequencing. PCR were done in a final volume of 50 μL containing 10 pmol of each primer, 125 nmol $MgCl_2$, 10 nmol dNTP, 50 ng DNA, 1× GoTaq flexi buffer and 1.25 U GoTaq polymerase (Promega, Madison, USA). Reactions were performed at 95 °C 1 min, 60 °C 30 s, 72 °C 1 min for 35 cycles. Sequencing reactions were done in a volume of 10 μL containing 20 pmol of either forward or reverse primer (Table 1), 2 μL of PCR products, 1× buffer and 1 μL of BigDye Terminator v3.1 (Applied Biosystems, Cheshire, UK). Reactions were performed at 96 °C 10 s, 50 °C 5 s, 60 °C 4 min for 25 cycles. Products were purified on Millipore Montage SEQ96 plates before bidirectional sequencing in an ABI 3130xl sequencer (Applied Biosystems, Courtaboeuf, France; analysis with CodonCode Aligner Software). Genotype frequencies were compared using Fisher's exact test (BiostaTGV server, http://marne.u707.jussieu.fr/biostatgv/).

Comparison of sequences, 2D structures and 3D modeling

The potential presence of a PP1i-coding sequence in LIMK2 isoforms in different species was studied using blastn (http://blast.ncbi.nlm.nih.gov/Blast.cgi). 2D structure comparison and 3D modeling of the PP1i domain of LIMK2-1 was done first by searching the Brookhaven Protein Data Bank for the most similar protein(s) to this domain. Among the crystallized proteins, PKC-potentiated inhibitory protein of PP1, CPI-17 chain A, showed the highest sequence identity with the PP1i of LIMK2-1 (38%). Protein phosphatase 1 regulatory subunit 14B (PHI-1, PPP1R14B) presented a higher percentage of identity but its 3D structure is not known. 2D structure comparison of the PP1i domain of LIMK2-1 and CPI-17 was done using the ESPRIT software and PDB data (#1J2M). We used the coordinates of CPI-17 structure in the Swiss-model workspace (http://swissmodel.expasy.org/workspace/; default parameters) to model the wild type and mutant forms of the PP1i domain of LIMK2-1. Ribbon

Please cite this article in press as: Tastet J et al. LIMK2-1 is a Hominidae-Specific Isoform of LIMK2 Expressed in Central Nervous System and Associated with Intellectual Disability. Neuroscience (2019), https://doi.org/10.1016/j.neuroscience.2018.12.017

representations of the wild type and mutant forms were obtained using the molecular graphics tool PyMOL v1.3.

Cell line cultures

HEK-293 cells (85120602, European Collection of Cell cultures) and C6 cells (a rat brain glial tumor, ATCC® CCL-107) were cultured in Dulbecco's modified Eagle's medium (DMEM) 1 g/L glucose (Sigma-Aldrich) supplemented with 10% heat inactivated fetal calf serum (Sigma-Aldrich). Neuronal cell line NSC-34 (CLU140-A, Tebu-Bio) was cultured in DMEM containing 4.5 g/L glucose, 0.58 g/L L-glutamine (Sigma-Aldrich) and 10% fetal bovine serum, 100 U/mL penicillin and 100 μg/mL streptomycin (Sigma-Aldrich).

Mouse primary neuronal culture and transfection

All mouse experiments were performed according to protocols approved by the University François-Rabelais of Tours and the INSERM. Primary cortical neuron cultures were prepared from postnatal days 0–2 C57bl/6J mice. Briefly, pups were euthanized by decapitation, and heads were placed in ice-cold 1× Hank's Balanced Salt Solution (HBSS; Life Technologies). Brains were dissected out of the skull in ice-cold HBSS in a glass petri dish. Cerebral cortices were isolated and processed individually. Samples were centrifuged (400*g*), digested using trypsin (2.5 mg/mL) (Sigma-Aldrich) and diluted 20× in HBSS with DNase I (0.65 mg/mL) (Roche) and magnesium chloride (2 mM) for 30 min at 37 °C. The reaction was halted using trypsin inhibitor (0.5 mg/mL) (Roche) in HBSS. Samples were centrifuged (400*g* at room temperature), the supernatant was removed and the cells in the resulting pellet were run through a 100-μm cell strainer (BD Falcon) and resuspended in plating media (Neurobasal media with B27 and N_2 supplements, 1% penstrep, and 1× Glutamax (all Life Technologies). Cells were plated onto poly-D-lysine (20 μg/ml) and laminin (40 μg/ml) (Sigma-Aldrich)-coated glass coverslips at a density of 1.5×10^5 cells/well in 12-well plates.

At DIV2, cortical neurons in culture were cotransfected with the EGFP plasmid and the different HA-LIMK2 coding plasmids using Lipofectamine 2000 (Life Technologies) in neurobasal serum free medium. 48 h after transfection, neurons were washed with PBS, fixed with 4% PFA and 4% Sucrose in PBS, pH 7.4 for 20 min at 37 °C before washing three more times with PBS. After immunostaining, images from the Zeiss Axioscop A1 were taken. For analysis of neuronal morphological parameters, about 110 transfected neurons were examined per condition of each independent experiment ($n = 3$).

PCR

A specific cDNA region of *LIMK2-1* (exons 15 to 16-1, corresponding to a 149 bp DNA fragment) and of *GAPDH* (corresponding to a 105 bp fragment) were amplified using GoTaqR Flexi DNA Polymerase (Promega) in a 25 μL reaction mixture containing 1 μL of human fetal brain, adult cortex, hippocampus and cerebellum cDNA (BioChainR, Newark, CA), HEK cDNA (prepared as described in Tastet et al., 2012), Rattus cortex cDNA (prepared as described in Vourc'h et al., 2003) or mouse cortex cDNA (prepared as described in Laumonnier et al., 2005), according to the supplier's instructions. Primer sequences are given in Table 1. Amplification consisted in 35 cycles of 94 °C 10 s, 60 °C 30 s and 72 °C 30 s.

Cell lines transfection

Plasmids used in this study are listed in Table 2. HEK-293 cells were transfected with 10 μg of plasmid/10-mm dish with Calcium Phosphate method. NSC-34 cells (30% confluence) were transfected with Lipofectamine 2000 according to manufacturer's instructions (Life Technologies) one hour after plating. Medium was replaced with DMEM without serum 4 h after transfection. Neurite outgrowth was induced by this serum starvation during 36 h.

Protein extraction and Western blotting

Total proteins from HEK-293, and C6 cells were extracted using a lysis buffer containing 50 mM Tris, 100 mM NaCl, 5 mM EDTA, 1% Triton X-100, 50 mM sodium fluoride, 10 μg/mL aprotinin, 10 mM pyrophosphate, 1 mM sodium orthovanadate, 20 mM *para*-nitrophenylphosphate, 1 μg/mL leupeptin, 50 ng/mL okadaic acid, 1 mM phenylmethane sulfonyl fluoride and 20 mM β-glycerophosphate. Fifteen to twenty micrograms of total proteins and proteins from human fetal brain, adult cortex, hippocampus and cerebellum (BioChainR, Newark, CA) were separated by SDS-PAGE and transferred to a polyvinylidene fluoride membrane. Membrane was first incubated within 5% milk in Tris buffer saline, 0.1% Tween-20. Membrane was then incubated with rabbit anti-PP1i antibody developed for us by Eurogentec (1/2000) overnight at 4 °C. Horseradish peroxidase-conjugated rabbit anti-goat antibody (656120, Life Technologies, 1/33,000) was used as secondary antibody before

Table 2. List of plasmids used in this study

Plasmid	Description	Source
pcDNA3-$(HA)_2$-LIMK2-2b	P_{CMV}-$(HA)_2$-*LIMK2-2b*	H. Bénédetti
pcDNA3-$(HA)_2$-LIMK2-1	P_{CMV}-$(HA)_2$-*LIMK2-1*	H. Bénédetti
pcDNA3-$(HA)_2$-LIMK2-1S668P	P_{CMV}-$(HA)_2$-*LIMK2-1S668P*	H. Bénédetti
pcDNA3	P_{CMV}	Invitrogen
pCMV LIMK2-1	P_{CMV}-*LIMK2-1*	Biovalley (Openbiosystem)
pEGFP	P_{CMV} *EGFP*	Clontech

Please cite this article in press as: Tastet J et al. LIMK2-1 is a Hominidae-Specific Isoform of LIMK2 Expressed in Central Nervous System and Associated with Intellectual Disability. Neuroscience (2019), https://doi.org/10.1016/j.neuroscience.2018.12.017

chemiluminescence analysis using the SuperSignal West Dura Chemiluminescent Substrate (Pierce).

Immunofluorescence assessment of neurite length and branching complexity

The neurite length in NSC-34 cells was assessed after immunofluorescence staining. Cell medium was removed and the cells were washed with cold Phosphate Buffer Saline (PBS) (Life Technologies). Cells were then fixed with 4% paraformaldehyde (Sigma-Aldrich) in PBS for 30 min. After washing step with cold PBS, cells were incubated with 2% bovine serum albumin and 0.3% Triton X-100 in PBS for 1 h. After additional washing step, cells were incubated overnight at 4 °C with a rat monoclonal primary antibody against hemagglutinin tag (HA) (11-867-423-001, 1/100, Roche) and 2 h with Cy3-conjugated donkey antibody against rat IgG (712-165-150, 1/200, Zymed-Life Technologies). Preparations were mounted with Prolong Gold Antifade (Life Technologies) and observed under Olympus Fluoview 500 confocal laser scanning microscope. The length of the longest neurite of NSC-34 cells expressing HA-LIMK2-2b, HA-LIMK2-1 or HA-LIMK2-1S668P was measured as previously described (Tastet et al., 2012) using ImageJ (http://imagej.nih.gov/ij/) and utilizing a Sholl analysis plugin with 10 μm separating concentric circles that centered at the cells soma. ImageJ was used to threshold the confocal z-stack projections of NSC-34 arbors prior to using the plugin. Statistical analysis was performed using a Mann–Whitney non-parametric test (StatPlusR:mac software, version 5.8.3.8. 2001–2009 Analyst Soft Inc.). Significance was defined as $p < 0.05$ (NS, non-significant; $^{*}p < 0.05$).

WIS-Neuromath (Weizmann Institute) software was used for determining cortical neuron morphological parameters (Rishal et al., 2013), which included total branch number, total outgrowth and maximal process length. Statistical analyses were carried out using unpaired Student's test.

RESULTS

LIMK2-1 is a Hominidae primate-specific isoform

In the protein databanks (NCBI, Uniprot and Ensembl), three human isoforms of LIMK2 are described: LIMK2a, LIMK2b and LIMK2-1 (Fig. 1A,B,C). They differ only at their extremities. Isoforms 2b and 2-1 have a truncated first LIM domain compared to LIMK2a and isoform 2-1 lacks a few amino acids at the C-terminal end of the kinase domain and possesses an extra C-terminal domain compared to LIMK2a and 2b (Fig. 1B, C). This C-terminal part is predicted to be a PP1i based on its high identity (93%) with the phosphatase 1 inhibitor protein PHI-1 (PPP1R14B) (Pfam *E* value: 1.1×10^{-30} and superfamily *E* value: 4.18×10^{-32}).

In order to determine whether *LIMK2-1* was present in other species, *in silico* analyses were performed in NCBI and Ensembl databases. LIMK2-1 was only found in Hominidae primates (Fig. 2A). Using blastp, we did not find such a sequence encoding a PP1i domain in proximity (30 kb) of the last *Limk2* exon in rodents (*i.e.* rat). To confirm these *in silico* data, we analyzed *LIMK2*-1 mRNA expression by RT-PCR in HEK cells, human, rat and mouse cortex cDNA samples (Fig. 2B, C). We could detect LIMK2-1 mRNA in HEK cells and human cortex but not in rat or mouse cortex. We then took advantage of an antibody we developed against a peptide of the specific PP1i C-terminal domain of LIMK2-1 (depicted in Fig. 1C). Using this specific antibody, we could detect LIMK2-1 protein in HEK cells but not in rat C6 cells.

Altogether, these data show that LIMK2-1 isoform is specific of Hominidae primate.

LIMK2-1 is expressed in the human central nervous system

In a recent study, we showed that LIMK2-1 protein is highly expressed in liver and pancreas and in a lesser extent in testis and lung. However, LIMK2-1 was not detected in brain (Vallée et al., 2018). These last data are quite surprising as LIMK2 was shown to play a role in neuronal functions. We wondered about the role of LIMK2-1 isoform in neuronal compartments. Firstly, we checked its existence at the mRNA level by RT-PCR. We showed *LIMK2-1* mRNA expression in human fetal brain as well as in adult hippocampus, cortex and cerebellum (Fig. 3A, C). Then, using our anti-PP1i antibody (Fig. 3B), we demonstrated the expression of LIMK2-1 at a protein level in human fetal brain and adult cortex and faintly in cerebellum and in adult brain (Fig. 3B).

LIMK2-1 contains a rare missense variation in the PP1i encoding region

In order to get insights into LIMK2-1 brain function, we analyzed the coding sequence of the PP1i region in patients with ID. One rare variation, rs151191437 (c.2232T > C, p.S668P), was identified. Genotype, either heterozygous or homozygous, and allele frequencies of this mutation were significantly different in ID patients when compared with our controls and Exome Variant Server database (Fisher exact test; $p < 0.0001$, odds ratio = 20.9821, IC 95%: [5.5725–55.9716] for genotype comparisons and $p < 0.0001$, odds ratio = 20.5992, IC 95%: [5.5028–54.4072] for allele comparisons) (Table 3). This variation causes the substitution of serine 668 to a proline (S668P) in the PP1i domain of LIMK2-1. The thymine 2232 was conserved during evolution in Hominidae primates suggesting a potential important role for this codon (Fig. 4A). This is further supported by the fact that serine 668 is also conserved in the PP1i domain of PHI-1 in several species during a long evolutionary period (Fig. 4B). Submission of LIMK2-1 sequence to PolyPhen2 program (http://genetics.bwh.harvard.edu/pph2/) predicted that the mutation had a high probability of damaging protein function with a score of 0.956/1 (sensitivity 0.79, specificity 0.95). We next modeled the 3D structure of the PP1i domain of LIMK2-1 using PKC-potentiated inhibitory protein of PP1, CPI-17 as a template (PDB ID: 1J2M chain A) (model: *E* value 1.10–

Please cite this article in press as: Tastet J et al. LIMK2-1 is a Hominidae-Specific Isoform of LIMK2 Expressed in Central Nervous System and Associated with Intellectual Disability. Neuroscience (2019), https://doi.org/10.1016/j.neuroscience.2018.12.017

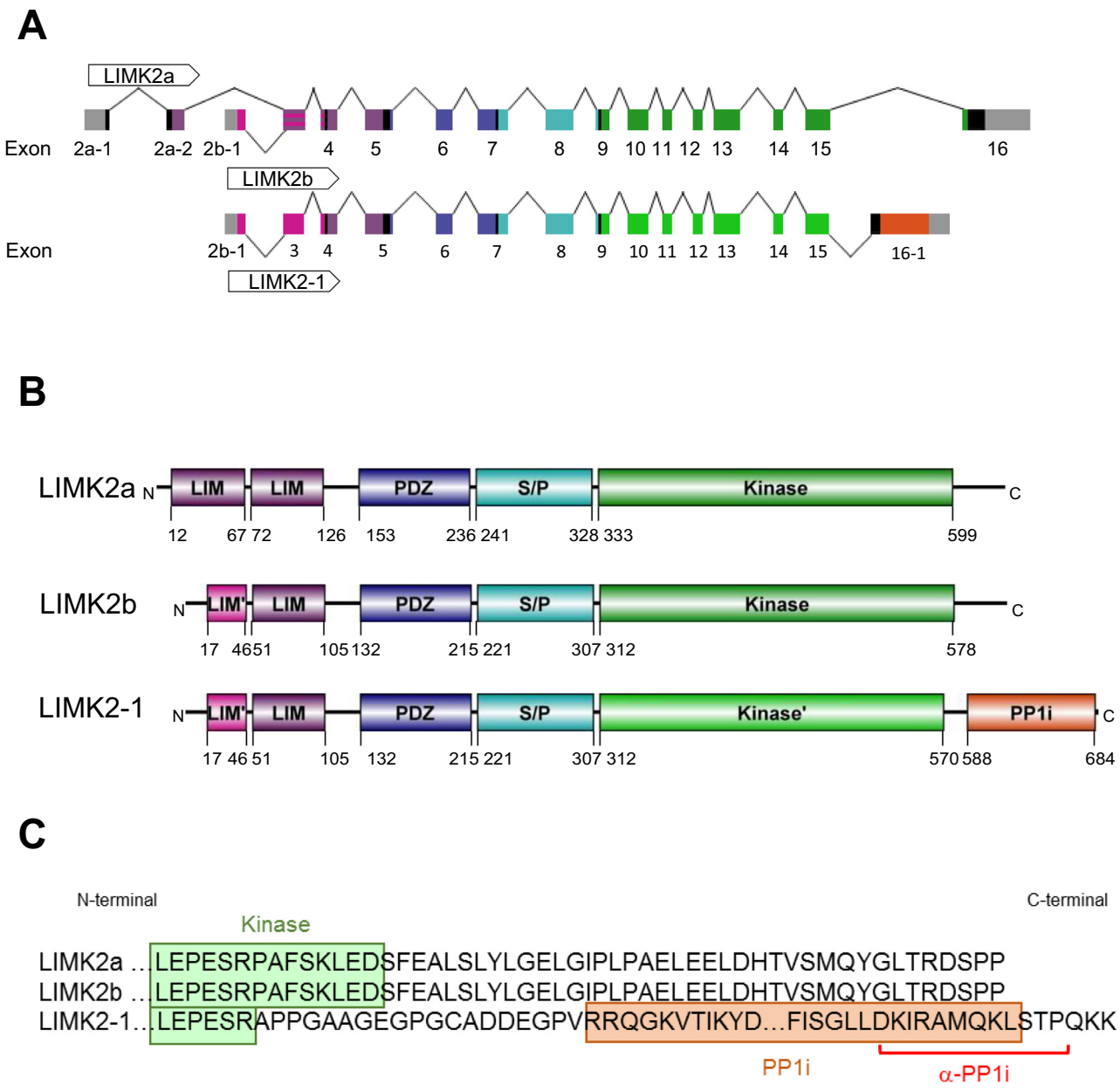

Fig. 1. Schematic diagram of LIMK2a, LIMK2b and LIMK2-1 pre-mRNA (A) and protein (B). (C) Focus on their C-terminal domains. The peptide used to develop anti-PP1i antibodies is underlined in red. (For interpretation of the references to colour in this figure legend, the reader is referred to the web version of this article.)

39, QMEAN Z-Score −4.78) (Fig. 4C, D). When the p.S668P mutation was introduced, the model predicted a change in the shape of the first turn of the α4 helix (Fig. 4D), which corresponds to classical proline properties. Altogether, these data support the idea that the rare mutation c.2232T > C in the PP1i domain of LIMK2-1 could constitute a risk factor in ID.

The impact of LIMK2-1 on neurite outgrowth and branching complexity is disturbed by the p.S668P mutation

The inhibition of LIMK2-2a and 2b expression by a siRNA targeting a region of the mRNA encoding the PDZ domain decreased neurite outgrowth in rat PC12 cells thereby indicating that these isoforms stimulate the growth of neurites (Endo et al., 2007). To assess if isoform LIMK2-1 might play a role in neurite extension, the neuronal NSC-34 cell line was transfected with plasmids encoding HA-tagged LIMK2-1 or LIMK2-2b (as a positive control), and neurite extension was compared. The expression of the proteins was confirmed by immunocytochemistry and their presence was detected in the soma and neurites (Fig. 5A). The length of the longest neurites was measured in transfected cells. HA-LIMK2-1 expressing cells displayed smaller neurites compared to those expressing HA-LIMK2b ($p < 0.05$, Fig. 5B). The presence of the p.S668P variation abrogates this phe-

Please cite this article in press as: Tastet J et al. LIMK2-1 is a Hominidae-Specific Isoform of LIMK2 Expressed in Central Nervous System and Associated with Intellectual Disability. Neuroscience (2019), https://doi.org/10.1016/j.neuroscience.2018.12.017

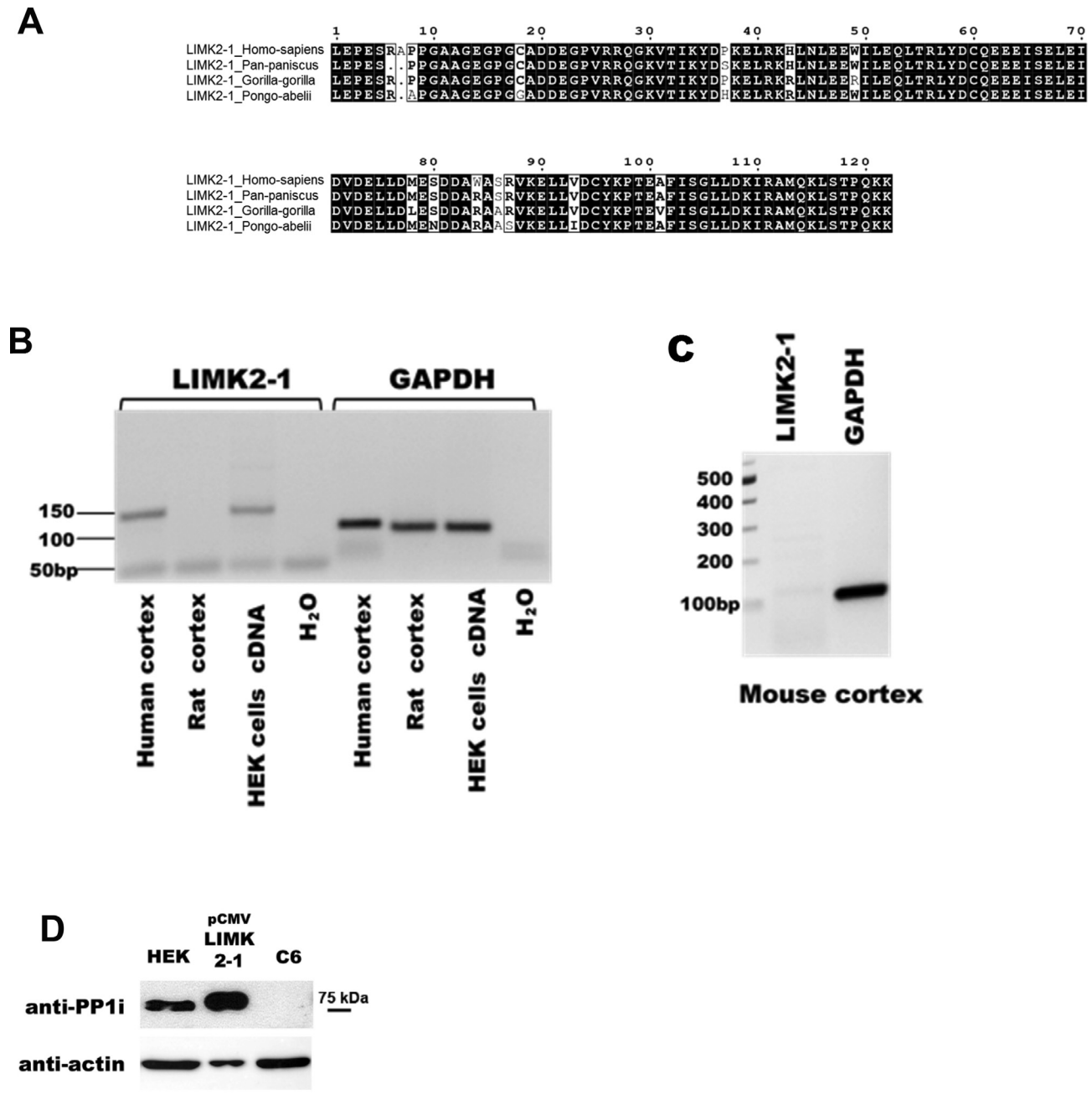

Fig. 2. LIMK2-1 is an Hominidae – specific isoform. (A) Sequence alignment of the C-terminal region of four Hominidae LIMK2-1: *Homo sapiens* (sp|P53671-3|), *Pan paniscus* (tr|A0A2R9BY75|), *Gorilla gorilla* (tr|A0A2I2Y889|) and *Pongo abelii* (tr|A0A2J8UVE6|). (B) RT-PCR products of LIMK2-1 and GAPDH in HEK cells, human and rat cortex. H_2O designates a negative control without cDNA. Molecular weight markers are indicated on the left. (C) RT-PCR products of LIMK2-1 and GAPDH in mouse cortex. Molecular weight markers are indicated on the left. (D) Detection of LIMK2-1 with the anti-PP1i antibody in HEK-293 cells expressing native LIMK2-1 or overexpressing LIMK2-1 (pCMV-LIMK2-1), but not in rat C6 cells.

nomenon and increased the length of neurites compared to LIMK2-1 ($p < 0.05$, Fig. 5B). The length of the longest neurite was similar in cells overexpressing LIMK2-1 S668P and LIMK2b (Fig. 6).

Then, to get closer to physiological conditions, mice neurons were co-transfected by the EGFP plasmid and the different HA-LIMK2 coding plasmids (HA-LIMK2b, HA-LIMK2-1, HA-LIMK2-1 S668P) or an empty related plasmid (pcDNA3-HA) as a negative control. The length of neurites and the branching complexity were analyzed in the GFP-expressing neurons. For neurite length, neurons transfected with HA-LIMK2-1 showed longer neurites compared to HA-LIMK2b. This effect was abrogated in the presence of S668P mutation. The number of cells with such long neurites appeared to be significantly lower for HA-LIMK2-1 S668P transfected neurons than HA-LIMK2-1 transfected ones and closer from the number of cells with such neurites in HA-LIMK2b transfected neurons (Fig. 6). Branching complexity was also significantly affected by the S668P

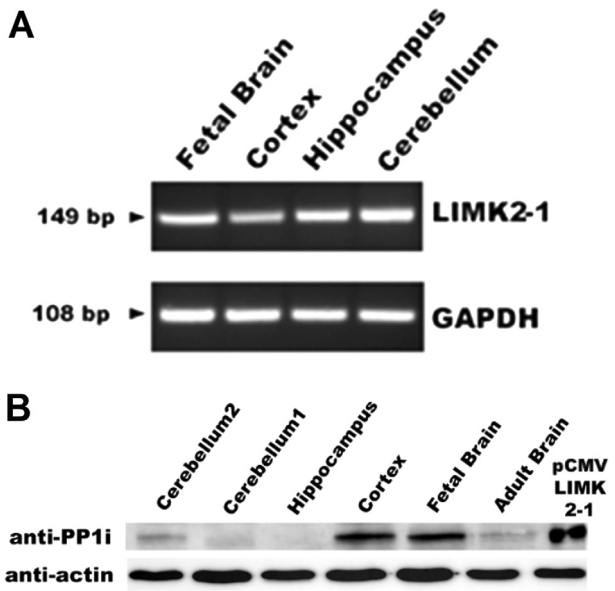

Fig. 3. Expression of LIMK2-1 protein in human central nervous system. (A) RT-PCR products of LIMK2-1 and GAPDH in human fetal brain and adult cortex, hippocampus and cerebellum. (B) Analyses of human fetal brain and adult cortex, hippocampus and cerebellum (two different batches for this last sample) and in HEK cells overexpressing LIMK2-1 (pCMV-LIMK2-1), by Western-blot using the anti-PP1i antibody.

mutation as compared to wild-type LIMK2-1 and comparable to that associated to HA-LIMK2b-producing neurons (Fig. 6).

DISCUSSION

In this study, we focused our attention on a particular human isoform of LIMK2, LIMK2-1. Unlike LIMK2a and LIMK2b, which are found in many species, we showed that LIMK2-1 is a Hominidae primate-specific isoform. LIMK2b and LIMK2-1 differ from LIMK2-2a at their N-terminal domain while LIMK2-1 differs from LIMK2a and LIMK2b by a truncated kinase domain and an extra PP1i domain at its C-terminal extremity. PP1i domain sequence is highly similar (93% identity) to the one of PHI-1 protein for which the inhibitory activity on PP1 is clearly established (Eto et al., 1999). Protein phosphatase 1 (PP1) has been involved in both neurite outgrowth (Han et al., 2007; Li et al., 2007; Monroe and Heathcote, 2013) and synaptic plasticity (Morishita et al., 2001; Munton et al., 2004; Hu et al., 2007; Siddoway et al., 2013). We can then reasonably assume that PP1 regulation is of crucial importance in these mechanisms and recently we obtained data strongly suggesting that LIMK2-1, via its PP1i domain, inhibits PP1 activity toward cofilin dephosphorylation, resulting in an increase of the pool of phospho-cofilin in the cell (Vallée et al., 2018).

We decided to further characterize human LIMK2-1 isoform, and its potential role in the CNS. In this work, we demonstrated its expression as a transcript in human fetal brain and in human adult cortex, hippocampus and cerebellum, which are involved in cognition processes. Moreover, we showed its expression as a protein in human fetal brain and in human adult cortex. Its expression is much lower in cerebellum and in adult brain, and absent from the hippocampus. These two sets of data may seem contradictory. Nevertheless, it is important to note that the expression pattern could be age-dependent. Indeed, we could hardly detect LIMK2-1 protein in adult brain, whereas it is strongly expressed in fetal brain (Fig. 3B). So, our cortex total protein sample might come from a younger person than the cerebellum (60 years old) and the hippocampus (82-year-old woman) samples. As the donors of RNA and protein samples are not the same and might not therefore have the same age, this might explain this discrepancy between mRNA and protein level in cerebellum and hippocampus. Furthermore, we have shown that LIMK2-1 protein expression is sensitive to extraction conditions (data not published), we can hypothesize that the purchased samples for cerebellum and hippocampus are not optimized to detect LIMK2-1 protein expression. However, LIMK2-1 expression in the central nervous system strengthens the interest to investigate its role in cognitive functions.

We therefore searched for the existence of variations in *LIMK2-1* in a population of patients with ID. ID is a complex cognitive disorder characterized by below average intellectual functioning (IQ < 70). Etiologies of ID are highly heterogeneous, including environmental factor and genetic defects that affect development and functioning of the nervous system (Srivastava and Schwartz, 2014). We showed that the rs151191437 variation is significantly more frequent in the population with ID, compared to controls. This missense mutation is located in the PP1i domain of LIMK2-1. The absence of the variation in our control population indicates that it is a rare mutation in our ethno-geographic population. This fact is confirmed by the ExAC Browser database where

Table 3. Genotype frequencies of the rs151191437 variation (p.S668P) in the coding sequence of the PP1i domain of *LIMK2-1* in French patients with ID and controls. Database: Exome Variant Server

	Patients with ID	Our controls	Controls in database	All controls
Genotype	*Distribution of genotype, n (%)*			
T/T	169 (97.69)	206 (100)	121,246 (99.89)	121,452 (99.89)
C/T	4 (2.31)	0 (0)	136 (0.11)	136 (0.11)
C/C	0 (0)	0 (0)	1 (0)	1 (0)
Allele	*Distribution of allele, n (%)*			
T	342 (98.84)	412 (100)	242,628 (99.94)	243,040 (99.94)
C	4 (1.16)	0 (0)	138 (0.06)	138 (0.06)

Please cite this article in press as: Tastet J et al. LIMK2-1 is a Hominidae-Specific Isoform of LIMK2 Expressed in Central Nervous System and Associated with Intellectual Disability. Neuroscience (2019), https://doi.org/10.1016/j.neuroscience.2018.12.017

A

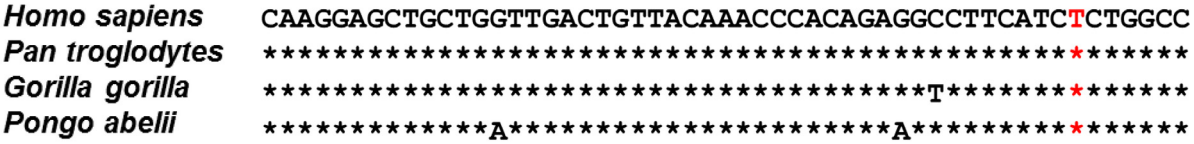

B

C

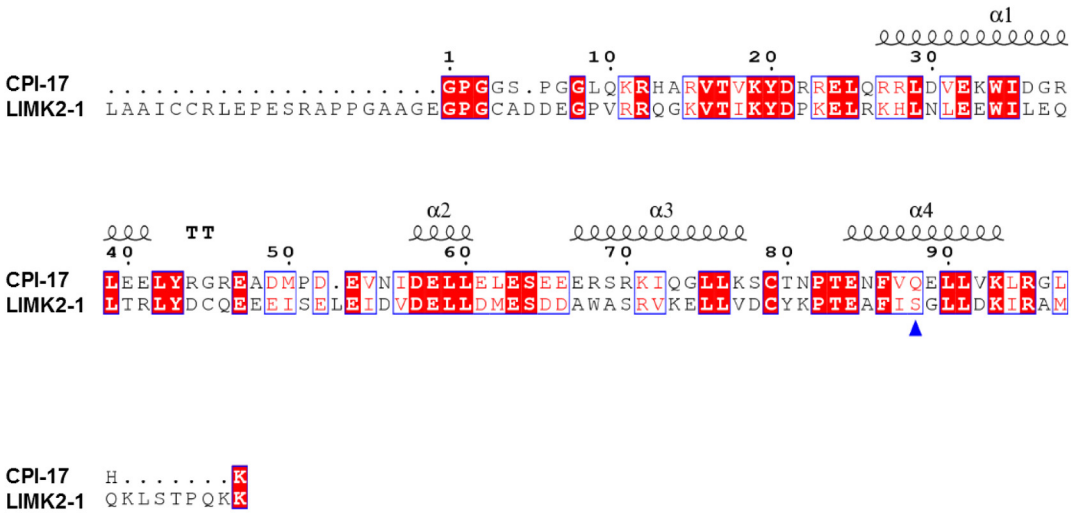

D

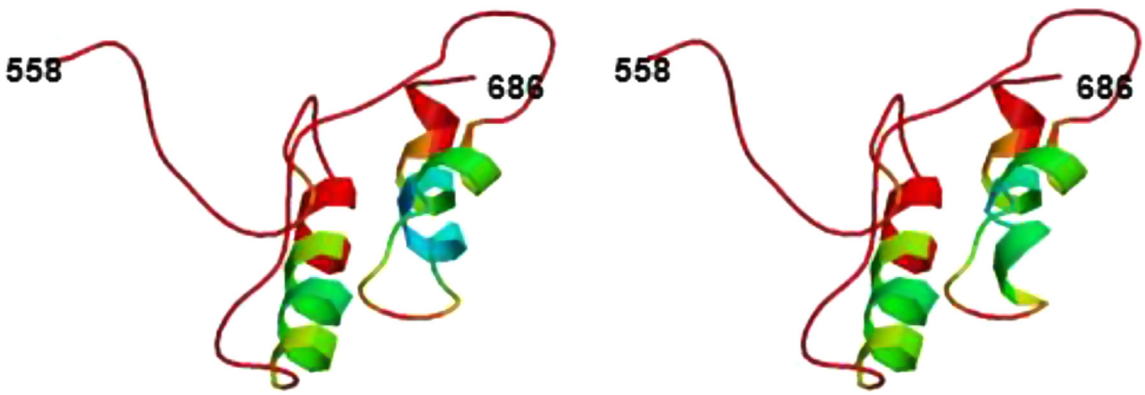

Please cite this article in press as: Tastet J et al. LIMK2-1 is a Hominidae-Specific Isoform of LIMK2 Expressed in Central Nervous System and Associated with Intellectual Disability. Neuroscience (2019), https://doi.org/10.1016/j.neuroscience.2018.12.017

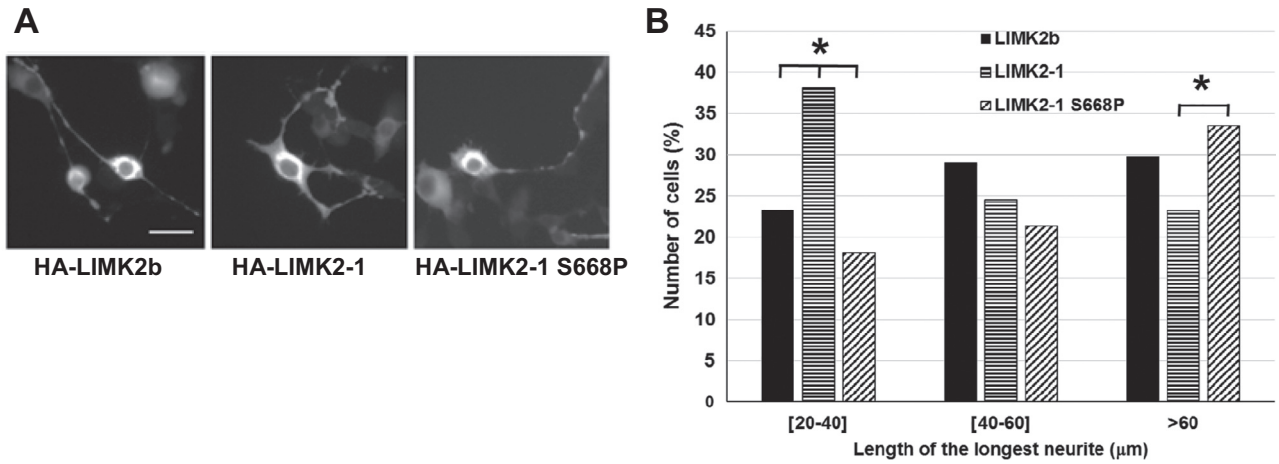

Fig. 5. Role of LIMK2-1 on neurite length in NSC-34 transfected cells. (A) Immunocytochemistry with anti-HA antibody on NSC-34 cells expressing HA-LIMK2-2b, HA-LIMK2-1 or HA-LIMK2-1-S668P. Scale bar = 20 μm. (B) Effect of HA-LIMK2-2b, HA-LIMK2-1 or HA-LIMK2-1-S668P expression on neurite length of NSC-34 cells. Data are mean ± SEM of three independent experiments ($^{*}p \leq 0.05$, Mann–Whitney test).

the frequency is 0.11%. The presence of the variation in the general population may be explained by a polygenic susceptibility model or by the presence of a lower range IQ population in this group. Considered as probably damaging by the PolyPhen2 program, this variation could affect the function of LIMK2-1. Moreover, serine 668 is highly conserved in the PP1i domain of LIMK2-1 in Hominidae primates and its substitution by proline is predicted to disrupt one α-helical turn in the PP1i domain.

Numerous genes with variations associated with ID regulate neurite outgrowth (Ramakers, 2002; Jolly et al., 2013; Van Maldergem et al., 2013; Doers et al., 2014). We therefore assessed the role of LIMK2-1 in this cellular process. Previous studies demonstrated that LIMK2a and 2b are involved in neurite outgrowth (Endo et al., 2007). We showed that NSC-34 cells overexpressing HA-LIMK2-1 displayed significantly smaller neurites compared with NSC-34 cells overexpressing LIMK2b. Thus, LIMK2-1 does not exert the same action than LIMK2b on neurite outgrowth. Since LIMK2-1 and LIMK2b only differ by their C-terminal region including the last amino acids of the kinase domain and the PP1i domain, we can assume a role of this extra C-terminal region in the control of neurite outgrowth. Furthermore, we showed that cells overexpressing HA-LIMK2-1 S668P displayed longer neurites than cells expressing wild-type HA-LIMK2-1, suggesting more precisely that the PP1i domain is involved in LIMK2-1 function on neurite outgrowth and that the p.S668P variation disturbs this function. The impact of S668P mutation on PP1i function was confirmed on mouse neurons. Indeed, data on transfected neurons harboring neurites longer than 400 nm corroborate a potential role of the PP1i domain in neurite extension that would be greatly affected by the S668P mutation. It has to be noted that LIMK2-1 has opposite effects on neurite length of NSC-34 cells (decrease) than of mouse neurons (increase). This might be due to the nature of NSC-34 cell line which is a mixture of motor neurons and neuroblastoma and which might disturb LIMK2-1 function. A role of the PP1i domain in branching complexity was also suggested by our quantification of this process on HA-LIMK2 constructs producing neurons. Indeed, S668P mutation significantly increases neuron arborization compared to wild-type HA-LIMK2-1 and neurons producing this mutant have a branching complexity comparable to those producing HA-LIMK2b. Therefore, HA-LIMK2-1 seems to induce longer but less branched neurites in mouse neurons.

In conclusion, we report for the first time that the hominidae-specific isoform LIMK2-1 is expressed in the central nervous system during neurodevelopment and in adult. We also report a variation in the PP1i domain associated with ID. A replication of this association needs to be obtained in independent ID populations to confirm the involvement of the p.S668P variation in ID. Our findings highlight the necessity to assess the implication of LIMK2 in ID etiology and confirm the importance of hominidae-specific proteins in cognitive disorders (Huffaker et al., 2009; Drews et al., 2013). Finally, we suggest a role for LIMK2-1 in neurite morphology through its PP1i domain consisting in stimulating neurite outgrowth but inhibiting its branching. Further

Fig. 4. Conservation and 3D structure model of the PP1i domain of LIMK2-1. (A) Alignments of genomic sequences of the regions coding the serine 668 of the PP1i domain of LIMK2-1 in four primates: *Homo sapiens* (NM_001031801.1), *Pan troglodytes* (NC_006489.3), *Gorilla gorilla* (NC_018446.1) and *Pongo abelii* (NW_002891525.1). (B) Alignment of primary sequences of the PP1i domain of LIMK2-1 in *Homo sapiens* (P53671-3) with sequences of the PP1i domain of the phosphatase inhibitor 1 (PHI-1) of several species: *Homo sapiens* (Q96C90), *Pan troglodytes* (K7BGM2), *Callithrix jacchus* (F6Q451), *Macacamulata* (H9YV07), *Canis lupus* (F1PCV4), *Feliscatus* (M3WW18), *Rattusnorvegicus* (Q8K3F3), *Mus musculus* (Q62084), *Equuscaballus* (F6Q2M3), *Susscrofa* (Q8MIK9), *Ailuropodamelanoleuca* (G1MI51) and *Xenopustropicalis* (F7C4E8). (C) Alignment of primary and secondary structures of the PP1i domain of human LIMK2-1 with the PP1i domain of human CPI-17 using the ESPRIT software. (D) Model structures of the PP1i domain of LIMK2-1 (left panel) and LIMK2-1S668P (right panel).

Please cite this article in press as: Tastet J et al. LIMK2-1 is a Hominidae-Specific Isoform of LIMK2 Expressed in Central Nervous System and Associated with Intellectual Disability. Neuroscience (2019), https://doi.org/10.1016/j.neuroscience.2018.12.017

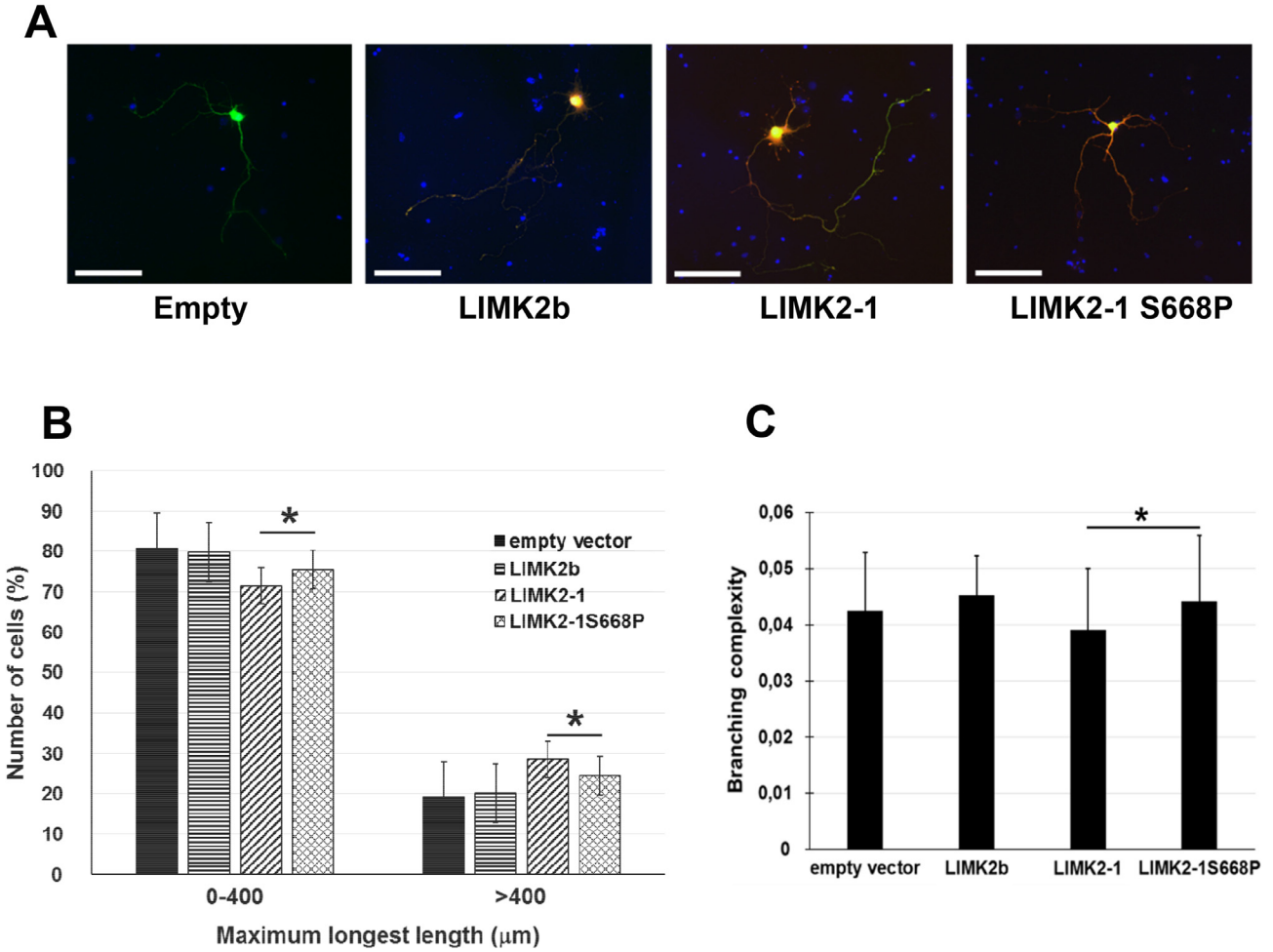

Fig. 6. Role of LIMK2-1 on neuron morphology in primary cortical neurons co-transfected with HA-LIMK2 constructs and EGFP. Primary cortical neurons co-transfected with a EGFP vector and an empty vector or a vector expressing HA-LIMK2b, HA-LIMK2-1 or HA-LIMK2-1 S668P. (A) Representative pictures of co-transfected neurons expressing GFP. Scale bar: 100 μm. (B) Effect of different LIMK2 isoforms on the length of the longest neurite. Data are mean ± SEM of three independent experiments. ($^{*}p \leq 0.05$) (C) Effect of different LIMK2 isoforms expression on branching complexity. Data are mean ± SEM of five independent experiments. ($^{*}p \leq 0.05$).

investigations are required to define the molecular mechanisms involved and the precise role of this isoform in brain functions.

CONFLICT OF INTEREST

None to declare.

ACKNOWLEDGMENTS

This work was supported by the Région Centre Val de Loire, Ligue contre le Cancer, Association Neurofibromatoses et Recklinghausen, Centre National de la Recherche Scientifique, Institut National de la Santé et de la Recherche Médicale, Université François-Rabelais de Tours, and Ministère de l'Enseignement Supérieur et de la Recherche. We thank the Département Génomique of the Plateforme Pluri-Formation Analyses Systèmes Biologiques (Université François-Rabelais de Tours).

REFERENCES

Acevedo K, Moussi N, Li R, Soo P, Bernard O (2006) LIM kinase 2 is widely expressed in all tissues. J Histochem Cytochem 54:487–501. https://doi.org/10.1369/jhc.5C6813.2006.

Aizawa H, Wakatsuki S, Ishii A, Moriyama K, Sasaki Y, Ohashi K, Sekine-Aizawa Y, Sehara-Fujisawa A, Mizuno K, Goshima Y, Yahara I (2001) Phosphorylation of cofilin by LIM-kinase is necessary for semaphorin 3A-induced growth cone collapse. Nat Neurosci 4:367–373. https://doi.org/10.1038/86011.

Arber S, Barbayannis FA, Hanser H, Schneider C, Stanyon CA, Bernard O, Caroni P (1998) Regulation of actin dynamics through phosphorylation of cofilin by LIM-kinase. Nature 393:805–809. https://doi.org/10.1038/31729.

Birkenfeld J, Betz H, Roth D (2001) Inhibition of neurite extension by overexpression of individual domains of LIM kinase 1. J Neurochem 78:924–927.

Croft DR, Crighton D, Samuel MS, Lourenco FC, Munro J, Wood J, Bensaad K, Vousden KH, Sansom OJ, Ryan KM, Olson MF (2011) p53-mediated transcriptional regulation and activation of the actin cytoskeleton regulatory RhoC to LIMK2 signaling pathway promotes cell survival. Cell Res 21:666–682. https://doi.org/10.1038/cr.2010.154.

Cuberos H, Vallée B, Vourc'h P, Tastet J, Andres CR, Bénédetti H (2015) Roles of LIM kinases in central nervous system function

and dysfunction. FEBS Lett 589:3795–3806. https://doi.org/10.1016/j.febslet.2015.10.032.

Doers M, Musser M, Nichol R, Berndt E, Baker M, Gomez T, Zhang S, Abbeduto L, Bhattacharyya A (2014) iPSC-derived forebrain neurons from FXS individuals show defects in initial neurite outgrowth. Stem Cells Dev 23:1777–1787.

Drews E, Otte D-M, Zimmer A (2013) Involvement of the primate specific gene G72 in schizophrenia: From genetic studies to pathomechanisms. Neurosci Biobehav Rev 37:2410–2417. https://doi.org/10.1016/j.neubiorev.2012.10.009.

Edwards DC, Sanders LC, Bokoch GM, Gill GN (1999) Activation of LIM-kinase by Pak1 couples Rac/Cdc42 GTPase signalling to actin cytoskeletal dynamics. Nat Cell Biol 1:253–259. https://doi.org/10.1038/12963.

Endo M, Ohashi K, Mizuno K (2007) LIM kinase and slingshot are critical for neurite extension. J Biol Chem 282:13692–13702. https://doi.org/10.1074/jbc.M610873200.

Eto M, Karginov A, Brautigan DL (1999) A novel phosphoprotein inhibitor of protein type-1 phosphatase holoenzymes. Biochemistry (Mosc) 38:16952–16957.

Foletta VC, Moussi N, Sarmiere PD, Bamburg JR, Bernard O (2004) LIM kinase 1, a key regulator of actin dynamics, is widely expressed in embryonic and adult tissues. Exp Cell Res 294:392–405. https://doi.org/10.1016/j.yexcr.2003.11.024.

Gamell C, Schofield AV, Suryadinata R, Sarcevic B, Bernard O (2013) LIMK2 mediates resistance to chemotherapeutic drugs in neuroblastoma cells through regulation of drug-induced cell cycle arrest. PLoS One 8. https://doi.org/10.1371/journal.pone.0072850 e72850.

Gorovoy M, Niu J, Bernard O, Profirovic J, Minshall R, Neamu R, Voyno-Yasenetskaya T (2005) LIM kinase 1 coordinates microtubule stability and actin polymerization in human endothelial cells. J Biol Chem 280:26533–26542. https://doi.org/10.1074/jbc.M502921200.

Han J, Han L, Tiwari P, Wen Z, Zheng JQ (2007) Spatial targeting of type II protein kinase A to filopodia mediates the regulation of growth cone guidance by cAMP. J Cell Biol 176:101–111. https://doi.org/10.1083/jcb.200607128.

Heng Y-W, Lim H-H, Mina T, Utomo P, Zhong S, Lim C-T, Koh C-G (2012) TPPP acts downstream of RhoA-ROCK-LIMK2 to regulate astral microtubule organization and spindle orientation. J Cell Sci 125:1579–1590. https://doi.org/10.1242/jcs.096818.

Hsieh SH-K, Ferraro GB, Fournier AE (2006) Myelin-associated inhibitors regulate cofilin phosphorylation and neuronal inhibition through LIM kinase and Slingshot phosphatase. J Neurosci 26:1006–1015. https://doi.org/10.1523/JNEUROSCI.2806-05.2006.

Huffaker SJ, Chen J, Nicodemus KK, Sambataro F, Yang F, Mattay V, Lipska BK, Hyde TM, Song J, Rujescu D, Giegling I, Mayilyan K, Proust MJ, Soghoyan A, Caforio G, Callicott JH, Bertolino A, Meyer-Lindenberg A, Chang J, Ji Y, Egan MF, Goldberg TE, Kleinman JE, Lu B, Weinberger DR (2009) A primate-specific, brain isoform of KCNH2 affects cortical physiology, cognition, neuronal repolarization and risk of schizophrenia. Nat Med 15:509–518. https://doi.org/10.1038/nm.1962.

Hu X, Huang Q, Yang X, Xia H (2007) Differential regulation of AMPA receptor trafficking by neurabin-targeted synaptic protein phosphatase-1 in synaptic transmission and long-term depression in hippocampus. J Neurosci 27:4674–4686. https://doi.org/10.1523/JNEUROSCI.5365-06.2007.

Jolly LA, Homan CC, Jacob R, Barry S, Gecz J (2013) The UPF3B gene, implicated in intellectual disability, autism, ADHD and childhood onset schizophrenia regulates neural progenitor cell behaviour and neuronal outgrowth. Hum Mol Genet 22:4673–4687. https://doi.org/10.1093/hmg/ddt315.

Laumonnier F, Holbert S, Ronce N, Faravelli F, Lenzner S, Schwartz CE, Lespinasse J, Van Esch H, Lacombe D, Goizet C, Phan-Dinh Tuy F, van Bokhoven H, Fryns JP, Chelly J, Ropers HH, Moraine C, Hamel BC, Briault S (2005) Mutations in PHF8 are associated with X linked mental retardation and cleft lip/cleft palate. J Med Genet. 42:780–786.

Li T, Chalifour LE, Paudel HK (2007) Phosphorylation of protein phosphatase 1 by cyclin-dependent protein kinase 5 during nerve growth factor-induced PC12 cell differentiation. J Biol Chem 282:6619–6628. https://doi.org/10.1074/jbc.M606347200.

Manetti F (2012) LIM kinases are attractive targets with many macromolecular partners and only a few small molecule regulators. Med Res Rev 32:968–998. https://doi.org/10.1002/med.20230.

Meng Y, Zhang Y, Tregoubov V, Janus C, Cruz L, Jackson M, Lu WY, MacDonald JF, Wang JY, Falls DL, Jia Z (2002) Abnormal spine morphology and enhanced LTP in LIMK-1 knockout mice. Neuron 35:121–133.

Meng Y, Takahashi H, Meng J, Zhang Y, Lu G, Asrar S, Nakamura T, Jia Z (2004) Regulation of ADF/cofilin phosphorylation and synaptic function by LIM-kinase. Neuropharmacology 47:746–754. https://doi.org/10.1016/j.neuropharm.2004.06.030.

Monroe JD, Heathcote RD (2013) Protein phosphatases regulate the growth of developing neurites. Int J Dev Neurosci 31:250–257. https://doi.org/10.1016/j.ijdevneu.2013.01.005.

Morishita W, Connor JH, Xia H, Quinlan EM, Shenolikar S, Malenka RC (2001) Regulation of synaptic strength by protein phosphatase 1. Neuron 32:1133–1148.

Munton RP, Vizi S, Mansuy IM (2004) The role of protein phosphatase-1 in the modulation of synaptic and structural plasticity. FEBS Lett 567:121–128. https://doi.org/10.1016/j.febslet.2004.03.121.

Nomoto S, Tatematsu Y, Takahashi T, Osada H (1999) Cloning and characterization of the alternative promoter regions of the human LIMK2 gene responsible for alternative transcripts with tissue-specific expression. Gene 236(2):259–271.

Osada H, Hasada K, Inazawa J, Uchida K, Ueda R, Takahashi T, Takahashi T (1996) Subcellular localization and protein interaction of the human LIMK2 gene expressing alternative transcripts with tissue-specific regulation. Biochem Biophys Res Commun 229:582–589. https://doi.org/10.1006/bbrc.1996.1847.

Po'uha ST, Shum MSY, Goebel A, Bernard O, Kavallaris M (2010) LIM-kinase 2, a regulator of actin dynamics, is involved in mitotic spindle integrity and sensitivity to microtubule-destabilizing drugs. Oncogene 29:597–607. https://doi.org/10.1038/onc.2009.367.

Ramakers GJA (2002) Rho proteins, mental retardation and the cellular basis of cognition. Trends Neurosci 25:191–199.

Rishal I, Golani O, Rajman M, Costa B, Ben-Yaakov K, Schoenmann Z, et al. (2013) WIS-NeuroMath enables versatile high throughput analyses of neuronal processes. Dev Neurobiol 73:247–256.

Sacchetti P, Carpentier R, Ségard P, Olivé-Cren C, Lefebvre P (2006) Multiple signaling pathways regulate the transcriptional activity of the orphan nuclear receptor NURR1. Nucleic Acids Res 34:5515–5527. https://doi.org/10.1093/nar/gkl712.

Scott RW, Olson MF (2007) LIM kinases: function, regulation and association with human disease. J Mol Med Berl Ger 85:555–568. https://doi.org/10.1007/s00109-007-0165-6.

Siddoway BA, Altimimi HF, Hou H, Petralia RS, Xu B, Stellwagen D, Xia H (2013) An essential role for inhibitor-2 regulation of protein phosphatase-1 in synaptic scaling. J Neurosci 33:11206–11211. https://doi.org/10.1523/JNEUROSCI.5241-12.2013.

Srivastava AK, Schwartz CE (2014) Intellectual disability and autism spectrum disorders: causal genes and molecular mechanisms. Neurosci Biobehav Rev 46(Pt 2):161–174. https://doi.org/10.1016/j.neubiorev.2014.02.015.

Sumi T, Hashigasako A, Matsumoto K, Nakamura T (2006) Different activity regulation and subcellular localization of LIMK1 and LIMK2 during cell cycle transition. Exp Cell Res 312:1021–1030. https://doi.org/10.1016/j.yexcr.2005.12.030.

Sumi T, Matsumoto K, Nakamura T (2001a) Specific activation of LIM kinase 2 via phosphorylation of threonine 505 by ROCK, a Rho-dependent protein kinase. J Biol Chem 276:670–676. https://doi.org/10.1074/jbc.M007074200.

Sumi T, Matsumoto K, Shibuya A, Nakamura T (2001b) Activation of LIM kinases by myotonic dystrophy kinase-related Cdc42-binding kinase alpha. J Biol Chem 276:23092–23096. https://doi.org/10.1074/jbc.C100196200.

Please cite this article in press as: Tastet J et al. LIMK2-1 is a Hominidae-Specific Isoform of LIMK2 Expressed in Central Nervous System and Associated with Intellectual Disability. Neuroscience (2019), https://doi.org/10.1016/j.neuroscience.2018.12.017

Tastet J, Vourc'h P, Laumonnier F, Vallée B, Michelle C, Duittoz A, Bénédetti H, Andres CR (2012) LIMK2d, a truncated isoform of Lim kinase 2 regulates neurite growth in absence of the LIM kinase domain. Biochem Biophys Res Commun 420:247–252. https://doi.org/10.1016/j.bbrc.2012.02.134.

Todorovski Z, Asrar S, Liu J, Saw NMN, Joshi K, Cortez MA, Snead OC, Xie W, Jia Z (2015) LIMK1 regulates long-term memory and synaptic plasticity via the transcriptional factor CREB. Cell. Biol Mol. https://doi.org/10.1128/MCB.01263-14.

Van Maldergem L, Hou Q, Kalscheuer V, Rio M, Doco-Fenzy M, Medeira A, de Brouwer A, Cabrol C, Haas S, Cacciagli P, Moutton S, Landais E, Motte J, Colleaux L, Bonnet C, Villard L, Dupont J, Man H (2013) Loss of function of KIAA2022 causes mild to severe intellectual disability with an autism spectrum disorder and impairs neurite outgrowth. Hum Mol Genet 22:3306–3314. https://doi.org/10.1093/hmg/ddt187.

Vallée B, Cuberos H, Doudeau M, Godin F, Gosset D, Vourc'h P, Andres CR, Bénédetti H (2018) LIMK2-1, a new isoform of Human-LIMK2, regulates actin cytoskeleton remodeling via a different signaling pathway than its two homologs, LIMK2a/2b. Biochem J. https://doi.org/10.1042/BCJ20170961.

Yang EJ, Yoon J-H, Min DS, Chung KC (2004) LIM kinase 1 activates cAMP-responsive element-binding protein during the neuronal differentiation of immortalized hippocampal progenitor cells. J Biol Chem 279:8903–8910. https://doi.org/10.1074/jbc.M311913200.

Yi F, Guo J, Dabbagh D, Spear M, He S, Kehn-Hall K, Fontenot J, Yin Y, Bibian M, Park CM, Zheng K, Park HJ, Soloveva V, Gharaibeh D, Retterer C, Zamani R, Pitt ML, Naughton J, Jiang Y, Shang H, Hakami RM, Ling B, Young JAT, Bavari S, Xu X, Feng Y, Wu Y (2017) Discovery of novel small-molecule inhibitors of LIM domain kinase for inhibiting HIV-1. J Virol 91(13). https://doi.org/10.1128/JVI.02418-16.

(Received 19 November 2018, Accepted 13 December 2018)
(Available online xxxx)

OPEN ACCESS Freely available online

PLOS ONE

Nf1 RasGAP Inhibition of LIMK2 Mediates a New Cross-Talk between Ras and Rho Pathways

Béatrice Vallée, Michel Doudeau, Fabienne Godin, Aurélie Gombault[¤a], Aurélie Tchalikian[¤b], Marie-Ludivine de Tauzia, Hélène Bénédetti*

Centre de Biophysique Moléculaire, Centre Nationale de la Recherche Scientifique (CNRS), University of Orléans and Institut National de la Santé et de la Recherche Médicale (INSERM), Orléans, France

Abstract

Background: Ras GTPases mediate numerous biological processes through their ability to cycle between an inactive GDP-bound form and an active GTP-bound form. Guanine nucleotide exchange factors (GEFs) favor the formation of the active Ras-GTP, whereas GTPase activating proteins (GAPs) promote the formation of inactive Ras-GDP. Numerous studies have established complex signaling cross-talks between Ras GTPases and other members of the superfamily of small GTPases. GEFs were thought to play a major role in these cross-talks. However, recently GAPs were also shown to play crucial roles in these processes. Among RasGAPs, Nf1 is of special interest. Nf1 is responsible for the genetic disease Neurofibromatosis type I, and recent data strongly suggest that this RasGAP connects different signaling pathways.

Methodology/Principal Findings: In order to know if the RasGAP Nf1 might play a role in connecting Ras GTPases to other small GTPase pathways, we systematically looked for new partners of Nf1, by performing a yeast two-hybrid screening on its SecPH domain. LIMK2, a major kinase of the Rho/ROCK/LIMK2/cofilin pathway, was identified in this screening. We confirmed this interaction by co-immunoprecipitation experiments, and further characterized it. We also demonstrated its specificity: the close related homolog of LIMK2, LIMK1, does not interact with the SecPH domain of Nf1. We then showed that SecPH partially inhibits the kinase activity of LIMK2 on cofilin. Our results furthermore suggest a precise mechanism for this inhibition: in fact, SecPH would specifically prevent LIMK2 activation by ROCK, its upstream regulator.

Conclusions/Significance: Although previous data had already connected Nf1 to actin cytoskeleton dynamics, our study provides for the first time possible detailed molecular requirements of this involvement. Nf1/LIMK2 interaction and inhibition allows to directly connect neurofibromatosis type I to actin cytoskeleton remodeling, and provides evidence that the RasGAP Nf1 mediates a new cross-talk between Ras and Rho signaling pathways within the superfamily of small GTPases.

Citation: Vallée B, Doudeau M, Godin F, Gombault A, Tchalikian A, et al. (2012) Nf1 RasGAP Inhibition of LIMK2 Mediates a New Cross-Talk between Ras and Rho Pathways. PLoS ONE 7(10): e47283. doi:10.1371/journal.pone.0047283

Editor: Robert Alan Arkowitz, Institute of Developmental Biology and Cancer Research, France

Received January 24, 2012; **Accepted** September 13, 2012; **Published** October 17, 2012

Funding: Ligue Nationale contre le cancer, Conseil régional du Centre, Cancéropole Grand-Ouest, and the Association Neurofibromatoses et Recklinghausen. The funders had no role in study design, data collection and analysis, decision to publish, or preparation of the manuscript.

Competing Interests: The authors have declared that no competing interests exist.

* E-mail: helene.benedetti@cnrs-orleans.fr

¤a Current address: Immunologie et Embryologie Moléculaires, CNRS, Orléans, France
¤b Current address: Institut Universitaire Hématologie, CNRS, Paris, France

Introduction

Ras GTPases act as molecular switches cycling between an inactive GDP bound form and an active GTP bound form. In response to various extracellular stimuli, the activated form of Ras GTPases interacts with specific downstream effectors thus regulating many major cellular processes, such as cell proliferation and differentiation, morphology, migration, and apoptosis. GDP/GTP cycling is controlled by two categories of proteins. Guanine nucleotide exchange factors (GEFs) catalyze the release of GDP thus allowing the binding of GTP, whereas GTPase Ativating Proteins (GAPs) enhance intrinsic Ras GTPase activity thus promoting hydrolysis of GTP into GDP.

RasGEFs have been extensively studied, and their connections with different signaling pathways have been well established [1]. In contrast, RasGAPs have received relatively little attention and there is less information regarding their regulation. However, emerging pieces of evidence show that RasGAP interaction with other partners mediates cross-talk between Ras GTPases and other small GTPase signaling pathways. Along this line, p120 RasGAP was shown to interact with and to influence the activity of several RhoGAPs: p190 RhoGAP, p200 RhoGAP, and DLC1 RhoGAP [2,3]. Beside p120 RasGAP, various other mammalian RasGAPs have been identified, including neurofibromin, RASA2, IQGAP1, IQGAP3, SYNGAP and GAPVD1 [4]. However, only mutations in p120 RasGAP and neurofibromin result in a clinical expression and lead to human hereditary disorders.

Neurofibromin (Nf1) is encoded by *NF1* gene which has been identified as a tumor suppressor gene involved in Neurofibromatosis type I. Neurofibromatosis type I (NF1), also known as von Recklinghausen disease, is an autosomal dominant disorder and

one of the most common genetic diseases as it affects 1 individual in 3,500. The phenotype of NF1 is highly variable: "café au lait" spots on the skin, iris Lish nodules, and bone deformations are often encountered. However, the hallmark of NF1 is the development of nerve tumors with an increased risk of malignancies, and neurological disorders such as learning disabilities [5,6,7]. NF1 is due to mutations within the *NF1* gene which encodes neurofibromin, a large 2818 amino acid protein [8,9,10]. Initially, sequence analysis of neurofibromin revealed a GAP Related Domain (GRD) with high identity (31%) with the GAP domain of p120RasGAP. Biochemical studies confirmed that Nf1 has RasGAP activity [11,12,13]. Therefore, primary studies have focused on Ras regulation by Nf1. Loss or mutations of Nf1 in a wide variety of both human tumors and *NF1*-deficient mice result in increased levels of active Ras-GTP and consequently activate various Ras effectors thereby promoting cell proliferation and differentiation [14,15]. However, recent data show that, besides regulating Ras, Nf1 plays a critical role in other signaling pathways. Indeed, Nf1 has been shown to be involved in the regulation of intracellular cAMP in human [16], mouse [17,18,19], drosophila [20,21], and yeast [22]. On the other hand, Nf1 was also suggested to play a role in actin cytoskeleton remodeling. Indeed, Nf1 was demonstrated to regulate cell adhesion, cell motility and actin cytoskeleton reorganisation [23,24,25]. Nf1 was shown to associate with microtubular and microfilamentous cytoskeleton [26], and to interact with FAK (Focal Adhesion Kinases) [27] and syndecans thus modulating PKA-Ena/VASP pathway in the formation of filopodia and dendritic spine [28]. Nf1 was also shown to enhance cell motility by regulating actin filament dynamics *via* the inhibition of the Rho/ROCK/LIMK2/cofilin pathway [29]. Furthermore, Nf1 was shown to act as a negative regulator of the Rac1/Pak1/LIMK1/cofilin pathway independently of Ras signaling pathways [30]. Although Nf1 involvement in these different signaling pathways is now well established, most of its molecular targets are still unknown, and the molecular mechanisms of these involvements remain in most cases to be elucidated.

As the RasGAP Nf1 seems to connect several signal transduction pathways, it appears as a good candidate to link Ras GTPases to other small GTPase pathways. In this context, we decided to systematically look for new partners of Nf1 by performing a two-hybrid screening. We focused on a specific domain of Nf1, SecPH. We chose this domain as it appeared well appropriate for our study. Firstly, Sec and PH domains are well known to mediate protein-protein interactions. Secondly, Nf1 SecPH 3D structure has been resolved revealing a well defined structure *per se* [31].Thirdly, SecPH flanks the GRD of Nf1 and could regulate its activity in an allosteric way. Finally, we already demonstrated in yeast that this domain is able to mediate protein-protein interactions [32].

Our two-hybrid screening allowed us to identify LIMK2 as a partner of Nf1-SecPH. LIMK2 is a major kinase in the Rho/ROCK/LIMK2/cofilin pathway. This pathway plays a major role in actin cytoskeleton remodeling. We confirmed the interaction between Nf1-SecPH and LIMK2 by coimmunoprecipitation experiments and dissected the molecular requirements of this interaction. From a functional point of view, our data showed that SecPH is an inhibitor of LIMK2: in the presence of SecPH, LIMK2 phosphorylates less efficiently its substrate cofilin. Our experiments also strongly suggested that SecPH interferes with LIMK2 activation by ROCK (Rho-associated coiled-coil-forming protein kinase): SecPH specifically prevents LIMK2 phosphorylation by this upstream kinase. Our findings therefore propose a molecular explanation for the connection between Nf1 and actin cytoskeleton remodelling, and thus shed light on a new cross-talk between Ras and Rho signaling pathways.

Results

Two-hybrid screening results

In an effort to identify a connection between Ras GTPases and other small GTPases *via* the RasGAP Nf1, we decided to systematically look for new partners of the RasGAP Nf1. In this purpose, we performed a yeast two-hybrid screening of a human fetal brain cDNA library on a newly characterized domain of Nf1, SecPH [31] (Figure 1A). This screening was particularly successful as we could test 270 million of interactions, which means a recovery of the library of 70 times for a final number of 1464 positive candidates. Among these 1464 candidates, we identified LIMK2 (Figure 1B).

LIMK2 is a serine threonine kinase playing a major role in actin cytoskeleton dynamics *via* the Rho/ROCK/LIMK2/cofilin signaling pathway. LIMK2, and its sole homolog LIMK1, have a unique organization of signaling domains, with two amino-terminal LIM domains (each containing double zinc finger motifs), adjacent PDZ and serine/proline (SP)-rich regions, followed by a carboxy-terminal kinase domain. Upon their activation by ROCK, LIMK2 and LIMK1 phosphorylate cofilin, resulting in its inactivation. Cofilin is a member of ADF (actin depolymerizing factor) family. It promotes actin depolymerization at pointed ends and severes long actin filaments, which leads to a fast turnover of actin filaments [33,34]. By inhibiting cofilin, LIMK2 and LIMK1 play a central role in the regulation of actin cytoskeleton.

LIMK2 interacts with the SecPH domain of Nf1

To validate the interaction found by our two-hybrid screening between SecPH and LIMK2 (Figure 1B), we performed coimmunoprecipitation experiments. On the one hand LIMK2 was tagged by a HA epitope, on the other hand SecPH was tagged with a flag epitope. HEK-293 cells were cotransfected by LIMK2 and SecPH or its parental empty plasmid. Anti-flag immunoprecipitations were performed. Lysates and eluates were subjected to western blot analysis. As shown in Figure 1C, LIMK2 specifically coimmunoprecipitated with SecPH. Indeed, no LIMK2 was detected in the anti-flag-immunoprecipitates using cells transfected with the parental empty plasmid of SecPH (p3XFlag). Therefore, in transfected HEK293 cells, LIMK2 specifically interacts with SecPH.

To further study the interaction between LIMK2 and SecPH, recombinant 6His-SecPH was incubated with immunoprecipitated HA-LIMK2 for a complex formation assay. As shown in Figure 1D, recombinant 6His-SecPH is co-purified with immunoprecipitated HA-LIMK2.

SecPH does not interact with LIMK2 close related homolog, LIMK1

LIMK2 has a sole homolog, LIMK1. They share 50% identity. In our two-hybrid screening, we could identify LIMK2 but not LIMK1. As LIMK1 and LIMK2 are very close we wondered if the SecPH-LIMK2 interaction could be conserved with LIMK1.

Using the two-hybrid system, we could detect no interaction between LIMK1 and SecPH (Figure 1B).

By coimmunoprecipitation experiments on lysates of cells cotransfected with SecPH and LIMK1, no interaction could either be detected (Figure 1C).

In conclusion, SecPH binds to LIMK2 but not to its related homolog LIMK1.

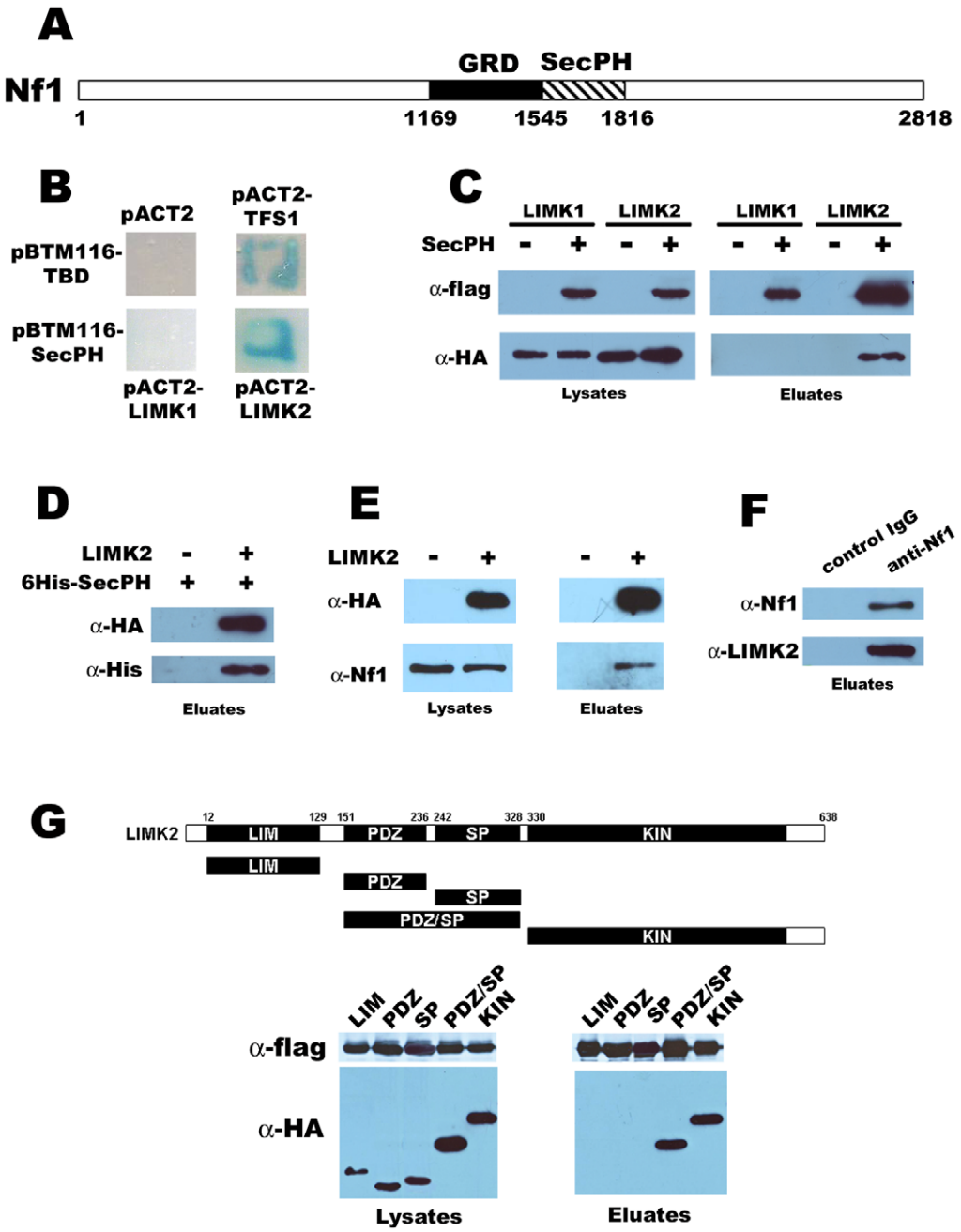

Figure 1. Interaction between LIMK2 and the SecPH domain of Nf1. *A. Diagram of Nf1*. GRD (GAP related domain) responsible for the main known function of Nf1 is depicted as well as SecPH, the region used for the two-hybrid screening. *B. Interaction revealed by the two-hybrid screening.* L40 cells transformed with pBTM116-TBD were mated with Y187 cells transformed with the empty plasmid pACT2 (as a negative control) or pACT2-TFS1 (as a positive control, as demonstrated by [32]). L40 cells transformed with pBTM116-SecPH were mated with Y187 cells transformed with pACT2-LIMK1 or pACT2-LIMK2. After mating on YPD, the resultant diploids were selected on a SD-LW medium. The interaction between the LexA fusion proteins encoded by the pACT2 plasmids and the Gal4 fusion proteins encoded by pBTM116 plasmids was tested by checking the growth of diploids on a SD-LWH media containing 3AT (1 mM) and their ability to cleave X-gal (1 mM) thereby attesting the production of β-galactosidase. *C. Interaction in HEK-293 transfected cells.* HEK-293 cells were cotransfected with either HA-LIMK2 or HA-LIMK1 and flag-SecPH or its parental empty plasmid (p3XFlag). Cell lysates and anti-flag immunoprecipitation eluates were analyzed by immunobloting. *D. Immunoprecipitated LIMK2 interacts with recombinant 6His-SecPH.* HEK-293 cells were transfected with HA-LIMK2 or its parental empty plasmid, pcDNA3. The corresponding cell lysates were immunoprecipitated with anti-HA beads. Beads were then incubated with 6His-SecPH in lysis buffer. Anti-HA immunoprecipitates were analyzed by immunobloting. *E. Transfected LIMK2 interacts with endogenous Nf1*. Cells were transfected with HA-LIMK2 or its parental empty plasmid, pcDNA3. Lysates and anti-HA immunoprecipitates were analyzed by immunobloting. *F. Endogenous LIMK2 interacts with endogenous Nf1* Anti-Nf1 immunoprecipitates from HEK-293 were analyzed by immunobloting. *G. Domains of LIMK2 involved in its interaction with SecPH*. Top. Schematic diagram of LIMK2 and its various fragments designed for this study. Bottom. Cells were cotransfected with SecPH and one of the domains of LIMK2. Lysates and anti-flag immunoprecipitates were analyzed by immunobloting.
doi:10.1371/journal.pone.0047283.g001

LIMK2 interacts with endogenous Nf1

We have shown that LIMK2 is able to interact with SecPH, a domain of Nf1. We wondered if this interaction was still observed with the full length protein Nf1.

To address this point, we first transfected HEK-293 cells, which naturally express Nf1, with HA-LIMK2, and proceeded to anti-HA immunoprecipitation. As shown in Figure 1E, immunoprecipitated HA-LIMK2 interacts specifically with endogenous Nf1.

We then immunoprecipitated endogenous Nf1 from HEK-293 lysed cells with anti-Nf1 antibodies coupled to sepharose beads and checked for endogenous LIMK2 interaction. As shown in Figure 1F, we could detect a specific band of endogenous LIMK2 interacting with endogenous Nf1.

Domains of LIMK2 involved in its interaction with SecPH

To further dissect the regions of LIMK2 involved in its interaction with SecPH, different domains of LIMK2 were tested for their abilities to coimmunoprecipitate with SecPH. Five domains of LIMK2 were tested (Figure 1G - Top): LIM (the N-terminal extremity of LIMK2 containing 2 LIM domains), PDZ, SP, PDZ/SP, and KIN (the C-terminal domain of LIMK2 comprising the kinase domain).

As shown in Figure 1G - Bottom, LIM domain is unable to interact with SecPH, neither PDZ nor SP domains. In contrast, KIN and PDZ/SP domains are able to interact with SecPH. It is quite intriguing that SecPH interacts with the double domain PDZ/SP but not with one of these single domains PDZ or SP, this may be explained by conformational requirements.

Therefore, SecPH interacts with LIMK2 *via* two domains: the kinase and the PDZ/SP domains.

SecPH affects LIMK2 induced formation of actin stress fibers

LIMK2 belongs to the Rho/ROCK/LIMK2/cofilin signal transduction pathway and phosphorylates cofilin. Once phosphorylated, cofilin, an actin depolymerisation factor, is then no longer able to depolymerise actin, and an accumulation of stress fibers is observed. Using *NF1* siRNA, Ozawa *et al.* have shown that Nf1 is an inhibitor of this pathway [29]. However, they provided no molecular explanation for this phenomenon. Our new data have prompted us to test if the target of Nf1 in the Rho/ROCK/LIMK2/cofilin pathway could be LIMK2.

We first focused our attention on actin cytoskeleton organisation driven by this pathway by performing immunofluorescence experiments on fixed intact cells.

HeLa cells were cotransfected with HA-LIMK2 and SecPH or with HA-LIMK2 and the parental empty plasmid of SecPH. The actin filaments were visualized by phalloidin staining. As previously observed [35], expression of LIMK2 enhanced the formation of actin stress fibers compared to mock-transfected cells, a consequence of cofilin inactivation by LIMK2 (Figure 2A- Left and Middle pannels). When SecPH was cotransfected with LIMK2, there was a marked decrease in the accumulation of actin stress fibers (Figure 2A – Right and Middle pannels). These data suggest that SecPH affects actin stress fiber formation due to LIMK2 overexpression.

SecPH partially inhibits cofilin phosphorylation by LIMK2

We then decided to test directly SecPH activity on LIMK2 by measuring LIMK2 kinase activity on cofilin *in vitro* in the presence or not of SecPH.

Cells were cotransfected by LIMK2 and either SecPH or Galectin-3, a non-specific flag-tagged protein control. Galectin-3 is a member of the lectin family which binds beta-galactoside [36]. We measured the kinase activity of the anti-HA-LIMK2 immunoprecipitates using recombinant GST-cofilin as a substrate.

As shown in Figure 2B, anti-HA immunoprecipitate from cells cotransfected with LIMK2 and SecPH showed a slight but significant and reproducible decrease of around 20% in the intensity of phospho-cofilin (P-cofilin) compared with anti-HA immunoprecipitate from cells cotransfected with LIMK2 and the non-specific protein control Galectin-3. These data are statistically significant as $p = 0.0289$ (* $p<0.05$).

These results suggest that SecPH partially inhibits cofilin phosphorylation by LIMK2.

SecPH dose dependent inhibition of cofilin phosphorylation by LIMK2

To further characterize SecPH inhibition of cofilin phosphorylation by LIMK2, we repeated the kinase assay on cofilin, but this time we incubated anti-HA-LIMK2 immunoprecipitate with increasing amounts of immunoprecipitated SecPH. Cells were transfected on one hand with LIMK2 and on the other hand with SecPH or the non-specific protein control Galectin-3. SecPH and Galectin-3 were immunoprecipitated from transfected cell lysates with anti-flag beads, and then eluted from the beads with flag peptide. For the kinase assay, immunoprecipitated HA-LIMK2 and GST-cofilin were used, in the presence of increasing amounts of eluted SecPH or Galectin-3.

As shown in Figure 2C, we observed a dose-dependent response of cofilin phosphorylation upon SecPH addition, whereas Galectin-3 addition had no influence on cofilin phosphorylation. The more SecPH was added, the less P-cofilin was observed. Therefore, the more SecPH was added, the more LIMK2 kinase activity on cofilin was inhibited.

SecPH inhibition of cofilin phosphorylation is specific to LIMK2

We already demonstrated that SecPH specifically interacts with LIMK2 and not with its close related homolog LIMK1 (Figures 1B and 1C). In order to make sure that SecPH activity on cofilin phosphorylation *in vitro* specifically went through LIMK2, and not through its close related homolog, LIMK1, we repeated the kinase assay on GST-cofilin with HA-LIMK1 immunoprecipitate in the presence of increasing amounts of immunoprecipitated SecPH. It appeared that SecPH has no effect on LIMK1 kinase activity on cofilin (Figure 2D).

SecPH inhibition of cofilin phosphorylation by LIMK2 requires ROCK activation of LIMK2

To deepen our understanding of SecPH inhibition on cofilin phosphorylation by LIMK2, we took advantage of two mutants of LIMK2 at Threonin 505. Consequently to T505 phosphorylation by ROCK, LIMK2 is activated and phosphorylates cofilin. The two mutants used in this study were LIMK2-T505A, which is inactive, and LIMK2-T505EE, which is constitutively active [35].

First, we checked if these two mutants were still able to interact with SecPH. Cells were cotransfected with HA-LIMK2 WT, LIMK2-TA or LIMK2-TEE and with flag-SecPH. Anti-flag immunoprecipitations were performed. As depicted in Figure 3A, SecPH interacts with wild-type LIMK2, as well as with LIMK2-TA and LIMK2-TEE. We also checked if these two mutants were still able to interact with endogenous Nf1. Cells were transfected with either HA-LIMK2-WT, or LIMK2-TA or LIMK2-TEE. Anti-HA immunoprecipitations were performed. As shown in Figure 3B, the two mutants interact with endogenous Nf1.

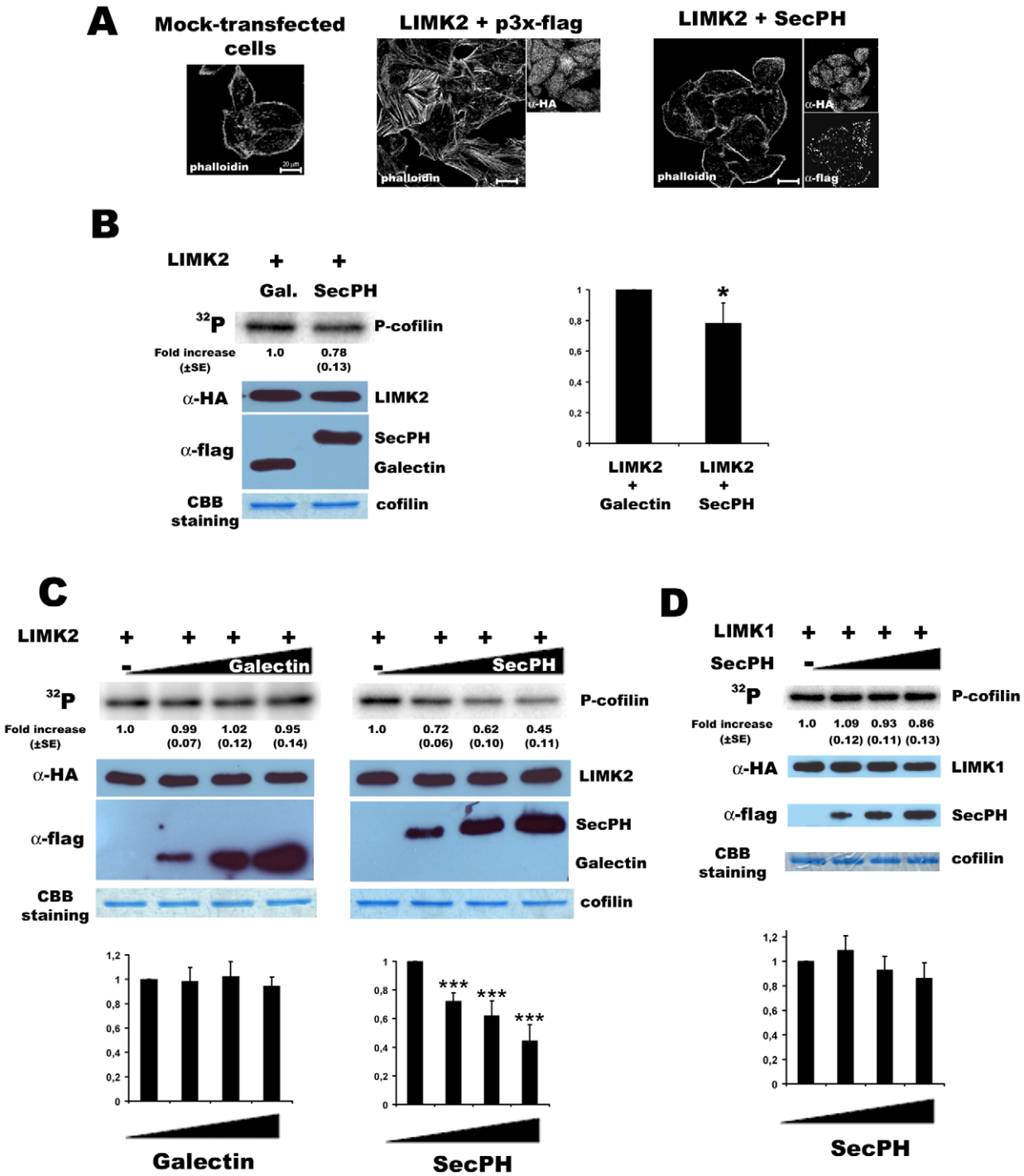

Figure 2. SecPH partially inhibits cofilin phosphorylation by LIMK2, but not by LIMK1. *A. Actin cytoskeleton organisation*. HeLa cells were cotransfected with pcDNA3, LIMK2 and SecPH or its parental empty plasmid, p3XFlag. Cells were fixed and stained with phalloidin, or anti-HA or anti-flag antibodies. *B. Inhibition of LIMK2 cofilin phosphorylation by SecPH.* Cells were cotransfected with LIMK2 and SecPH or Galectin-3 (a non-specific control protein). Immunoprecipitated HA-LIMK2 and GST-cofilin were used in the kinase assay. The kinase activity on cofilin of immunoprecipitated HA-LIMK2 from cells cotransfected with Galectin-3 was taken as 1.0. Each value represents the mean ± SE (standard error) of four independent experiments. Statistical significance was determined relative to control using one-way ANOVA (* $p<0.05$). The HA-immunoprecipitates were also submitted to HA-immunoblotting and to coomassie blue staining. Lysates were submitted to flag-immunoblotting. *C. Dose dependent inhibition of LIMK2 cofilin phosphorylation by SecPH.* Cells were transfected with LIMK2 and either SecPH or Galectin-3. SecPH and Galectin-3 cell lysates were immunoprecipitated with anti-flag beads, beads were then eluted flag peptide. Immunoprecipitated HA-LIMK2 and GST-cofilin were used for kinase assay and were incubated with increasing amount of immunoprecipitated SecPH or Galectin-3 (0, 6, 12, 18 ul respectively). The kinase activity on cofilin of immunoprecipitated HA-LIMK2 with no addition of immunoprecipitated SecPH or Galectin-3 was taken as 1.0. Each value represents the mean ± SE of four independent experiments. Statistical significance was determined relative to control using one-way ANOVA (*** $p<0.0001$). Immunoprecipitates were also subjected to immunoblotting and to coomassie blue staining. *D. SecPH does not inhibit cofilin phosphorylation by LIMK1*. Cells were transfected either with SecPH or with LIMK1. SecPH cell lysates were immunoprecipitated with anti-flag beads, beads were then

eluted with flag peptide. Immunoprecipitated HA-LIMK1 was used for kinase assay and was incubated with increasing amount of immunoprecipitated SecPH (0, 6, 12, 18 ul respectively). The kinase activity on cofilin of immunoprecipitated HA-LIMK1 with no addition of immunoprecipitated SecPH was taken as 1.0. Each value represents the mean ± SE of two independent experiments. Immunoprecipitates were also subjected to immunoblotting and to coomassie blue staining.
doi:10.1371/journal.pone.0047283.g002

We then tested the ability of SecPH to inhibit cofilin phosphorylation by these two mutants. Cells were cotransfected by SecPH or its empty parental plasmid and by either LIMK2-WT, LIMK2-TA, or LIMK2-TEE. We measured the kinase activity of the different anti-HA-LIMK2 immunoprecipitates using GST-cofilin as a substrate. P-cofilin signal was very weak with the inactive LIMK2-TA and particularly intense with the constitutively active LIMK2-TEE (Figure 3C). These results are in good accordance with data from the literature [35]. Neither of these P-cofilin signals was modulated by SecPH (Figure 3C). These results are not so surprising for P-cofilin produced by LIMK2-TA, considering the mutant has a weak activity. SecPH was interestingly unable to inhibit cofilin phosphorylation by the constitutively active LIMK2-TEE whereas it can still interact with it (Figure 3A).

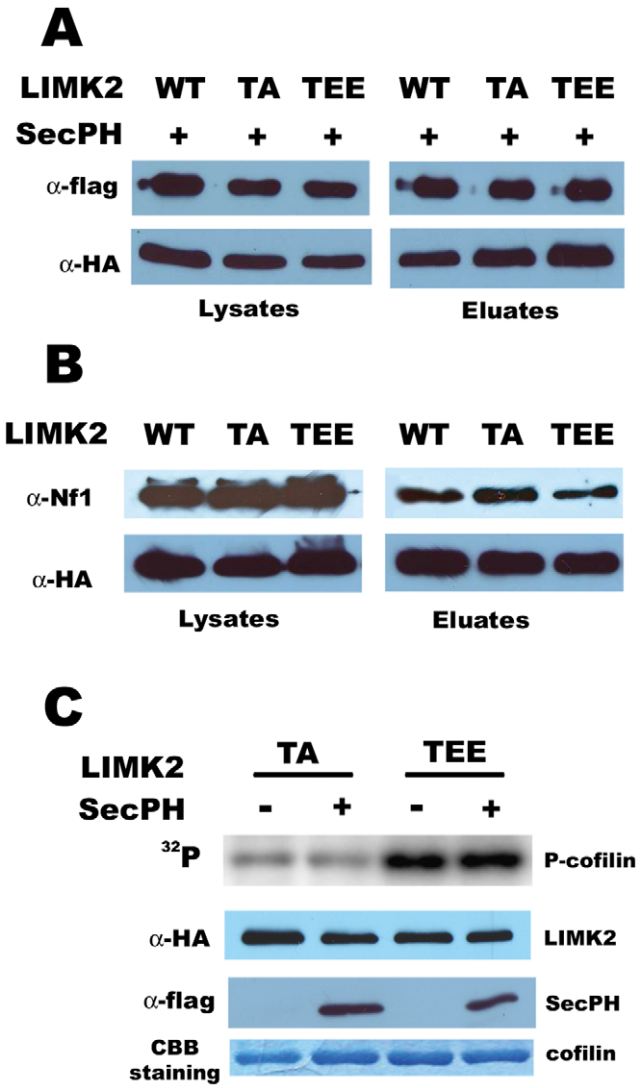

Figure 3. SecPH inhibition of cofilin phosphorylation by LIMK2 requires ROCK activation of LIMK2. *A. SecPH interacts with LIMK2 whatever its activation state.* Cells were cotransfected with SecPH and either LIMK2-WT, or LIMK2-TA or LIMK2-TEE. Lysates and anti-flag immunoprecipitates were subjected to immunoblotting. *B. Nf1 interacts with LIMK2 whatever its activation state.* Cells were transfected with either LIMK2-WT, or LIMK2-TA or LIMK2-TEE. Lysates and anti-HA immunoprecipitates were subjected to immunoblotting. *C. SecPH is unable to modulate cofilin phosphorylation by LIMK2-T505 mutants.* Cells were cotransfected with either LIMK2-WT, or LIMK2-TA or LIMK2-TEE and SecPH or its parental empty plasmid. Immunoprecipitated HA-LIMK2 and GST-cofilin were used in the kinase assay. Anti-HA immunoprecipitates were also subjected to immunoblotting and to coomassie blue staining.
doi:10.1371/journal.pone.0047283.g003

SecPH inhibits LIMK2 phosphorylation of cofilin by preventing ROCK activation of LIMK2

In an attempt to elucidate the mechanism of SecPH inhibition of cofilin phosphorylation by ROCK activated LIMK2, we postulated that SecPH might prevent LIMK2 from interacting with ROCK. To check this hypothesis, we cotransfected cells with HA-LIMK2, cMyc-ROCK1 and flag-SecPH or its empty parental plasmid. We then performed HA-immunoprecipitations. In these conditions, ROCK1 interacts with LIMK2 in the absence as well as in the presence of SecPH (Figure 4A). Therefore, SecPH does not disturb the interaction between ROCK1 and LIMK2.

Another attractive hypothesis is that SecPH might prevent the T505 phosphorylation of LIMK2 by ROCK.

This hypothesis was in accordance with ^{32}P gels from the LIMK2 kinase assay on cofilin described in Figure 2B. Indeed, a slower mobility band compared to cofilin could be observed on ^{32}P labeled gels. This band corresponded to LIMK2 molecular weight. So in this assay, we could also observe HA-immunoprecipitated LIMK2 phosphorylation. The intensity of LIMK2 phosphorylated band was decreased in the presence of SecPH (Figure 4B) indicating that SecPH might affect LIMK2 phosphorylation.

In order to know if this phosphorylation was mediated by ROCK activity on T505 of LIMK2, and was not due to LIMK2 autophosphorylation, we used anti-P-LIMK1 (T508)/LIMK2 (T505) antibodies. However, in conditions where cells were transfected with LIMK2, this antibody appeared to be non specific for P-LIMK2 (T505) detection. Indeed, a signal could be observed with the LIMK2-T505A mutant on lysate and even on LIMK2-T505A immunoprecipitate. To circumvent this problem, we cotransfected cells with LIMK2 and ROCK1, in order to enhance LIMK2-T505 phosphorylation. In these conditions, no signal was observed for LIMK2-T505A mutant (Figure 4D).

In these conditions *i.e.* when ROCK1 was cotransfected with LIMK2, SecPH was still able to inhibit cofilin phosphorylation by LIMK2, although HA-LIMK2 immunoprecipitates showed an increased kinase activity on cofilin (Figure 4C).

When cells were cotransfected with ROCK1, LIMK2 and SecPH, the signal detected with anti-phosphoT505 antibodies was significantly decreased compared to cells cotransfected with ROCK1, LIMK2 and a non-specific control protein, Galectin-3

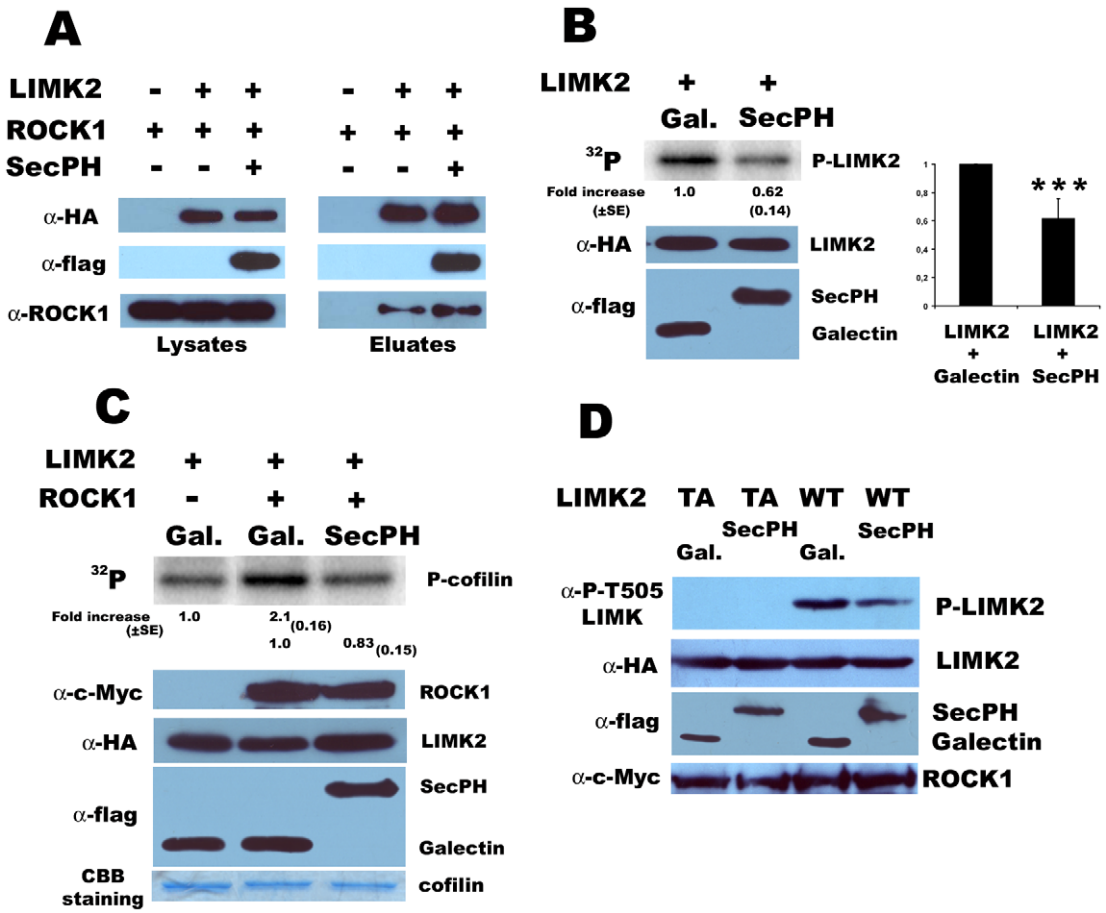

Figure 4. Mechanism of SecPH inhibition of LIMK2 kinase activity. *A. SecPH does not prevent LIMK2 from interacting with ROCK1*. Cells were cotransfected with HA-LIMK2, ROCK1 and SecPH or its empty parental plasmid. Lysates and anti-HA immunoprecipitates were subjected to immunoblotting. *B. SecPH affects LIMK2 phosphorylation.* Same as Figure 2B. Statistical significance was determined relative to control using one-way ANOVA (*** $p<0.0001$). *C. Inhibition of LIMK2 cofilin phosphorylation by SecPH in the presence of ROCK1*. Cells were cotransfected with ROCK1, LIMK2 and SecPH or Galectin-3 (a non-specific control protein). Immunoprecipitated HA-LIMK2 and GST-cofilin were used for the kinase assay. The kinase activity on cofilin of immunoprecipitated HA-LIMK2 from cells cotransfected with Galectin-3 was taken as 1.0. Each value represents the mean ± SE (standard error) of four independent experiments. The HA-immunoprecipitates were also submitted to immunoblotting and to coomassie blue staining. Lysates were also submitted to flag-immunoblotting. *D. SecPH affects LIMK2 T505 phosphorylation by ROCK1*. Cells were cotransfected with either LIMK2-TA or LIMK2-WT and SecPH or Galectin-3 (a non-specific control protein). Lysates were subjected to immunoblotting.
doi:10.1371/journal.pone.0047283.g004

(Figure 4D). These results suggest that SecPH affects LIMK2-T505 phosphorylation by ROCK1.

Altogether these data suggest that SecPH inhibition of cofilin phosphorylation by LIMK2 is due to SecPH inhibition of LIMK2 phosphorylation and therefore activation by ROCK1.

SecPH affects ROCK kinase activity specifically with respect to LIMK2

Our results suggest that SecPH affects LIMK2 phosphorylation by ROCK. We next wondered if SecPH affects ROCK kinase activity in general or specifically with respect to LIMK2. In this purpose, we studied the kinase activity of ROCK on Myosin Light Chain (MLC), another ROCK substrate, in the presence or in the absence of SecPH.

First, we repeated our kinase assay on HA-LIMK2 immunoprecipitates in the presence of SecPH or Galectin-3 as described in Figure 2B but we added MLC in the kinase reaction mixture. Indeed, as shown in Figure 4B, we know that in this assay, SecPH inhibits LIMK2 phosphorylation and we wanted to know if it was also the case for MLC. In these conditions, MLC phosphorylation did not seem to be affected by SecPH (Figure 5A).

Then, we transfected cells with c-Myc-ROCK1 and SecPH or Galectin-3. We measured the kinase activity of the anti-c-Myc immunoprecipitates but this time by using recombinant LIMK2 or MLC as substrates. As shown in Figure 5B, SecPH seemed to have no influence on MLC phosphorylation by ROCK1. In this experiment, SecPH inhibition of the recombinant LIMK2 phosphorylation was faint but this can be explained by the fact that the recombinant LIMK2 we used was already activated and phosphorylated. It has also to be noted that ROCK1 autophosphorylated during the assay and that SecPH did not seem either to inhibit this phosphorylation.

Altogether, these results suggest that SecPH inhibition of ROCK kinase activity is specific to LIMK2.

Discussion

The human superfamily of small GTPases presents more than 150 members. Ras GTPases are the founding members of this family, which is divided into five main branches: Ras, Rho, Rab,

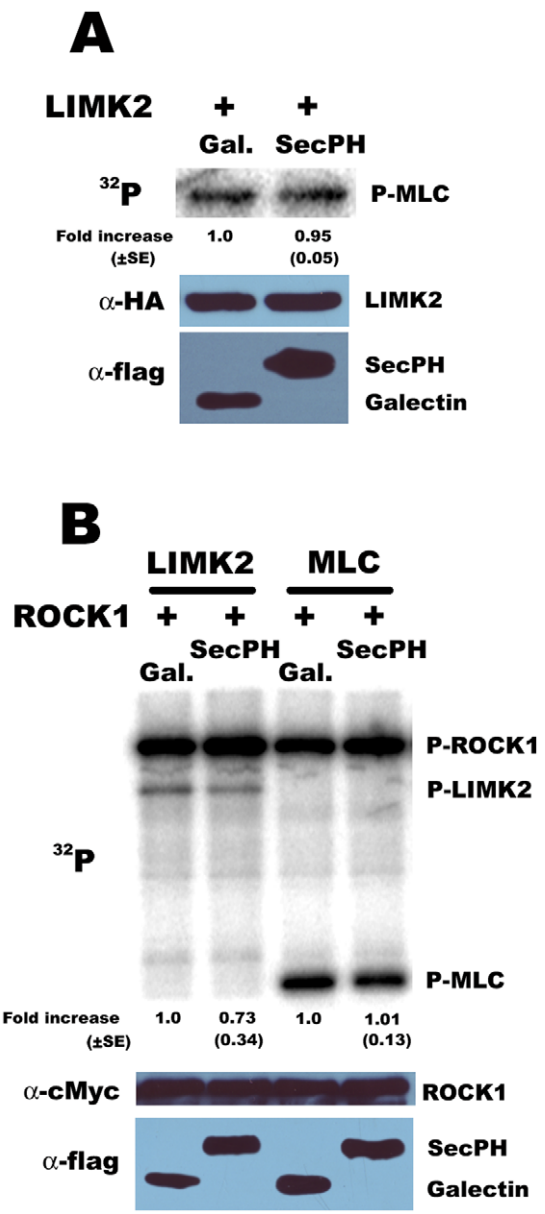

Figure 5. SecPH affects ROCK kinase activity specifically with respect to LIMK2. *A. MLC phosphorylation is not affected by SecPH.* Same as Figure 2B, except 0.5 µg of MLC were added in the kinase reaction mixture. Each value represents the mean ± SE (standard error) of two independent experiments. B. *MLC phosphorylation by ROCK-1 is not affected by SecPH.* Cells were cotransfected with ROCK1 and SecPH or Galectin-3. Immunoprecipitated c-Myc-ROCK1 was used for the kinase assay in the presence of recombinant LIMK2 or MLC (0.5 µg each). The kinase activity on LIMK2/MLC of immunoprecipitated c-Myc-ROCK from cells cotransfected with Galectin-3 was taken as 1.0. Each value represents the mean ± SE (standard error) of four independent experiments. Immunoprecipitates were also submitted to c-Myc-immunoblotting and lysates to flag-immunoblotting.
doi:10.1371/journal.pone.0047283.g005

Ran and Arf. Acting as molecular binary switches, these small GTPases regulate many major biological processes, such as cell cycle progression, cell survival, actin cytoskeleton organization, cell polarity and movement, and vesicular and nuclear transport. Extensive cross-talks between these different small GTPases have been demonstrated [1,37,38,39].

In order to find new cross-talks between Ras GTPases and other small GTPases, we decided to focus on the RasGAP Nf1, which was already shown to integrate several signal transduction pathways. By a yeast two-hybrid screening, we identified LIMK2 as a new partner of the SecPH domain of Nf1. LIMK2 is a major kinase of the Rho/ROCK/LIMK2/cofilin pathway. Upon activation by ROCK, LIMK2 phosphorylates cofilin, resulting in its inactivation. Cofilin is a member of the ADF (actin depolymerizing factor) family. It promotes actin depolymerization at pointed ends and severes long actin filaments, which leads to a fast turnover of actin filaments [33,34]. By inhibiting cofilin, LIMK2 plays a central role in the regulation of actin cytoskeleton reorganisation and thereby contributes to diverse cellular functions such as cell motility, morphogenesis, division, differentiation, apoptosis, neurite extension and oncogenesis.

We confirmed the interaction between LIMK2 and the SecPH domain of NF1 by coimmunoprecipitation experiments. Our results also suggest a molecular mechanism explaining the physiological relevance of this interaction. Indeed, by interacting with LIMK2, Nf1, *via* its SecPH domain, seems able to inhibit LIMK2 activation by ROCK and its subsequent activity on cofilin.

Our results are in accordance with data from a recent proteomic study on ROCK, whose goal was to identify new substrates of this kinase [40]. Nf1 and LIMK2 were found to be part of the ROCK complexome.

Our findings are also in good agreement with previous data from Ozawa *et al.* [29], who showed that Nf1 regulated actin cytoskeleton reorganization by inhibiting the Rho/ROCK/LIMK2/cofilin pathway. They performed *NF1* siRNA experiments on HeLa cells and observed an excessive actin stress fiber formation and an increase of P-cofilin due to LIMK2. However, they could not establish a direct molecular link between Nf1 and this pathway. Our data indicate that this missing link might be the interaction between LIMK2 and the SecPH domain of Nf1, although we cannot exclude another partner as we worked on immunoprecipitated and not recombinant proteins. We also went further into the understanding of the molecular mechanism of Nf1 inhibition of the Rho/ROCK/LIMK2/cofilin pathway by suggesting that Nf1-SecPH might prevent LIMK2 activation by ROCK and therefore prevent LIMK2 phosphorylation and inhibition of cofilin. SecPH inhibition of ROCK kinase activity seems to be specific to LIMK2, as phosphorylation of another ROCK substrate, Myosin Light Chain, is not affected by SecPH. It would be very interesting to go deeper into the understanding of the mechanistics of this process. Our study raised two hypotheses (Figure 6) : (1) we have shown that SecPH does not disrupt LIMK2/ROCK interaction (Figure 4A), however when SecPH binds to LIMK2, a steric hindrance might prevent ROCK from accessing its target residue, Thr505 of LIMK2 (2) when SecPH and ROCK bind to LIMK2, they get nearby, then the PH domain of SecPH might interact with the kinase domain of ROCK and inhibit it, thereby mimicking the action of the PH domain of ROCK in its inactive closed conformation. However, as we showed that SecPH has no intrinsic influence on ROCK kinase activity in general, this inhibition would specifically occur when ROCK and SecPH simultaneously interact with LIMK2. Further studies are currently in progress to bring an answer to these intriguing mechanistics.

Our results also corroborate previous data suggesting a role of Nf1 in actin cytoskeleton dynamics.

First of all, many of the clinical features of Neurofibromatosis type I, such as neurofibroma and glioma formation as well as learning disabilities, may be related to actin cytoskeletal organi-

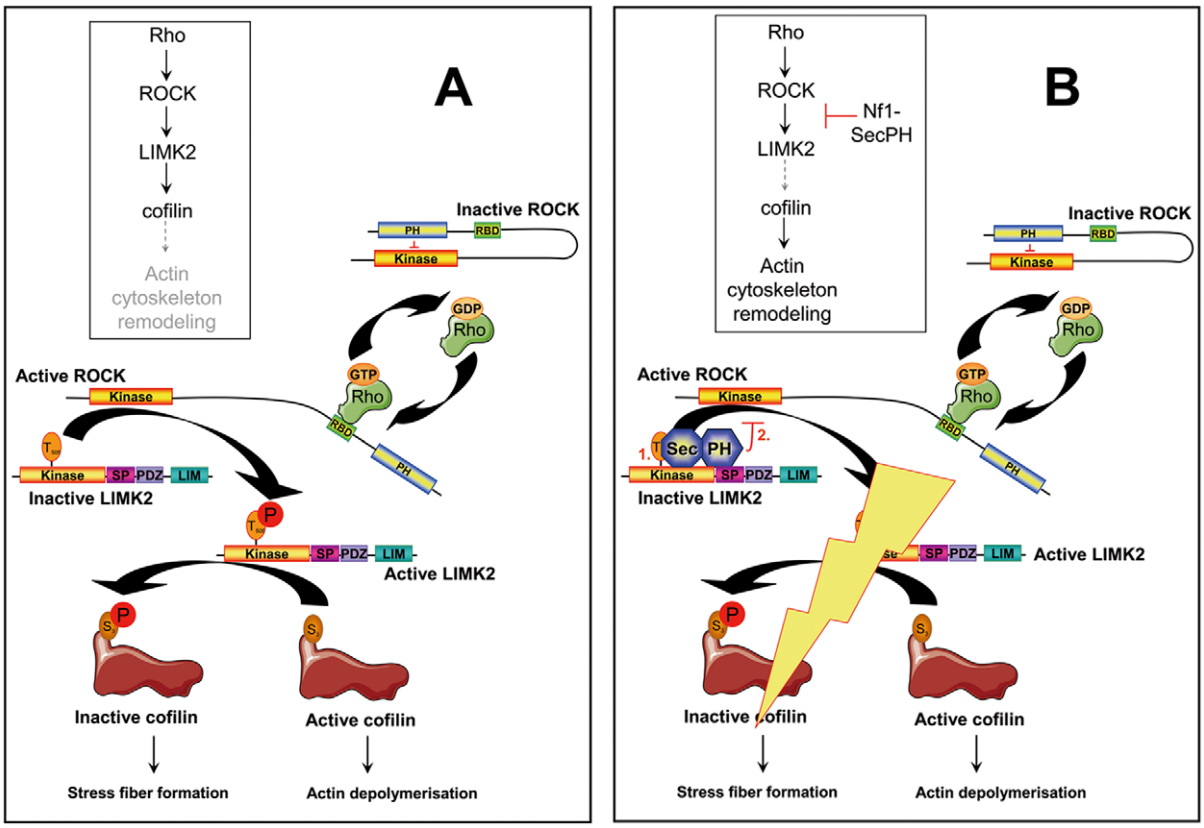

Figure 6. Schematic representation of our findings: A molecular connection between neurofibromin and the Rho/ROCK/LIMK2/cofilin pathway. *A.* Upon Rho activation *via* binding to its RBD (Rho Binding domain), ROCK activates LIMK2 by phosphorylation at its Thr505. Activated LIMK2 will then phosphorylate cofilin on its Ser3, resulting in its inhibition. An invasive phenotype is then observed with accumulation of actin stress fibers. *B. SecPH, a new inhibitor of this Rho/ROCK/LIMK2/cofilin pathway*. By interacting with LIMK2, SecPH prevents ROCK activation of LIMK2. Our data raises two possible hypotheses for this inhibition of ROCK activation of LIMK2 by SecPH: (1) by steric hindrance, SecPH hides Thr505 of LIMK2 from ROCK accessibility, (2) the PH domain of SecPH substitutes to the PH domain of ROCK by inhibiting the kinase activity of ROCK; this inhibition would specifically occur when ROCK and SecPH are simultaneously bound to LIMK2.
doi:10.1371/journal.pone.0047283.g006

sation defect. Indeed, neurofibromas are composed of an aggregation of multiple cell types and they are infiltrated by surrounding hypermotile *Nf1*+/− mast cells (which secrete mediators that remodel the extracellular matrix and initiate angiogenesis). Both features are related to the deregulation of the actin cytoskeleton. Beyond the tumorigenic symptoms, NF1 patients frequently exhibit cognitive deficits. Along this line, regulation of actin cytoskeleton reorganization and the Rho/ROCK/LIMK/cofilin pathway have been shown to play a role in neuronal cell development [41,42].

Secondly, enhanced migration and motility as well as abnormal actin cytoskeleton organization were observed in *Nf1* deficient or haploinsufficient Schwann cells, astrocytes and osteoclasts [43,44,45,46]

Finally, in addition to the Rho/ROCK/LIMK2/cofilin pathway, several other specific signaling pathways were identified to connect Nf1 to actin cytoskeleton dynamics. *NF1* overexpression was shown to induce an increase in the expression levels of the Focal Adhesion Kinase (FAK) [24]. A direct interaction between Nf1 and FAK has also been described [27], suggesting a role of Nf1 in cell adhesion. Moreover, by interacting with syndecan-2, another adhesion protein, Nf1 mediates the activation of PKA, which phosphorylates two actin-associated proteins Ena and VASP, thus promoting actin polymerisation for the formation of filopodia and dendritic spines [28]. In addition to its negative regulation of the Rho/ROCK/LIMK2/cofilin pathway [29], Nf1 also independently negatively regulates the Rac1/Pak1/LIMK1/cofilin pathway [30]. In both cases, *NF1* depletion leads to an increased phosphorylation and consequently inhibition of cofilin, thus promoting actin stress fiber formation. Along the same line, the effect of the drug schweinfurthin A is most probably related to the role of Nf1 in the Rho/ROCK/LIMK2 pathway [47]. Recently, Nf1 was shown to activate Rho/ROCK/MLC pathway *via* cAMP/PKA signaling. These latter results seem in contradiction with the previous data described above and our findings, but can be easily reconciliated. Indeed, they were obtained specifically in neurons of the central nervous system and not in neurons of the peripheral nervous system, therefore they appear to be cell type specific [48].

From a signal transduction point of view, we identified a new cross-talk between Ras GTPases and another small GTPase, namely between Ras and RhoA.

About twenty years ago, several studies already suggested cross-talks between Ras and Rho signaling pathways [37,49,50]. The preliminary ideas limiting Ras to cell proliferation and Rho to actin cytoskeleton reorganization and considering these pathways as linear and disconnected became quickly obsolete. A complex scheme interconnecting the different small GTPase pathways was more accurate. Different approaches, sometimes combined, allowed to establish these connections: (i) the use of dominant

negative and constitutively active versions of small GTPases (created through specific amino acid substitution); (ii) the use of transient activation or chemical drugs to stimulate or inhibit upstream regulators of small GTPases; (iii) more recently the use of RNAi and gene knockout models. Although these studies brought invaluable data on cross-talks between Ras and Rho, mainly *via* Rac, they suffered from a lack of molecular data. Indeed, most of the time they did not identify precisely the different proteins or the biochemical mechanisms involved in these connections. In parallel, studies based on GEFs and GAPs, the main regulators of small GTPases, also established connections between the different small GTPases. Sequence analysis showed that some GEFs, and in a lower extent a few GAPs, possess GEF or GAP domains for other small GTPases. By interacting with various specific partners, GAPs or GEFs appear to trigger different cell responses. As an example, when the GEF SOS is in complex with Grb2, it activates Ras, whereas when it is in complex with Eps8, it activates Rac [1,51]. Special interest has focused on p120RasGAP, the first RasGAP identified. p120RasGAP was found to interact with several RhoGAPs, triggering different cell responses according to which RhoGAP is involved. p120RasGAP was found to interact with p190RhoGAP [49,52]. It appears to recruit it to the cell periphery where it inhibits Rho [53]. p120RasGAP was also found to interact with p200RhoGAP. This interaction is required for p200RhoGAP to activate Ras, promoting cell growth and transformation [54]. Finally, p120RasGAP was found to interact with the DLC1 RhoGAP thereby inhibiting its GAP activity towards RhoA and resulting in RhoA activation [3].

In our present study, the RasGAP Nf1 does not interact with a RhoGAP but with a downstream effector of RhoA, LIMK2. By interacting with the SecPH domain of Nf1 Ras GAP, LIMK2 partially loses its kinase activity on cofilin. We have shown that this process is specific to LIMK2. Nf1 RasGAP-SecPH has no effect on LIMK1, the close related homolog of LIMK2. One may think that, in these conditions, cofilin may still be inactivated by LIMK1. However, another domain of the RasGAP Nf1, its pre-GAP region, has been shown to negatively regulate the Rac1/Pak1/LIMK1/cofilin pathway [30]. So, *via* two of its domains, the RasGAP Nf1 may coordinate the inhibition of both LIM kinases shutting down their activity on cofilin. The regulation of these two branches of the pathway by two independent domains suggests an independent regulation for these processes.

In conclusion, our study suggests a new connection into the complex network of small GTPase signaling. The RasGAP Nf1 might regulate the activity of a downstream effector of RhoA. Our results bring unprecedented details of the molecular mechanism that might be involved in this connection. Further characterization of the interactome of the different members of this network will certainly establish new cross-talks between small GTPases. A special effort on the molecular requirements of these interactions is needed for a better understanding of the role and the interconnections between each member in this network.

Materials and Methods

Materials

Antibodies against Nf1 (sc-67), ROCK1 (sc-6055), and LIMK2 (sc-8390) and anti-Nf1 beads were from Santa Cruz Biotechnology, Inc. Anti-flag M2 affinity gel, anti-flag M2 monoclonal antibody, flag-peptide and anti-HA and anti-c-Myc affinity gels were from Sigma-Aldrich Co. HA antibody was from Roche Applied Science and P-LIMK2 antibody from Cell Signalling Technology. Lipofectamine LTX was from Invitrogen, Opti-MEM from Gibco. Recombinant GST-fused cofilin was purchased from Upstate cell signalling Inc. Recombinant Myosin Light Chain and LIMK2 were from Calbiochem and Life Technologies, respectively. Plasmids used in this study are listed in Table 1.

Table 1. List of plasmids used in this study.

Plasmid	Description	Source/ Reference
pBTM116	P_{ADH1} *-LEXA TRP1* 2μ	[57]
pBTM116-SecPH	P_{ADH1} *–LEXA-SecPH TRP1* 2μ	This study
pBTM116-TBD	P_{ADH1} *–LEXA-Ira2 TBD TRP1* 2μ	This study
pACT2	2μ*LEU2*	Clontech
pACT2-TFS1	2μ*LEU2-TFS1*	This study
pACT2-LIMK1	2μ*LEU2-LIMK1*	This study
pACT2-LIMK2	2μ*LEU2-LIMK2-2a*	This study
p3XFlag-*myc*-CMV-24	P_{CMV}-Flag	Sigma
p3XFlag-SecPH	P_{CMV}-Flag-SecPH	This study
p3XFlag-Galectin-3	P_{CMV}-Flag-Galectin-3	A. Legrand
pUC2SR-*myc*-LIMK2-2a	*LIMK2-2a*	K. Mizuno
pUC2SR-*myc*-LIMK2-2a-T505A	*LIMK2-2a*-T505A	K. Mizuno
pFC1-*myc*-hLIMK1	*LIMK1*	K. Mizuno
pcDNA3-$(HA)_2$-LIMK2	P_{CMV}-$(HA)_2$-*LIMK2-2a*	This study
pcDNA3-$(HA)_2$-LIMK1	P_{CMV}-$(HA)_2$-*LIMK1*	This study
pcDNA3-$(HA)_2$-LIMK2-T505A	P_{CMV}-$(HA)_2$-*LIMK2-2a-T505A*	This study
pcDNA3-$(HA)_2$-LIMK2-T505EE	P_{CMV}-$(HA)_2$-*LIMK2-2a-T505EE*	This study
pcDNA3-$(HA)_2$-LIM-LIMK2	P_{CMV}-$(HA)_2$-*LIM-LIMK2-2a*	This study
pcDNA3-$(HA)_2$-PDZ-LIMK2	P_{CMV}-$(HA)_2$-*PDZ-LIMK2-2a*	This study
pcDNA3-$(HA)_2$-PDZ-SP-LIMK2	P_{CMV}-$(HA)_2$-*PDZ-SP-LIMK2-2a*	This study
pcDNA3-$(HA)_2$-KIN-LIMK2	P_{CMV}-$(HA)_2$-*KIN-LIMK2-2a*	This study
pCAG ROCK1	*ROCK1-myc*	[58]
pET14-6his-SecPH	*6his-SecPH*	This study

doi:10.1371/journal.pone.0047283.t001

Two-hybrid screening

The two-hybrid system used was obtained from Clontech (Yeast Matchmaker). All media, buffers and methods used for yeast cells were adapted from previously described procedures [55,56] and from the Clontech *Yeast Protocols Handbook*. pBTM116-SecPH encoding the SecPH domain of Nf1 fused in N-terminus to the LexA DNA-binding protein was transformed into the *Saccharomyces cerevisiae* strain L40 (MATa, *his3Δ200*, *trp1-901*, *leu2-3*, *112*, *ade2*, *LYS::(lexAop)$_4$-HIS*, *URA3::(lexAop)$_8$-lacZ*. The human foetal brain cDNA library, cloned in pACT2 (and fused in N-terminus to the activation domain of Gal4) was transformed in the Y187 strain (MATa, *ade2-101*, *met-his3-200*, *leu2-3*, *112*, *trp1-901*, *ura3-52*, *gal4Δ gal80Δ*, *URA3::GAL1*, *UAS-GAL1*, *TATA-lacZ MEL1*) and was purchased from Clontech. It contained 3.5 millions of independent clones. After mating of the two strains, 270 millions of interactions were tested and plated on restricted medium lacking leucin, tryptophan and histidin. Growing colonies were restreaked and tested for β-galactosidase activity, yielding 1464 positive clones that were collected and stored at −80°C in glycerol. 173 of these clones were identified by PCR-amplifying the corresponding prey fragments and sequencing them. Two of these clones encoded the full length LIMK2.

Cell culture and transfection

HEK-293 (ATCC, CRL1573) and HeLa cells (ATCC, CCL-2) were cultured under 5% CO_2 at 37°C in Dulbecco's modified Eagle's medium supplemented with 10% fetal calf serum. Cells were transiently transfected with 10 ug of plasmid/100-mm dish with Lipofectamine LTX according to manufacter's recommendations. Experiments were performed 24 h to 48 h after transfection.

Immunoprecipitation

HEK-293 cells were transiently transfected with expression plasmids as described above, and cultured for 24 to 48 h. Cells were lysed in 0.5 ml of lysis buffer (50 mM Tris/HCl, pH 7.5, 100 mM NaCl, 5 mM EDTA, 0.1% Triton X-100, 50 mM NaF, 10 mM sodium pyrophosphate, 1 mM Na_3VO_4, 20 mM p-nitrophenyl phosphate, 20 mM β-glycerophosphate, 10 µg/ml aprotinin, 0.05 µg/ml okaidic acid, 1 µg/ml leupeptin, and 1 mM PMSF), and incubated on ice for 10 min. After centrifugation, the supernatants were incubated for 3 h at 4°C either with anti-HA affinity gel for HA-LIMK2 or its derivatives or with anti-flag M2 affinity gel for SecPH and Galectin-3 or with anti-Nf1 affinity gel for endogenous Nf1. Beads were washed five times with lysis buffer. HA-LIMK2 or its derivatives and Nf1 were eluted by Laemmli sample buffer and flag-SecPH or flag-Galectin-3 was eluted by incubating the beads for 30 minutes on ice with 0.2 mg/ml of the flag peptide.

6His-SecPH purification

6His-SecPH was expressed in *Escherichia coli* using the pET14 plasmid. The protein was purified from the bacterial extract by using TALON Metal Affinity Resin (Clontech). Elution was performed with 100 mM imidazole. Protein concentration was measured by using Bradford method.

To test the interaction between 6His-SecPH and LIMK2, HA-LIMK2 was immunoprecipitated as described in the previous section. Immunoprecipitated beads were then incubated with 6His-SecPH (12 µg) in lysis buffer for 2 hours, and further washed three times with lysis buffer, and then eluted by Laemmli sample buffer. For the negative control, the anti-HA immunoprecipitation was performed on lysates of HEK-293 cells transfected with the pcDNA3 empty plasmid (parental plasmid of HA-LIMK2).

Kinase assay

Immunoprecipitates bound to HA- or flag-beads, as described above, were washed twice with lysis buffer and then three times with kinase buffer (50 mM HEPES-NaOH pH 7.5, 150 mM NaCl, 5 mM $MgCl_2$, 5 mM $MnCl_2$, 50 mM, NaF, 1 mM Na_3VO_4, 20 mM β-glycerophosphate, 1 µg/ml leupeptin, and 1 mM PMSF). HA-LIMK2 or its derivatives were used bound on beads. Flag-SecPH or Flag-Galectin-3 were eluted by incubating the beads with the flag peptide. Immunoprecipitates were incubated for 20 min at 30°C in 22 µl of kinase buffer containing 50 µM ATP, 5 µCi of $\gamma[^{32}P]$ATP (3,000 Ci/mmol) and 2.5 µg of GST-fused cofilin. The reaction was terminated by heating 5 minutes at 90°C in Laemmli sample buffer. Samples were then subjected to SDS-PAGE, and analyzed by autoradiography.

Cell staining

HeLa cells were fixed with 4% paraformaldelyde in PBS for 20 min and permeabilized with 0.5% Triton-X100 in PBS for 15 min at room temperature. After blocking with 1% fetal calf serum in PBS for 30 min, these cells were incubated with anti-HA, anti-flag antibodies for 1 h and subsequently with FITC-conjugated anti-rat IgG and AlexaFluor647-conjugated anti-mouse IgG, respectively, and simultaneously with AlexaFluor568-conjugated phalloidin for 1 h. The cells were then washed three times with PBS, mounted on glass slides, and then analyzed by confocal microscopy using a Zeiss Axiovert 200 M microscope coupled with a Zeiss LSM 510 scanning device (Carl Zeiss Co. Ltd., Iena, Germany).

Acknowledgments

We are very grateful to P. Billuart who provided us the Clontech matchmaker human fetal brain library, P. Roux and K. Mizuno for LIMK and ROCK plasmids, and A. Legrand for Galectin-3 plasmid. We also thank J.V. Barnier for invaluable advices and encouragements, D. Gosset for immunofluorescence image treatment, S. Morisset for helpful discussions, and L. Cobret for technical help.

Author Contributions

Conceived and designed the experiments: BV HB. Performed the experiments: BV MD FG AG AT MLDT HB. Analyzed the data: BV MD FG AG AT MLDT HB. Contributed reagents/materials/analysis tools: BV MD FG AG AT MLDT HB. Wrote the paper: BV HB.

References

1. Mitin N, Rossman KL, Der CJ (2005) Signaling interplay in Ras superfamily function. Curr Biol 15: R563–574.
2. Pamonsinlapatham P, Hadj-Slimane R, Lepelletier Y, Allain B, Toccafondi M, et al. (2009) p120-Ras GTPase activating protein (RasGAP): a multi-interacting protein in downstream signaling. Biochimie 91: 320–328.
3. Yang XY, Guan M, Vigil D, Der CJ, Lowy DR, et al. (2009) p120Ras-GAP binds the DLC1 Rho-GAP tumor suppressor protein and inhibits its RhoA GTPase and growth-suppressing activities. Oncogene 28: 1401–1409.
4. Bos JL, Rehmann H, Wittinghofer A (2007) GEFs and GAPs: critical elements in the control of small G proteins. Cell 129: 865v877.
5. Freidman JM, Gutmann DH, MacCollin M, Riccardi VM (1999) Neurofibromatosis: Phenotype, Natural History, and Pathogenesis.
6. Cichowski K, Jacks T (2001) NF1 tumor suppressor gene function: narrowing the GAP. Cell 104: 593–604.
7. Riccardi VM (1992) Neurofibromatosis: Phenotype, Natural History, and Pathogenesis. Baltimore and London: The Johns Hopkins University Press Second Edition.
8. Cawthon RM, Weiss R, Xu GF, Viskochil D, Culver M, et al. (1990) A major segment of the neurofibromatosis type 1 gene: cDNA sequence, genomic structure, and point mutations. Cell 62: 193–201.
9. Upadhyaya M, Cooper DN (1998) Neurofibromatosis type 1-from genotype to phenotype. Bios Scientific Publishers, Oxford, Washington.
10. Wallace MR, Marchuk DA, Andersen LB, Letcher R, Odeh HM, et al. (1990) Type 1 neurofibromatosis gene: identification of a large transcript disrupted in three NF1 patients. Science 249: 181–186.
11. Xu GF, Lin B, Tanaka K, Dunn D, Wood D, et al. (1990) The catalytic domain of the neurofibromatosis type 1 gene product stimulates ras GTPase and complements ira mutants of S. cerevisiae. Cell 63: 835–841.
12. Martin GA, Viskochil D, Bollag G, McCabe PC, Crosier WJ, et al. (1990) The GAP-related domain of the neurofibromatosis type 1 gene product interacts with ras p21. Cell 63: 843–849.
13. Ballester R, Marchuk D, Boguski M, Saulino A, Letcher R, et al. (1990) The NF1 locus encodes a protein functionally related to mammalian GAP and yeast IRA proteins. Cell 63: 851–859.
14. Bollag G, Clapp DW, Shih S, Adler F, Zhang YY, et al. (1996) Loss of NF1 results in activation of the Ras signaling pathway and leads to aberrant growth in haematopoietic cells. Nat Genet 12: 144–148.
15. Gutmann DH, Giordano MJ, Mahadeo DK, Lau N, Silbergeld D, et al. (1996) Increased neurofibromatosis 1 gene expression in astrocytic tumors: positive regulation by p21-ras. Oncogene 12: 2121–2127.
16. Dang I, De Vries GH (2011) Aberrant cAMP Metabolism in NF1 Malignant Peripheral Nerve Sheath Tumor Cells. Neurochem Res 36: 1697–705.
17. Tong J, Hannan F, Zhu Y, Bernards A, Zhong Y (2002) Neurofibromin regulates G protein-stimulated adenylyl cyclase activity. Nat Neurosci 5: 95–96.
18. Hegedus B, Dasgupta B, Shin JE, Emnett RJ, Hart-Mahon EK, et al. (2007) Neurofibromatosis-1 regulates neuronal and glial cell differentiation from neuroglial progenitors in vivo by both cAMP- and Ras-dependent mechanisms. Cell Stem Cell 1: 443–457.

19. Dasgupta B, Dugan LL, Gutmann DH (2003) The neurofibromatosis 1 gene product neurofibromin regulates pituitary adenylate cyclase-activating polypeptide-mediated signaling in astrocytes. J Neurosci 23: 8949–8954.
20. Guo HF, The I, Hannan F, Bernards A, Zhong Y (1997) Requirement of Drosophila NF1 for activation of adenylyl cyclase by PACAP38-like neuropeptides. Science 276: 795–798.
21. The I, Hannigan GE, Cowley GS, Reginald S, Zhong Y, et al. (1997) Rescue of a Drosophila NF1 mutant phenotype by protein kinase A.Science 276: 791–794.
22. Harashima T, Anderson S, Yates JR 3rd, Heitman J (2006) The kelch proteins Gpb1 and Gpb2 inhibit Ras activity via association with the yeast RasGAP neurofibromin homologs Ira1 and Ira2. Mol Cell 22: 819–830.
23. Boyanapalli M, Lahoud OB, Messiaen L, Kim B, Anderle de Sylor MS, et al. (2006) Neurofibromin binds to caveolin-1 and regulates ras, FAK, and Akt. Biochem Biophys Res Commun 340: 1200–1208.
24. Corral T, Jimenez M, Hernandez-Munoz I, Perez de Castro I, Pellicer A (2003) NF1 modulates the effects of Ras oncogenes: evidence of other NF1 function besides its GAP activity. J Cell Physiol 197: 214–224.
25. Mangoura D, Sun Y, Li C, Singh D, Gutmann DH, et al. (2006) Phosphorylation of neurofibromin by PKC is a possible molecular switch in EGF receptor signaling in neural cells. Oncogene 25: 735–745.
26. Gregory PE, Gutmann DH, Mitchell A, Park S, Boguski M, et al. (1993) Neurofibromatosis type 1 gene product (neurofibromin) associates with microtubules. Somat Cell Mol Genet 19: 265–274.
27. Kweh F, Zheng M, Kurenova E, Wallace M, Golubovskaya V, et al. (2009) Neurofibromin physically interacts with the N-terminal domain of focal adhesion kinase. Mol Carcinog 48: 1005–1017.
28. Lin YL, Lei YT, Hong CJ, Hsueh YP (2007) Syndecan-2 induces filopodia and dendritic spine formation via the neurofibromin-PKA-Ena/VASP pathway. J Cell Biol 177: 829–841.
29. Ozawa T, Araki N, Yunoue S, Tokuo H, Feng L, et al. (2005) The neurofibromatosis type 1 gene product neurofibromin enhances cell motility by regulating actin filament dynamics via the Rho-ROCK-LIMK2-cofilin pathway. J Biol Chem 280: 39524–39533.
30. Starinsky-Elbaz S, Faigenbloom L, Friedman E, Stein R, Kloog Y (2009) The pre-GAP-related domain of neurofibromin regulates cell migration through the LIM kinase/cofilin pathway. Mol Cell Neurosci 42: 278–287.
31. D'Angelo I, Welti S, Bonneau F, Scheffzek K (2006) A novel bipartite phospholipid-binding module in the neurofibromatosis type 1 protein. EMBO Rep 7: 174–179.
32. Chautard H, Jacquet M, Schoentgen F, Bureaud N, Benedetti H (2004) Tfs1p, a member of the PEBP family, inhibits the Ira2p but not the Ira1p Ras GTPase-activating protein in Saccharomyces cerevisiae. Eukaryot Cell 3: 459–470.
33. Pollard TD, Borisy GG (2003) Cellular motility driven by assembly and disassembly of actin filaments. Cell 112: 453–465.
34. Scott RW, Olson MF (2007) LIM kinases: function, regulation and association with human disease. J Mol Med 85: 555–568.
35. Sumi T, Matsumoto K, Nakamura T (2001) Specific activation of LIM kinase 2 via phosphorylation of threonine 505 by ROCK, a Rho-dependent protein kinase. J Biol Chem 276: 670–676.
36. Gaudin JC, Monsigny M, Legrand A (1995) Cloning of the cDNA encoding rabbit galectin-3. Gene 163: 249–252.
37. Bar-Sagi D, Hall A (2000) Ras and Rho GTPases: a family reunion. Cell 103: 227–238.
38. Scita G, Tenca P, Frittoli E, Tocchetti A, Innocenti M, et al. (2000) Signaling from Ras to Rac and beyond: not just a matter of GEFs. Embo J 19: 2393–2398.
39. Takai Y, Sasaki T, Matozaki T (2001) Small GTP-binding proteins. Physiol Rev 81: 153–208.
40. Amano M, Tsumura Y, Taki K, Harada H, Mori K, et al. (2010) A proteomic approach for comprehensively screening substrates of protein kinases such as Rho-kinase. PLoS ONE 5: e8704.
41. Schmandke A, Strittmatter SM (2007) ROCK and Rho: biochemistry and neuronal functions of Rho-associated protein kinases. Neuroscientist 13: 454–469.
42. Luo L (2000) Rho GTPases in neuronal morphogenesis. Nat Rev Neurosci 1: 173–180.
43. Huang Y, Rangwala F, Fulkerson PC, Ling B, Reed E, et al. (2004) Role of TC21/R-Ras2 in enhanced migration of neurofibromin-deficient Schwann cells. Oncogene 23: 368–378.
44. Gutmann DH (2001) The neurofibromatoses: when less is more. Hum Mol Genet 10: 747–755.
45. Sandsmark DK, Zhang H, Hegedus B, Pelletier CL, Weber JD, et al. (2007) Nucleophosmin mediates mammalian target of rapamycin-dependent actin cytoskeleton dynamics and proliferation in neurofibromin-deficient astrocytes. Cancer Res 67: 4790–4799.
46. Yan J, Chen S, Zhang Y, Li X, Li Y, et al. (2008) Rac1 mediates the osteoclast gains-in-function induced by haploinsufficiency of Nf1. Hum Mol Genet 17: 936–948.
47. Turbyville TJ, Gursel DB, Tuskan RG, Walrath JC, Lipschultz CA, et al. (2010) Schweinfurthin A selectively inhibits proliferation and Rho signaling in glioma and neurofibromatosis type 1 tumor cells in a NF1-GRD-dependent manner. Mol Cancer Ther 9: 1234–1243.
48. Brown JA, Diggs-Andrews KA, Gianino SM, Gutmann DH (2012) Neurofibromatosis-1 heterozygosity impairs CNS neuronal morphology in a cAMP/PKA/ROCK-dependent manner. Mol Cell Neurosci 49: 13–22.
49. Settleman J, Albright CF, Foster LC, Weinberg RA (1992) Association between GTPase activators for Rho and Ras families. Nature 359: 153–154.
50. Ridley AJ, Paterson HF, Johnston CL, Diekmann D, Hall A (1992) The small GTP-binding protein rac regulates growth factor-induced membrane ruffling. Cell 70: 401–410.
51. Innocenti M, Tenca P, Frittoli E, Faretta M, Tocchetti A, et al. (2002) Mechanisms through which Sos-1 coordinates the activation of Ras and Rac. J Cell Biol 156: 125–136.
52. Moran MF, Polakis P, McCormick F, Pawson T, Ellis C (1991) Protein-tyrosine kinases regulate the phosphorylation, protein interactions, subcellular distribution, and activity of p21ras GTPase-activating protein. Mol Cell Biol 11: 1804–1812.
53. Bradley WD, Hernandez SE, Settleman J, Koleske AJ (2006) Integrin signaling through Arg activates p190RhoGAP by promoting its binding to p120RasGAP and recruitment to the membrane. Mol Biol Cell 17: 4827–4836.
54. Shang X, Moon SY, Zheng Y (2007) p200 RhoGAP promotes cell proliferation by mediating cross-talk between Ras and Rho signaling pathways. J Biol Chem 282: 8801–8811.
55. Maniatis T, Fritsch EF, Sambrook J (1989) Molecular cloning: a laboratory manual, 2nd ed.
56. Guthrie C, Fink GR (1991) Guide to yeast genetics and molecular biology.
57. Vojtek AB, Hollenberg SM (1995) Ras-Raf interaction: two-hybrid analysis. Methods Enzymol 255: 331–342.
58. Ishizaki T, Naito M, Fujisawa K, Maekawa M, Watanabe N, et al. (1997) p160ROCK, a Rho-associated coiled-coil forming protein kinase, works downstream of Rho and induces focal adhesions. FEBS Lett 404: 118–124.

The EMBO Journal (2005) 24, 730–741 | © 2005 European Molecular Biology Organization | All Rights Reserved 0261-4189/05
www.embojournal.org

THE EMBO JOURNAL

Lip1p: a novel subunit of acyl-CoA ceramide synthase

Béatrice Vallée[1] and Howard Riezman*

Department of Biochemistry, Sciences II, University of Geneva, Geneva, Switzerland

Ceramide plays a crucial role as a basic building block of sphingolipids, but also as a signalling molecule mediating the fate of the cell. Although Lac1p and Lag1p have been shown recently to be involved in acyl-CoA-dependent ceramide synthesis, ceramide synthase is still poorly characterized. In this study, we expressed tagged versions of Lac1p and Lag1p and purified them to near homogeneity. They copurified with ceramide synthase activity, giving unequivocal evidence that they are subunits of the enzyme. In purified form, the acyl-CoA dependence, fatty acyl-CoA chain length specificity, and Fumonisin B1/Australifungin sensitivity of the ceramide synthase were the same as in cells, showing that these are properties of the enzyme and do not depend upon the membrane environment or other factors. SDS–PAGE analysis of purified ceramide synthase revealed the presence of a novel subunit of the enzyme, Lip1p. Lip1p is a single-span ER membrane protein that is required for ceramide synthesis *in vivo* and *in vitro*. The Lip1p regions required for ceramide synthesis are localized within the ER membrane or lumen.

The EMBO Journal (2005) **24,** 730–741. doi:10.1038/sj.emboj.7600562; Published online 3 February 2005
Subject Categories: membranes & transport; cellular metabolism
Keywords: C26-fatty acyl-CoA; Fumonisin B1; *LAC1*, *LAG1*; sphingolipids; yeast

Introduction

Recently, sphingolipids and their precursors have attracted great attention because these compounds have been shown to play roles in cell signalling, heat stress response, calcium homeostasis, and have been implicated in the formation of specialized membrane microdomains. Sphingolipids also function in membrane trafficking, influencing the intracellular targeting of glycosylphosphatidylinositol-anchored proteins and regulating the internalization step of endocytosis (Dickson, 1998; Dickson and Lester, 2002; Merrill, 2002; Futerman and Hannun, 2004). Although our knowledge of sphingolipid metabolism, in particular in yeast, has increased greatly over the past years (Dickson and Lester, 1999, 2002; Funato *et al*, 2002; Figure 1), many important questions remain to be answered concerning the regulation of their synthesis and its response to environmental cues. To address these issues, it is necessary to characterize the sphingolipid biosynthetic machinery as well as the enzymes that modify them.

Among sphingolipid precursors, ceramide is a central molecule. Structurally critical for cell growth, ceramide also mediates different cellular events, such as apoptosis, growth arrest, endocytosis and stress response (Perry and Hannun, 1998; Hannun and Luberto, 2000; Hannun and Obeid, 2002; Acharya *et al*, 2003). Moreover, the balance between sphingoid bases (DHS/PHS/sphingosine), their phosphorylated counterparts and ceramide seems to control cell fate (Merrill, 2002; Spiegel and Milstien, 2002). The term 'sphingolipid rheostat' has been used to describe this critical balance (Cuvillier *et al*, 1996; Mandala *et al*, 1998; Maceyka *et al*, 2002; Kobayashi and Nagiec, 2003). It is vital to our understanding of these signalling events to characterize the enzymes that convert sphingoid bases into ceramide.

Ceramide is synthesized mainly from the reaction of a fatty acyl-CoA with a sphingoid base by an acyl-CoA-dependent ceramide synthase (Morell and Radin, 1970; Akanuma and Kishimoto, 1979). In yeast, C26 fatty acyl-CoA is the major acyl chain donor (Smith and Lester, 1974; Lester and Dickson, 1993; Lester *et al*, 1993; Oh *et al*, 1997), while in animal cells various acyl chain lengths are used (Morell and Radin, 1970). However, the origin of the fatty acyl chain length specificity is unknown. In addition to acyl-CoA-dependent ceramide synthesis, *YPC1* and *YDC1* have been shown to encode for a minor acyl-CoA-independent ceramide synthase activity due to their reverse ceramidase action (Mao *et al*, 2000a, b). CoA-dependent ceramide synthase activity is specifically inhibited by Fumonisin B1. Two genes, *LAG1* and *LAC1*, have been shown to be required for ceramide synthase activity in *Saccharomyces cerevisiae* (Guillas *et al*, 2001; Schorling *et al*, 2001). Lag1p and Lac1p are homologous multispanning transmembrane proteins of the endoplasmic reticulum (ER). Homologs have been found in a wide variety of eukaryotes (Jiang *et al*, 1998; Brandwagt *et al*, 2000). Mutant *lag1*Δ *lac1*Δ cells have reduced sphingolipid levels due to a loss of the Fumonisin B1-sensitive and acyl-CoA-dependent ceramide synthase reaction. This activity was characterized using crude microsomal membranes (Guillas *et al*, 2001; Schorling *et al*, 2001).

Here, we have purified the ceramide synthase and show that it has the same properties as in membranes. These data provide direct and definitive evidence that Lag1p and Lac1p are subunits of the acyl-CoA-dependent ceramide synthase. Moreover, we have identified another essential component of the ceramide synthase, Lip1p, which forms a heteromeric complex with Lac1p and Lag1p. Lip1p is required for ceramide synthesis *in vivo* and *in vitro*. Like Lac1p and Lag1p, it

*Corresponding author. Department of Biochemistry, Sciences II, University of Geneva, 30 quai Ernert Ansermet, 1211 Geneva 4, Switzerland. Tel.: +41 22 379 6469; Fax: +41 22 379 6465; E-mail: howard.riezman@biochem.unige.ch
[1]Present address: CBM, CNRS, Rue Charles Sadron, 45071 Orleans Cedex 2, France

Received: 30 June 2004; accepted: 29 December 2004; published online: 3 February 2005

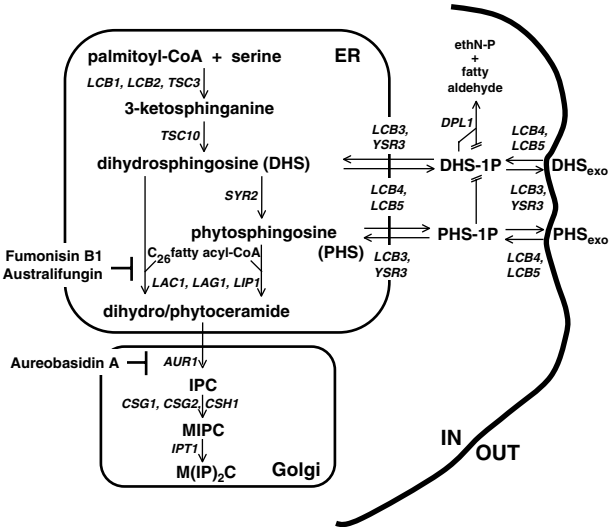

Figure 1 Sphingolipid biosynthetic pathway in yeast. DHS: dihydrosphingosine, PHS: phytosphingosine, IPC: inositolphosphorylceramide, MIPC: mannose inositolphosphorylceramide, $M(IP)_2C$: mannose di(inositolphosphoryl)ceramide, ER, endoplasmic reticulum. Yeast genes required for the individual enzymatic steps are shown.

is localized to the ER. It is also an integral membrane protein, with one transmembrane domain. Its short N-terminal part is cytoplasmic and not required for ceramide synthesis.

Results

Purified Lac1p and Lag1p show ceramide synthase activity

Lac1p and Lag1p are integral membrane proteins with six to eight predicted transmembrane domains. We tagged Lac1p and Lag1p at their N-termini to preserve their ER retention signals. The resulting fusion proteins are functional, because they restored growth and sphingolipid synthesis to the *lac1*Δ*lag1*Δ strain (data not shown). We used different epitope-tagged versions of the proteins: Flag, c-*myc*, double GST-Flag or HA epitopes. We found the same results whichever epitope was used. We show the data obtained with the Flag-tagged proteins, unless specified otherwise.

We assayed different detergents (25 mM CHAPS, 1% decylmaltoside, 1% digitonin, 1% dodecylmaltoside, 1% octylglycoside, 1% Triton X-100) and 2 M urea to assess their solubilization ability towards Lac1p and Lag1p. Decylmaltoside, digitonin, dodecylmaltoside and Triton X-100 showed the best solubilization efficiency (data not shown). Triton X-100 and digitonin were chosen to test ceramide synthase activity of the proteins purified by Flag pulldown of microsomes solubilized with either 1% Triton X-100 or 1% digitonin. Digitonin was the more suitable detergent, because it preserved the ceramide synthase activity of the purified proteins in contrast to Triton X-100 (Figure 2A). Therefore, the enzymatic activity of ceramide synthase was characterized with proteins purified in the presence of digitonin.

Microsomal membranes were solubilized by incubation with the nonionic detergent digitonin. After high-speed centrifugation, the supernatant, corresponding to solubilized membranes, was recovered and incubated with anti-Flag antibody-coupled beads. Proteins bound to the beads were then eluted with a buffer containing the Flag peptide. The immunoisolation step was very effective for purification of ceramide synthase, because it resulted in about a 3500-fold enrichment of the specific activity (Table I). The purification procedure was efficient because we could obtain 68% yield of ceramide synthase activity from the detergent-treated membranes.

Characterization of ceramide synthase activity

A mixture of [4,5-^{3}H]D-erythro-dihydrosphingosine ([^{3}H]DHS)/DHS was dried under a stream of nitrogen and the residue was resuspended in BSA solution to prevent spontaneous reaction of the activated fatty acyl-CoA with DHS. Membrane extracts or eluates containing purified Lag1p and Lac1p were added to this mixture, followed by C26 fatty acyl-CoA to initiate the ceramide synthase reaction.

The time course of ceramide formation by purified Lac1p and Lag1p was virtually linear for the first 30 min, and then reached a plateau (Figure 2B, upper panel). The activity was proportional to the amount of enzyme to at least 50 ng (Figure 2B, lower panel), was acyl-CoA-dependent (Figure 2C, left panel) and showed strong specificity for very-long-chain fatty acyl-CoA with an apparent Km of ~3 μM for C26 FA-CoA, and ~30 μM for C20 FA-CoA (Figure 2C). This is in agreement with previous data showing that the major ceramide species in yeast carries a C26 fatty acid moiety (Smith and Lester, 1974; Lester and Dickson, 1993; Oh *et al*, 1997) and that microsomal fractions had higher activity towards long-chain rather than short-chain acyl-CoA (Guillas *et al*, 2003). Purified ceramide synthase was highly sensitive to Fumonisin B1 ($K_i \approx 400$ μM) and Australifungin ($K_i \approx 15$ μM) (data not shown), potent inhibitors of ceramide synthase activity (Wang *et al*, 1991; Mandala *et al*, 1995; Wu *et al*, 1995).

Characterization of the ceramide synthase complex

Protein patterns of the purified Flag-Lac1p were analyzed by SDS–PAGE. The elution fraction displayed four bands visible by silver staining, two major bands at M_r 48 000 and 28 000, and two minor bands at M_r ~70 000 (A) and M_r ~40 000 (B) (Figure 3A, lane 2, digitonin). Protein patterns of purified Flag-Lag1p were similar (data not shown). Band (A) was nonspecific as it also appeared in isolations performed on cells without Flag-tagged proteins (Figure 3A, lane 1, digitonin and Triton X-100). Band (B) was identified by mass spectrometry as a degradation product of Lac1p. The major band at M_r 48 000 corresponded to Lac1p. The other major band at M_r 28 000 was co-immunoprecipitated specifically with Lac1p upon digitonin solubilization, but not when we used Triton X-100 as a detergent (Figure 3A, lane 2, digitonin and Triton X-100). The loss of this specific partner coincided with the loss of ceramide synthase activity (Figures 2A and 3A). Quantitation of protein bands after silver staining allowed us to detect at least 10 ng of a standard protein, BSA. No other bands than the ones seen in the ceramide synthase preparation (Figure 3A) could be detected while visualizing as much as 170 ng of Lac1p and 200 ng of Lip1p, suggesting that, apart from the shown contaminant (Band A), the enzyme is greater than 95% pure. To ascertain whether proteins escaped detection by silver staining, we used Sypro

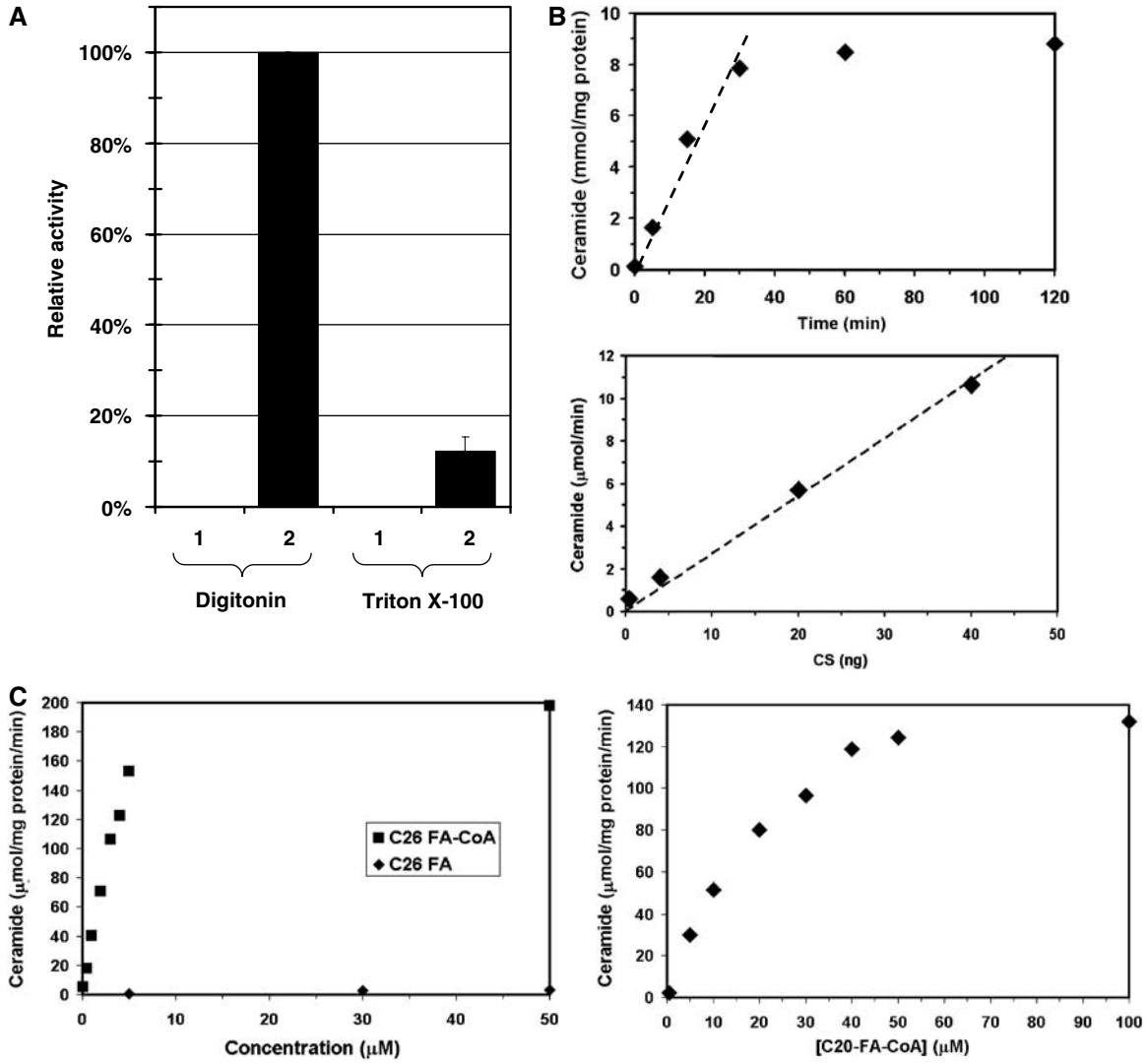

Figure 2 Enzymatic characterization of purified ceramide synthase. Microsomal membranes were solubilized with either digitonin or Triton X-100, and Flag-Lac1p-containing protein complexes were purified by immunoisolation and eluted from the beads. Ceramide synthase activity was measured. (**A**) Lanes 1, 2: membranes were solubilized with 1% digitonin, lanes 3, 4: membranes were solubilized with 1% Triton X-100. Lane (1) corresponds to experiments with strain RH 5665 and lane (2) to strain RH 5666. (**B**) Time course (upper panel) and protein concentration dependence (lower panel) of ceramide synthase activity. (**C**) Fatty acyl-CoA concentration and CoA dependence of ceramide synthase activity. C26 fatty acid substrates are shown in the left panel and C20 fatty acyl-CoA in the right panel.

Table I Purification of the ceramide synthase

Fraction	Protein	Ceramide synthase activity	Yield	Enrichment
	mg/ml	nmol/mg of protein/min	Percentage	Fold
Digitonin-treated membranes[a]	5.6	6.1	100	1
Solubilized membranes[b]	4.6	6.0	80	0.98
Elution of anti-Flag M2 affinity beads	5.4×10^{-3}[c]	20 678	68	3420

Ceramide synthase was purified from membranes as described in Materials and methods. Data are the average of five sets of experiments. Each time similar results were found.
[a]Membranes resuspended in the presence of 1% digitonin prior to incubation.
[b]Supernatant after centrifugation (100 000 *g* for 1 h) of the digitonin-treated membranes.
[c]Protein concentrations were estimated by densitometric comparison of silver-stained proteins of the fraction with stained calibration bands of bovine serum albumin of known concentrations in SDS–PAGE.

Ruby as an alternative, as well as purification from ^{35}S-labelled cells, visualizing the radioactivity by a phosphorimager. No other bands than the ones observed by silver staining appeared (data not shown).

The new partner (M_r 28 000) was termed Lip1p, standing for Lag1p/Lac1p interacting protein. Lip1p was identified by mass spectrometry as Ymr298wp. The function of this protein had not previously been identified, although its interaction

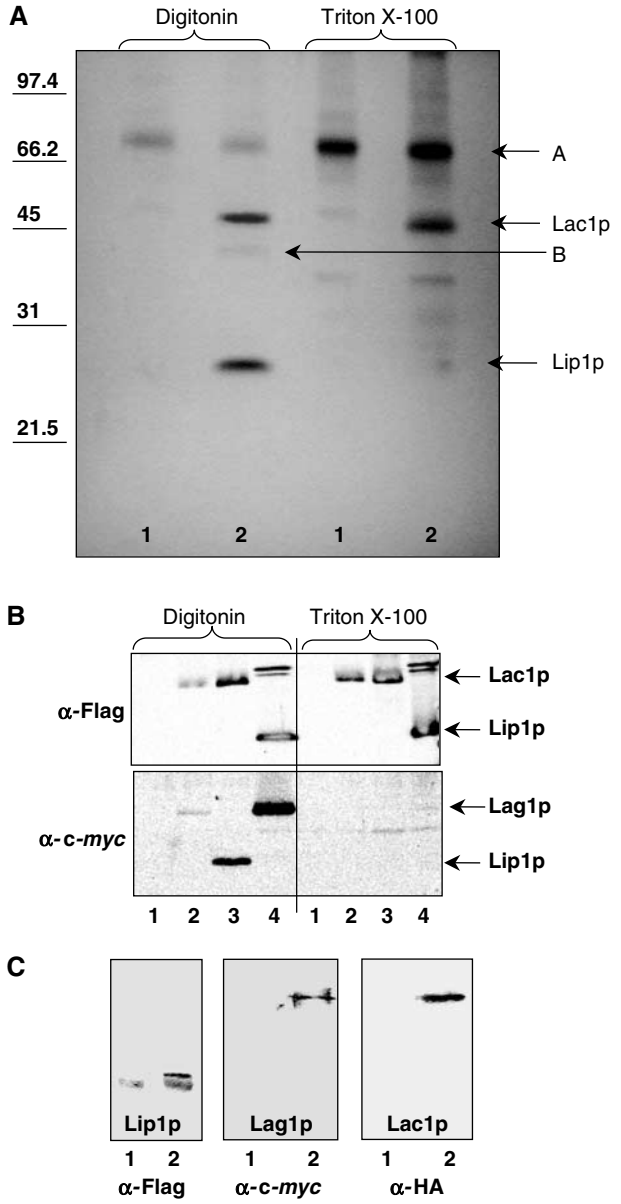

Figure 3 Ceramide synthase complex. (**A**) Eluates after immunoisolation from a strain RH5665 (1) or RH5668 (2) were separated by SDS–PAGE. Membranes were solubilized with 1% digitonin (first two lanes) or with 1% Triton X-100 (last two lanes). (**B**) Strains co-expressing Flag-tagged and c-*myc* tagged proteins. Immunoprecipitation against the Flag-tagged protein was performed and the eluate was submitted to Western blotting against Flag epitope (upper panel) and against c-*myc* epitope (lower panel). (1) Assay performed with strain RH5665, (2) strain RH5666, (3) strain RH6047, (4) strain RH6067. Membranes were solubilized with 1% digitonin (first four lanes) or with 1% Triton X-100 (last four lanes). (**C**) Flag immunoprecipitation of digitonin-solubilized membranes of a strain expressing HA-Lac1p, c-*myc*-Lag1p and Flag-Lip1p (RH6344, lane 2) was performed. Western blotting against Flag, c-*myc* and HA epitopes. Lane (1) corresponds to the control experiment, performed with strain RH6345.

with Lac1p and Lag1p had already been suggested from systematic two-hybrid studies (Ito *et al*, 2001). The predicted molecular mass of Lip1p is 17 kDa, but its sequence contains many prolines, and the protein has a predicted acidic pI, which could explain the higher apparent molecular mass (~28 kDa). Furthermore, it is possible that Lip1p is modified by O-linked glycosylation, but this has not been tested. One transmembrane domain is predicted near to the amino-terminal end of the protein by different programs (HMMTOP, SOSUI, TMHMM, TMpred and TopPred2). No strong homologs in animals or plants were found using sequence alignments (Clustal W protein alignment), but were found in other fungi (Figure 4).

In order to provide additional evidence for Lac1p/Lag1p/Lip1p interaction, we used the pESC plasmid co-expressing two proteins, one Flag tagged and the other c-*myc* tagged, and carried out co-immunoprecipitation experiments. Immunoprecipitations were performed against the Flag-tagged versions of the different proteins, and beads were eluted with Flag peptide. Immunoprecipitation efficiency was checked by Western blotting of the eluates against Flag epitope (Figure 3B, upper panel). Eluates were then tested for c-*myc*-tagged partners by Western blotting (Figure 3B, lower panel). We could confirm that Lag1p interacts with Lac1p and Lip1p, that Lac1p interacts with Lag1p and Lip1, that Lip1p interacts with Lac1p and Lag1p (Figure 3B), and that Lip1p interacts with itself (data not shown) when membranes were solubilized by digitonin. These interactions were lost if membranes were solubilized by Triton X-100 (Figure 3B). Using a similar approach, we confirmed the interaction between the three partners, Lac1p, Lag1p and Lip1p, by Flag immunoprecipitation, and anti-c-*myc* and anti-HA Western blotting in a strain expressing Flag-Lip1p, c-*myc*-Lag1p and HA-Lac1p (Figure 3C).

Next, we determined the apparent molecular mass of ceramide synthase in a strain expressing Flag-Lac1p and Lip1p, but not Lag1p, by glycerol gradient centrifugation. Eluates from a Flag pulldown were separated by centrifugation on glycerol gradients containing 1% digitonin, fractions were collected and analyzed by Western blotting. Flag-Lac1p was found in fractions 4–8, peaking in fraction 6 (Figure 5A). We analyzed the fractions by silver staining (Figure 5B). The protein pattern was similar to the one observed in Figure 3A (lane 2 digitonin). The nonspecific band (A) did not cofractionate exactly with the ceramide synthase, whereas band (B) (degradation product of Lac1p) and Lip1p exhibited the same distribution as Lac1p. The glycerol gradient fractions were also tested for ceramide synthase activity, which cofractionated with the Lac1p peak (data not shown). Similar results were obtained with strains expressing Lag1p and Lac1p, or either of the two individually always giving a complex of apparent mass of approximately 250–260 kDa. The complex is large enough to accommodate two of the homologous large subunits and two Lip1p included in a digitonin micelle of 73–86 kDa (aggregation number 60–70, Calbiochem catalog).

Lip1p is an integral membrane protein, localized to the ER

Analysis of the sequence of Lip1p predicted one transmembrane domain (Figure 4). To investigate the nature of its membrane association, we treated cell lysates with different reagents able to extract proteins from the membranes, and then centrifuged the samples at 100 000 *g* for 1 h. The presence of proteins in the supernatant (S) and pellet (P) was determined by Western blotting. The Lip1p pattern was similar to the one of Lac1p, and Wbp1p (an integral ER protein taken as a control) (Figure 6A). Lip1p was found in

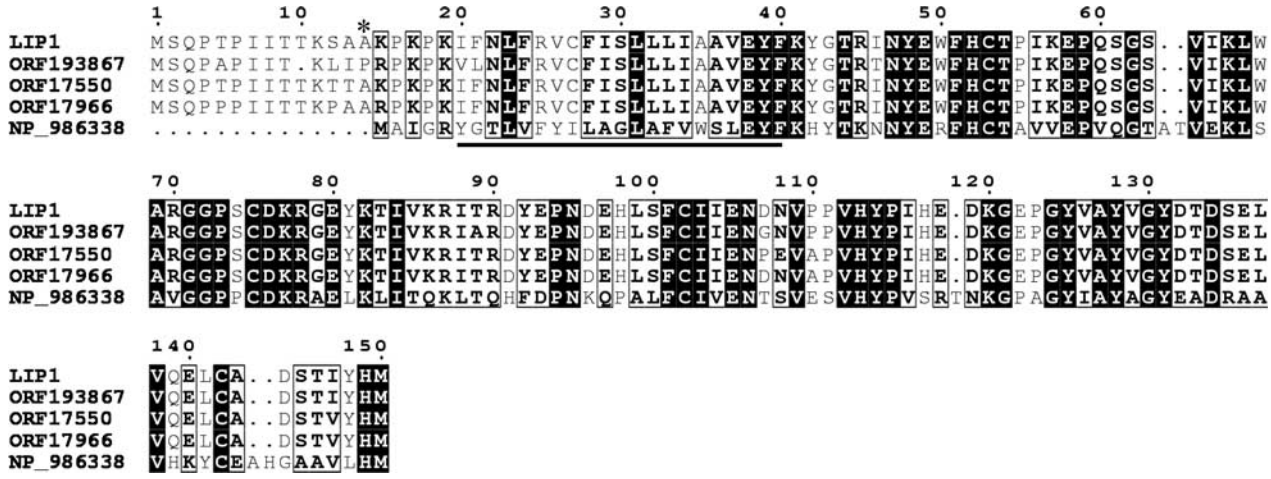

Figure 4 Multiple alignment of *LIP1* with fungal homologs. The alignment includes the deduced protein sequence of *S. cerevisiae LIP1* (*YMR298w*), *S. bayanus* predicated ORF19386, *S. mikatae* predicated ORF17550, *S. paradoxus* predicated ORF17966 and *Asbia gossypii* predicated NP_986338. The alignment was generated using the T-coffee (Notredame *et al*, 2000) and ESPript (Gouet *et al*, 1999) programs. Black boxes indicate identical residues, black borders show similar amino acids. The predicted transmembrane domain is underlined. The beginning of the truncated Lip1p (ΔNT-Lip1p) is labelled by a star.

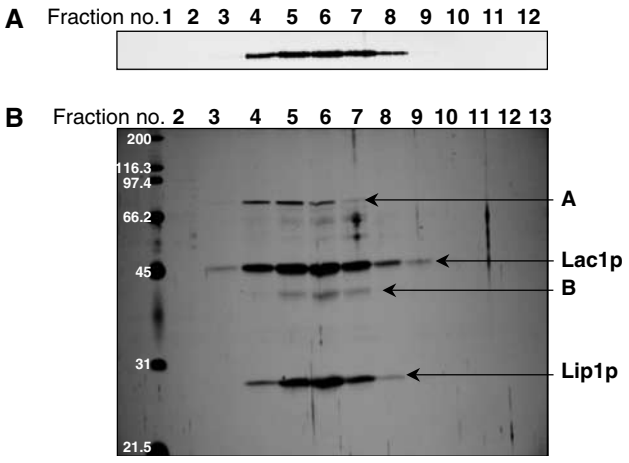

Figure 5 Glycerol gradient centrifugation of the ceramide synthase complex. Eluate from Flag immunoisolation of digitonin-solubilized membranes of the strain RH5668 was separated by glycerol gradient centrifugation and fractions were collected from the top of the tube. (**A**) Western blotting against the Flag tag of Lac1p. (**B**) Silver staining.

the membrane pellet (Figure 6A, last two columns). When the lysates were treated with either 1% Triton X-100 or 1% SDS, Lip1p was partially released into the soluble fraction. When lysates were treated with either 1 M NaCl or 0.1 M Na_2CO_3 (pH 11.5), Lip1p remained in the pellet fraction. These results show that Lip1p, like Lac1p, behaves like an integral membrane protein.

Lac1p and Lag1p and ceramide synthase activity have been shown to be localized to the ER (Barz and Walter, 1999; Funato and Riezman, 2001). We verified that Lip1p is also localized to the ER by subcellular fractionation using sucrose gradient centrifugation followed by Western blotting. Lip1p and Lac1p both appeared in fractions 7–9, which were enriched in the ER marker Wbp1p, whereas Emp47p, a Golgi marker, was present in fractions 3–6 (Figure 6B). We further verified the ER localization of the different proteins by indirect immunofluorescence microscopy against their Flag tag. Flag-Lip1p colocalized with Kar2p, an ER marker (Figure 6C, upper panel). Flag-Lip1p and Flag-Lac1p had a characteristic ER staining, that is, a ring around the nucleus. However, when compared to the Kar2p pattern, the staining was more perinuclear and less in the peripheral ER. Such a perinuclear staining was also observed for Lcb1p, a protein involved in the first step of sphingolipid metabolism (Yasuda *et al*, 2003). Some dots were also present in the cytoplasm, but they were not experimentally significant as they could also be found in the cells carrying an empty plasmid and visualized under the same conditions (Figure 6C, lower panel). Lip1p staining in the perinuclear ER seemed to be concentrated in specific areas of the nuclear envelope/ER that are not enriched for Kar2p, but this could be an effect of its overproduction. Additional evidence will be required to determine if the ceramide synthase is found in specialized ER microdomains.

Lip1p is required for ceramide synthase activity

Our experiments described above suggest that Lip1p is required for ceramide synthase activity because its loss from the complex coincides with a loss of activity (Figures 2A and 3). To definitively address if Lip1p is essential for the ceramide synthase activity, we created *lip1*Δ mutant cells. In a systematic high-throughput study, deletion of *LIP1* was found to be lethal (Winzeler *et al*, 1999; Uetz *et al*, 2000). However, as the *lag1*Δ*lac1*Δ double mutant grows extremely slowly, we suspected that the same could be true for *lip1*Δ mutant, and that this slow growth had been missed. We disrupted one of the alleles of *LIP1* gene in a diploid strain, sporulated the heterozygous diploids and dissected tetrads. After short growth periods of 2–3 days, there was a 2/0 segregation pattern, indicating that the two *lip1*Δ strains were either inviable or grew very slowly (Figure 7A, left panel). However, after more than 1 week, we obtained *lip1*Δ mutant colonies (Figure 7A, middle panel) whose growth was very

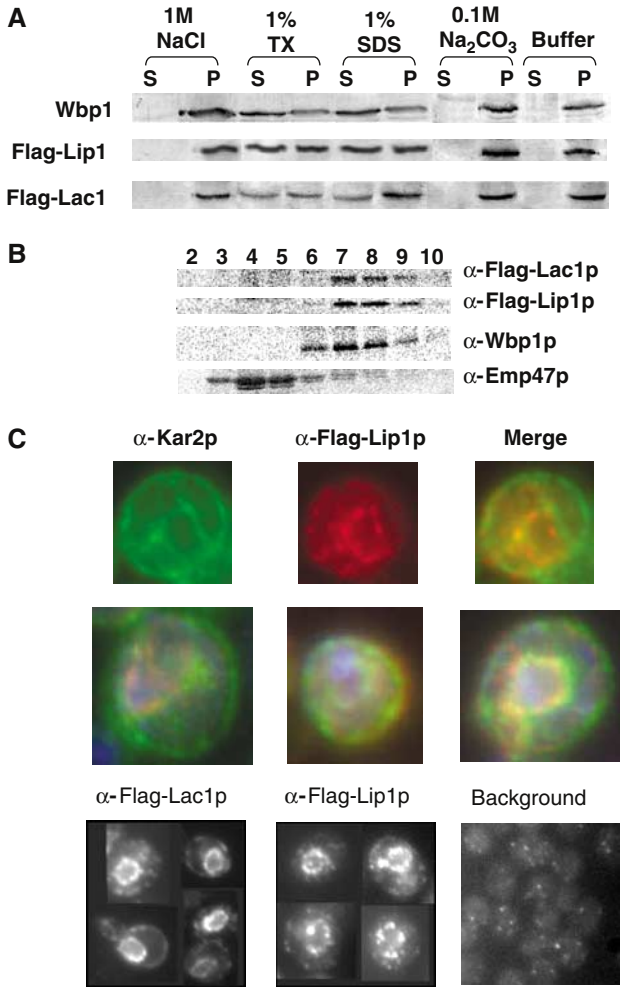

Figure 6 Lip1p is an integral ER membrane protein. The strains used were RH 5666 and RH 6068. (**A**) Cell lysates were treated with different chemical reagents as indicated, centrifuged, and pellet (P) and soluble (S) fractions were analyzed by Western blotting. (**B**) Cell homogenates were separated on sucrose density gradients. Fractions were collected from the top of the tube and analyzed by Western blotting. Wbp1p is a marker of the ER, Emp47p of the Golgi apparatus. (**C**) Colocalization of Kar2p and Lip1p by indirect immunofluorescence (upper panels), additional merged images with DAPI (middle panels). Immunofluorescence of Flag-Lac1p and Flag-Lip1p (lower panels).

slow even after colonies were restreaked onto rich medium plate (Figure 7A, right panel).

Previously, we developed a quick and easy test to assess if a strain is likely to be deficient in ceramide synthesis (Schorling *et al*, 2001). Cells are streaked on a plate containing aureobasidin A, an inhibitor of inositolphosphorylceramide (IPC) synthesis, known to be highly toxic (Endo *et al*, 1997; Nagiec *et al*, 1997). If cells are deficient in ceramide synthesis, they are resistant to aureobasidin A, as they cannot accumulate ceramide. Wild-type (WT) cells were sensitive to aureobasidin A, but *lip1*Δ strains grew on plates containing aureobasidin A, as did the double *lac1*Δ*lag1*Δ mutant, suggesting strongly that Lip1p is involved in ceramide synthesis (Figure 7B).

Next, we measured ceramide synthase activity by performing *in vivo* labellings on the *lip1*Δ strain. Strains were labelled with [^{3}H]-*myo* inositol and their lipids were analyzed by TLC. A *lip1*Δ strain had a pattern similar to the one of *lac1*Δ*lag1*Δ strain (Figure 8A). The complex sphingolipids were absent (see quantification; Figure 8A, lower panel) and lyso-PI accumulated. Moreover, an extra product (*) was observed as for *lac1*Δ*lag1*Δ strain. This spot has been found and identified in extracts from the *lac1*Δ*lag1*Δ strain as a PI with a very-long-chain fatty acid (Guillas *et al*, 2001). We also labelled cells with [^{3}H]DHS and analyzed ceramide production by TLC. Mutant *lip1*Δ cells were defective in synthesis of ceramide from DHS (Figure 8B). These results show that *LIP1* is required for ceramide synthesis *in vivo*. However, *in vivo* labellings would still be consistent with an indirect role of Lip1p in ceramide synthesis, including preparation or delivery of one of the substrates to the enzyme or biogenesis of the complex. To address this point, we assayed ceramide synthesis using Flag–Lac1p complexes purified from a *lip1*Δ strain. Complexes isolated from this strain were not able to synthesize ceramide (Figure 8C), even though Lac1p and Lag1p were expressed, could interact together and were purified by immunoisolation (data not shown).

The N-terminal part of Lip1p is cytoplasmic and not required for sphingolipid synthesis

Lip1p is an integral membrane protein (Figure 6A) predicted to have one transmembrane domain close to its N-terminus. Due to the distribution of negative and positive charges surrounding the transmembrane domain (Goder *et al*, 2004), we predicted that the N-terminus would be cytoplasmic (Figure 4). To assess Lip1p topology, we performed a protease protection assay. Lip1p as well as Lac1p were tagged with a Flag epitope at their N-terminus, and Lip1p was also tagged with a Flag epitope at its C-terminus. Microsomal membranes were incubated with or without Triton X-100 in the presence or absence of proteinase K. Kar2p, an ER lumenal protein, was used to check the integrity of the ER membrane. In the absence of Triton X-100, the N-termini of Lip1p and Lac1p were sensitive to proteinase K, whereas the C-terminus of Lip1p was preserved (Figure 9A). Kar2p was unaffected, showing that the ER had remained intact. In the presence of Triton X-100, both Lip1p-Flag and Kar2p were degraded (Figure 9A). These results show that the N-terminus of Lip1p is cytoplasmic and its C-terminus is lumenal.

Next, we deleted the first 14 amino acids of Lip1p, comprising most of its cytoplasmic domain. A few charged amino acids were kept prior to the transmembrane domain to preserve its integration into the membrane (Figure 4). The localization of the truncated protein by indirect immunofluoresence microscopy was the same as the tagged WT protein (Figure 9B), showing that the N-terminal part of Lip1p is not required for its correct localization. Next, we checked sphingolipid composition of the Lip1p-ΔNT strain by [^{3}H]DHS labelling *in vivo*. The lipid pattern was very similar to that of a WT strain (Figure 9C). Therefore, the cytoplasmic N-terminal part of Lip1p is not necessary for ceramide synthesis. These results suggest that the functional domain of Lip1p is most likely located in the lumen of the ER or in its transmembrane domain.

Discussion

In recent years, sphingolipids have attracted the attention of many researchers and striking advances in the field have

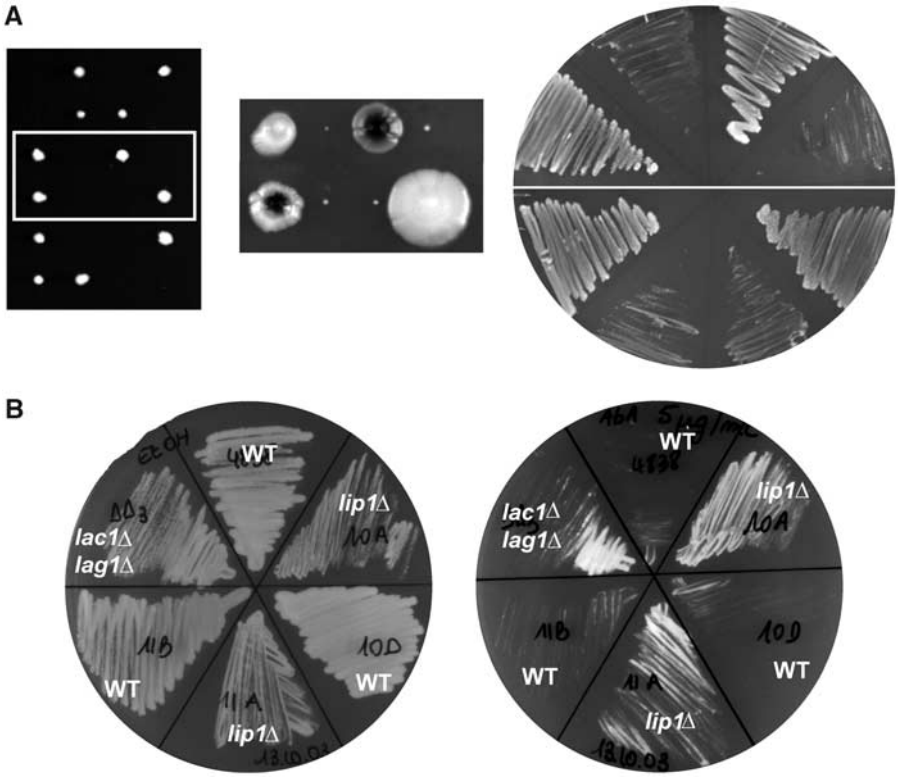

Figure 7 Growth of the *lip1*Δ strain. (**A**) Tetrads were dissected from a heterozygous *lip1*Δ diploid. Left panel: tetrads after 3 days. Middle panel: two tetrads after 10 days. Right panel: growth on rich medium after re-streaking these two tetrads. (**B**) Aureobasidin A (final concentration ≈5 μg/ml, right) or ethanol (left) was spread onto YPD agar plates. These strains were streaked on the plates and incubated at 24°C. RH4838, RH5308, RH6013, RH6016, RH5994, RH5995.

been made. While most of the enzymes involved in this biosynthetic pathway have been identified genetically, only serine palmitoyltransferase from Chinese hamster ovary cells and from *Sphingomonas paucimobilis* (Hanada *et al*, 2000; Ikushiro *et al*, 2004) and yeast 3-ketosphinganine reductase expressed in *Escherichia coli* (Beeler *et al*, 1998) have been purified. All the other enzymes of this pathway, in particular the integral membrane enzymes, have not yet been purified and fully characterized, most likely due to technical difficulties. As most of the molecules of this pathway are not only biosynthetic intermediates, but also signalling molecules, characterization of these enzymes is crucial for our understanding of cell physiology.

Using tagged versions of Lac1p and Lag1p, we purified an active ceramide synthase complex to near homogeneity with more than a 3400-fold increase in specific activity starting from a detergent-treated microsomal fraction (Table I). The fold purification from whole cells is much greater, but very difficult to determine exactly, because of the difficulty in measuring the enzyme activity quantitatively in crude extracts. The activity of the purified ceramide synthase was similar to the ceramide synthesis activity detected in intact cells or isolated microsomal membranes (Morell and Radin, 1970; Akanuma and Kishimoto, 1979; Wu *et al*, 1995; Guillas *et al*, 2003; Kobayashi and Nagiec, 2003). Purified yeast ceramide synthase activity was CoA dependent, preferred very-long-chain fatty acyl-CoA, which is consistent with the acyl-CoA specificity of the activity characterized in cells or membranes (Guillas *et al*, 2003; Kobayashi and Nagiec, 2003) and shows that this specificity does not depend upon the membrane environment. This is consistent with the fact the human homologs of Lag1p expressed in yeast show ceramide synthase activity with slightly different preferences for fatty acid length (Guillas *et al*, 2003).

After SDS–PAGE and silver-staining analysis, the active purified ceramide synthase containing Lac1p and Lag1p displayed an additional protein, Lip1p, which was shown to be essential for ceramide synthase activity *in vivo* and *in vitro* (Figures 2A, 3A, and 8). Lip1p can be found in complexes with both Lac1p and Lag1p, and with itself (Figure 3B and C). These results show that the ceramide synthase consists of Lac1p, and/or Lag1p, and Lip1p. Lip1p, corresponds to Ymr298wp, a protein of previously unknown function. *LIP1* has numerous homologs among fungi, but no obvious homologs were found in mammals (Figure 4). However, as the open reading frame is quite short (450 bp), it may not have been properly annotated, in particular if a mammalian ortholog contains several introns. Since human homologs of *LAC1* and *LAG1* have been recently isolated and can complement the *lac1* and *lag1* mutations (Venkataraman *et al*, 2002; Guillas *et al*, 2003; Riebeling *et al*, 2003), it would be surprising if no functional homologs of Lip1p were found.

To definitively determine if Lip1p is required for ceramide synthase activity, we created a deletion mutant. The *lip1*Δ strain behaved almost identically to the *lag1*Δ*lac1*Δ deletion strain. Lip1p is necessary for ceramide synthase activity, but its precise role is not known. Several hypotheses can be raised: Lip1p could be necessary for stability of the ceramide

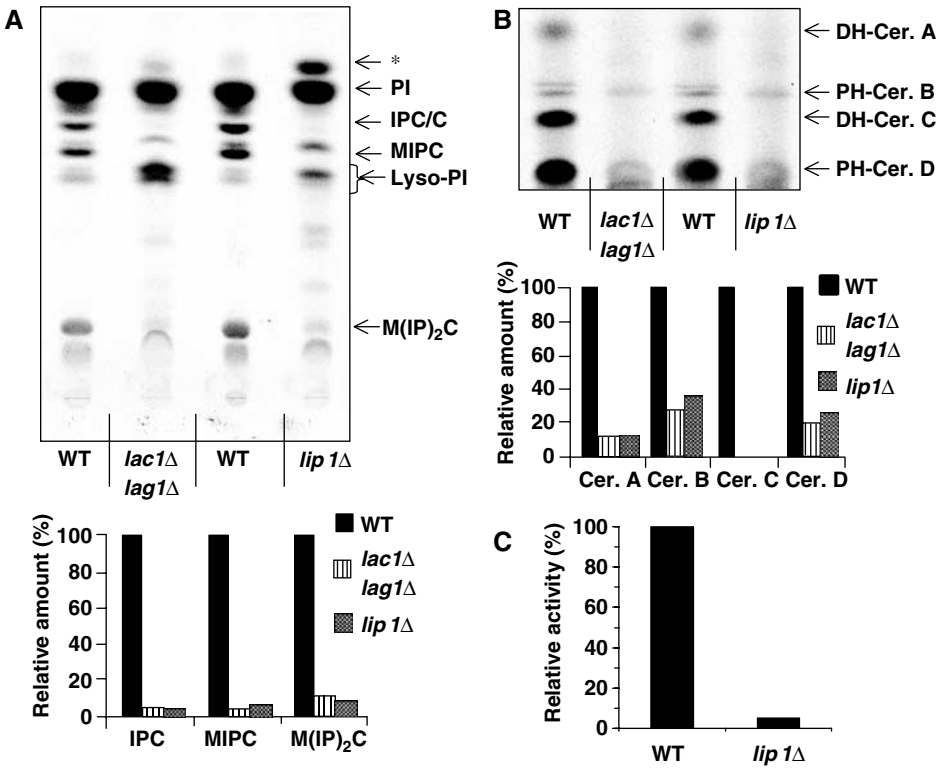

Figure 8 Labellings of *Lip1*Δ mutant. (**A**) Cells (strains RH4838, RH5308 and RH 6013) were labelled with [^{3}H]*myo* inositol, lipids were analyzed on TLC and detected using a phosphorimager. Radioactivity in sphingolipids was quantified, and the relative amount of each species was determined as a percentage of the amount in WT cells. PI, phosphatidylinositol; IPC/C: inositolphosphorylceramide C; MIPC: mannose inositolphosphorylceramide; M(IP)$_2$C: mannose di(inositolphosphoryl)ceramide; * indicates a spot that migrates identically to that previously identified as a C26 fatty acid containing PI. (**B**) The same cells were labelled with [^{3}H]DHS and lipids were analyzed as above. Radioactivity in sphingolipids was quantified as in (A). (**C**) Ceramide synthesis activity of eluates from a Flag immunoisolation of digitonin-solubilized membranes from strains RH5666 and RH6075.

synthase or for an upstream step in ceramide synthesis. These are both unlikely because Lac1p and Lag1p were copurified from a strain lacking Lip1p (data not shown), but the complex was inactive (Figure 8). Lip1p could be a regulatory subunit of the ceramide synthase complex or be required for the enzymatic activity of the ceramide synthase complex. If the latter were the case, this would suggest that the ceramide synthase reaction requires a component in the ER lumen or within the membrane.

To get the first idea about the subunit stoichiometry of purified ceramide synthase complex, we estimated its molecular mass by glycerol gradient centrifugation. The ceramide synthase complex that we have purified could be mixtures of Lag1p–Lac1p heteromers with at least two Lip1p or Lag1p or Lac1p homodimers with at least two Lip1p. The different complexes could have different enzymatic characteristics, such as slightly different specificities for chain length or hydroxylation rate of the fatty acyl-CoAs or for the sphingoid bases (C16 versus C18). It has been suggested that *LAG1* proteins function in substrate recognition (Guillas *et al*, 2003) and several mammalian homologs of Lag1p exist, making them ideal candidates to explain the wide variety of fatty acid chains that are incorporated into ceramide in animal cells.

Like Lac1p and Lag1p, Lip1p is localized to the ER where the synthesis of ceramide occurs (Funato and Riezman, 2001). Ceramide synthase has been proposed to have its active site on the cytoplasmic surface of the ER membrane (Hirschberg *et al*, 1993) because its activity is protease sensitive in isolated microsomal membranes. Now that we have shown that Lag1p, Lac1p and Lip1p comprise the ceramide synthase, these results must be reinterpreted. Lag1p and Lac1p span the ER membrane multiple times and their susceptibility to protease digestion cannot be taken as an indication of the topology of the active site. To synthesize ceramide from exogenous sphingoid bases, these have to be phosphorylated by Lcb4p and dephosphorylated by Lcb3p, sphingoid base kinase and phosphatase, respectively (Funato *et al*, 2003). Lcb4p is a peripheral membrane protein mainly found on the ER membrane (Funato *et al*, 2003) and Lcb3p is an integral ER membrane protein (Mao *et al*, 1999) whose active site has been shown to be in the lumen of the ER (Kihara *et al*, 2003). Therefore, after the phosphorylation/dephosphorylation cycle, the sphingoid bases should be found in the lumen of the ER. On the other hand, the 3-ketosphinganine reductase that generates dihydroshingosine seems to have its active site localized to the cytoplasmic face of the ER (Kihara and Igarashi, 2004), suggesting that one of the substrates, dihydrosphingosine, can be made available from either side of the ER membrane. Lip1p is an integral membrane protein with one predicted transmembrane domain. We found that its short, highly charged N-terminus is cytoplasmic and dispensible for ceramide synthase activity. These data suggest that the functional region of Lip1p is localized in the lumen of the ER, or in its transmembrane domain. Lac1p and Lag1p initially attracted interest because of significant sequence similarity

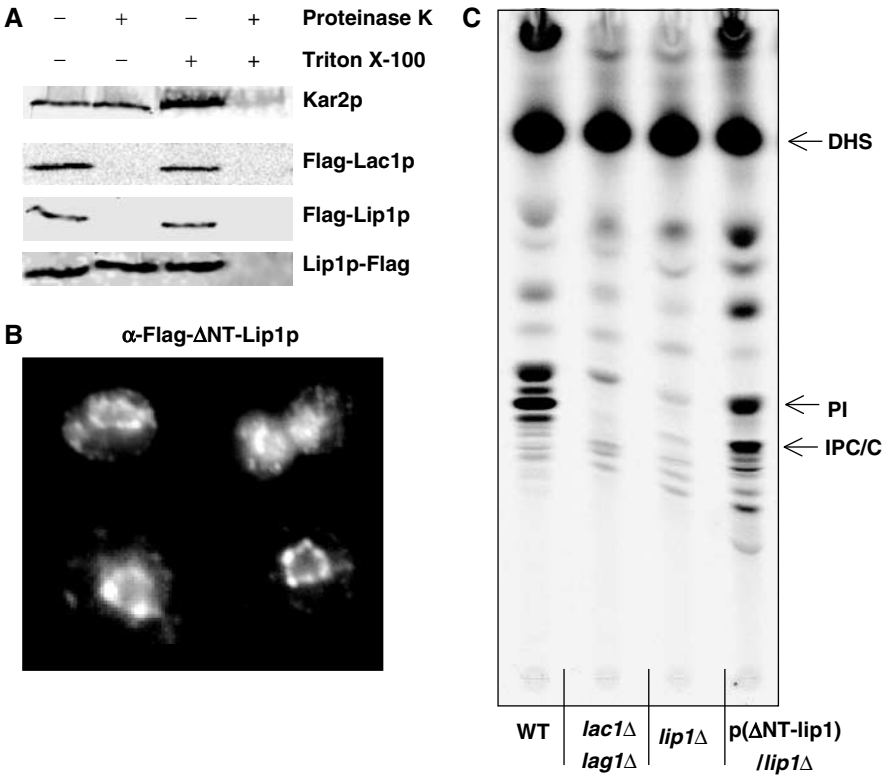

Figure 9 Lip1p topology. (**A**) Microsomal membranes from strains RH6068, RH5666 or RH6348 were incubated with or without Triton X-100 in the presence or absence of Proteinase K. The samples were analyzed by Western blotting to reveal the Flag tag and Kar2p. (**B**) Flag-Lip1p-ΔNT (RH6069) was visualized by indirect immunofluorescence. (**C**) Cells (strains RH4838, RH5309, RH6013 and RH6069) were labelled with [^{3}H]DHS and analyzed as in Figure 8.

Table II Plasmids used in this study

Plasmid number	Plasmids	Inserts	Source
372	pEG(KT)	None	Deschenes
1118	pESC-URA3	None	Dieter Oesterhelt
1119	pSTS30a	*LAG1* (N-term. c-*myc* tagged)	Dieter Oesterhelt
1120	pSTS30	*LAG1* and *LAC1* (N-term. c-*myc* and Flag tagged, resp.)	Dieter Oesterhelt
1121	pSTS30b	*LAC1* (N-term. Flag tagged)	Dieter Oesterhelt
1285	pWB94	*LAC1* (N-term. HA tagged)	This study
1479	pEG(KT)-(GST-Flag-Lac1p)	*LAC1* (N-term. GST and Flag tagged)	Barz and Walter (1999)
1548	pSTS30c	*LAG1* (N-term. Flag tagged)	This study
1551	pESC(Flag-Lip1p)	*LIP1* (N-term. Flag tagged)	This study
1552	pESC(Flag-ΔNT-Lip1p)	*LIP1* (N-term. Flag tagged) without the first 14 amino acids	This study
1559	pESC(c-*myc*Lag1p/Flag-Lip1p)	*LAG1* and *LIP1* (N-term. c-*myc* and Flag tagged, resp.)	This study
1560	pESC(c-*myc*Lip1p/Flag-Lac1p)	*LIP1* and *LAC1* (N-term. c-*myc* and Flag tagged, resp.)	This study
1700	pESC(Lip1p-Flag)	*LIP1* (C-term. Flag tagged)	This study
1701	pESC(c-*myc*Lip1p/Flag-Lip1p)	*LIP1* and *LIP1* (N-term. c-*myc* and Flag tagged)	This study

with TRAM (translocating chain associating membrane protein), a mammalian protein thought to be involved in protein translocation across the ER membrane (Barz and Walter, 1999). Even if they do not share functional homologies, these proteins could share common structural features. Based on TRAM characteristics, we speculate that ceramide synthase complex would form a 'channel' across the ER membrane and this may permit the enzyme active site to accept dihydrosphingosine from either side of the membrane. Predictions (Jazwinski and Conzelmann, 2002) and our preliminary evidence (N Yahara and H Riezman) suggest that the conserved Lag domain, presumably containing the active site, is indeed mostly embedded in the membrane. Given the multiple spanning membrane structure of ceramide synthase, only a high-resolution structure is likely to resolve these important topology questions.

Materials and methods

Yeast strains, media and reagents

The strains and plasmids used in this study are listed in Tables II and III. To construct deletion strains, entire open reading frames were deleted and replaced with the designated genes. Deletions were confirmed by PCR.

Yeast strains were grown in rich medium (20 g/l glucose, 20 g/l peptone and 10 g/l yeast extract with adenine, uracil and tryptophan at 40 mg/l) at 24°C.

Table III Strains used in this study

Strain	Genotype	Source
RH4838	Mat a his3 leu2 ura3 trp1 bar1 *AUR1*::3HA::*HIS3*	Lab strain
RH5308	Mat a his3 leu2 ura3 trp1 bar1 *AUR1*::3HA::*HIS3* lac1::*LEU2* lag1::*TRP1*	Schorling *et al* (2001)
RH5660	Strain RH5308 transformed with the plasmid no. 1285 (HA-*LAC1*)	This study
RH5664	Strain RH5308 transformed with the plasmid no. 1479 (GST-Flag-*LAC1*)	This study
RH5665	Strain RH4838 transformed with the plasmid no. 1118 (Vector control)	This study
RH5666	Strain RH5308 transformed with the plasmid no. 1120 (c-*myc-LAG1*, Flag-*LAC1*)	This study
RH5668	Strain RH5308 transformed with the plasmid no. 1121 (Flag-*LAC1*)	This study
RH5994	Mat alpha leu2 ura3 trp1 bar1 *lip1*::*HIS3*	This study
RH5995	Mat a leu2 ura3 trp1 his3 lys2 ade2 bar1	This study
RH6013	Mat alpha leu2 ura3 trp1 bar1 *lip1*::*HIS3*	This study
RH6016	Mat alpha leu2 ura3 trp1 his3 lys2 bar1	This study
RH6044	Strain RH5308 transformed with the plasmid no. 1548 (Flag-*LAG1*)	This study
RH6046	Strain RH5308 transformed with the plasmid no. 1559 (c-*myc-LAG1*, Flag-*LIP1*)	This study
RH6047	Strain RH5308 transformed with the plasmid no. 1560 (c-*myc-LIP1*, Flag-*LAC1*)	This study
RH6067	Strain RH6013 transformed with the plasmid no. 1559 (c-*myc-LAG1*, Flag-*LIP1*)	This study
RH6068	Strain RH6013 transformed with the plasmid no. 1551 (Flag-*LIP1*)	This study
RH6069	Strain RH6013 transformed with the plasmid no. 1552 (Flag-*LIP1*-Δ*NT*)	This study
RH6075	Strain RH6013 transformed with the plasmid no. 1120 (c-*myc-LAG1*, Flag-*LAC1*)	This study
RH6344	Strain RH2881 transformed with the plasmids no. 1285 and no. 1559 (HA-*LAC1*, c-*myc-LAG1*, Flag-*LIP1*)	This study
RH6345	Strain RH2881 transformed with the plasmids no. 1285 and no. 1118 (HA-*LAC1*, vector control)	This study
RH6348	Strain RH 6013 transformed with the plasmid no. 1700 (*LIP1*-Flag)	This study
RH6349	Strain RH 6013 transformed with the plasmid no. 1701 (c-*myc-LIP1*, Flag-*LIP1*)	This study

Protein concentration was determined using the detergent compatible Bio-Rad protein assay kit. [^{3}H]DHS was from Anawa Trading SA or American Radiolabeled Chemical Inc. (ARC, St Louis, MO). DHS, Fumonisin B1, C20:0 fatty acyl-CoA, C26:0 fatty acid, Flag beads, Flag antibody and Flag peptide were from Sigma. HA rat antibody was purchased from Roche. Digitonin was from Acros, and high-purity digitonin from Calbiochem. Australifungin was a gift from Merck.

Purification of Lac1p, Lag1p and Lip1p

Cells were grown in rich medium, washed twice and resuspended at 200 OD/ml in TNE buffer (50 mM Tris–HCl, pH 7.5, 150 mM NaCl, 5 mM EDTA, 1 mM PMSF, 1 μg/ml protease inhibitor mixture). Cells were disrupted with glass beads, and the cell debris and glass beads were removed by centrifugation at 1000 *g* for 10 min at 4°C. The supernatant was then centrifuged at 100 000 *g* for 1 h at 4°C. The pellet corresponding to microsomal membranes was resuspended in TNE, the appropriate volume of a 10 × stock solution of detergent (Triton X-100 or digitonin (Acros)) was then added to a final concentration of detergent of 1%. Microsomal membranes were solubilized for 1 h at 4°C with a rotating movement. The unsolubilized membranes were removed by centrifugation at 100 000 *g* for 1 h at 4°C. Immunoprecipitation using the HA epitope was performed using rat antibody and protein G beads for 2–4 h at 4°C with a rocking movement. The immunoprecipitated beads were then washed three times with TNE/1% digitonin or Triton X-100, and eluted with sample buffer. Immunoprecipitation using the Flag epitope was performed using Flag beads at 4°C for 2–4 h with rocking. The immunoprecipitated beads were then washed three times with TNE/1% digitonin or Triton X-100, and eluted with a 2 mg/ml solution of Flag peptide in TNE/1% digitonin or Triton X-100 on ice for 20–30 min. In the case of double-tagged protein (GST-Flag), the eluate from the Flag beads was further incubated with glutathione beads at 4°C for 3–5 h with rocking. The beads were washed three times with TNE/1% digitonin or Triton X-100, and eluted with a solution of 20 mM reduced glutathione in TNE (pH 9.4)/1% digitonin or Triton X-100 on ice for 30 min.

In vitro ceramide synthesis assay

The enzyme was purified as described above, but the beads were washed three times with TNE and twice with B88 (20 mM HEPES, pH 6.8, 150 mM KAc, 5 mM MgAc, 250 mM sorbitol). In case of HA-tagged proteins, the assay was performed directly on the beads. For the Flag-tagged version, the immunoprecipitated beads were eluted with 2 mg/ml of Flag peptide in B88 and detergent.

For the assay, 5 μl of a mixture of [^{3}H]DHS/DHS (1/4, 20 μM) in ethanol was dried under a stream of nitrogen, the residue was resuspended in 5 μl of a 40 μM solution of BSA. Eluates or beads in B88 were added to this mixture, followed by C26 fatty acyl-CoA. The final volume of the reaction was 100 μl, with a 2 μM final concentration of BSA, 1 μM final concentration for [^{3}H]DHS/DHS and 0.5 μM for C26 fatty acyl-CoA, unless specified otherwise. The samples were incubated at 24°C for 30 min, and the reaction was stopped by adding 600 μl of chloroform/methanol (1/1, v/v). The lipids were extracted by *n*-butanol/water partitioning as previously described (Schorling *et al*, 2001), and analyzed by TLC using the solvent system I, chloroform/acetic acid (9/1, v/v). The TLC plates were visualized and quantified by using tritium-sensitive screens and a Cyclone phosphorimager (Packard, Meriden, CT). The radioactivity extracted from enzyme-negative controls was regarded as the background level and subtracted. On each TLC, a known amount of [^{3}H]DHS was loaded, and used as a standard.

Glycerol gradient

In all, 200 μl of proteins were loaded onto a glycerol gradient. A 4 ml-step gradient from 15% (v/v) to 40% (v/v) glycerol in TNE + 1% digitonin (Calbiochem) or Triton X-100 was prepared and centrifuged at 200 000 *g* in a SW60 rotor (Beckman) for 6 h at 4°C. Fractions of 250 μl were collected from the top. The sample buffer was added, and fractions were analyzed either by Western blotting or by silver staining (according to either Mann or Blum protocols (Blum *et al*, 1987; Shevchenko *et al*, 1996)).

In vivo lipid labelling

In vivo lipid labellings were performed as previously described (Zanolari *et al*, 2000). Sphingolipids were extracted by chloroform/methanol (1/1) in presence of glass beads and then by butanol/water. For ceramide analysis, lipids were extracted first by ethanol/diethylether/pyridine/4.2 N ammonium hydroxide (15/5/1/0.018), and then by butanol/water partitioning. Lipids were analyzed on TLC using solvent system II, chloroform/methanol/0.25% KCl (55/45/10) for sphingolipid labelled with [^{3}H]*myo*-inositol, solvent system III, chloroform/methanol/4.2 N ammonium hydroxide (9/7/2) for sphingolipid labelled with [^{3}H]DHS, and solvent system IV, chloroform/methanol/acetic acid (190/9/1) for ceramide.

Protein extraction and subcellular fractionation

To characterize the nature of membrane association of proteins, cells were grown in rich medium, washed and resuspended in TNE buffer. Cells were disrupted with glass beads, and the cell debris and glass beads were removed by centrifugation at 720 *g* for 5 min at 4°C. One volume of TNE buffer containing 2 M NaCl, 2% Triton X-100, 2% SDS, or 200 mM Na_2CO_3 (pH 11.5) was added to the supernatants. The mixture was incubated on ice for 30 min and

centrifuged at 100 000 *g* for 1 h at 4°C. The resulting pellet and supernatant fractions were subjected to SDS–PAGE and then analyzed by Western blotting using a rabbit polyclonal antibody against Wbp1p, or a mouse mAb M2 against Flag. Subcellular fractionation was performed as described (Funato *et al*, 2003). Samples were subjected to SDS–PAGE, followed by Western blotting using a mouse Ab against Flag epitope, a rabbit polyclonal Ab against Wbp1p or Emp47p.

Indirect immunofluorescence microscopy

Indirect immunofluorescence on whole fixed yeast cells was performed as described (Beck *et al*, 1999). A mouse Ab against Flag followed by an indocarbocyanine, Cy-3-conjugated goat anti-mouse IgG (Jackson ImmunoResearch Laboratories, West Grove, PA) and a rabbit polyclonal Ab against Kar2 (kindly provided by R Schekman) followed by a fluorescein isothiocyanate donkey anti-rabbit IgG (Jackson ImmunoResearch Laboratories) were used. DNA was stained with 4′,6-diamidino-2-phenylindole (DAPI; Sigma) at a concentration of 1 μg/ml. Cells were visualized with a Axiophot 2 microscope (× 100).

Protease protection assay

Spheroplasts prepared as described above were lysed by Dounce homogenization in B88. The 3000 *g* supernatant was centrifuged at 10 000 *g* and then at 100 000 *g* for 1 h. The pellet was washed with B88 and centrifuged at 100 000 *g* twice more. Finally, the microsome pellet was resuspended at a concentration of 4000 OD/ml. The protein concentration was determined using BioRad protein assay kit. In all, 80 μg of proteins were incubated with or without 0.1% of Triton X-100 in the presence or absence of proteinase K (final concentration, 30 μg/ml) on ice for 30 min. The reaction was stopped by addition of PMSF (final concentration, 2 mM). The samples were subjected to SDS–PAGE, followed by Western blotting using a mouse Ab against Flag epitope, a rabbit polyclonal Ab against Kar2p.

Supplementary data

Supplementary data are available at *The EMBO Journal* Online.

Acknowledgements

We thank Dieter Oesterhelt, Jeanette Holenstein, Véronique Koerin and Brigitte Bernadets for reagents and help, as well as the Riezman laboratory, in particular Kouichi Funato and Reika Watanabe, for stimulating discussions and suggestions. Many thanks to Hélène Bénédetti for her patience and support. This work was funded by a FEBS fellowship (BV) and a grant from the Office Fédérale de la Santé (EC network grant HPRN-CT-2000-00077; HR).

References

Acharya U, Patel S, Koundakjian E, Nagashima K, Han X, Acharya JK (2003) Modulating sphingolipid biosynthetic pathway rescues photoreceptor degeneration. *Science* **299:** 1740–1743

Akanuma H, Kishimoto Y (1979) Synthesis of ceramides and cerebrosides containing both alpha-hydroxy and nonhydroxy fatty acids from lignoceroyl-CoA by rat brain microsomes. *J Biol Chem* **254:** 1050–1060

Barz WP, Walter P (1999) Two endoplasmic reticulum (ER) membrane proteins that facilitate ER-to-Golgi transport of glycosylphosphatidylinositol-anchored proteins. *Mol Biol Cell* **10:** 1043–1059

Beck T, Schmidt A, Hall MN (1999) Starvation induces vacuolar targeting and degradation of the tryptophan permease in yeast. *J Cell Biol* **146:** 1227–1238

Beeler T, Bacikova D, Gable K, Hopkins L, Johnson C, Slife H, Dunn T (1998) The *Saccharomyces cerevisiae* TSC10/YBR265w gene encoding 3-ketosphinganine reductase is identified in a screen for temperature-sensitive suppressors of the Ca2 + -sensitive csg2Delta mutant. *J Biol Chem* **273:** 30688–30694

Blum H, Beier H, Gross H (1987) Improved silver staining of plant proteins, RNA, and DNA in polyacrylamide gels. *Electrophoresis* **8:** 93–99

Brandwagt BF, Mesbah LA, Takken FL, Laurent PL, Kneppers TJ, Hille J, Nijkamp HJ (2000) A longevity assurance gene homolog of tomato mediates resistance to *Alternaria alternata* f. sp. lycopersici toxins and fumonisin B1. *Proc Natl Acad Sci USA* **97:** 4961–4966

Cuvillier O, Pirianov G, Kleuser B, Vanek PG, Coso OA, Gutkind S, Spiegel S (1996) Suppression of ceramide-mediated programmed cell death by sphingosine-1-phosphate. *Nature* **381:** 800–803

Dickson RC (1998) Sphingolipid functions in *Saccharomyces cerevisiae*: comparison to mammals. *Annu Rev Biochem* **67:** 27–48

Dickson RC, Lester RL (1999) Metabolism and selected functions of sphingolipids in the yeast *Saccharomyces cerevisiae*. *Biochim Biophys Acta* **1438:** 305–321

Dickson RC, Lester RL (2002) Sphingolipid functions in *Saccharomyces cerevisiae*. *Biochim Biophys Acta* **1583:** 13–25

Endo M, Takesako K, Kato I, Yamaguchi H (1997) Fungicidal action of aureobasidin A, a cyclic depsipeptide antifungal antibiotic, against *Saccharomyces cerevisiae*. *Antimicrob Agents Chemother* **41:** 672–676

Funato K, Lombardi R, Vallee B, Riezman H (2003) Lcb4p is a key regulator of ceramide synthesis from exogenous long chain sphingoid base in *Saccharomyces cerevisiae*. *J Biol Chem* **278:** 7325–7334

Funato K, Riezman H (2001) Vesicular and nonvesicular transport of ceramide from ER to the Golgi apparatus in yeast. *J Cell Biol* **155:** 949–959

Funato K, Vallee B, Riezman H (2002) Biosynthesis and trafficking of sphingolipids in the yeast *Saccharomyces cerevisiae*. *Biochemistry* **41:** 15105–15114

Futerman AH, Hannun YA (2004) The complex life of simple sphingolipids. *EMBO Rep* **5:** 777–782

Goder V, Junne T, Spiess M (2004) Sec61p contributes to signal sequence orientation according to the positive-inside rule. *Mol Biol Cell* **15:** 1470–1478

Gouet P, Courcelle E, Stuart DI, Metoz F (1999) ESPript: analysis of multiple sequence alignments in PostScript. *Bioinformatics* **15:** 305–308

Guillas I, Jiang JC, Vionnet C, Roubaty C, Uldry D, Chuard R, Wang J, Jazwinski SM, Conzelmann A (2003) Human homologues of LAG1 reconstitute Acyl-CoA-dependent ceramide synthesis in yeast. *J Biol Chem* **278:** 37083–37091

Guillas I, Kirchman PA, Chuard R, Pfefferli M, Jiang JC, Jazwinski SM, Conzelmann A (2001) C26-CoA-dependent ceramide synthesis of *Saccharomyces cerevisiae* is operated by Lag1p and Lac1p. *EMBO J* **20:** 2655–2665

Hanada K, Hara T, Nishijima M (2000) Purification of the serine palmitoyltransferase complex responsible for sphingoid base synthesis by using affinity peptide chromatography techniques. *J Biol Chem* **275:** 8409–8415

Hannun YA, Luberto C (2000) Ceramide in the eukaryotic stress response. *Trends Cell Biol* **10:** 73–80

Hannun YA, Obeid LM (2002) The ceramide-centric universe of lipid-mediated cell regulation: stress encounters of the lipid kind. *J Biol Chem* **277:** 25847–25850

Hirschberg K, Rodger J, Futerman AH (1993) The long-chain sphingoid base of sphingolipids is acylated at the cytosolic surface of the endoplasmic reticulum in rat liver. *Biochem J* **290:** 751–757

Ikushiro H, Hayashi H, Kagamiyama H (2004) Reactions of serine palmitoyltransferase with serine and molecular mechanisms of the actions of serine derivatives as inhibitors. *Biochemistry* **43:** 1082–1092

Ito T, Chiba T, Ozawa R, Yoshida M, Hattori M, Sakaki Y (2001) A comprehensive two-hybrid analysis to explore the yeast protein interactome. *Proc Natl Acad Sci USA* **98:** 4569–4574

Jazwinski SM, Conzelmann A (2002) LAG1 puts the focus on ceramide signaling. *Int J Biochem Cell Biol* **34:** 1491–1495

Jiang JC, Kirchman PA, Zagulski M, Hunt J, Jazwinski SM (1998) Homologs of the yeast longevity gene LAG1 in *Caenorhabditis elegans* and human. *Genome Res* **8:** 1259–1272

Kihara A, Igarashi Y (2004) FVT-1 is a mammalian 3-ketodihydrosphingosine reductase with an active site that faces the cytosolic side of the endoplasmic reticulum membrane. *J Biol Chem* **279:** 49243–49250

Kihara A, Sano T, Iwaki S, Igarashi Y (2003) Transmembrane topology of sphingoid long-chain base-1-phosphate phosphatase, Lcb3p. *Genes Cells* **8:** 525–535

Kobayashi SD, Nagiec MM (2003) Ceramide/long-chain base phosphate rheostat in *Saccharomyces cerevisiae*: regulation of ceramide synthesis by Elo3p and Cka2p. *Eukaryot Cell* **2:** 284–294

Lester RL, Dickson RC (1993) Sphingolipids with inositolphosphate-containing head groups. *Adv Lipid Res* **26:** 253–274

Lester RL, Wells GB, Oxford G, Dickson RC (1993) Mutant strains of *Saccharomyces cerevisiae* lacking sphingolipids synthesize novel inositol glycerophospholipids that mimic sphingolipid structures. *J Biol Chem* **268:** 845–856

Maceyka M, Payne SG, Milstien S, Spiegel S (2002) Sphingosine kinase, sphingosine-1-phosphate, and apoptosis. *Biochim Biophys Acta* **1585:** 193–201

Mandala SM, Thornton RA, Frommer BR, Curotto JE, Rozdilsky W, Kurtz MB, Giacobbe RA, Bills GF, Cabello MA, Martin I, Pelaez F, Harris GH (1995) The discovery of australifungin, a novel inhibitor of sphinganine *N*-acyltransferase from *Sporormiella australis*. Producing organism, fermentation, isolation, and biological activity. *J Antibiot (Tokyo)* **48:** 349–356

Mandala SM, Thornton R, Tu Z, Kurtz MB, Nickels J, Broach J, Menzeleev R, Spiegel S (1998) Sphingoid base 1-phosphate phosphatase: a key regulator of sphingolipid metabolism and stress response. *Proc Natl Acad Sci USA* **95:** 150–155

Mao C, Saba JD, Obeid LM (1999) The dihydrosphingosine-1-phosphate phosphatases of *Saccharomyces cerevisiae* are important regulators of cell proliferation and heat stress responses. *Biochem J* **3:** 667–675

Mao C, Xu R, Bielawska A, Obeid LM (2000a) Cloning of an alkaline ceramidase from *Saccharomyces cerevisiae*. An enzyme with reverse (CoA-independent) ceramide synthase activity. *J Biol Chem* **275:** 6876–6884

Mao C, Xu R, Bielawska A, Szulc ZM, Obeid LM (2000b) Cloning and characterization of a *Saccharomyces cerevisiae* alkaline ceramidase with specificity for dihydroceramide. *J Biol Chem* **275:** 31369–31378

Merrill Jr AH (2002) *De novo* sphingolipid biosynthesis: a necessary, but dangerous, pathway. *J Biol Chem* **277:** 25843–25846

Morell P, Radin NS (1970) Specificity in ceramide biosynthesis from long chain bases and various fatty acyl coenzyme A′s by brain microsomes. *J Biol Chem* **245:** 342–350

Nagiec MM, Nagiec EE, Baltisberger JA, Wells GB, Lester RL, Dickson RC (1997) Sphingolipid synthesis as a target for antifungal drugs. Complementation of the inositol phosphorylceramide synthase defect in a mutant strain of *Saccharomyces cerevisiae* by the AUR1 gene. *J Biol Chem* **272:** 9809–9817

Notredame C, Higgins D, Heringa J (2000) T-coffee: a novel method for multiple sequence alignments. *J Mol Biol* **302:** 205–217

Oh CS, Toke DA, Mandala S, Martin CE (1997) ELO2 and ELO3, homologues of the *Saccharomyces cerevisiae* ELO1 gene, function in fatty acid elongation and are required for sphingolipid formation. *J Biol Chem* **272:** 17376–17384

Perry DK, Hannun YA (1998) The role of ceramide in cell signaling. *Biochim Biophys Acta* **1436:** 233–243

Riebeling C, Allegood JC, Wang E, Merrill Jr AH, Futerman AH (2003) Two mammalian longevity assurance gene (LAG1) family members, trh1 and trh4, regulate dihydroceramide synthesis using different fatty acyl-CoA donors. *J Biol Chem* **278:** 43452–43459

Schorling S, Vallee B, Barz WP, Riezman H, Oesterhelt D (2001) Lag1p and Lac1p are essential for the Acyl-CoA-dependent ceramide synthase reaction in *Saccharomyces cerevisae*. *Mol Biol Cell* **12:** 3417–3427

Shevchenko A, Wilm M, Vorm O, Mann M (1996) Mass spectrometric sequencing of proteins silver-stained polyacrylamide gels. *Anal Chem* **68:** 850–858

Smith SW, Lester RL (1974) Inositol phosphorylceramide, a novel substance and the chief member of a major group of yeast sphingolipids containing a single inositol phosphate. *J Biol Chem* **249:** 3395–3405

Spiegel S, Milstien S (2002) Sphingosine 1-phosphate, a key cell signaling molecule. *J Biol Chem* **277:** 25851–25854

Uetz P, Giot L, Cagney G, Mansfield TA, Judson RS, Knight JR, Lockshon D, Narayan V, Srinivasan M, Pochart P, Qureshi-Emili A, Li Y, Godwin B, Conover D, Kalbfleisch T, Vijayadamodar G, Yang M, Johnston M, Fields S, Rothberg JM (2000) A comprehensive analysis of protein–protein interactions in *Saccharomyces cerevisiae*. *Nature* **403:** 623–627

Venkataraman K, Riebeling C, Bodennec J, Riezman H, Allegood JC, Sullards MC, Merrill Jr AH, Futerman AH (2002) Upstream of growth and differentiation factor 1 (uog1), a mammalian homolog of the yeast longevity assurance gene 1 (LAG1), regulates *N*-stearoyl-sphinganine (C18-(dihydro)ceramide) synthesis in a fumonisin B1-independent manner in mammalian cells. *J Biol Chem* **277:** 35642–35649

Wang E, Norred WP, Bacon CW, Riley RT, Merrill Jr AH (1991) Inhibition of sphingolipid biosynthesis by fumonisins. Implications for diseases associated with *Fusarium moniliforme*. *J Biol Chem* **266:** 14486–14490

Winzeler EA, Shoemaker DD, Astromoff A, Liang H, Anderson K, Andre B, Bangham R, Benito R, Boeke JD, Bussey H, Chu AM, Connelly C, Davis K, Dietrich F, Dow SW, El Bakkoury M, Foury F, Friend SH, Gentalen E, Giaever G, Hegemann JH, Jones T, Laub M, Liao H, Liebundguth N, Lockhart DJ, Lucau-Danila A, Lussier M, M'Rabet N, Menard P, Mittmann M, Pai C, Rebischung C, Revuelta JL, Riles L, Roberts CJ, Ross-MacDonald P, Scherens B, Snyder M, Sookhai-Mahadeo S, Storms RK, Veronneau S, Voet M, Vlockaert G, Ward TR, Wysocki R, Yen GS, Yu KX, Zimmermann K, Philippsen P, Johnston M, Davis RW (1999) Functional characterization of the *S. cerevisiae* genome by gene deletion and parallel analysis. *Science* **285:** 901–906

Wu WI, McDonough VM, Nickels Jr JT, Ko J, Fischl AS, Vales TR, Merrill Jr AH, Carman GM (1995) Regulation of lipid biosynthesis in *Saccharomyces cerevisiae* by fumonisin B1. *J Biol Chem* **270:** 13171–13178

Yasuda S, Nishijima M, Hanada K (2003) Localization, topology, and function of the LCB1 subunit of serine palmitoyltransferase in mammalian cells. *J Biol Chem* **278:** 4176–4183, (Epub 2002 December 4102)

Zanolari B, Friant S, Funato K, Sutterlin C, Stevenson BJ, Riezman H (2000) Sphingoid base synthesis requirement for endocytosis in *Saccharomyces cerevisiae*. *EMBO J* **19:** 2824–2833